

**A study of glutathione peroxidase 4 function in human intestinal
epithelial cells**

By

Patience Cole Ezea

MRes Newcastle University

BSc Sunderland University

A thesis presented for the degree of

Doctor of Philosophy

At Newcastle University

2012

Declaration

The information contained within this thesis is truly the author's work except where stated otherwise and has not been previously submitted for a degree at the University of Newcastle or any other university. All help given by others has been duly acknowledged and sources of materials and information are indicated in the text.

Patience Cole Ezea

September 2012

Acknowledgements

This thesis could not have been completed without the advice, enthusiasm, guidance and encouragement of my supervisors Professor John Hesketh and Dr Daryl Shanley. Their support throughout my studies was invaluable.

I would like to thank the many people who have spent time giving me help and advice in the lab. I am specifically indebted to Dr Guanyu Gong who help design the siRNA used throughout this study, Prof Robert Lightowlers and Dr Paul Smith for advice on respirometry experiment, Dr Owen Hughes and Dr Ian Harvey for assistance with flow cytometry experiment and Dr Daniel Swan for help with bioinformatics analysis of the microarray data.

I would like to thank Michael Owulu who have supported and encouraged me throughout my studies.

Finally, I would like to thank EPSRC for funding the project.

ABSTRACT

Intake of the micronutrient selenium, which is incorporated into selenoproteins in humans, has been implicated in affecting risk of colorectal cancer. A genetic variant in the gene encoding the selenoprotein glutathione peroxidase 4 (GPx4) has been reported to influence colorectal cancer risk. In this study the role of GPx4 was investigated in the Caco-2 intestinal cell line using RNA silencing. *GPX4* expression was knocked-down by ~60% and an unbiased gene microarray analysis of the total Caco-2 cell transcriptome was carried out using Illumina HumanHT-12v3 beadchips. The data were validated by real-time PCR. Ingenuity Pathway analysis showed that the major canonical pathways affected by *GPX4* knock-down were oxidative phosphorylation, ubiquinone biosynthesis and mitochondrial dysfunction and the top two toxicological lists were mitochondrial dysfunction and oxidative stress. Western blotting and real-time PCR confirmed that knock-down affected target genes encoding components of respiratory complexes I, IV and V as well as the protein apoptosis-inducing factor (AIF). *GPX4* knock-down increased levels of mitochondrial reactive oxygen species and oxidised lipid, and decreased mitochondrial adenosine triphosphate (ATP) levels and mitochondrial membrane potential. Time course experiments showed changes in AIF expression preceded those in the respiratory complexes. *GPX4* knock-down increased apoptosis and changed protein expression of Caspase-9, Bax and Bcl-2. Treatment of cells with the antioxidant mitoquinone prevented the effects of *GPX4* knockdown on mitochondrial reactive oxygen species, oxidised lipid and mitochondrial membrane potential but not the effect on AIF. These data suggest that in intestinal epithelial cells GPx4, through effects on lipid peroxidation and AIF, plays a complex role in maintaining the oxidative phosphorylation system and protecting mitochondria from oxidative damage and apoptosis.

List of publication related to this thesis

Cole-Ezea P, Swan D, Shanley D, Hesketh J. (2012) Glutathione peroxidase 4 has a major role in protecting mitochondria from oxidative damage and maintaining oxidative phosphorylation complexes in gut epithelial cells. *Free Radic Biol Med.* 53(3):488-97.

List of Abbreviations

A	Adenine
AA	Adenine-Adenine
A ₂₆₀	Absorbance reading at 260nm
ADP	Adenosine diphosphate
AIF	Apoptosis inducing factor
APS	Ammonium persulphate
ATP	Adenosine triphosphate
BAX	Bcl2-associated
Bcl-2	B-cell lymphoma 2
bp	Base pair
BSA	Bovine serum albumin
C	Carbon
C	Cytosine
Caco-2	Colonic adenocarcinoma cells
Carboxy-H2DCFDA	5'(and6)-carboxyl-2'7'-dichlorodihydrofluorescein diacetate
Caspases	Cysteine-aspartic proteases
Caspase3	Cysteine-aspartic protease 3

Caspase7	Cysteine-aspartic protease 7
Caspase9	Cysteine-aspartic protease 9
cDNA	copy DNA
CDS	Coding sequence
cGPx4	cytosolic glutathione peroxidase 4
Complex I	NADH dehydrogenase 1
Complex II	Succinate dehydrogenase
Complex III	Cytochrome <i>bc1</i> complex
Complex IV	Cytochrome c oxidase
COX	Cyclooxygenase
COX-1	Cyclooxygenase 1
COX-2	Cyclooxygenase 2
COX2	Cytochrome c oxidase mitochondria subunit 2
Cyt.c	Cytochrome Complex
DEPC	Diethylpyrocarbonate
dH ₂ O	Distilled water
DIO	Deiodinase
DMSO	Dimethyl sulfoxide

DNA	Deoxyribonucleic acid
dNTP	Deoxynucleotide triphosphate
DTPP	Decyltriphenylphosphonium
EB	Ethidium bromide
EDTA	Ethylenediaminetetraacetic acid
EFsec	Selenocysteine-specific elongation factor
EIF5	Eukaryotic translation initiation factor 5
ER	Endoplasmic reticulum
FCCP	Carbonylcyanide-p-trifluoromethoxyphenylhydrazone
FCS	Foetal calf serum
G	Guanine
GAPDH	Glyceraldehyde-3-phosphate dehydrogenase
GI	Gastrointestinal
GPx1	Glutathione peroxidase 1
GPx2	Glutathione peroxidase 2
GPx3	Glutathione peroxidase 3
GPx4	Glutathione peroxidase 4
GSH	Glutathione

GSSG	Glutathione disulphide
HBSS	Hank's Buffered Salt Solution
H ₂ O ₂	Hydrogen peroxide
5-HETE	5-Hydroxyeicosatetraenoic acid
HIV	Human immunodeficiency virus
5-HPETE	5-hydroperoxyeicosatetraenoic acid
HRP	Horseradish peroxidase
HUVEC	Human umbilical endothelial cells
I	Iodine
IBD	Inflammatory bowel disease
L	Lysine
kb	Kilo bases
LOX	lipooxygenase
5-LOX	5-Lipooxygenase
12-LOX	12-Lipooxygenase
15-LOX	15-Lipooxygenase
LPS	Lipopolysaccharide
mGPx4	mitochondrial glutathione peroxidase 4

MitoQ ₁₀	Mitoquinone ₁₀
MQH ₂ O	milli-Q water
mRNA	Messenger ribonucleic acid
NAD(H)	Nicotinamide mononucleotide adenylytransferase 1
NDUFA10	NADH dehydrogenase (ubiquinone) 1 alpha subcomplex subunit 10
NDUFB6	NADH dehydrogenase (ubiquinone) 1 beta subcomplex subunit 6
NDUFB8	NADH dehydrogenase (ubiquinone) 1 beta subcomplex subunit 8
NFκB	Nuclear factor kappa B
nGPx4	nuclear glutathione peroxidase 4
P	Phosphate
PBS	Phosphate buffered saline
PCR	Polymerase chain reaction
PG	Prostaglandin
PGE2	Prostaglandin E2
PG12	Prostaglandin 12
PI	Propidium Iodide
PS	Phosphatidylserine
PVDF	Polyvinylidene difluoride

Redox	Reduction-oxidation reaction
RISC	RNA-induced silencing complex
RNA	Ribonucleic acid
RNAi	Ribonucleic acid interference
ROOH	lipid peroxides
ROS	Reactive oxygen species
RT-PCR	Reverse transcriptase-polymerase chain reaction
RT-qPCR	Reverse transcriptase-quantitative polymerase chain reaction
S	Sulphur
SBP2	SECIS-binding protein 2
SDS-PAGE	Sodium dodecyl sulphate-polyacrylamide gel electrophoresis
Se	Selenium
Se-	Selenium-depleted
Se+	Selenium-supplemented
SECIS	Selenocysteine insertion sequence
SeCys	Selenocysteine
SEM	Standard error of the mean
Sel H	Selenoprotein H

Sel I	Selenoprotein I
Sel K	Selenoprotein K
Sel M	Selenoprotein M
Sel N	Selenoprotein N
Sel O	Selenoprotein O
Sel P	Selenoprotein P
Sel R	Selenoprotein R
Sel S	Selenoprotein S
Sel T	Selenoprotein T
Sel W	Selenoprotein W
Sep-15	Selenoprotein 15kDa
SiRNA	small interfering ribonucleic acid
SMAC	second mitochondria-derived activator of caspases
SOD	Superoxide dismutase
T	Thymine
tBOOH	tert-Butyl hydroperoxide
TEMED	N,N,N',N'-Tetramethylethylenediamine
T-PBS	Tween-20 Phosphate buffered saline

TNF α	Tumor necrosis factor α
TrxR	Thioredoxin reductase
TrxR1	Thioredoxin reductase 1
TrxR2	Thioredoxin reductase 2
TrxR3	Thioredoxin reductase 3
UTR	Untranslated region
UV	Ultra violet

List of Tables

Table 1. Identified selenoproteins, their possible functions, tissue distribution and subcellular localization.....	8
Table 2. Summary of observed effects of GPxs on eicosanoid biosynthesis through LOX/COX pathways	25
Table 3. Volumes and amount of reagents required for transfection in different format.....	41
Table 4. List of primers for generating products from cDNA by semi-quantitative RT-PCR or by real-time PCR.....	47
Table 5. List of primary and secondary antibodies used for Western blotting.....	57
Table 6. Pathway analysis of the transcriptomic data after <i>GPX4</i> knock-down.....	85
Table 7. Quantification of flow cytometric data to assess apoptosis in Caco-2 cells following <i>GPX4</i> knock-down.....	159

List of Figures

Figure 1. The pathway of ROS production and clearance in the cell environment.....	10
Figure 2. SECIS stem-loop structure and SeCys incorporation during selenoprotein biosynthesis.....	14
Figure 3. Structure of the GPx4 gene and the three isoforms of GPx4 mRNA.....	19
Figure 4. Repression of 5-LOX activation and leukotriene production by GPx.....	23
Figure 5. Hypothetical scheme illustrating the relationship of mitochondrial respiration, ROS, antioxidant enzymes and cytochrome c.....	32
Figure 6. Conversion of Resazurin by metabolically active cells results in the generation of a fluorescent product or a change in absorbance wavelength.....	58
Figure 7. A typical formation of MDA-TBA adduct.....	60
Figure 8. Detection of <i>GPX4</i> mRNA transcript variant in Caco-2 cells.....	75
Figure 9. Sequence information of <i>GPX4</i> mRNA transcript and <i>GPX4</i> -siRNA(1), siRNA(2), and scrambled negative control siRNA.....	75
Figure 10. Knock-down of <i>GPX4</i> mRNA expression in Caco-2 cells.....	78
Figure 11. Knock-down of GPx4 expression at protein level.....	79
Figure 12. Integrity of RNA used for microarray analysis.....	82
Figure 13. Network analysis of the transcriptomic data.....	86
Figure 14. Confirmation of <i>GPX4</i> knock-down transcriptomic data by quantitative RT-PCR.....	89
Figure 15. Expression of markers of mitochondrial complex I and IV after <i>GPX4</i> knock-down with siRNA(1).....	91

Figure 16. Expression of <i>GPX4</i> mRNA and protein and markers of mitochondrial complex I and IV after <i>GPX4</i> knock-down with siRNA(2).....	92
Figure 17. Assessment of lipid peroxide and superoxide level following <i>GPX4</i> knock-down with siRNA(1).....	106
Figure 18. Assessment of mitochondrial membrane potential and oxidative stress following <i>GPX4</i> knock-down with siRNA(2).....	107
Figure 19. Assessment of mitochondrial membrane potential and mitochondrial ATP following <i>GPX4</i> knock-down with siRNA(1).....	108
Figure 20. Assessment of mitochondrial respiration and overall cellular ROS following <i>GPX4</i> knock-down.....	109
Figure 21. Assessment of cell viability following cell treatment with siRNA(1).....	110
Figure 22. Expression of AIF protein following <i>GPX4</i> knock-down.....	121
Figure 23. Expression of AIF mitochondrial and cytosolic fractions following <i>GPX4</i> knock-down	122
Figure 24. A time course assessment of <i>GPX4</i> , NDUFB8, COX2 and AIF protein following <i>GPX4</i> knock-down with siRNA(1).....	124
Figure 25. Time course of mitochondrial integrity and oxidative stress following <i>GPX4</i> knock-down with siRNA(1).....	126
Figure 26. Structure of MitoQ ₁₀ and scheme illustrating its uptake into plasma membrane and mitochondria membrane.....	132
Figure 27. Confirmation of <i>GPX4</i> mRNA status following MitoQ ₁₀ and DTTP treatment.....	133
Figure 28. Confirmation of <i>GPX4</i> knock-down at protein level following siRNA(1) treatment in the presence of MitoQ ₁₀	134

Figure 29. Investigation of the Impact of MitoQ ₁₀ treatment on the effect of GPX4 knock-down on mitochondrial complex I and IV and on AIF.....	136
Figure 30. Effect of Mitoquinone on mitochondrial integrity and oxidative stress following GPX4 knock-down with siRNA(1).....	140
Figure 31. Assessment of DNA fragmentation following treatment with either <i>GPX4</i> -siRNA(1) or scrambled negative control.....	148
Figure 32. Expression of Caspase-3 and caspase-9 after <i>GPX4</i> knock-down.....	150
Figure 33. Enzymatic activity of caspase 3/7 following treatment with <i>GPX4</i> -siRNA(1) or scrambled negative control siRNA.....	152
Figure 34. Bax and Bcl-2 protein expression following Caco-2 cell treatment with either <i>GPX4</i> -siRNA(1) or scrambled negative control.....	153
Figure 34. Bax protein levels in mitochondrial and cytosolic fractions expression following treatment with either <i>GPX4</i> -siRNA(1) or scrambled negative control siRNA.....	156
Figure 36. Flow cytometric assessment of apoptosis in Caco-2 cells following <i>GPX4</i> knock-down.....	158
Figure 37. Hypothetical model of the role of GPx4 in Caco-2 cells.....	174

Table of Contents

Declaration.....	i
Acknowledgment.....	ii
Abstract.....	iii
List of publication related to thesis.....	iv
Abbreviations.....	v
List of tables.....	x
List of figures.....	xi

Chapter 1. Introduction.....	1
1.1.1 The importance of micronutrient selenium and its role in human health.....	1
1.2 The selenoproteins and their functions.....	6
1.2.1 The incorporation mechanism of selenium into selenoprotein.....	11
1.3 Glutathione Peroxidases (GPx).....	15
1.3.1 Glutathione Peroxidase 1 (GPx1).....	15
1.3.2 Glutathione Peroxidase 2 (GPx2).....	16
1.3.3 Glutathione Peroxidase 3 (GPx3).....	17
1.3.4 Glutathione Peroxidase 4 (GPx4).....	18
1.4 Proposed roles of GPx4.....	20
1.4.1 Effect of GPx4 on Eicosanoid biosynthesis.....	23
1.4.2 Mitochondrial regulation by selenoprotein GPx4.....	27
1.4.3 GPx4 protection against cell death.....	28
1.4.4 The role of mitochondrial GPx4 in apoptosis.....	30
1.4.5 Regulation of spermatogenesis and sperm function by GPx4.....	33
1.5 Aim and objectives of the projects.....	36
Chapter 2. Materials and Methods.....	37
2.1 General.....	37
2.1.1 Culture of mammalian cells.....	36
2.1.2 Growth and maintenance.....	38
2.2 Transient transfection of human intestinal epithelial (Caco-2) cells with small interfering RNA (siRNA).....	38
2.3 RNA lysate preparation using TRIzol® reagents.....	42
2.3.1 Preparation for RNA for microarray and qRT-PCR analysis.....	43
2.3.2 Determination of RNA concentration and integrity.....	43
2.3.3 Reverse transcription of RNA.....	43
2.3.4 Polymerase chain reaction (PCR) and semi-quantitative RT-PCR.....	44
2.3.5 Agarose gel electrophoresis.....	48
2.3.6 qRT-PCR (Real-Time PCR).....	49
2.3.7 DNase treatment of RNA used for qRT-PCR.....	49
2.3.8 Reverse transcription of RNA used for qRT-PCR.....	49

2.3.9	qPCR using the Roche LightCycler® 480.....	49
2.3.10	Global mRNA expression analysis.....	51
2.4	Whole cell lysate preparation, protein analysis and Western blotting.....	51
2.4.1	Cell lysate preparation.....	51
2.4.2	Preparation of mitochondrial and cytosolic fractions.....	52
2.4.3	Determination of protein concentration.....	53
2.4.4	Sodium dodecyl sulphate-polyacrylamide gel electrophoresis.....	53
2.4.5	Blotting and detection of protein.....	54
2.4.6	Staining of protein.....	56
2.5	Cell viability assay.....	58
2.6	Thiobarbituric acid reactive assay substance (TBARS) assay for lipid peroxidation.....	59
2.7	Measurement of ROS levels using Carboxy-H ₂ DCFDA.....	61
2.7.1	Measurement of superoxide production using MitoSOX™.....	63
2.8	Measurement of mitochondrial ATP production using a luminometer based luciferase assay.....	64
2.9	Measurement of mitochondrial membrane potential using the JC-1 5,5',6,6'-tetrachloro-1,1',3,3'-tetraethylbenzimidazolylcarbocyanine iodide assay.....	66
2.10	Measurement of mitochondrial respiration.....	67
2.11	DNA fragmentation assay.....	67
2.11.1	Measurement of Caspase 3/7 activity.....	69
2.11.2	Flow cytometry analysis of apoptosis.....	70
2.12	Mitoquinone (MitoQ ₁₀) treatment on Caco-2 cells.....	71
2.13	Statistical analysis.....	72

Chapter 3. Investigating the biological functions of GPx4 and down-stream effects of altered GPx4 expression in Caco-2 cells.....73

3.1	Introduction.....	73
3.1.1	Design of GPX4 siRNA and knock-down GPX4 mRNA and protein.....	74
3.1.2	Sequence information of GPx4 mRNA transcript and siRNA.....	76
3.1.3	Effect of <i>GPX4</i> knock-down on <i>GPX4</i> mRNA and protein expression.....	77
3.2	Investigating the genome-wide effects of <i>GPX4</i> on gene expression.....	81
3.2.1	Microarray hybridisation.....	83

3.2.2	Data analysis.....	83
3.2.3	Validation of transcriptomic data.....	88
3.2.4	Investigation of mitochondrial complex I and IV protein expression following <i>GPX4</i> knock-down.....	90
2.2.5	Effect of a second <i>GPX4</i> -specific siRNA on mitochondrial protein expression.....	92
3.2.6	Discussion.....	94

Chapter 4. Investigation of mitochondrial function and integrity following *GPX4* knock-down.....100

4.1	Introduction.....	100
4.1.1	Impact of <i>GPX4</i> knock-down on lipid peroxide and ROS.....	103
4.1.2	Impact of <i>GPX4</i> knock-down on mitochondrial membrane potential and ATP production.....	103
4.1.3	Effect of <i>GPX4</i> knock-down on mitochondrial respiration and cellular ROS.....	104
4.1.4	Impact of <i>GPX4</i> knock-down on cell viability.....	105
4.1.5	Effect of <i>GPX4</i> knock-down on mitochondrial superoxide and mitochondrial membrane potential with <i>GPX4</i> -siRNA(2).....	105
4.1.6	Discussion.....	111

Chapter 5. Investigation of the impact of *GPX4* knock-down on AIF protein expression.....119

5.1	Introduction.....	119
5.1.1	Impact of <i>GPX4</i> knock-down on AIF protein expression.....	120
5.1.2	A time-course study to investigate the impact of <i>GPX4</i> knock-down on NDUFB8, COX2 and AIF and on $\Delta\Psi_m$, lipid peroxide and ROS protein expression.....	123
5.1.3	Discussion.....	127

Chapter 6. Investigating the effect of Mitoquinone (MitoQ₁₀) on Caco-2 cells following *GPX4* knock-down.....131

6.1	Introduction.....	131
6.1.1	Effect of MitoQ10 on <i>GPX4</i> mRNA status n Caco-2 cells.....	133
6.1.2	Confirmation of <i>GPX4</i> knock-down at protein level following treatment with siRNA and MitoQ ₁₀	134
6.1.3	Effect of MitoQ10 treatment on NDUFB8, COX2 and AIF protein expression following <i>GPX4</i> knock-down in Caco-2 cells.....	135
6.1.4	Discussion.....	141

Chapter 7. Effect of <i>GPX4</i> knock-down on apoptosis in Caco-2 cells.....	145
7.1 Introduction.....	145
7.1.1 Results.....	147
7.1.2 DNA fragmentation assay to study apoptosis in Caco-2 cells.....	147
7.1.3 Impact of <i>GPX4</i> knock-down on Caspase-3 and -9 protein levels.....	149
7.1.4 Caspase 3/7 enzymatic activity following <i>GPX4</i> knock-down.....	151
7.1.5 Impact of <i>GPX4</i> knock-down on Bax and Bcl-2 protein levels.....	153
7.1.6 Flow cytometry analysis of apoptosis in Caco-2 cells.....	157
7.1.7 Discussion.....	160
Chapter 8. Final Discussion.....	165
Chapter 9. References.....	175

Chapter 1. Introduction

1.1 The importance of micronutrient selenium and its role in human health.

The identification of selenium (Se) as an essential micronutrient was first reported in cattle and sheep that exhibited Se-responsive disorders such as white muscle disease (Brown & Arthur, 2001). Subsequently, the importance of Se to human physiology was highlighted by report of a particular cardiovascular disease known as Keshan disease which occurred in the Keshan region of Heilongjiang province in China and which responded to Se supplementation. The soil Se is very low in this region (Combs, 2000). The aetiology of Keshan disease is not entirely known, however, a possible mechanism has been linked to low Se intake and susceptibility to virus infection in human heart muscle (Beck, 1999; Combs, 2000). Selenium supplementation of the diet prevented the high incidence of Keshan disease in this region of China (Beck, 1999). Health implications of Se intake have been widely studied with interest since its implication in Keshan disease. Selenium intake has been linked with the ability to protect against viral, bacterial infection and in carcinogenesis (review by Fairweather-Tait *et al.*, 2011; Rayman, 2012).

Deficiency in Se has been associated with susceptibility to Coxsackie virus (Beck *et al.*, 1995; Beck, 1997), human immunodeficiency virus (HIV) (Baum *et al.*, 1997; Fawzi *et*

al., 2005) and influenza virus (Beck *et al.*, 2001; Jaspers *et al.*, 2007). A Coxsackie B4 strain of virus was isolated from cardiac muscle samples of patients with Keshan disease (Beck, 1997), and a study in mice showed that that Coxackie virus reacted more virulently, and a benign strain Coxsackie B3 switched and became more virulent at low Se intake (Beck *et al.*, 1995; Beck, 1999). HIV patients exhibited a 10 fold lower level of plasma Se than healthy controls and these patients demonstrated a 6 fold increased risk of mortality from multiple infections in both adults and children (Baum *et al.*, 1997; Campa *et al.*, 1999). A clinical trial investigating the effects of Se and TRI on HIV-1 encoded transcriptional activator (Tat), and HIV-1 replication, in macrophages showed TRI knock-down by small interfering RNA to significantly increase Tat and HIV-1 in human macrophages, and 100-200ug/day of Se supplementation to increase TRI expression thereby inhibiting Tat and HIV-1 replication. These data might explain Se effects on HIV infection (Kalantari *et al.*, 2008).

Selenium enhances resistance to bacterial infection and low Se intake has been associated with increased progression of inflammatory bowel diseases (IBD) (Halliwell *et al.*, 2000; Karp & Koch, 2006). The aetiology of IBD has been linked with a combination of genetic variant (Hugot *et al.*, 2001; Stoll *et al.*, 2004), microbial infection (Marteau *et al.*, 2004; Hisamatsu *et al.*, 2008) and low Se intake (Geerling *et al.*, 2000; Karp & Koch, 2006). The colon is often a site for inflammation due to presence of pathogenic or commensal microbes (Wen & Fiocchi, 2004) and Se

supplementation has been shown to be useful in controlling IBD symptoms (Halliwell *et al.*, 2000; Tirosh *et al.*, 2007) and may reduce the need for therapeutic steroids as a clinical immunosuppressant (Karp & Koch, 2006).

Increased Se intake has been proposed to reduce cancer risk. Low Se intake has been associated with increased risk of developing various cancer types with prostate and gastrointestinal cancers showing strongest association (Willett *et al.*, 1983; Russo *et al.*, 1997; Whanger, 2004). Two analyses from a clinical trial following Se supplementation showed that Se lowered risk of prostate, lung and gastrointestinal tract cancer compared to placebo (Clark *et al.*, 1996, Duffield-Lillico *et al.*, 2002). The protective effect of Se has been implicated in some but not all cancer types, for example no significant reduction was observed in skin cancer after Se supplementation (Clark *et al.*, 1996).

Supplementation with Se has been reported to reduce gastrointestinal cancers by ~25% to 60% and other gastrointestinal associated cancers such as small intestine, biliary tract, esophageal, pancreatic, colorectal, gastric and liver (Wang *et al.*, 1994; Bjelakovic *et al.*, 2008; review by Fairweather-Tait *et al.*, 2011). Dietary supplementation of selenium in China showed significant reduction in prevalence of oesophageal cancer (Wang *et al.*, 1994; Blot *et al.*, 1995) and reduced gastric cancer mortality (Qiao *et al.*, 2009). A study of a Chinese cohort supplemented with 50 µg sodium selenite and allitridum (a garlic compound) showed significant effect on gastric cancer and overall cancer incidence (Li

et al., 2004). The Netherland Cohort study supplemented 2759 cancer esophageal patients and controls with Se and observed an inverse association between toenail Se content, gastric carcinoma and esophageal squamous carcinoma (Steevens *et al.*, 2010). Smokers with low-baseline Se showed significantly reduced incidence of adenomas and colorectal cancer (Reid *et al.*, 2006). Combined supplementation of Se and other antioxidants such as vitamin E, vitamin C, β -carotene and calcium resulted in the reduced incidence of adenomas in Norwegian patients (Hofstad *et al.*, 1998). Combined supplementation of Se and other antioxidants reduced the risk of prostate cancer (Meyer *et al.*, 2005). A case-control study in the United States reported the association between higher serum Se concentration and reduced risk of prostate cancer (Vogt *et al.*, 2003).

Selenium has been reported to play a crucial role in the brain (see review by Burk & Hill, 2009; Rayman, 2012). Selenoprotein P (Sel P) is a selenium derived protein responsible for distribution of Se to different organs and tissues. A study in mice lacking Sel P reported enhanced spasticity, abnormality in movement and spontaneous seizures (Schweizer *et al.*, 2004). Studies in humans implicated Se deficiency in seizures, Parkinson's disease coordination and decline in cognitive capability (Ashrafi *et al.*, 2007; Mahyar *et al.*, 2010). Children and adults with epilepsy and seizures (Ashrafi *et al.*, 2007a;b) and children with febrile seizures (Amiri *et al.*, 2010; Mahyar *et al.*, 2010) exhibited significantly lower Se levels than controls and Se supplementation has been reported to reduce intractable childhood seizures (reviewed by Rayman, 2000). Patients

with low plasma Se exhibited significant low coordination and a trend towards increased risk of developing Parkinson's disease (Shahtar *et al.*, 2010). Low plasma Se has been associated with cognitive decline in a French sample cohort (Akbaraly *et al.*, 2007) and cognitive decline in a Chinese sample cohort (Gao *et al.*, 2007).

The highest Se concentration of all tissues is in the thyroid gland (Schomburg *et al.*, 2008). Various roles of Se in the thyroid gland have been reported. Iodothyronine deiodinases are Se-dependent selenoproteins that produce active thyroid hormone, triiodothyronine (T3) from its inactive precursor thyroxine (T4) (Schomburg *et al.*, 2008). GPx3 is a Se-dependent enzyme reported to protect cells from effects of hydrogen peroxide in the thyroid gland (Schomburg *et al.*, 2008). This function is consistent with thyroid tissue damage and goitre, thyroid volume and Se status in French women (Derumeaux *et al.*, 2003), and the incidence of low prediagnostic serum-Se concentration and thyroid cancer in Norway (Glattre *et al.*, 1989). Selenium has been widely implicated in Hashimoto's thyroiditis, the most common type of autoimmune thyroid disease. Hashimoto's thyroiditis is characterized by accumulation of complement-fixing autoantibodies to thyroid peroxidase and Se supplementation between 80 µg to 200 µg per day (in form of sodium-selenite or selenomethionine) was effective against Hashimoto's thyroiditis (Nacamulli *et al.*, 2010; Toulis *et al.*, 2010). A meta-analysis study and systematic review reported that Se supplementation significantly reduced titre of autoantibody targeting thyroid peroxidase at 3 months

(Toulis *et al.*, 2010). Se supplementation of 200 µg reduced thyroid inflammation, permanent hypothyroidism and post-partum thyroid disease (Negro *et al.*, 2007). Selenium supplementation has been reported to reduce effects of Graves disease and these patients showed less eye involvement, improved quality of life and reduction towards progression to Graves' orbitopathy after supplementation (Marcocci *et al.*, 2011). However, a randomized control trial study in elderly UK adults with low-to-moderate Se levels did not show any evidence of an effect on thyroid hormone (Rayman *et al.*, 2008).

1.2 The selenoproteins and their functions

Twenty seven selenoproteins have so far been identified in the human proteome (Kryukov *et al.*, 2003). Glutathione peroxidase (GPx) family (GPx1-7) and the Thioredoxin Reductase (TrxR) family (TrxR1-3) are two groups of selenoprotein which have been characterized as antioxidants and play crucial role in the reduction of reactive oxygen species (ROS) (Lu & Holmgren, 2009; Fairweather-Tait *et al.* 2011). The deiodinase (DIO) families (DIO1-3), through their reductive activity, play an important role in metabolism of Iodine (I) in the thyroid (Kohrle, 2000; Brown & Arthur, 2001). Some other selenoproteins such as selenoprotein W (SelW) and selenoprotein H (SelH) have been reported to have antioxidant function (Dikiy *et al.*, 2007), selenoprotein P,

(Sel P) is responsible for the absorption and transportation of Se (Kato *et al.*, 1992), and selenophosphate synthetase 2 synthesis of SeCys tRNA such as, (SPS2) (Xu *et al.*, 2007). Seven selenoproteins including Selenoprotein K (SelK), SelM, SelN, SelS, SelT, Sep 15 and DIO2 are found in the endoplasmic reticulum (ER) where their functions have been suggested to involve modulation of protein folding particularly in response to ER stress (Labunskyy *et al.*, 2009; Shchedrina *et al.*, 2010). Table 1 shows the list of the 27 selenoproteins together with their respective tissue distributions, subcellular localizations and functions.

Selenoprotein	Function	Tissue distribution	Subcellular localization
GPx1(c-GPx)	Antioxidant	All tissues	Cytoplasm
GPx2(GiGPx)	Antioxidant	Gastrointestinal epithelium, liver	Cytoplasm
GPx3(p-GPx)	Antioxidant Circulation plasma	Circulation plasma	Extracellular
GPx4(phGPx)	Antioxidant	All tissues	Cytoplasm, Mitochondria
GPx5	Antioxidant?	Unknown	Unknown
GPx6	Antioxidant?	Unknown	Unknown
GPx7	Antioxidant?	Unknown	Unknown
TrxR1	Antioxidant	All tissues	Cytoplasm; Mitochondria
TrxR2	Antioxidant	Liver, kidney, heart	Mitochondria
TrxR3	Antioxidant	Testis	Cytoplasm
IOD1	T3 T4 metabolism	Thyroid	Plasma membrane
IOD2	T3 T4 metabolism	Thyroid	ER membrane
IOD3	T3 T4 metabolism	Brain, muscle, placenta	Plasma membrane
SPS2	Wide SeCys tRNA synthesis	Wide	Cytoplasm
SeIS	Protein folding	Unknown	ER
SeIP	Se transportation	Liver and others?	Extracellular
Sep 15	Protein folding	Wide	ER
SeIW	Antioxidant	Muscle	Cytoplasm
SeIN	Calcium homeostasis	Wide	ER membrane
SeIR	Unknown	Liver, kidney, pancreas	Cytoplasm
SeIT	Protein folding?	Prostate	Unknown
SeIH	Antioxidant	Unknown	Cytoplasm
SeII	Unknown	Unknown	Cytoplasm
SeIK	Protein folding?	Unknown	Plasma membrane
SeIM	Protein folding?	Unknown	Perinuclear?
SeIO	Unknown	Unknown	Cytoplasm?
SeIV	Unknown	Unknown	Cytoplasm

Table 1. Identified selenoproteins, their possible functions, tissue distribution and subcellular localizations. Adapted from Moghadaszadeh and Beggs, 2006 and modified according to Voudouri et al., 2003, Labunskyy et al., 2009, Brigelius-Flohe, 1999, 2008, Shchedrina et al., 2010, Curran et al., 2005, Dikiy et al., 2007, Jablonska et al. (?= not well characterized)

As shown in Table 1, the majority of the 27 selenoproteins function as antioxidants and have the ability to reduce reactive oxygen species (ROS) due to the presence of SeCys in their catalytic sequence. Selenium is a chemical family member of Oxygen (O) and Sulphur (S), but it has a high ability to transfer electrons. In the case of glutathione peroxidases, two electrons are donated to unsaturated oxygen radicals catalytically and this results in a formation of reduced glutathione (Moghadaszadeh & Beggs, 2006; Brigelius-Flohe & Kipp, 2009). A typical example is the reaction with hydrogen peroxide (H_2O_2) shown in Figure 1 and the overall resulting reaction is as follows: $2 \text{GSH} + \text{H}_2\text{O}_2 \rightarrow \text{GSSG} + 2\text{H}_2\text{O}$. Following this reaction, glutathione disulphide (GSSG), at the expense of NADPH, is recycled to glutathione by Glutathione reductase. In addition to H_2O_2 , selenoproteins have the ability to reduce other free radicals such as superoxide and lipid peroxide (ROOH) by *GPX4* (Imai & Nakagawa, 2003), and reduction of thioredoxin by thioredoxin reductase (TrxRs) utilizing NADH as a substrate (Ganther, 1999). However, it is important to emphasize that ROS are produced continuously in cells and their clearance requires collective cooperation of many antioxidants in which selenium and selenoproteins play a crucial role. The pathway through which ROS are produced and cleared (Droge, 2002) is shown in Figure 1.

Pathways of ROS production and clearance

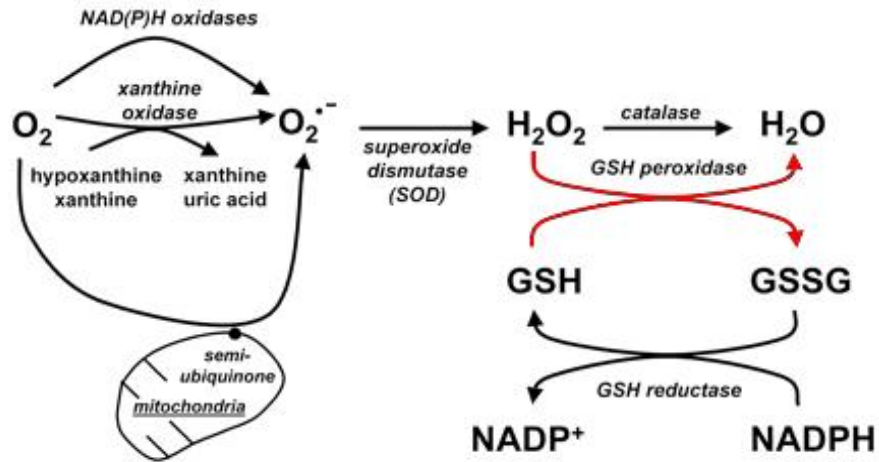


Figure 1. The pathway of ROS production and clearance in the cell environment

A constant production and reduction of ROS occurs in the cell environment. This requires a cooperative system of antioxidants to function in ROS clearance, of which selenoproteins play a crucial role. (taken from Droge, 2002).

1.2.1 Incorporation mechanism of selenium into selenoproteins

Selenium is incorporated into proteins known as selenoproteins in form of Selenocysteine (SeCys) amino acid (Kryukov *et al.*, 2003). Insertion of the amino acid selenocysteine (Sec) is the key step in selenoprotein biosynthesis and this process requires a UGA codon in the coding region and the Selenocysteine Insertion Sequence (SECIS) in the 3' untranslated region (UTR) which are present in the mRNA of all selenoproteins (Kryukov *et al.*, 2003; Brigelius-Flohe, 2008). Three different triplicate nucleotides (UAG, UAA and UGA) function as a stop signal, which stops the synthesis of polypeptide during translation. The biosynthesis of protein is not terminated at UGA during the coding of selenoproteins because the UGA is translated into amino acid SeCys (Bellinger *et al.*, 2009). A stem-loop structure (SECIS) situated within the 3'untranslated region (3'UTR) of the selenoprotein mRNA recognizes UGA as the codon for the SeCys but not as a stop codon (Kryukov *et al.*, 2003). In the selenoproteins of eukaryotes, SECIS share a conserved stem-loop structure with low similarity between sequence of the selenoprotein mRNA within the 3'UTR (Berry, 2005). A typical predicted SECIS structure of human GPx4 (Villette *et al.*, 2002) is given in Figure 2. UGA codon interacts with SECIS to recruit additional proteins which include SeCys-synthesizing tRNA^{sec} (Bosl *et al.*, 1997), an elongation factor EFsec and a binding protein known as SECIS-binding protein 2 (SBP2) (Copeland *et al.*, 2000).

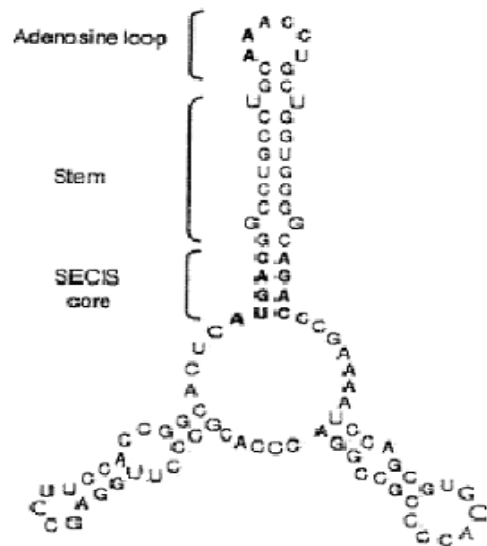
Typical machinery required for SECIS incorporation is illustrated in Figure 2. Selenium incorporation into selenoproteins is crucial as shown by the tRNA^{sec} knock-out mouse exhibiting a lethal phenotype of prenatal death (Bosl *et al.*, 1997).

The importance of SECIS and 3'UTR in Se incorporation is shown by the observation that mutations or genetic polymorphisms in regions of the selenoprotein gene corresponding to the 3'UTR affects the expression of the selenoproteins concerned (Hesketh, 2008). Indeed, various polymorphisms with functional implications in the 3'UTR of selenoprotein genes have been reported: *GPX4*: 718T/C close to SECIS (Meplan *et al.*, 2007) *SEP15*: 811 C/T and 1125 G/A (Villette *et al.*, 2002; Jablonka *et al.*, 2008) and *SEL P*: r25191G/A (Kumaraswamy *et al.*, 2000).

The polymorphism 718T/C in the 3'UTR of GPx4 gene has been linked with increase risk of colorectal cancer (Bemano *et al.*, 2007; Meplan *et al.*, 2010) and alteration in 5-Lipoxygenase metabolism pathway (Villette *et al.*, 2002). The SEP15 polymorphism 1125 G/A has been linked with increased susceptibility to lung cancer (Jablonska *et al.*, 2008). Additionally, early onset myopathy has been associated with mutations in SEPNI gene which encodes selenoprotein N (Maiti *et al.*, 2009), a regulator of calcium homeostasis in muscle (Arbogast & Ferreiro, 2010).

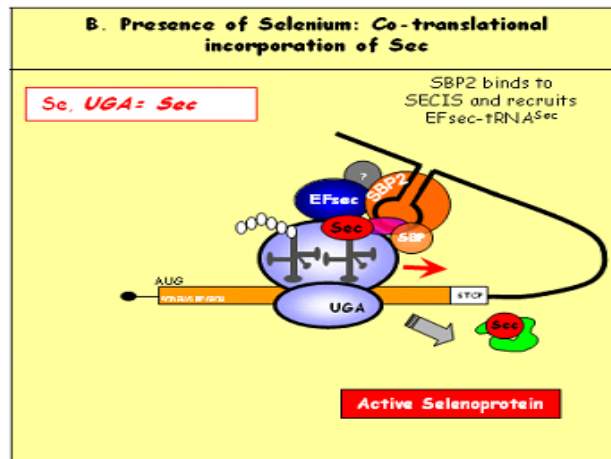
Despite the shared stem-loop structure amongst selenoproteins, the variability in their SECIS mRNA sequence has influenced their ability to incorporate Se (Kryukov *et al.*,

2003; Berry, 2005). Such difference influences the response of selenoproteins to change in Se status resulting in differences in selenoprotein hierarchy with some being synthesized in higher priority and others in relatively lower priority particularly at low Se supply (Bermano *et al.*, 1996; Brigelius-Flohe, 1999). Considering this effect, reduction in Se supply has been reported to lower the synthesis of some selenoproteins more than others e.g. GPx1, SelW and SelH (Pagmantidis *et al.*, 2005; Sunde *et al.*, 2009). The order of GPxs hierarchy during low Se status are GPx2>GPx4>GPx1=GPx3.



SECIS stem-loop structure
(Human GPx4 mRNA)

(A)



Incorporation of SeCys
(Selenoprotein assembly)

(B)

Figure 2 SECIS stem-loop structure and SeCys incorporation during selenoprotein biosynthesis.

Interaction between SECIS (a conserved stem-loop structure in the 3' untranslated region of all selenoprotein mRNA) and UGA is required for appropriate incorporation of Se into selenoproteins. (A) SECIS structure of human GPx4 mRNA and (B) Recruitment of additional factors such as EFsec, SBP2 and tRNA^{Sec} which allows SeCys incorporation into selenoprotein sequence by SECIS and UGA codon encoding SeCys. (Taken from (Villette et al., 2002 and Meplan et al., 2006)).

1.3 Glutathione Peroxidases (GPxs)

The glutathione peroxidase family comprises six members (GPx1-7), which are evolutionary conserved, particularly in their catalytic sequences. GPx1 to GPx4 and GPx6 incorporate SeCys during translation and require Se incorporation for their synthesis whereas GPx5 uses cysteine (Brigelius-Flohe, 1999); information about GPx7 biosynthesis is yet to be elucidated. One of the characteristics of GPxs is their ability to catalyze ROS at the expense of glutathione (GSH) which results in the reduction of ROS and a balance between ROS production and clearance (redox). Selenoprotein glutathione peroxidases vary in their ability to incorporate Se (i.e. in the hierarchy of Se incorporation), in tissue distribution and cellular localization, and in their catalytic target to oxidative targets (Brigelius-Flohe, 1999). GPx1 and GPx4 are the most widely studied glutathione peroxidases and their biological functions are described below:

1.3.1 GPx1: The ubiquitously expressed GPx1 (Moghadaszadeh & Beggs, 2006) is localized in cell cytoplasm and its expression has been reported to exhibit a high sensitivity to low Se supply. GPx1 mRNA is reduced to 60% in Caco-2 cells depleted of Se (Pagmantidis *et al.*, 2005) and in mice fed with Se deficient diet (Sunde *et al.*, 2009; Bermanno *et al* 1995). The major function of GPx1 is to detoxify hydrogen peroxide but may also be involved in the clearance of water soluble hydroperoxides (Grossmann & Wendel, 1983; Brigelius-Flohe, 2006). Mice lacking GPx1 (GPx1^{-/-}) did not exhibit any

apparent abnormalities during embryonic development (Ho *et al.*, 1997), but showed high susceptibility to coxsackievirus B3 infection (Beck *et al.*, 1998). This finding emulates the aetiology of Keshan diseases where reduced Se intake leads to high vulnerability to coxsackievirus infection. Additionally, GPx1 knockout mice (GPx1^{-/-}) exhibited increased sensitivity to secondary necrosis and liver injury (Bajt *et al.*, 2002), to heart injury induced by doxorubicin (Gao *et al.*, 2008), to brain ischemia reperfusion injury (Crack *et al.*, 2006) and increased sensitivity to insulin induced glucose uptake in muscle cells (Loh *et al.*, 2009). The lack of antioxidant protection offered by GPx1 has been implicated with reduced cell tolerance to oxidative stress and apoptosis (Crack *et al.*, 2006; Loh *et al.*, 2009).

1.3.2 GPx2: GPx2 is a gastrointestinal GPx, known to be localized in the cytoplasm and expressed in the liver and gastrointestinal epithelium (Chu *et al.*, 1993). GPx2 specifically reduce hydrogen peroxide in the same manner as GPx1 (Brigelius-Flohe, 1999). As observed in mice fed a Se depleted diet, GPx2 is highest in the Se incorporation hierarchy in tissues where it is expressed and as a result GPx2 expression is barely affected by Se depletion (Bermano *et al.*, 1995; Sunde *et al.*, 2009; Kipp *et al.*, 2009). Furthermore, a non-significant increase in GPx2 mRNA expression in cells following Se supplementation has been reported (Pagmantidis *et al.*, 2005). As a selenoprotein which is specifically expressed in the intestinal epithelium, GPx2 has been studied in combination (double knockout model) with GPx1. Mice lacking both GPx1

(GPx1^{-/-}) and GPx2 (GPx2^{-/-}) showed increased sensitivity to challenges by microflora, resulting in colonic inflammation (Esworthy et al., 2003). Knockout mice of both GPx1 and GPx2 exhibited increased susceptibility to gastrointestinal cancer probably as a result of reoccurring of colitis compared to normal littermates (Lee *et al.*, 2006). The double knockout mice also exhibited increased malignancy (tumor growth) mediated by Cyclooxygenase (COX) (Banning *et al.*, 2008) and aberrant DNA methylation (Hahn *et al.*, 2008). The protective function of GPx2 has been reported in the intestinal epithelium and deficiency in both GPx1 and GPx2 resulting in reduced tolerance to oxidative challenges (reviewed by Brigelius-Flohe, 1999). Mice lacking GPx4 exhibited increased inflammation and tumor numbers (Krehl *et al.*, 2012). This finding suggests that GPx4 inhibit inflammation-mediated tumorigenesis (Krehl *et al.*, 2012). It has been shown that GPx2 promoter is activated by the Wnt pathway and knock out of B-catenin (a subunit of the cadherin protein complex, which, acts as an intracellular signal transducer in the Wnt signaling pathway) in isolated colonic crypt reduced GPx2 expression (Kipp *et al.*, 2012). This finding suggests GPx2 as a novel Wnt target, highlighting its potential role(s) in proliferation, apoptosis and cancer development (Kipp *et al.*, 2012).

1.3.3 GPx3: GPx3 is also known as plasma GPx, is secreted from the kidney and has been reported to be present in blood circulation (Avisar *et al.*, 1994). The *GPX3* gene encodes one transcript and is low in the Se incorporation hierarchy. One of its major

functions is to reduce soluble hydroperoxides in extracellular environment (Bjornstedt *et al.*, 1994).

1.3.4 GPx4: GPx4 is also known as phospholipid hydroperoxide GPx. GPx4 is ubiquitously expressed in all tissues including the gastrointestinal tract (Imai *et al.*, 1995). GPx4 is located in the mitochondria and cytoplasm, and is present in the nucleus in some cell types e.g. testes cells (Imai & Nakagawa, 2003). GPx4 is an unusual selenoprotein with broad substrate specificity and has a protective role in various cellular compartments. GPx4 is expressed ubiquitously in all tissues and cells with the highest amount being in the testis (Baek *et al.*, 2007).

The expression of GPx4 has been shown to be reduced (by ~ 20%) in low Se conditions (Bermano *et al.*, 1996; Pagmantidis *et al.*, 2005; Kipp *et al.*, 2009) and increased Se has been shown to increase GPx4 activity (Bao *et al.*, 1996). The major function of GPx4 is the reduction of fatty acid hydroperoxides and removal of phospholipid hydroperoxides. A wide range of oxidative targets including phospholipid hydroperoxide (Ursini *et al.*, 1985), reducing phospholipid hydroperoxide to phospholipid hydroxide (Bao *et al.*, 1996), reduction of thymine hydroperoxides (Bao *et al.*, 1997) and lipid hydroperoxide derived from cholesteryl esters and cholesterol (Thomas *et al.*, 1990) can be catalyzed by GPx4. Additionally, GPx4 can use substrates other than glutathione for its catalytic function (Aumann *et al.*, 1997).

The *GPX4* gene produces three different transcript variants (Figure 3), namely: cytosolic GPx4 (cGPx4), mitochondrial GPx4 (mGPx4) and nuclear GPx4 (nGPx4). Cytosolic GPx4 is located in the cytoplasm (Maiorino *et al.*, 1991) and mitochondrial and nuclear GPx4 contain additional leader sequences required for mitochondrial and nuclear translocation (Arai *et al.*, 1996; Pfeifer *et al.*, 2001). Nuclear GPx4 has been reported to be present only in the testis and to play an important role in sperm maturation.

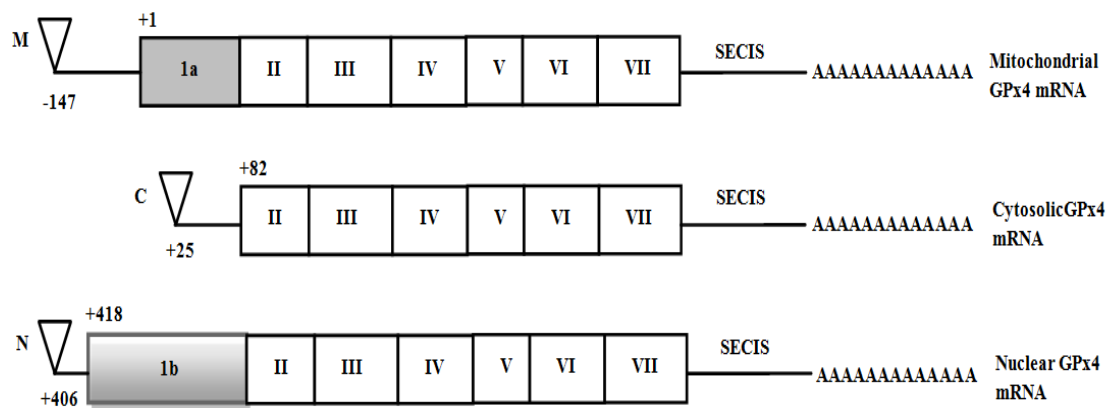


Figure 3 Structure of the GPx4 gene, and the three types isoforms of GPx4 mRNA.

Seven exons of human GPx4 gene containing exons of the three types of GPx4 mRNA. Exon 1a (gray box) contains the translational first start codon ATG (+1) for mGPx4 and the second ATG (+82) for cGPx4. Exon 1b (shaded box) contains the start codon ATG (+418) for nGPx4. Three transcriptional start codon (ATG) are shown on the reverted open triangles; the transcriptional start site for mGPx4 is shown in position -147 (M), cGPx4 at position +25 (C) and nGPx4 at position +406 (N). TGA in exon III encodes selenocysteine and TAG in exon VII encodes the stop codon. SECIS is the selenocysteine insertion sequence. (Taken from Imai, 2010).

1.4 Proposed roles of GPx4

GPx4 has been implicated in the repression of oxidative radicals particularly in lipid environments and in protecting mitochondria from oxidative damage (Arai *et al.*, 1996; Normura *et al.*, 1999; Liang *et al.*, 2007). The biological role of GPx4 has been investigated using mouse knockout models. Lack of the *GPX4* gene is embryonically lethal with the mice dying at prenatal stage with dysfunctional embryonic development (Imai *et al.*, 2003). Failure to restructure cavity development during embryogenesis suggests the importance of GPx4 in apoptosis (Imai *et al.*, 2003). GPx4 haploid insufficient mice (GPx4^{+/-}) with GPx4 mRNA, protein and activity lowered to approximately 50% exhibited increased sensitivity to oxidative challenges following exposure to γ -irradiation and reduced survival rate compared with normal littermates (Yant *et al.*, 2003). Additionally, cultured embryonic fibroblasts from mice lacking a copy of *GPX4* (GPx^{+/-}) gene showed increased sensitivity to treatment with paraquat, t-butyl hydroperoxide and hydrogen peroxide, which led to increased membrane peroxidation and activation of caspase-3 dependent cell death (Ran *et al.*, 2003). On the other hand, GPx4 overexpression in mice liver presented resistance to oxidative challenges such as diquat and fibroblasts derived from these mice exhibited resistance following treatment with diquat and t-butyl hydroperoxide (Ran *et al.*, 2004). On the

basis of this evidence, GPx4 appears to be crucial for cell protection from oxidative stress.

Compared to other GPx isoenzymes, GPx4 has a unique capacity to repress 12/15-lipoxygenase-derived lipid peroxidation and reduce phospholipid hydroperoxides (Seiler *et al.*, 2008). GPx4 has been reported to play a role in preventing mutagenesis through its ability to repair oxidatively damaged DNA and through reduction of thymine hydroperoxide (Bao *et al.*, 1997). Murine embryonic fibroblast cells from GPx4^{+/-} mice exhibited increased levels of mutagenic DNA adduct and increased sensitivity to oxidative stress following exposure to oxidizing agent t-butyl hydroperoxide (t-BOOH) (Ran *et al.*, 2003). Identification of a single nucleotide polymorphism (SNP) of human GPx4 (718T/C) has been reported (Bermano *et al.*, 2007) and this SNP has been linked with increased risk of colorectal cancer and colorectal adenoma (Peters *et al.*, 2008; Meplan *et al.*, 2010). GPx4 mRNA transcript is one of the most abundant selenoprotein mRNAs in the murine intestine (Hoffmann *et al.*, 2007). GPx4 mRNA levels are relatively resistant to Se depletion in Caco-2 cells (Wingler *et al.*, 1999). Contrary to this finding, reduced Se was reported to down-regulate GPx1 mRNA and up-regulate GPx2 mRNA respectively. During limited Se availability, GPx4 maintains a relatively stable mRNA level indicating the high ranking of GPx4 in the selenoprotein hierarchy (Brigelius-Flohe, 2006).

GPx4 is the only GPx with the ability to regulate lipid hydroperoxides and the metabolism of arachidonic acid. It is crucial in the detoxification of a broad spectrum of hydroperoxide substrates such as complex membrane lipid hydroperoxides as well as thymine hydroperoxide (Bao *et al.*, 1997; Conrad *et al.*, 2007; Yoo *et al.*, 2010). Indeed, GPx4 has been reported to possess the highest enzymatic activity (compared to other hydroperoxide reducing enzymes tested) against thymine hydroperoxide as a substrate *in vitro* (Bao *et al.*, 1997). This finding led to a hypothesis suggesting that GPx4 may protect DNA integrity against DNA damage-induced lipid peroxidation such as etheno-nucleotide adducts and repair of oxidative DNA damage caused by DNA adduct such as thymine hydroperoxide (Bao *et al.*, 1997; Bartsch *et al.*, 2002).

To conclude, glutathione peroxidases (GPxs) are important antioxidant selenoproteins and their fundamental functions appear to be to reduce reactive oxygen species, reactive nitrogen species and to protect cells from lipid peroxidation. However, GPx4 has been suggested to have additional biological role. A study of mice with reduced GPx4 (GPx4^{+/-}) exposed to diquat showed activation of the intrinsic apoptotic pathway and damage to mitochondrial inner membrane (Liang *et al.*, 2009). Transgenic mice overexpressing GPx4 exposed to diquat presented resistance to oxidative challenge through reduced mitochondrial ROS, increased mitochondrial membrane potential and ATP compared to wild type controls (Liang *et al.*, 2007). These data suggest the importance of GPx4 for functional mitochondria and appropriate regulation of apoptosis.

1.4.1 Effects of GPx4 on eicosanoid biosynthesis

GPx4 has been suggested to repress leukotriene (LT) and prostaglandin (PG) biosynthesis through its mediation with cyclooxygenase (COX) and lipoxygenase (LOX) catalyzed arachidonic acid metabolic pathways, known for their sensitivity to redox signaling, (Brigelius-Flohe, 1999, Imai & Nakagawa, 2003). Leukotrienes are fatty acid signaling molecules which are products of 5-LOX. Their formation involves conversion of arachidonic acid to 5-hydroperoxyeicosatetraenoic (5-HPETE) by 5-LOX and a further dehydration of 5-HPETE is then required to form LT (Hyde & Missailidis, 2009) (Figure 3). The oxidized 5-HPETE, through an autonomous feedback cycle, activates 5-LOX (Rouzer & Samuelsson, 1986). GPx4 has been suggested to reduce 5-HPETE to 5-HETE, which is then proposed to block the activation feedback of 5-LOX pathway (Imai *et al.*, 1998; Straif *et al.*, 2000) (Figure 5).

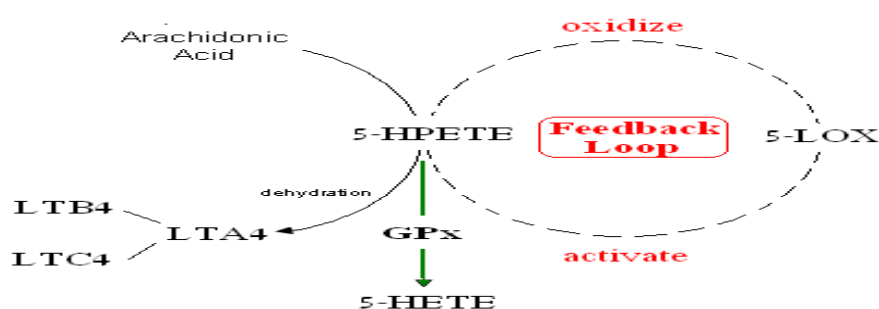


Figure 4. Repression of 5-LOX activation and Leukotriene production by GPx. Leukotriene biosynthesis requires metabolism of arachidonic acid to 5-HPETE by 5-LOX. 5-HPETE can activate 5-LOX through a positive feedback cycle. A reduction of 5-HPETE into 5-HETE results to a break in the 5-LOX feedback cycle which inhibits leukotriene production and this reduction can be carried out by both GPx1 and GPx4.

Likewise, GPx4 has been implicated in the regulation of 12-LOX, 15-LOXS and COX pathways, and the repression of their oxidised intermediary products respectively (Sakamoto *et al.*, 2000; Chen *et al.*, 2003; Heirman *et al.*, 2006). A number of investigations have identified these links and are listed in Table 2.

Cell Type	LOX/COX Pathway	Inhibitor	Enhancer	Key Observations	References
Rat Basophilic leukemia cell line (RBL-2H3)	5-LOX	GPx4 ↑	5-HPETE; 12-HPETE; DEM(GPx4 inhibitor)	1. GPx4 inhibits 5-LOX activity by reducing 5-HPETE.	(Imai et al., 1998)
Polymononuclear cells line (PMNs)	5-LOX	GPx4 ↑	n.a.	1. GPx4 is up-regulated by GRO but not TNF α or IL1 β . 2. GPx4 inhibits 5-LOX	(Hattori et al., 2005)
Human Quamous Carcinoma (A431)	12-LOX; 5-LOX; COX;	GPx4	n.a.	1. GPx4 inhibits of 12-LOX, 5-LOX and COX	(Huang et al., 1998)
Human Quamous Carcinoma (A431)	5-LOX; 12-LOX; 15-LOX; COX1 and COX2	GPx4	Exogenous oxidative stress	1. 12- and 15-LOX and COX-2 are 10 times sensitive to GPx4 than 5-LOX and COX-1 2. Increase levels of GPx4 inhibits 12-LOX.	(Huang et al., 1999)
Human Quamous Carcinoma (A431)	COX; 12-LOX	n.a.	GPx4 ↓ (antisense).	1. Inhibition of GPx4 enhances the metabolic activity of 12LOX and COX.	(Chen et al., 2000)
Monocyte	5-LOX	GPx1	n.a.	At low thiol concentration, GPx1 but not GPx4 is involved in inhibition of 5-LOX in monocytes	(Straif et al., 2000)
Rat insulin-secreting cell line (RINm5f)	12-LOX	GPx4	n.a.	Treatment with Hepoxilin A3 stimulates GPx4 expression which in turn, represses 12-LOX to protect the cells.	(Zafiriou et al., 2007)
Fibrosarcoma cell (L929) and melanoma cell (B16BL6)	COX-2	GPx4 ↑	n.a.	GPx4 represses COX-2 and PGE2 production, which results in impediment of tumor growth and malignancy.	(Heirman et al., 2006)
Human colon adenocarcinoma grade II (HT29)	COX-2	GPx2	GPx2 siRNA	GPx2 represses COX-2 and GPx2 knockdown enhances tumor migration and invasion.	(Banning et al., 2008)
Human colon adenocarcinoma grade II (HT29)	COX-2	n.a.	GPx2 siRNA	GPx2 knockdown results in enhanced expression of COX-2 and following IL1 stimulation, enhanced synthesis of PGE2.	(Banning et al., 2008)
Mice and mouse neurons	12-LOX; 15-LOX	GPx4 PD146176	GPx4 -/-	GPx4 represses 12/15-LOX and GPx4 -/- activates 12/15-LOX and AIF-mediated apoptosis	(Seiler et al., 2008)
Human platelets	12-LOX	n.a.	Iodoacetate (GPx4 inhibitor)	1. GPx4 was found in platelets & megakaryocytes. 2. GPx4 blocks the 12-LOX pathway and the generation of hepoxilins in platelets.	(Sutherland et al., 2001)
Human Quamous Carcinoma (A431)	12-LOX; COX	GPx4 ↑	n.a.	1. GPx4 reduces the metabolism of 12-LOX and COX to form eicosanoids.	(Chen et al., 2002)
Human Quamous Carcinoma (A431)	12-LOX; COX1	n.a.	GPx4 ↓ (antisense).	1. GPx4 depletion by antisense enhances 12-HETE and COX1 activity.	(Chen et al., 2003)
Submitochondrial particles from beef heart mitochondria and Human LDL	15-LOX	GPx4	n.a.	1. GPx4 represses 15-LOX metabolism on mitochondria membrane and lipoprotein.	(Schnurr et al., 1996)
Rat Basophilic leukemia cell line (RBL-2H3)	COX2	GPx4 ↑	Exogenous oxidative stress	1. GPx4 represses COX2 to convert PGH2 to PGD2 in nucleus and endoplasmic reticulum.	(Sakamoto et al., 2000)
Colonic adenocarcinoma cell line (HT29 cl.19A)	COX2	n.a.	GPx4 ↑	1. GPx4 enhances COX2 metabolism and activates COX2 mRNA expression.	(Barriere et al., 2004)

Table 2. Summary of observed effects of GPxs on eicosanoid biosynthesis through LOX/COX pathways.

Prostaglandins (PG) and Leukotrienes (LT) mediate biological processes such as contraction of smooth muscle, vasodilation and pain sensing using prostaglandin E2 (PGE2) and prostaglandin 12 (PG12) (Henderson, 1994). LT also play a role in leukocyte adhesion using leukotriene B4 (LTB4) and has been associated with carcinogenic events, including cell differentiation and apoptosis (Shureiqi *et al.*, 2005; Eisinger *et al.*, 2007; Sordillo *et al.*, 2008). *GPX4* inhibits 5-LOX activity by reducing 5-HPETE (Imai *et al.* 1998). Metabolic activities of 12/LOX and COX are enhanced as a result of *GPX4* inhibition (Chen *et al.*, 2000) and treatment with Hepoxilin A3 stimulates *GPX4* expression, which represses 12-LOX and protects Rat insulin-secreting cell line from lipid damage and ROS (Zafiriou *et al.*, 2007).

Platelet-type 12-LOX has been identified as an inducer of inflammation in endothelial cells, human monocytes and prostate cancer cells (Laniado-Schwartzman *et al.*, 1994; Huang *et al.*, 2004; Kandouz *et al.*, 2003). 12-LOX, COX-2 and 5-LOX have been associated with eicosanoid biosynthesis and increased oxidised lipid in guineas pigs (Chopra *et al.*, 1992), human neuronal cells (Kaltschmidt *et al.*, 2002) and human erythroleukemia cells (Arakawa *et al.*, 1995). Reduced *GPX4* in mice cells and mice neuron have been linked with activated 12/15 LOX activity (Seiler *et al.*, 2008).

1.4.2 Mitochondrial regulation by selenoprotein GPx4

Overexpression studies suggest GPx4 is important in mitochondrial function. A study of cardiac function following ischemia reperfusion in transgenic mice overexpressing the mitochondria-specific form of GPx4 (mPHGPx) showed reduced lipid peroxidation and increased mitochondrial electron transport chain complex I, III and IV activities compared to littermate controls (Babkowski *et al.*, 2008). Overexpression of GPx4 protected cultured lung fibroblasts from phosphatidylcholine hydroperoxide (PCOOH)-induced loss of mitochondrial membrane potential and blocked apoptosis induced by different apoptosis agents (Garry *et al.*, 2008). Transgenic mice overexpressing GPx4 exposed to diquat showed resistance to loss of mitochondrial membrane potential and increased ATP production compared to wild type, suggesting the relevance of GPx4 in maintaining mitochondrial function and stability (Liang *et al.*, 2007).

1.4.3 GPx4 Protection against cell death

One of the major known functions of GPx4 is to protect cell membranes against oxidative damage particularly since GPx4 has the ability to metabolize phospholipid hydroperoxides in membranes. The importance of GPx4 in other aspects of regulation of cell function became apparent following overexpression of GPx4 in various cell lines. Rat basophil leukemia 2H3 (RBL2H3) cells overexpressing cytosolic-GPx4 exhibited increased resistance to apoptosis induced by free radical initiators and fatty acid hydroperoxides (Imai *et al.*, 1996). The guinea-pig cell line 104C1 overexpressing GPx4 showed increased resistance to oxidative injury caused by exogenous phosphatidylcholine hydroperoxide (Yagi *et al.*, 1996). Overexpression of mitochondrial GPx4 (mGPx4) in RBL2H3 cells protected the cells from cell death induced by 2-deoxyglucose (2-DG), etoposide, staurosporine, UV radiation, cycloheximide, and actinomycin D, but not from cell-death induced by either Fas-specific antibodies or A23187 (a Ca²⁺ ionophore) (Nomura *et al.*, 1999). Cells overexpressing cytosolic-GPx4 were not protected from apoptosis following exposure to these stimuli (Nomura *et al.*, 1999). GPx4 overexpression in rabbit aortic smooth muscle cells cultured with sodium selenite blocked apoptosis induced by linoleic acid hydroperoxide (Brigelius-Flohe *et al.*, 2000). Overexpression of mitochondrial GPx4 protected cells from necrotic cell death-induced chemical hypoxia following treatment with mitochondrial respiratory

inhibitors rotenone and potassium cyanide (KCN) (Arai *et al.*, 1999). mGPx4 blocked hydroperoxide generation, loss of mitochondrial membrane potential and plasma membrane potential induced by KCN (Arai *et al.*, 1999). Breast tumor epithelial cells (COH-BR1) overexpressing mGPx4 were protected from cell death induction following exposure to photochemically generated cholesterol hydroperoxide (Hurst *et al.*, 2001). Findings from these studies suggest that overexpression of mGPx4 may prevent alterations in mitochondrial functions such as ATP synthesis and apoptosis through repressing intracellular hydroperoxides.

RBL2H3 cells overexpressing mGPx4 are more resistant to apoptosis induced as a result of direct damage to mitochondria and exposure to t-butylhydroperoxide, H₂O₂ and 15-hydroperoxyeicosatetraenoic acid than cells overexpressing cGPx4 (Arai *et al.*, 1999). Human breast cancer cell line (MCF-7) overexpressing mGPx4 showed increased resistance to lipid peroxide induced-singlet oxygen and photosensitizer induced cell death, whereas cells overexpressing cGPx4 did not (Wang *et al.*, 2001). Increased resistance to mitochondrial abnormalities in mouse NSC-34 motor neuron-like cells was observed following overexpression of both mGPx4 and manganese superoxide dismutase (Mn-SOD) (Liu *et al.*, 2002). Since hydroperoxides in the mitochondria ultimately play a crucial role as apoptotic signalling molecules, this overexpression study of mGPx4 and Mn-SOD suggest that generation of superoxide, lipid hydroperoxide and hydrogen peroxide may activate the mitochondrial apoptosis

pathway (Figure 4), and that mitochondrial antioxidant enzymes may effectively modulate apoptotic signalling. The findings from these studies indicate that GPx4 may have a primary role in protecting cells from mitochondrial oxidative stress. Low *GPX4* expression has been associated with increased levels of 12/15 lipoxygenase-derived lipid hydroperoxides and increased Apoptosis inducing factor (AIF)-induced apoptosis (Villette *et al.*, 2002; Seiler *et al.*, 2008; Conrad, 2009; Conrad *et al.*, 2010).

1.4.4 The role of mitochondrial GPx4 in apoptosis

Electrons are shuttled from cytochrome c reductase to cytochrome c oxidase by cytochrome c (cyt.c), a mitochondrial peripheral membrane protein functioning within the inner mitochondrial membrane of the mitochondrial respiratory chain. Cytochrome.c release from the mitochondria, into the cytoplasm, is a crucial step in the activation of the mitochondrial apoptotic pathway (Kroemer *et al.*, 1998; Skulachev, 1998). Following the release of cyt.c from the mitochondria, pro-apoptotic proteins such as caspase-9, and Apaf-1 are activated and as a result may activate caspase-3 (Li *et al.*, 1997).

RBL2H3 cells overexpressing mGPx4 exhibited less hydroperoxides and showed increased resistance to the release of cyt.c, caspase-3 activation and 2-deoxyglucose (2-DG) induced cell death (Nomura *et al.*, 1999). The well characterized Bcl-2 and Bcl-xl

are anti-apoptotic proteins and their major function is to inhibit the release of cyt.c (Yang *et al.*, 1997). Mouse neuron-like cells overexpressing Mn-SOD and/or mGPx4 exhibited increased resistance to lipid peroxide-induced apoptosis and cyt.c release (Liu *et al.*, 2002), suggesting that generation of lipid hydroperoxide in the mitochondria may be crucial for activation of apoptotic signalling through the release of cyt.c, and that mGPx4 might be an important anti-apoptotic agent. The release of cyt.c from the mitochondria into the cytoplasm is an important process of apoptosis. Recently, mGPx4 has been reported to block the release of cyt.c from the mitochondria into the cytoplasm (Schneider *et al.*, 2009).

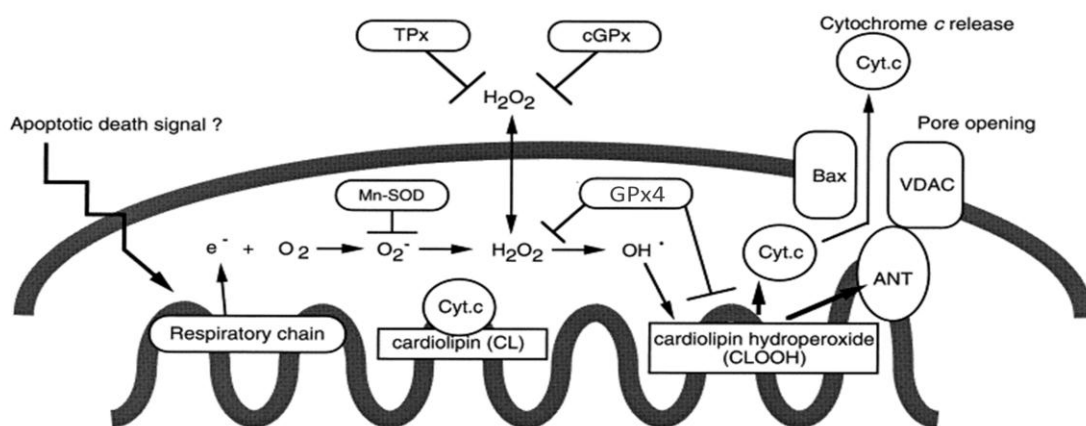


Figure 5. A hypothetical scheme illustrating the relationships of mitochondrial respiration, ROS, antioxidant enzymes and cyt. c release.

The release of cyt. c from the inner mitochondrial membrane is inhibited by mGPx4, resulting in reduction of cardiolipin hydroperoxide. Mitochondrial superoxide (O_2^-) and hydrogen peroxide (H_2O_2) generation has been reported in various apoptotic models. The figure illustrates possible mechanisms for this. A reaction of H_2O_2 with iron (Fe^{2+}) generates highly reactive hydroxyl radical (HO^\cdot) and the production of lipid hydroperoxide and lipid radicals in the mitochondrial membrane. The disassociation of cyt.c from mitochondrial inner membrane, the loss of Adenine nucleotide translocator (ANT) activity, the release of cyt.c, the loss of mitochondrial respiratory activity and mitochondrial membrane potential are affected by the production of cardiolipin in the mitochondria via cardiolipin hydroperoxide (CLOOH) cascade. mGPx4 overexpression could inhibit the release of cyt .c through the elimination of cardiolipin-induced peroxidation and activation of mitochondrial apoptosis. ANT = Adenine nucleotide translocator; CL = Cardiolipin; CLOOH = Cardiolipin hydroperoxide; Cyt. c = Cytochrome c; PHGPx = GPx4; cGPx = cytosolic glutathione peroxidase; Mn-SOD: Mn-superoxide dismutase; TPx = Thioredoxin peroxidase; VDAC: = Voltage dependent anion channel (taken from Imai & Nagakawa, 2003).

1.4.5 Regulation of spermatogenesis and sperm function by GPx4

Jones and Mann (1973), were the first to associate male infertility to increased susceptibility to oxidative stress in human sperm. A high concentration of polyunsaturated fatty acids (PUFA), including docosahexaenoic acid, is found in human sperm (Kim & Parthasarathy, 1998; Aitken, 1999). Sperm are vulnerable to peroxides such as oxygen radicals. Generation of ROS and lipid peroxidation of sperm can result in sperm motility defects (Alvarez & Storey, 1982), sperm midpiece abnormalities, and impaired fusion of sperm and oocyte (Aitken *et al.*, 1989) each of which can inhibit fertilization (Rao *et al.*, 1989).

During mitochondrial respiration, the process which enables ATP synthesis for sperm motility, ROS are generated in the sperm mitochondria (Bourgeron, 2000). Mitochondrial abnormalities, including those associated with mitochondrial pathologies, have been associated with loss of sperm motility and infertility in male (Folgero *et al.*, 1993). Various antioxidant enzymes in the spermatozoon and seminal plasma provide protection to sperm. GPx4 has been identified in midpieces and sperm heads in ejaculated human sperm, and epididymal rat sperm (Godeas *et al.*, 1996; Godeas *et al.*, 1997; Ursini *et al.*, 1999; Imai *et al.*, 2001). Nuclear GPx4 (nGPx4), has also been reported to be present in human sperm and functions as a hydrogen peroxide scavenger (Imai *et al.*, 2001).

It has been shown in rat epididymal spermatozoa that GPx4 plays an important role in protecting sperm from oxidative damage (Weir & Robaire, 2007). Selenium has been found to be important for male fertility of rodents (Wallace *et al.*, 1983a). Severe deficiency of Se reduced sperm count and motility (Wallace *et al.*, 1983a, b). Sperm from Se-deficient rats exhibited abnormal mitochondrial morphology and abnormal midpiece formation, which resulted from increased oxidative damage affecting sperm, sperm production (Wallace *et al.*, 1983a, b). Complete absence of mitochondrial GPx4 affects early stages of spermatogenesis (Wallace *et al.*, 1983a, b). Seven out of 73 infertile men showed reduced level of GPx4 expression in their sperm following an immunoblotting study using anti-GPx4 antibodies whereas the expression of GPx4 in the sperm of 31 normal volunteers was unaffected (Imai *et al.*, 2001). These seven subjects were classified as belonging to the group with oligo-asthenozoospermia which is characterized by reduced sperm motility and number. These results suggest that severe impairment of fertility may be due to reduced GPx4 expression and this is supported by a study which identified reduced mitochondrial membrane potential in sperm with reduced GPx4 expression compared with normal sperm (Imai *et al.*, 2001). It is proposed that the spermatozoa are defective due to dysfunctional mitochondria and that reduced expression of mitochondrial GPx4 in sperm is a contributing factor to infertility since reduced expression of GPx4 has been identified in ejaculated sperm from infertile males (Imai *et al.*, 2001).

1.5 Aims and Objectives

Generation of ROS results in oxidative stress and oxidative stress has been linked to increased apoptosis (Tarin, 1996; Liu & Keefe, 2000; Liu *et al.*, 2000; Fissore *et al.*, 2002). Cells require a precise control of cellular redox homeostasis that enables regular cell function (Castagne *et al.*, 1999). Cellular redox homeostasis has been widely shown to affect various cell functions including ATP synthesis (Noji & Yoshida, 2001), cell death, cell proliferation, differentiation and maturation (Salas-Vidal *et al.*, 1998), and has also been shown to be involved in the regulation of gene expression (Ufer *et al.*, 2010). Modification of biological molecules and biological functions by ROS results in deleterious outcome and cellular dysfunction, which can induce cell death (Chen *et al.*, 1999; Hansen, 2006).

The selenoprotein GPx4 has been reported to have regulatory effects on oxidative stress, (Section 1.3.4) eicosanoid biosynthesis (Section 1.4.1), mitochondria regulation (Section 1.4.2) and apoptosis (Sections 1.4.3 & 1.4.4), but to date little is known about the precise role of GPx4 in intestinal cells and how alterations of GPx4 activity affect intestinal cell function. For this reason, investigations into the role of GPx4 in human gut epithelial cells in response to GPx4 silencing was carried out and this thesis describes studies to investigate GPx4 function by silencing its expression using siRNA in Caco-2 cells.

The aim was to use gene microarray approach to study the function of GPx4 in intestinal epithelial cells using siRNA to knock-down GPx4 expression. The data obtained suggest the major effects were on mitochondrial function and therefore the subsequent objectives were:

- To study the effects of GPx4 knock-down on global gene expression in human intestinal epithelial cell line (Caco-2 cells).
- To use real-time PCR to study the effect of GPx4 knock-down on expression of genes encoding components of the respiratory complex I and IV in Caco-2 cells.
- To study the effect of GPx4 knock-down on functional markers of mitochondrial electron transport chain complexes I and IV in Caco-2 cells.
- To study the effect of GPx4 knock-down on oxidative stress and on overall mitochondrial function and integrity in Caco-2 cells.
- To study the relationship between GPx4 and mitochondria targeting-antioxidant Mitoquinone 10 (MitoQ₁₀).
- To study the effect of GPx4 knock-down on apoptosis in Caco-2 cells.

Chapter 2. Materials and methods

2.1 General

Glassware and microcentrifuges tubes were sterilized with ethanol where necessary and autoclaved at 121°C and 2100 mBar for at least 20 minutes. All solutions and buffers were sterilized by autoclaving at 121°C using a pressure thermostat for 20 minutes or where necessary by filtration using a 0.2 µm syringe filters (Whatman). Tissue culture experiments were undertaken in a sterile environment, employing good cell culture practice. Two hundred and fifty µl of Diethylpyrocarbonate (DEPC) was added to 500 ml distilled water to make up DEPC-treated water and this was mixed thoroughly and autoclaved at 121°C for 20 minutes. Unless otherwise stated, all DNA, RNA including (cDNA and PCR products) and associated buffers and solutions were diluted in DEPC-treated water, RNAase free water (Invitrogen), milli-Q water (MQH₂O) or deionised water (ddH₂O).

2.1.1 Culture of mammalian cells

Mammalian cell stocks were trypsinized and re-suspended at 3×10^6 cells/ml in 8ml of complete Dulbecco's modified Eagle medium (DMEM) plus additional 10% fetal calf serum and 10% DMSO. Aliquots of cell suspension were transferred into 1.8 ml cryovials and frozen in isopropanol at -80 °C. Following 24 h in isopropanol, cryovials were transferred to liquid nitrogen for storage.

2.1.2 Growth and maintenance

Human colon adenocarcinoma cell line (Caco-2 cells) were cultured routinely in DMEM medium (DMEM+GlutaMAX-1 containing pyruvate 4.5g/L D-Glucose (Gibco®) containing 1% (v/v) penicillin-streptomycin (P/S), 10% (v/v) fetal calf serum (FCS) in either 75 cm³ tissue culture flasks, 6 well plates or 96 well plates at 37 °C in an atmosphere of 5% CO₂.

Caco-2 cells were sub-cultured from a 75 cm³ flask once they had reached 80% confluence by discarding the medium, washing the confluent monolayer with 25 ml of sterile PBS (pH 7.4) and addition of 2ml trypsin (10 X Solution Trypsin-EDTA; Sigma). Cells were incubated at 37°C for 5 minutes, collected from the culture dish into a clean 25 ml universal tube, centrifuged at 1,500 x g for 5 minutes and the supernatant was discarded. Cells were re-suspended in 10 ml of medium, 1 ml of cell suspension was transferred into a new 75 cm³ flask, 15 ml of medium was added and cells grown at 37 °C. The composition of the cell culture medium is shown in Appendix C

2.2 Transient transfection of human intestinal epithelial cells (Caco-2) with small interfering RNA (siRNA).

Small interfering RNA (siRNA) can be delivered into eukaryotic cells through transient transfection using a cationic lipid transfection agent. siRNA transfection experiments described in this study used Lipofectamine 2000™ (Invitrogen). siRNA is a small dimeric double-stranded RNA, generally consisting of a 21 nucleotide strand with a minimum of a 19 nucleotide complementary sequence and a

two nucleotide AA overhang. Experimental design of siRNA requires a 21 nucleotide sequence homologous to a target mRNA transcript. Following siRNA delivery into cells, the double stranded siRNA disassociates into two strands to bind to the target mRNA. The binding of the siRNA strand to the target mRNA recruits an enzymatic complex known as RNA-induced silencing complex (RISC) and mRNA degradation by the RISC complex (a process known as RNA interference). Therefore, target transcript of cells can be transiently degraded through the use of siRNA and can also be used to reduce gene expression for a period between 2-5 days.

Generally, gene expression is more efficiently reduced by siRNA after 2-3 days; mRNA level is generally reduced after 2 days and protein level after 3 days. In the present experiments, siRNAs were designed to reduce human *GPX4* gene expression both at mRNA and protein levels. Two commercially synthesized *GPX4*-specific siRNA were obtained (20nmol siRNA annealed with standard purity, AM16104 Ambion). Additionally, a negative control siRNA was designed by scrambling the sequence. Details of the siRNA, negative control siRNA and mRNA target sequences are given in Chapter 3 Section 3.2.1 and Section 3.2.2.

Human colonic epithelial cells were transiently transfected with siRNA by seeding 5×10^5 cells in a 6-well plate 24 h before transfection. Each well of the 6-well plate contained 2 ml cell growth medium containing DMEM + GlutaMAX-1 (4.5g/L D-Glucose and pyruvate, Gibco®, 10% (v/v) foetal calf serum (FCS) and 1% (v/v) penicillin-streptomycin (P/S). Cells were grown to 30-50% confluence. Prior to transfection with siRNA, the cell growth medium in each well was changed with new 2 ml of

modified growth medium containing DMEM + GlutaMAX-1 (Gibco®) supplemented with 5% (v/v) FCS and no P/S, as recommended in the manuals provided by the manufacturer (Ambion).

Additionally, 5 μ l of Lipofectamine 2000™ was added to 250 μ l Optimem in a universal tube, gently mixed and incubated at room temperature for 5 minutes. At the same time, 20 nmoles siRNA or scrambled control siRNA was diluted in 200 μ l RNase free H₂O to make a 100 μ M stock. The 100 μ M stock was further diluted 1:10 (i.e. 20 μ l of the 100 μ M stock into 80 μ l of RNase free H₂O) to make 20 μ M working stock. 2.5 and 5 μ l of the 20 μ M siRNA and scrambled control siRNA was added to 250 μ l Optimem, mixed gently by shaking and allowed to incubate at room temperature for 5 minutes. The Lipofectamine mix and the siRNA mix were added together, mixed gently by shaking and left at room temperature to incubate for 20 minutes. 500 μ l of the transfection mix was added into 6 well containing 2 ml reduced-serum medium in a drop-wise manner. The 2.5 ml medium containing either siRNA or negative control siRNA and Lipofectamin resulted to 20 nM or 40 nM siRNA concentrations. These concentrations are within the range of working concentration recommended by Ambion (10-100 nM).

Following treatment with GPX4 siRNA, cells were grown for 24 h and the medium was discarded and replaced with 2 ml serum-reduced medium (5% FCS) for additional 24 and 48 h before harvest. Volumes and amount of reagents required for transfections are listed in Table 3.

	96 well	6 well
Surface area (cm ²)	0.3	10
Cells	1.5x10 ⁴	5x10 ⁵
Lipofectamine™ 2000 (μl)	0.2	5
Opti-MEM® I Reduced Serum Medium (μl)	7.5 x 2	250 x 2
siRNA (nM)	20 & 40	20 & 40
siRNA (μl)	0.1 & 1.5	2.5 & 5
Plating volume	60 μl	2 ml
Total volume	75 μl	2.5 ml

Table 3. siRNA transfection.

Volumes and amounts of reagents required for transfection in different formats.

2.3 RNA lysate preparation using TRIzol® reagent

Total RNA was extracted from Caco-2 cells using a modification of the method of Chomczynski and Sacchi, (1987). Cells were washed twice with 1X PBS and further incubated with 0.5 ml (in each well of a 6-well plate) or 1ml (in a 75 cm³ flask) of TRIzol® (Invitrogen) for 5 minutes at room temperature. Using a cell scraper, cells were detached from the 6-well plate or flask. Each cell sample containing TRIzol was transferred into a sterile 1.5 ml microcentrifuge tube and 200 µl of chloroform (Sigma) was added. The mixture was vigorously mixed for 15 seconds and further incubated for 3 minutes at room temperature. TRIzol comprises of phenol and guanidinium isothiocyanate, guanidinium isothiocyanate is used for cell lysing and nucleoprotein complex disassociation whereas phenol and chloroform dissolves genomic DNA and RNA and allows the separation of these components.

Total RNA was retained in the upper clear aqueous phase following centrifugation of samples at 12,000 x g for 15 minutes at 4°C. A mixture of un-dissolved DNA and protein and cell debris was retained in the white-colour intermediate phase whereas the majority of DNA and protein remained in the pink lower organic phase. The upper aqueous phase was carefully transferred into another sterile 1.5 ml microcentrifuge tube.

Five hundred µl of isopropanol (Sigma) was added into the upper aqueous phase solution (~ 200-400 µl) to precipitate the RNA and the tube was inverted 10 times to mix the mixture and incubated for 10 minutes at room temperature. Total RNA was pelleted at the bottom of the tube by centrifugation at 12,000 x g for 15 minutes at 4°C. The supernatant was discarded and the RNA pellet was washed once

with 1ml 75% ethanol and tube vortexed for 10 seconds. The sample was centrifuged again at 7,500 x g for 5 minutes at 4°C, and the pelleted total RNA was briefly air dried and dissolved in 50 µl of DEPC-treated water.

2.3.1 Preparation of RNA for microarray and qRT-PCR analysis

Seventy two hours following transfection with siRNA, cells were harvested and RNA prepared as described in Section 2.1. Further purification of RNA was performed using PureLink™ RNA Mini Kit (Invitrogen) according to the manufacturer's instructions.

2.3.2 Determination of RNA concentration and integrity

A Nanodrop 1000 spectrophotometer (Thermo Scientific, UK) was used to analyse RNA concentrations. RNA with an A260/A280 nm \geq 2.0 and an A260/A230 nm \geq 1.8 was considered suitable for further analysis. An Agilent 2100 bioanalyser (Agilent Technologies) was used to analyse RNA integrity. Samples with a RIN (RNA Integrity Number) above the threshold of seven were judged suitable for microarray or qRT-PCR analysis.

2.3.3 Reverse transcription of RNA

Single-stranded RNA can be reverse transcribed into double-stranded DNA (cDNA) by using reverse transcriptase (also known as RNA-dependent DNA polymerase). In this study, RNA was reverse transcribed using Transcriptor Reverse Transcriptase® kit (Roche) according to manufacturer's

instructions. One microgram of total RNA was used as template and added to 2µl of ddNTP mix (Bioline) at a concentration of 10mM, and 0.5µl of RNase inhibitor (40U/µl) (Roche), 4µl of 5X Transcription buffer (provided in kit), 1µl of Oligo(dt)15 primer (100µM) (Roche) and DEPC-treated water to a final volume of 19.5µl added. Finally, 0.5µl of Transcriptor Reverse Transcriptase® (20U/µl) was added to a total volume of 20 µl and the mixture was mixed gently by pipetting. A programme for reverse transcription was set up on a Thermohybrid PX2™ PCR machine allowing incubation of samples for 30 minutes at 55°C and then allowed to cool at 4°C. The resulting cDNA was stored at -20°C before use.

2.3.4 Polymerase chain reaction (PCR) and semi-quantitative RT-PCR

The polymerase chain reaction (PCR), using a thermostable DNA polymerase enzyme allows the amplification of DNA. A combination of reverse transcription and RT-PCR is used frequently for gene expression studies and the process of involves the amplification of the cDNA product.

The first step of PCR (Denaturation stage) requires the dissociation of double-stranded DNA into single stranded DNA by denaturing the DNA through heating at 94°C for 5 minutes. Subsequent DNA amplification utilizes a pair of short oligonucleotides (single-stranded DNA also known as forward and reverse PCR primers) designed to complement the DNA template.

Initial denaturation involves a brief heating of the template DNA and primer DNA at 94°C for 30 seconds, after which the temperature is lowered to 50-70°C for 30 seconds. The denatured single-stranded primer DNA anneals to the DNA template at an annealing temperature which varies according

to the GC content of the oligonucleotide primers. The next stage of the PCR process is the elongation stage, which involves heating of the template DNA and primer at 72°C for 1 minute and a new DNA strand is synthesized by the DNA polymerase from the 3' end of the oligonucleotide primer in the presence of dNTP (10 mM each dATP, dTTP, dCTP and dGTP). Altogether, a single cycle of PCR amplification comprises all of the above three steps series denaturation, annealing and elongation. A continuation of one cycle after another allows increased copy numbers and around 20-40 cycle numbers are generally used in PCR amplification. Following PCR amplification, the last stage is to heat the PCR sample for 12 minutes at 72°C. In this study, the programme used for PCR in a Thermohybrid PX2™ was as follows:

95°C 5 minutes initial denaturation

29-35 cycles { 95°C 30 seconds denaturation
 *55 - 66°C 30 seconds -1 minute annealing
 72°C 1 minutes elongation

72°C 12 minutes

4°C hold

* At temperature given in Table 4 for specific primer pairs

PCR primers (MWG Biotech) were designed to be 19-24 bases in length, to optimally have 50 % GC content and to preferably terminate at both ends in a G or a C. All primers used are listed in Table 4.

Each PCR reaction contained 0.5 µl of cDNA sample (RT product used as a template DNA), 2.5 µl of 10X PCR buffer (Bioline), 2.5 µl of 10 mM dNTP mix (Bioline), 1.2 µl of 50 mM MgCl₂, and 2.5 µl of forward and reverse primers (each in solution at concentration of 20 pmol/ µl) and to 0.5 µl of Taq polymerase (Bioline). The final volume of each samples was adjusted to 20 µl with the addition of DEPC-water.

One of the principles of semi-quantitative RT-PCR is that amplification of the PCR is required to be at the linear stage before saturation, which ensures effective amplification of the PCR in all samples and ensures reliability of the semi-quantification. For each set of primers used, the cycle number was optimized experimentally. For instance to compare the expression of *GPX4* in Caco-2 cells treated with negative control siRNA and cells treated with *GPX4*-siRNA, amplification of *GPX4* expression by PCR was performed at 25, 27, 29 and 31 cycles and results showed that PCR cycle 29 or 30 was appropriate for both samples at the linear stage.

Primers	Sequences	T _m °C	b
GPX4 FWD	5'-CGA TAC GCT GAG TGT GGT TTG C-3'	66	22
GPX4 REV	5'-CAT TTC CCA GGA TGC CCT TG-3'		20
GPX4 m-FWD	5'-CAT TGG TCG GCT GGA CGA G-3'	65	19
GAPDH FWD	5'-TGA AGG TCG GAG TCA ACG GAT TTG-3'	55	24
GAPDH REV	5'-CAT GTA AAC CAT GTA GTT GAG GTC-3'		24
AIF FWD	5'-ACA TAG TGG CAG CTG TGG GC-3'	60	20
AIF REV	5'-CAT GGT GCT CTA CCC GCC TC-3'		20
COX17 FWD	5'-AGT GAC TGC GGA CGA ATC GG-3'	60	20
COX17 REV	5'-TTC TTG GTC TCC GGG CAA GC-3'		20
NDUFA10 FWD	5'-CAG TTC AGA GAG CTG CCG GG-3'	62	20
NDUFA10 REV	5'-CCA GGA GAG TGC GGC TGA TG-3'		20
NDUFB6 FWD	5'-GTC CGT AGT TCG AGG GTG CG-3'	60	20
NDUFB6 REV	5'-TCA GCC ATC GCC TTC TCA GC-3'		20
BAX FWD	5'-TGG ACT TCC TCC GGG AGC GG-3'	60	20
BAX REV	5'-TGG TGA GTG AGG CGG TGA GCA-3'		21
βeta-Actin FWD	5'-TGT TAC AGG AAG TCC CTT GCC ATC-3'	60	24
βeta-Actin REV	5'-CTC CCC TGT GTG GAC TTG GG-3'		20

Table 4. List of primers for generating products from cDNA by semi-quantitative RT-PCR or by real-time PCR. T_m (°C)=Primer annealing temperature, b= number of primer bases.

2.3.5 Agarose gel electrophoresis

Negatively charged DNA molecules migrate towards the positive electrode in agarose gel electrophoresis. Large sized DNA molecules electrophoresce move slowly through the agarose gel compared to small DNA molecules resulting in less migration during electrophoresis. The use of agarose gel electrophoresis allows the separation of DNA molecules on the basis of size and this approach is used frequently for separation of DNA fragments harvested from PCR. Known sized DNA molecules (DNA markers) are generally co-electrophoresized alongside the DNA fragment and comparison between the two allows the estimation of the size of the DNA products.

In the present experiments, PCR products were analysed on 1% agarose gels. The gel was prepared by boiling 0.5 g Agarose (Sigma) in 50 ml of 1X TAE buffer (Promega) diluted from a stock of 10X TAE buffer (Tris base 242 g, Glacial acetate acid 57.1 ml, EDTA 100 ml of 0.5 M pH 8, 1 L MQH₂O pH 8.3) plus 2 µl of 10 mg/ml ethidium bromide (EB Promega) added to enable DNA visualization. The mixture was poured into a gel casting tray containing a comb to generate spaces for loading DNA samples and left at room temperature until solid. Two microlitres of 5X loading dye (50 mM Tris-HCl pH 8, 5 mM EDTA, 20 % glycerol and 0.1 % Bromophenol Blue) (Bioline) was mixed with 8 µl of the PCR product and samples were loaded onto the gel.

The samples were electrophoresized for 40 minutes at 70 V and DNA bands were visualized using a gel documentation system (Uvitec (model BTS-26M), UK) under UV light. For semi-quantitative RT-PCR, the intensity of the band was measured using the Uvitec software.

2.3.6 qRT-PCR (Real-time PCR)

2.3.7 DNase treatment of RNA used for qRT-PCR

Prior to qRT-PCR, RNA was treated with DNAase to remove any contaminating DNA. Four and a half (4.5) µg of RNA was added to a mixture of 2 µl 10X DNase buffer (Roche), 4.5 U DNase (Roche) with RNase free water to a final volume of 20 µl (Invitrogen). The reaction was incubated for 30 minutes at 37 °C after which 4 µl of stop solution (EDTA, 20 mM, pH 8.0) was added. Further incubation for 10 minutes at 65 °C was carried out and the RNA was placed on ice or stored at -80°C for future use.

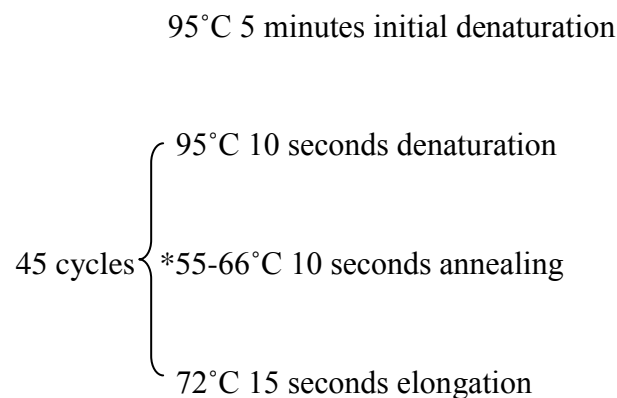
2.3.8 Reverse transcription of RNA used for qRT-PCR

RNA used for qRT-PCR was reverse transcribed as described in section 2.3.3

2.3.9 qPCR using the Roche LightCycler® 480

Real time PCR was performed on the Roche LightCycler® 480 (Roche). PCR reactions were set up in LightCycler® 480 96 Multiwell plates (Roche) using SYBR Green I Master (Roche). One microlitre of cDNA was used in a standard reaction PCR using primers for the target and housekeeping genes. PCR products were purified using PCR purification kit (Qiagen). One in 10 serial dilutions of the PCR products were prepared in triplicate in order to construct a standard curve. One in 10 serial dilutions of the cDNA was also prepared for each target gene and housekeeping gene sets. Each PCR reaction

contained 3 µl of water, 1 µl forward and reverse primers (MWG) (Table 4), 10 µl LightCycler® 480 SYBR Green I Master (Roche) and 5 µl of the serial dilution or the target samples were added to a final volume of 20 µl. The plates were sealed with Roche LightCycler® 480 plate sealing foil (Roche) and centrifuged at 1500 x g for 2 minutes at 4°C. Samples were analysed using the following cycling parameters:



* At temperature given in Table 4 for specific primer pairs.

Fluorescence for each PCR cycle was detected and the threshold crossing points (CT values) determined. At the end of all reactions, a melting curve peak analysis was carried out to ensure single product amplification. Each PCR sample was measured in duplicate and typical amplification curves for each analysed gene are shown in Appendix B.

To calculate the expression of all target and reference genes for each samples the gene specific standard curve generated during each run was used. Using the cDNA samples, each target cDNA concentration was normalised to the average value of the reference gene. Relative mRNA levels of *GPX4*, *AIF*, *BAX*, *NDUFA10*, *NDUFB6*, *COX17*, *beta-Actin* and *GAPDH* of the negative control siRNA and siRNA

samples were determined using the Δ cycle threshold (Δ Ct) method as outlined in Livak's protocol. (Livak & Schmittgen 2001). In brief, a Δ Ct value was the Ct difference between the target gene and the reference genes (Δ Ct = $CT_{\text{target}} - CT_{\text{reference}}$). *GAPDH* and *beta-Actin* were used as the reference genes. Data were calculated as a % mean of value for cells treated with negative control siRNA.

2.3.10 Global mRNA expression analysis

RNA was extracted from Caco-2 cells as described in Section 2.3 and 2.3.1, and quality and integrity was checked as described in Sections 2.3.2. RNA of sufficient integrity was sent for analysis. After being re-checked by Service XS, RNA were labelled, hybridized and scanned as described in Chapter 3 Section 3.4.1.

2.4 Whole cell lysate preparation, protein analysis and Western blotting

2.4.1 Cell lysate preparation

Cells were harvested 72 h (except where stated otherwise) following transfection. Cells in each well of a 6-well plate were washed with 1 ml of ice cold PBS, and collected into 1 ml cold PBS containing 1 protease inhibitor (Roche). Cells were collected using a cell scraper (Greiner), transferred into a 1.5 ml microcentrifuge tube and centrifuged at 13,000 x g for 15 minutes at 4 °C. The supernatant was discarded and the pellet was resuspended in 200 μ l PBS containing 0.1% (v/v) Triton. The cell suspension was sonicated twice for 10 seconds with a 30-50% pulse using a sonicator (4710 Series Cole

Palmer) to cause cell disruption. Cells were further centrifuged at 3,500 x g for 10 minutes at 4 °C. The resulting supernatant was collected, snap-frozen in liquid nitrogen and further stored at -80 °C until analysis.

2.4.2 Preparation of mitochondrial and cytosolic fractions

Cells were washed in ice-cold PBS and re-suspended in 2 ml of homogenisation buffer containing 0.6 M mannitol, 10 mM Tris-HCL pH7.4, 1 mM EGTA, 1 mM phenylmethylsulfonyl fluoride (PMSF) and 0.1% BSA. The cell suspension was subjected to 15 homogenisation passes with a glass-teflon homogeniser, followed by centrifugation at 400 x g for 10 minutes at 4°C. The supernatant fluid containing the cytosolic fraction was kept on ice, whilst the remaining pellet was re-suspended in 2 ml of homogenisation buffer and the homogenisation and centrifugation steps were repeated. The combined supernatant fluids were centrifuged at 12,000 x g for 10 minutes at 4°C and stored at -80°C (cytosolic fraction). The resulting mitochondrial pellets were re-suspended in homogenisation buffer, combined into one tube and centrifuged again at 12,000 x g for 10 minutes at 4°C. The resulting final pellet (mitochondrial fraction) was re-suspended in a small volume of homogenisation buffer (without BSA), snap-frozen in liquid nitrogen and further stored at -80 °C for further analysis.

2.4.3 Determination of protein concentration

Protein concentration was determined using the Bradford assay. Standards of 0, 20, 40, 60, 80 and 100 µg/ml were made in triplicate using a 100 µg/ml bovine serum albumin standard solution and 50 µl of each were pipetted into a 96 well plate (SLS Ltd, UK). Cell lysates were diluted 1 in 50 for analysis and 50 µl was used in the assay. Biorad dye reagent (Biorad, UK) was diluted 1 in 5 from the stock with MQH₂O and 200 µl was added to the 96 well plate containing the samples and standards, and absorbance was measured at 595 nm on a multiwell plate reader (ThermoLab Systems Multiscan Ascent).

2.4.4 Sodium dodecyl sulphate-polyacrylamide gel electrophoresis

Sodium dodecyl sulphate-polyacrylamide gel electrophoresis (SDS-PAGE) is an electrophoretic approach, which allows separation of protein molecules according to their molecular weight. Binding of SDS to the polypeptide sequences results to a disruption of the non-covalent bonds and opening of their folding confirmation resulting in distribution of negative charges on the SDS-polypeptide proportional to the polypeptide length.

Work described in this study separated protein molecules using 12.5% SDS-polyacrylamide gels prior to Western blotting. The 12.5% SDS-polyacrylamide gel (resolving gel) was prepared by mixing together 3.75 ml of 1 M Tris-HCl buffer (pH=8.8) (Promega), 2.925 ml of ddH₂O, 100 µl of 10% SDS solution (obtained from 20% SDS stock solution, Sigma), 3.125 ml of 30% Acrylamide/Bis-acrylamide solution

(ratio 29:1) (Sigma), 10 μ l of N, N, N', N'-tetramethylethylenediamine (Sigma) in 10 ml total volume and 100 μ l of 10% Ammonium persulphate (Sigma). The same procedure was used to prepare the stacking gel except 3.75 ml of 1 M Tris-HCl buffer (pH=6.8) was used. The 1 X SDS-PAGE running buffer was diluted from 5 X stock. To prepare the 5 X running buffer, 144.1 g Glycine, 65 g SDS and 0.6 g Tris-HCl (Promega) were dissolved in 800 ml of water, adjusted to pH 8.8 and water added to a final volume of 1000 ml. To prepare a 5 x protein loading buffer, 5 ml of Glycerol (Sigma), 2.5 ml of 1 M DTT, 2.25 ml of 1 M Tris-HCl solution (pH=6.8) and 0.5 g SDS (Promega) was mixed and dissolved. Ten milliliter of each stock solution was aliquoted and stored at -20°C before use. Twenty micrograms of protein cell lysate was mixed with the 5 X loading buffer in a ratio of 1:1 (v/v) for each sample. To denature the protein molecules, the mixture of protein samples and protein loading buffer was heated at 90°C for 5 minutes. Following incubation, protein samples were loaded into wells in the stacking gel and electrophoresis was performed at 80-120 V for 1 h and 30 minutes.

2.4.5 Western Blotting and detection of protein

Following separation by SDS-PAGE proteins were transferred to a PVDF membrane (Roche) and the protein of interest detected with specific antibodies. The gel was placed next to a sheet of PVDF membrane with two pieces of filter paper (Whatman) above and below, placed on the bottom of transfer apparatus (Atto, GRI, UK) and wetted lightly with transfer buffer. To prepare the transfer buffer, 1 X SDS-PAGE running buffer was mixed with methanol (Fisher Scientific) in a ratio of 4:1 (v/v) and the

stack was gently rolled with a roller to squeeze out air bubbles between gel and PVDF membrane. To avoid the membrane becoming over-dry, a small amount of the transfer buffer was pipetted on top of the stack and transfer was carried out for 1 h at 15 volts.

The PVDF membrane was placed into 10 ml of 5% (w/v) non-fat milk powder solution in 5 x TPBS buffer and incubated either for 1 h at room temperature or overnight at 4°C. To prepare the TPBS, 0.05% (v/v) Tween-20 (Sigma) was added into 1X PBS and was thoroughly mixed. This blocking step was designed to prevent non-specific binding of antibodies to the PVDF membrane. The PVDF membrane was incubated with the primary antibody for 1 h diluted in 3% (w/v) milk-TPBS. The membrane was washed three times using 10 ml of TPBS, each time for 10 minutes. Incubation of the PVDF membrane with a secondary antibody was carried out for 1 h with horseradish peroxidase (HRP)-labeled anti-rabbit IgG diluted in 3% (w/v) milk-TPBS. Ten milliliter of PBS was used to wash the membrane three times, each time for 10 minutes. A list of primary and secondary antibodies used in work described in this thesis, and the dilutions used is given in Table 5.

Hyperfilm ECL™ reagent (GE Healthcare) was used to detect the bound secondary antibody. Two milliliters of Solution A and Solution B of the ECL solution in a ratio of 40:1 were gently mixed and added to the PVDF membrane, covered with plastic film and incubated for 5 minutes in darkness. ECL allows emission of fluorescence following catalysis by HRP and the fluorescence signal can be captured on Kodak Biomax XAR film in a Hypercassette™ (Amersham Bioscience) film using Kodak GBX developer (Sigma). The intensity of the fluorescent signal reflects the abundance of protein blotted on to

the membrane. Band intensities of proteins were assessed using densitometry software (UVItec (UVIBand software), UK) on a gel documentation system (UVItec (model BTS-26M), UK).

2.4.6 Staining of protein

To assess transfer efficiency of proteins onto a membrane, PVDF membranes were stained with a Ponceau S staining kit (Sigma) according to the manufacturer's instructions. The membrane was incubated (with shaking) in 100 ml Ponceau S stain for 1 h. After 1h incubation, the membrane was washed twice and further incubated in 200 ml of deionised water until the background of the PVDF membrane became clear.

1° ANTIBODY	SOURCE	DILUTION	CAT-NO
Rabbit Anti-Human GPX4	ABCAM	1 in 500	AB41787
Rabbit Anti-Human AIF	SIGMA	1 in 1000	A7549
Rabbit Anti-Human BAX	SIGMA	1 in 1000	B3428
Rabbit Anti-Human Bcl-2	SIGMA	1 in 1000	PRS3337
Rabbit Anti-Human CASPASE-3	CELL SIGNALLING	1 in 1000	#9662
Rabbit Anti-Human CASPASE-9	PTGLAB	1 in 1000	10380-1- AP
2° ANTIBODY Anti-Rabbit IgG-peroxidase produced in goat, affinity isolated antibody adsorbed with human IgG	SIGMA	1 in 5000	A0545
Mouse- Anti-Human COX2	MitoScience	1 in 1000	AB110258
Mouse- Anti-Human NDUFB8	MitoScience	1 in 1000	AB110242
Mouse- Anti-Human SDH	ABCAM	1 in 1000	AB14714
Mouse- Anti-Human β -Actin	SIGMA	1 in 2000	A1978
2° ANTIBODY Anti-Mouse IgG-peroxidase produced in rabbit, IgG fraction of antiserum	SIGMA	1 in 10000	A9044

Table 5. List of primary and secondary antibodies used for Western blotting.

2.5 Cell viability assay

CellTiter-Blue® provides an absorbance and fluorometric approach to estimate the number of viable cells in a multiwell plate assay. It uses resazurin indicator dye to assess the metabolic capacity of viable cells. The ability to reduce resazurin into resorufin is retained in viable cells and the resulting resorufin is highly fluorescent (Figure 6). Non-viable cells lack the ability to reduce resazurin into resorufin. Resazurin has little intrinsic fluorescence and remains dark blue until it is reduced to resorufin which, is pink in colour and highly fluorescence (579Ex/584Em). Either fluorescence or absorbance can be used to measure cell viability results. The maximum absorbance for resazurin is 605 nm whereas that of resorufin is 573 nm.

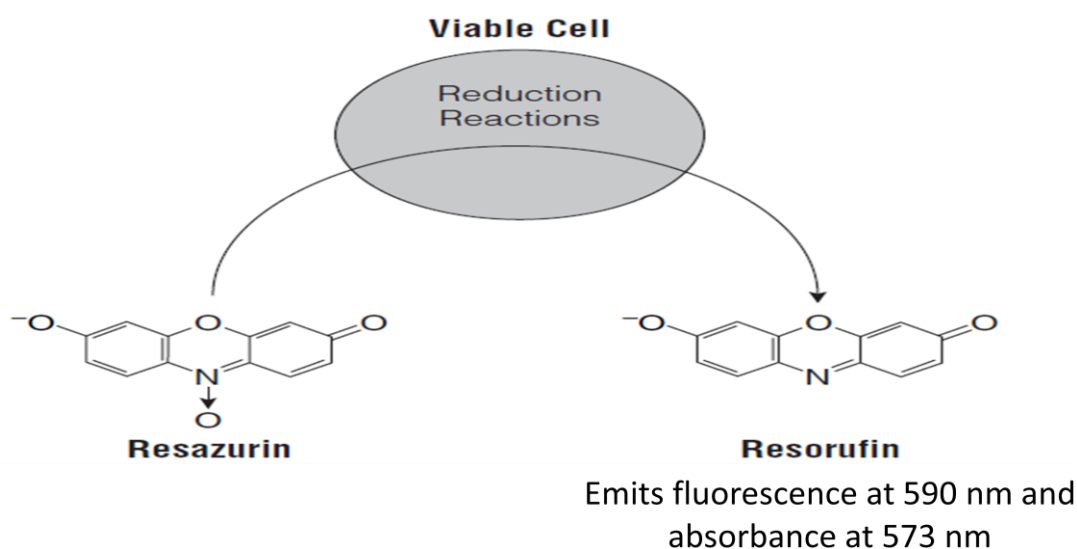


Figure 6. Conversion of resazurin to resorufin by metabolically active cells results in the generation of a fluorescent product or a change in absorbance wavelength

For work described in this thesis, 96 well plates were seeded with 1×10^4 cells/well, and after 24 h, half the cells were treated with GPx4 siRNA and half with the scrambled control siRNA. 72 h following transfection, medium was removed and 180 μ l fresh medium added to the cells. Cell viability was assessed by the addition of 20 μ l of CellTiter-Blue[®] reagent (Promega) and after 4 h absorbance was measured at 573 nm using (Thermo Labsystem Multiscan Ascent).

2.6 Thiobarbituric acid reactive assay substance (TBARS) assay for lipid peroxidation.

Measurement of lipid peroxidation is widely used as a marker of oxidative stress in cell and tissues. Due to their unstable nature, lipid peroxides, decompose to form a series of complex compounds which include reactive carbonyl compounds, such as malondialdehyde (MDA). Measurement of MDA is widely recognised as an indicator of lipid peroxidation and thiobarbituric acid reactive substance measurement (TBARS) is a well established approach to measure MDA and lipid peroxidation. The MDA-TBA adduct is formed by the reaction of MDA and TBA (Figure 6) under high temperature (40-100°C) and acidic conditions. The MDA-TBA can be measured colorimetrically at 530-540 nm or fluorometrically at an excitation wavelength of 530 nm and emission wavelength of 550 nm.

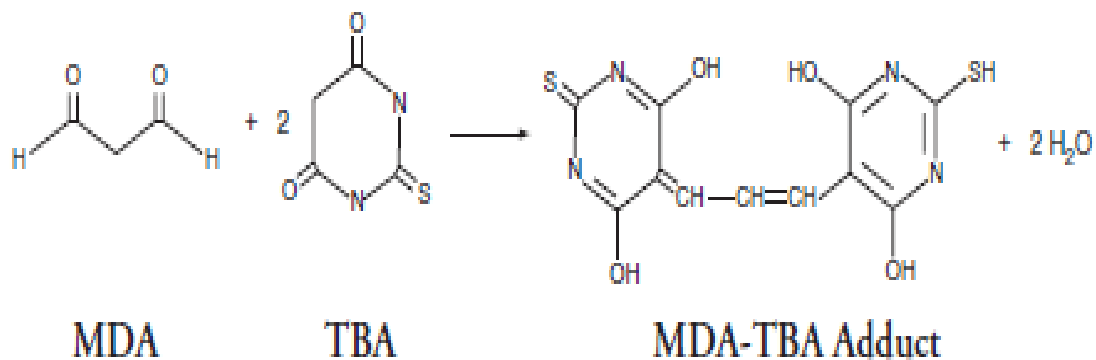


Figure 7. Formation of a MDA-TBA adduct.

A typical MDA-TBA adduct formed by the reaction of MDA and TBA under high temperature (~ 90-100°C).

To prepare the colour reagent used for both the sample and standards, 530 mg of TBA (Sigma) was added to 50 ml of TBA acetic acid solution (TBA acetic acid Sigma) diluted 1 in 50. 50 ml of TBA sodium hydroxide (Sigma) diluted 1 in 50 was added to the mixture and mixed until the TBA is completely dissolved.

For colorimetric standard preparation, 250 µl of the MDA standard (Sigma, UK) was diluted with 750 µl of water to obtain a stock solution of 125 µM and target concentrations of standards were 0-50 µM.

Caco-2 cells were grown to confluency in 6 well plates, washed with PBS, trypsinised and transferred into 1.5 ml microcentrifuge tubes and centrifuged at 12,000 x g for 10 minutes. Cells were transferred into fresh 1.5 ml microcentrifuge tubes containing PBS and sonicated 3X for 5 seconds intervals at 40V setting over ice. Two hundred µl ice cold 10% trichloroacetic acid was added to 100 µl cell lysate,

incubated on ice for 15 minutes and centrifuged at 2,200 x g for 15 minutes at 4°C. 200 µl supernatant were transferred to a clean 1.5 ml microcentrifuge tubes each containing 100 µl of TBA sodium hydroxide (adjusted to pH 8.3) and mixed. Tubes were placed in vigorously boiling water for 1 h, and then placed in ice for 10 minutes to stop the reaction. The microcentrifuge tubes containing the mixture were centrifuged at 1,600 x g for 10 minutes at 4°C and left to stabilize at room temperature for 30 minutes. 150 µl of the mixture from the tubes were loaded in duplicate into 96-well plate and absorbance measured colorimetrically at 532 nm using a colorimetric plate reader (Thermo Labsystem Multiscan Ascent).

The average absorbance of each standard and samples were calculated, and the absorbance value of standard A (0 µM) was subtracted from all other values (both standards and samples) and this was considered a corrected absorbance. The corrected absorbance values of each standard were plotted as a function of MDA concentration and the values of MDA for each sample calculated from the standard curve.

2.7 Measurement of ROS levels using carboxy-H2DCFDA

Detection of reactive oxygen species (ROS) can be carried out through the use of the cell membrane-permeable fluorescent dye 5-(and-6)-carboxy-2',7'-dichlorodihydrofluorescein diacetate (carboxy-H2DCFDA). Following cleavage of the compound by ROS, a luminometer or fluorescence microscope can be used to capture the fluorescence emission of the product. Comparison of ROS levels in test and

control groups can be performed in a semi-quantitative manner and data expressed as a percentage relative to the level of control.

ROS levels were assessed by staining cells with Image-iT™ LIVE Green Reactive Oxygen Species (ROS) Detection Kit (Invitrogen) according to manufacturer's instructions and the carboxy-H2DCFDA fluorescence signal was read using a luminometer (POLARstar Omega). The ROS Detection Kit (Invitrogen) comprises Component A (carboxy-H2DCFDA as powder, 275 µg/vial), Component B (Hoechst 33342, 400 µl of a 1 mM solution), Component C (*tert*-butyl hydroperoxide solution) and Component D (500 µl DMSO). A stock of 10 mM solution of carboxy-H2DCFDA was prepared by adding 50 µl of DMSO into one vial of carboxy-H2DCFDA and mixed to dissolve. To prepare a working 25 µM solution of H2DCFDA 5 µl of 10 mM stock solution was added to 2 ml of pre-warmed 1X HBSS/Ca/Mg solution and gently mixed. Additionally, a nucleic acid targeting dye Hoechst 33342 was used as a control dye. Two microlitres of 1 mM Hoechst 33342 solution was mixed with 2 ml of 25 µM carboxy-H2DCFDA working solution to make a final concentration of 1 µM Hoechst 33342.

Cells were grown to confluency in 96-well plates. 50 µl of carboxy-H2DCFDA-Hoechst 33342 was added to each well and incubated for 30 minutes at 37°C. Due to the light sensitivity of the assay, the 96-well plate was wrapped with foil. Following incubation, cells were washed three times with 100 µl of warm 1 X HBSS/Ca/Mg solution per well and 50 µl of 1X HBSS/Ca/Mg solution was added into each well. Fluorescent signal for carboxy-H2DCFDA was read at 495/529 nm (emission/excitation) wavelength whereas that of Hoechst 33342 was read at 350/460 nm using a POLARstar Omega

fluorometer. Twenty repeat measurements were taken for each signal in each well and calculation of the signal value was taken from the average of the 20 readings. The difference in ROS level of cells treated with *GPX4*-siRNA was compared using the carboxy-H₂DCFDA signal value of cells treated with negative control siRNA expressed as a percentage of the average value. Readings from the Hoechst 33342 analyses used as a control for cell number and staining efficiency.

2.7.1 Measurement of superoxide production using MitoSOX™

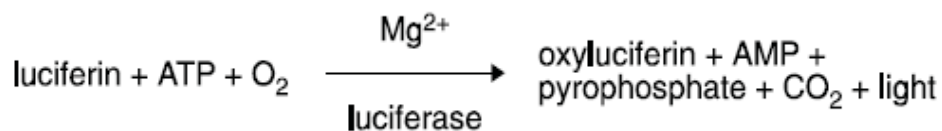
Superoxide indicator MitoSOX™ Red is a fluorogenic dye, which is selective for detection of mitochondrial superoxide in live cells. The dye selectively and rapidly targets the mitochondria. Superoxide dismutase (SOD) prevents the oxidation of MitoSOX™ but once oxidized by superoxide in the mitochondria MitoSOX™ exhibits red fluorescence. Although MitoSOX™ Red has been suggested to specifically detect superoxide in the mitochondria there are some reports which have also implicated its oxidation by other ROS generating systems (Kalyanaraman *et al.*, 2012). Following its cleavage by ROS MitoSOX™ Red emits a fluorescence signal and this signal can be captured using a luminometer. This method was used to analyse the effect of *GPX4* knock-down on mitochondrial superoxide levels in Caco-2 cells.

Caco-2 cells were seeded to a black, flat-bottomed 96-well plate (Greiner) at 3×10^4 cells/well, washed gently with 100µl/well of pre-warmed 1X HBSS (Hank's Balanced salt Solution)/Ca/Mg solution

(without phenol red;Sigma) and mitochondrial superoxide formation measured using the MitoSOX™ LIVE Detection Kit (Invitrogen) following the manufacturer's instructions. Essentially, twenty five µl of MitoSOX-Hoechst 33342 mix was added to each well of a 96-well plate and incubated at 37°C for 10 minutes whilst wrapped in foil. After incubation, cells were washed three times with 100 µl/well of pre-warmed 1X HBSS/Ca/Mg solution, and finally 50 µl of 1X HBSS/Ca/Mg solution was added. MitoSOX fluorescent signal was measured at 510/580 nm (emission/excitation) wavelength and the Hoechst 33342 fluorescent signal read at 350/460 nm using a fluorometer (POLARstar Omega-BMG Labtech); the Hoechst 33342 fluorescence was used as a control for cell number and staining efficiency.

2.8 Measurement of mitochondrial ATP production using a luminometer based luciferase assay.

A luciferase based assay using Molecular Probes' ATP Determination Kit containing recombinant firefly luciferase and its substrate D-luciferin was used for a quantitative determination of ATP. This assay offers a convenient bioluminescence approach for ATP determination and is based on luciferase' s requirement for ATP in producing light (emission maximum ~560 nm) from the reaction below:



This assay is sensitive and can detect as little as 0.1 picomole of either pre-existing ATP, or ATP as it is being formed in kinetic systems. Cells were washed with ice cold PBS before the addition of 50 µl ice

cold lysis buffer (25 mM HEPES pH7.8, 5 mM MgCl₂, 140 mM NaCl) and a detergent supplied with the kit which releases ATP. Briefly, 1 ml of a 10 mM D-luciferin stock solution was prepared by adding 1mL of 1x reaction buffer to one vial of D-luciferin. This mixture was protected from light until it was ready to be used. 100 mM DTT stock solution was prepared by adding 1.62 ml of dH₂O to the bottle containing 25 mg of DTT and was aliquoted into ten 160 µl volumes and stored frozen at -20 °C until it was ready to be used. 1µM ATP standard solution was used. To prepare a 10 ml standard reaction solution, 8.9 ml dH₂O was added to 0.5 ml of 20X reaction buffer, plus 0.1mL of 0.1 M DTT, 0.5 ml of 10 mM D-luciferin and 2.5 µl of firefly luciferase 5 mg/ml stock solution. The tube was gently inverted to avoid denaturation of the firefly luciferase enzyme, and was kept away from light.

Background luminescence was measured by taking a luminescence reading of 100 µl of a standard reaction performed by adding 10% of the diluted ATP standard solution to the standard assay solution (i.e. 10 µl of ATP standard solution in 90 µl of standard reaction solution). Background luminescence was subtracted, and a standard curve for series of ATP concentration of 0,0.2,0.4,0.6,0.8 and 1 µM/µl was measured using the luminometer (POLARstar Omega-BMG Labtech). The amount of ATP in the experimental samples were calculated from the standard curve.

2.9 Measurement of mitochondrial membrane potential using the JC-1 5,5',6,6'-tetrachloro-1,1',3,3'-tetraethylbenzimidazolylcarbocyanine iodide assay

One of the hallmarks of apoptosis and mitochondrial damage is the loss of mitochondrial membrane potential. A unique cationic dye JC-1 (5,5',6,6'-tetrachloro-1,1',3,3'-tetraethylbenzimidazolylcarbocyanine iodide) can be used to detect the loss of mitochondrial membrane potential. The mitochondria stains bright red in healthy cells since the mitochondrial membrane potential allows the dye to accumulate and aggregate in the mitochondrial matrix where it fluoresces red. The collapse of mitochondrial membrane potential inhibits the accumulation of JC-1 within the mitochondria and JC-1 remains in a green fluorescent monomeric form in the cytoplasm. The aggregate red form has absorption/emission maxima of 585/590 nm whereas the green monomeric form has absorption/ emission maxima of 510/527 nm. Mitochondrial depolarization is consequently detected by reduction in red/green fluorescence intensity ratio.

10X JC-1 assay buffer (Biotum) was heated in a warm water bath for 10 minutes to dissolve any crystals that may be present in the JC-1 reagent. Assay buffer was diluted 1:10 in DI water. 100 X JC-1 reagent (Biotum) was diluted 1:100 in 1X assay buffer to generate JC-1 working solution. 1×10^6 cell/ml (i.e. 10^4 cells/well) Caco-2 cells were seeded in 96 well plates and were grown for 24 h before treatment with siRNA. Three days following cell treatment, medium was aspirated out of the wells, cells washed twice with 100 μ l PBS and then incubated for 30 minutes with 100 μ l of 10 μ g/ml JC-1 at 37°C. Cells were washed twice more with 100 μ l PBS, 100 μ l PBS was added to cells and fluorescence was

measured at excitation 550 nm, emission 590 nm (red) and fluorescence excitation 480 nm, emission 520 nm (green) using a fluorescence plate reader (POLARstar Omega-BMG Labtech). The ratio of red fluorescence to green fluorescence was calculated.

2.10 Measurement of mitochondrial respiration

Cellular oxygen consumption activities of mitochondrial complex I, IV and V were measured in a respirometer (Oroboros Oxygraph 2k). 5×10^6 cells/ml Caco-2 cells were washed twice with warm PBS and trypsinized. Cells were collected into universal tubes each containing 5 ml of glucose-free DMEM with 10% FCS, 0.11 mg/ml Na pyruvate, 0.9 mg/ml galactose and centrifuged at $12,000 \times g$ at 4°C for 5 minutes. Cells were re-suspended in 250 μl of glucose free medium, 80 μl of these re-suspended cells were added into each oxygen electrode chamber resting respiration measured. Oxygen consumption was measured successively in presence of 2 $\mu\text{g/mL}$ Oligomycin, 0.5 μM Carbonyl cyanide p-(trifluoromethoxy) (FCCP), 0.5 μM Rotenone and 2.5 μM Antimycin A with the respiration rate being allowed to stabilise between additions.

2.11 DNA fragmentation assay.

DNA fragmentation is considered as a hallmark of apoptosis (Nagata, 2000). Towards the end stage of apoptosis, the higher order chromatin structure of DNA is degraded into fragments of 50 to 500 kilo bases pairs in length by activated nucleases. The fragmented DNA can be extracted from cells and visualized by agarose gel electrophoresis and ethidium bromide staining.

Cells were grown in 6-well plate, washed with 1 ml 1X PBS, trypsinized with 0.5 ml trypsin (10 X Solution Trypsin-EDTA; Sigma) and cell count was performed. Following cell counting, 5×10^5 cells were resuspended in 2 ml of DMEM medium. 1 ml of cell suspension was aliquoted into a fresh 1.5 microcentrifuge tube and centrifuged at $2,000 \times g$ for 5 minutes at 4°C . The supernatant was discarded and 200 μl of lysis buffer (20 mM EDTA, 100 mM Tris HCL pH 8.0, 0.8% (w/v) SDS) was added to the cell pellet. Cells were lysed by repeated (10 X) homogenisation with a glass homogeniser. The cell lysate was stored at -80°C for further analysis.

Genomic DNA was extracted from Caco-2 cells using the DNA Isolation Kit (Ambion). Briefly, 10 μl of RNAase A/TI cocktail mix (500 units/ml RNAase A, 20,000 unit/ml RNAase TI) (Ambion) was added to the cell lysate and mixed well by flipping the tip of the tube. The mixture was incubated at 37°C for 90 minutes, 10 μl of proteinase K (20 mg/ml) (Ambion) was added, mixed and further incubated at 50°C for 90 minutes. 2 μl of 5X DNA loading dye (50 mM Tris-HCl pH 8, 5 mM EDTA, 20 % glycerol and 0.1 % Bromophenol Blue) and 18 μl of the DNA was loaded into dry wells (DNA was viscous and had to be loaded into a dry well before adding TAE run buffer) of a 1.5% agarose gel in 50X TAE buffer (Tris base 242 g, Glacial acetic acid 57.1 ml, EDTA 100 ml of 0.5 M pH 8, 1 L MQH₂O pH 8.3) (containing ethidium bromide). Hyperladder IV (Bioline) (a 1000 bp ladder) was used as DNA size markers. Electrophoresis was carried out in TAE buffer at 35V for 30 minutes and DNA bands were visualised under UV light using a gel documentation system (Uvitec model BTS-26M, UK).

2.11.1 Measurement of Caspase 3/7 activity

The luminescence-based Caspase-Glo assay measures the combined activities of caspase-3 and -7. The Caspase-Glo assay kit provides a luminogenic caspase-3/7 substrate containing tetrapeptide sequence DEVD and optimized reagents for detection of luciferase activity and cell lysis. In the assay the proluminescent caspase substrate containing DEVD is cleaved to aminoluciferin which in turn is a substrate for luciferase. The amount of luminescence present is proportional to the amount of caspase activity present and the reagent relies on the properties of thermostable luciferase (Ultra-Glo™ Recombinant Luciferase) that is generated to produce a luminescent signal.

Caspase-Glo assay was used to investigate the activation of caspase-3 and -7 activity in cells treated with *GPX4*-siRNA or negative control siRNA. The following reactions were prepared: Blank reaction-Caspase-Glo®3/7 reagent (Promega), DMSO (Sigma) and DMEM medium without cells, Assay reaction-Caspase-Glo®3/7 reagent or cells treated with siRNA and scrambled control siRNA in DMEM medium.

Caspase-Glo®3/7 reagent was allowed to equilibrate to room temperature for 20 minutes and the 96-well plate containing cells from the incubator was also allowed to equilibrate to room temperature for 10 minutes. 100 µl Caspase-Glo®3/7 reagent was added to each well of a white walled 96-well plate (Greiner) containing 100 µl of blank reaction, negative control siRNA treated cells or siRNA treated cells in culture medium and the plate sealed with a plate sealer. Well contents were gently mixed using a plate shaker at 500 x g for 30 seconds and incubated at room temperature for either 30 minutes, or 60

minutes, or 90 minutes, and 120 minutes. Luminescence of each sample was measured in a plate reader (POLARstar Omega-BMG Labtech).

2.11.2 Flow cytometry analysis of apoptosis

Detection of apoptosis by Annexin V-FITC is based on the observation that phosphatidylserine (PS) is translocated from the inner face of the plasma membrane to the cell surface at the onset of apoptosis. Once PS is on the cell surface, it can be detected easily by staining with a protein that has a high affinity for PS such as Annexin V-FITC. Detection of apoptosis using Annexin V can be determined by flow cytometry or by fluorescence microscopy. Differentiation between apoptotic cells vs necrotic cells can be performed using both Annexin V-FITC and Propidium iodide (PI) staining.

For the analysis of apoptosis in this study, Caco-2 cells were treated with Annexin V-FITC Apoptosis Detection kit (Abcam). Cells were seeded and allowed to grow to 30-50% confluency before transfection with either *GPX4*-siRNA, negative control siRNA or siRNA plus Mitoquinone 10 (MitoQ₁₀) (a blocker of lipid peroxides). Seventy two hours following transfection, cells were washed with PBS and collected into microcentrifuge tubes and centrifuged at 12,000 x g for 5 minutes at 4°C. The supernatant was discarded and the pellet resuspended in 500µl of Solution A (1x Annexin binding buffer solution Abcam). This was repeated twice more to remove any remaining media. A cell count was performed and 5X10⁵ cells were taken and resuspended into 500 µl 1x Annexin binding buffer solution. This was incubated for 10 minutes at room temperature, then 5 µl of Solution B (Annexin V-

FITC) and 5 μ l of Solution C (50mg/ml propidium iodide stain solution) was added to the suspension and incubated for further 10 minutes in the dark at room temperature. Annexin V-FITC binding was analyzed by flow cytometry (Excitation=488 nm; emission=530 nm) using FITC signal detector (FL1) and PI staining by the phycoerythrin emission signal detector (F2) with FACS Canto (USA) and analyzed statistically using FACSDiva software.

2.12 Mitoquinone₁₀ treatment on Caco-2 cells.

MitoQuinone₁₀ (MitoQ₁₀) is a ubiquinone that accumulates within mitochondria driven by a conjugated lipophilic triphenylphosphonium cation (TPP⁺) attached to a ubiquinone moiety by saturated 10-carbon chain. Once there, MitoQ₁₀ is reduced to its active ubiquinol form. The lipophilic cation leads to the extensive accumulation of MitoQ₁₀ within mitochondria where the ubiquinone is reduced to its active antioxidant ubiquinol form. Accumulation and subsequent reduction of MitoQ₁₀ leads to protection against mitochondrial oxidative damage in a number of *in vitro* and *in vivo* systems (Orsucci *et al.*, 2001; Cortes-Rojo & Rodriguez-Orozco, 2011).

Caco-2 cells were seeded and grown for 24 h before transfection with siRNA and negative control siRNA and addition of 1 μ M MitoQ₁₀ or its control compound, decyltriphenylphosphonium bromide (DecylTPP). 1 μ M was considered optimal dose for MitoQ₁₀ and DecylTPP as recommended by the supplier (Dr R.A.J. Smith, Department of Chemistry, and University of Otago, New Zealand). Twenty

four, 36 and 72 h post-transfection, cells were washed with 1X PBS and parameters such as levels of lipid peroxide, mitochondria superoxide, mitochondrial membrane potential and apoptosis were measured as described in sections 2.6, 2.7.1, 2.9 and 2.11.2.

2.13 Statistical Analysis

All the data described in this thesis except for the microarray data was analyzed statistically using SPSS 17.0 (Statistical Product and Service Solutions 17.0, Chicago, IL, USA). Where necessary, results were presented as mean \pm standard deviation (SD) and standard error of mean (SEM). A Mann-Whitney U test was performed for statistical analysis, and a P-value of < 0.05 was considered significant.

Chapter 3: Investigation into the biological functions of *GPX4* and downstream effects of altered *GPX4* expression in Caco-2 cells.

3.1 Introduction

Glutathione peroxidase 4 (*GPX4*), a phospholipid hydroperoxidase gene, has been shown to be ubiquitously expressed in various tissues including the gastrointestinal tract (Imai *et al.*, 1995). GPx4 variants are localized in the mitochondria and cytoplasm, and are associated with cell membranes, (Imai and Nakagawa, 2003). GPx4 is a catalyst of a wide range of oxidative targets such as thymine hydroperoxide (Bao *et al.*, 1997), lipid hydroperoxides (from cholesterol and cholesteryl esters) (Thomas *et al.*, 1990), phospholipid hydroperoxides (Ursini *et al.*, 1985), and additionally has the ability to use other substrates in catalysis of oxidative targets outside glutathione (GSH) (Aumann *et al.*, 1997). Overexpression of *GPX4* in transgenic mice helped protect from oxidative damage (Ran *et al.*, 2004; Liang *et al.*, 2007). Overexpression studies have also suggested that GPx4 has a role in mitochondrial function, eicosanoid metabolism and apoptosis. Using a hypothesis-free approach, this study aimed to investigate the effects of altered expression of *GPX4* in a human gut epithelial cell line through the use of *GPX4*-targeting siRNAs.

3.2 Design of *GPX4* siRNA and knock-down of *GPX4* mRNA and protein

The use of synthetic microRNAs (siRNA) has become an effective tool for gene silencing within mammalian cells. siRNA act upon an mRNA target sequence for degradation and this mechanism has been widely accepted for the study of effects of gene knockdown. RNA interference (RNAi) is a process by which a gene loses its function through processing of dsRNA into smaller (~21 nucleotides) RNAs by an enzyme known as dicer and their incorporation into a RNA-induced silencing complex (RISC). This allows the loading of the siRNA antisense strand which recognises and cleaves the target mRNA sequence by the complex. In this way, mRNA that has been cleaved is targeted for degradation and ultimately prevents protein synthesis. siRNA are processed by dicer when introduced into cells. To achieve *GPX4* knockdown in the Caco-2 cell line, two non-overlapping siRNAs targeting *GPX4* mRNA were designed (Guanyu Gong, personal communication) and purchased from Ambion. Knockdown was assessed using 20 and 40 nM siRNA at 48 and 72 h after transfection to ascertain the most effective concentration and time.

Three different transcript variants are encoded in the *GPX4* gene; namely cytosolic *GPX4* (*cGPX4*), mitochondrial *GPX4* (*mGPX4*) and nuclear *GPX4* (*nGPX4*) (Arai *et al.*, 1996, Pfeifer *et al.*, 2001). An initial experiment was carried out to determine which *GPX4* transcript variants are expressed in Caco-2 cells. Caco-2 cells were seeded at 3×10^5 cells/well in a six well plate and allowed to grow to 80% confluency before extraction of RNA. The extracted RNA was reverse transcribed and the resulting cDNA was amplified by PCR using primers specific to either all *GPX4* or only *mGPX4* and to the

reference gene GAPDH as a control. Primer sequences and annealing temperatures are described in Table 4. Using RT-PCR, as shown in Figure 8, amplification of both cGPX4 and mGPX4 isoforms was achieved but, the expression of mGPX4 was very low. Thus, the short form is the major GPX4 isoform in undifferentiated Caco-2 cells, as reported to be the case in other somatic cells.

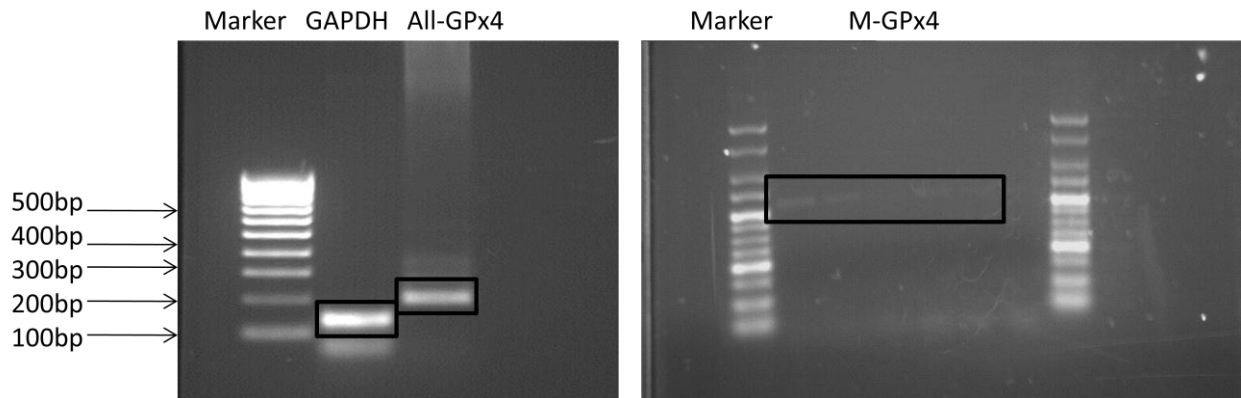


Figure 8. Detection of GPX4 transcript variants in Caco-2 cells.

Duplicate RNA samples from Caco-2 cells were reverse transcribed and the cDNA subjected to PCR using primers specific to GPX4 and GAPDH. PCR amplification was carried out for 30 cycles, the expression of GPX4 transcript variants in Caco-2 cells was detected using RT-PCR. GAPDH (house keeping gene), All-GPx4: amplification of both cytosolic GPX4 and mitochondrial GPX4; M-GPx4: amplification of mGPX4 only.

Following the published methods of (Reynolds *et al.*, 2004, Ui-Tei *et al.*, 2004), two GPX4-specific siRNA were designed (GPX4-siRNA(1) and GPX4 siRNA(2) that had low sequence homology (≥ 15 nt out of 21nt length of siRNA) with other human mRNA transcripts so as to limit the non-specific binding of siRNA to off target mRNAs. The sequences of both GPX4-siRNAs together with the corresponding sequence information for the GPX4 mRNA transcripts are shown in Figure 9.

3.2.1 Sequence of *GPX4* mRNA transcript and specific siRNA

A Exon 1a:

[ATGAGCCTCGGCCGCTTTGCCGCTACTGAAGCCGGCGCTGCTCTGTGGGGCTCTGGCCGCGCTGGCCTGGCCGGGACCATG]

Exon 2-7:

[TGCGCGTCCCGGGACGACTGGCGCTGTGCGCGCTCCATGCACGAGTTTTCCGCCAAGGACATCGACGGGCACATGGTTAACCTGGACAAGTACCG][GGGCTTCGTGTGCATCGTCACCAACGTGGCCTCCCAGTGAGGCAAGACCGAAGTAAACTACACTCAGCTCGTCGACCTGCACGCCC GATACGCTGAGTGTGGTTTGGCGATCCTGGCCTTCCCCTGTAACCAAGTTCGGGAAGCAG][GAGCCAGGGAGTAACGAAGAGATCAAAGAG TTCGCCGCGGGCTACAACGTCAAAATTCGATATGTTTCAGCAAGATCTGCGTGAACGGGGACGACGCCACCCGCTGTGGAAGTGGATGAA GATCCAACCAAGGGCAAGGGCATCTGGGAA][TGCCATCAAGTGGAACCTCACCAAG][TTCCTCATCGACAAGAACGGCTGCGTGGTGAA GCGCTACGGACCCATGGAGGAGCCCTG][GTGATAGAGAAGGACCTGCCCACTATTCTAG]

B *GPX4* siRNA (1)

Target mRNA: AAGACCGAAGTAAACTACACT

GACCGAAGUAAACUACACU-UU (sense strand)

UU-CUGGCUUCAUUUGAUGUGA (antisense-strand)

C Sequence of *GPX4* siRNA (2)

Target mRNA: AATTCGATATGTTTCAGCAAGA

SiRNA(2): UUCGAUAUGUUCAGCAAGA-UU (sense strand)

UU-AAGCUAUACAAGUCGUUCU (antisense-strand)

Scrambled negative control siRNA: CAGUCAGAUAUUAGAACCU (sense strand)

UCCAAGAUUAAACUAGACUGAC (antisense-strand)

Figure 9. Sequence information of *GPX4* mRNA transcript and *GPX4* siRNA(1), (2) and scrambled negative control siRNA.

(A) The *GPX4* gene encodes 7 exons (exon 1a and exon 2 to 7). *mGPx4* is transcribed from exon 1a to exon 7 and *cGPX4* is transcribed from exon 2 to 7. *GPX4* gene also encodes an alternative exon 1 as exon 1b, which is used to transcribe *nGPX4* but this is not shown above. Exon 1a is suggested to translate a mitochondrial translocation leader sequence whereas exon 2 to 7 was suggested to translate the main part of *GPX4* with catalytic function (Arai et al., 1996). Exons are separated by brackets and the mRNA targets of *GPX4* siRNA (1) and *GPX4* siRNA (2) are respectively underlined. (B) Sequence of *GPX4* siRNA (1) (design 1) and *GPX4* (design 2).

Since a short sequence of 84 nucleotides is the only differential sequence between m*GPX4* and c*GPX4* both *GPX4*-siRNAs was designed to sequences within exon 3 and exon 4.

GPX4 siRNA(1) and *GPX4* siRNA(2) target sequences were present in both c*GPX4* and m*GPX4* transcripts and therefore these siRNAs were unable to differentiate between the c*GPX4* and m*GPX4* transcripts expressed and would deplete both the c*GPX4* and m*GPX4* in Caco-2 cells. However, as indicated by RTPCR c*GPX4* is the major form in these cells.

3.3 Effect of GPx4 knock-down on *GPX4* mRNA and protein expression

To test the ability of siRNA to knockdown *GPX4* expression, Caco-2 cells were seeded in a 6-well plate 24 h before transfection with either 20 or 40 nM of *GPX4*-siRNA (1), or scrambled control siRNA. Treatment with siRNA was maintained for 48-72 h following transfection and knock-down at mRNA level assessed by semi-quantitative RT-PCR using total RNA harvested from cells after 48 h. The mRNA expression of *GPX4* and *GAPDH* was assessed; the ratio of *GPX4/GAPDH* was calculated and further normalized as mean percentage of the scrambled control siRNA. To assess the knockdown at the protein level, treatment by each *GPX4*-siRNA was maintained for 72 h following transfection. Total cell lysate was harvested and GPx4 expression was determined by western blot using polyclonal anti-GPx4 as described in (Chapter 2 Section 2.4-2.4.6).

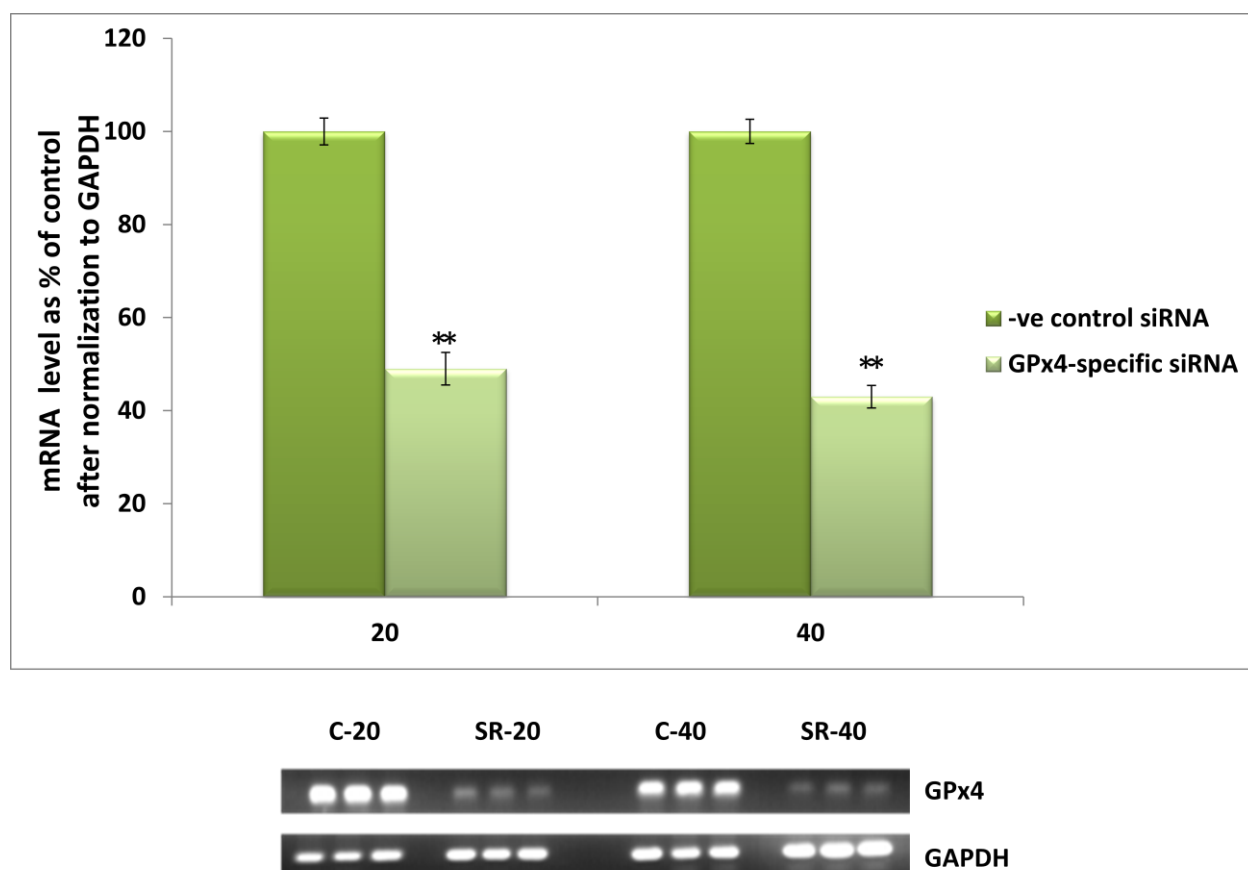


Figure 10. Knock-down of GPX4 mRNA expression in Caco-2 cells.

*Undifferentiated Caco-2 cells were treated with 20 or 40 nM GPX4-siRNA(1) or a scrambled negative control siRNA for 48 h. RNA was isolated, reverse transcribed and subjected to PCR using primers specific to both long and short forms of GPX4. Semi-quantitative RTPCR was used to assess levels of GPX4 knock-down at mRNA level (SR=siRNA, C=negative control siRNA). GPX4 mRNA levels were calculated relative to that of the GAPDH transcript and expressed as a percentage of the mean value for cells treated with the scrambled negative control siRNA. Values shown are mean \pm s.e.m. of n=6. Groups were compared using a Mann-Whitney U test, * p<0.05, ** p<0.01.*

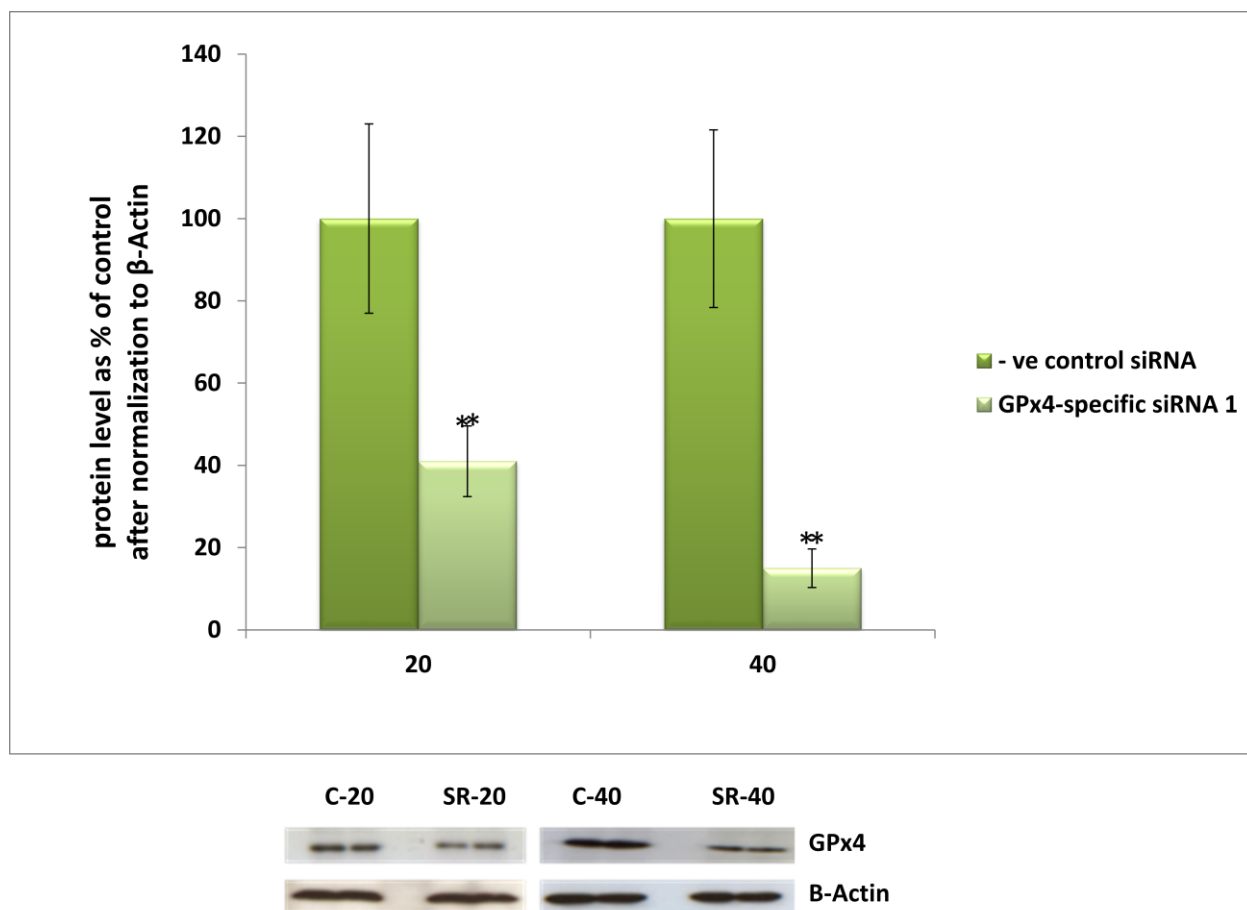


Figure 11. Knockdown of GPx4 expression at the protein level.

*Caco-2 cells treated with either 20 or 40 nM of GPX4-siRNA(1) or a scrambled negative control for 72 h. Following transfection, total protein was extracted and protein expression assessed by Western blotting using an anti-GPx4 antibody. Protein expression was calculated relative to that of B-Actin and then as a percentage of the mean value for cells treated with the scrambled negative control siRNA. Western panels =2 wells, values shown are mean \pm S.D of n=6. Groups were compared using a Mann-Whitney U test, * $p<0.05$, ** $p<0.01$.*

As shown in Figure 10, treatments with 20 and 40 nM of *GPX4*-siRNA(1) resulted in a clear decrease in *GPX4* mRNA expression, compared to the control group treated with scrambled negative control siRNA. In addition, *GAPDH* expression was not affected by *GPX4*-siRNA treatments. Quantification by densitometry of the RT-PCR bands allowed calculation of the *GPX4* expression as a ratio of *GPX4/GAPDH* transcript levels. As shown in Figure 10, *GPX4* mRNA levels were reduced by ~50-60% with 20 and 40 nM respectively, compared to the group treated with scrambled control siRNA. Therefore, *GPX4*-siRNA was able to cause *GPX4* knockdown in Caco-2 cells. Cells treated with 40 nM *GPX4*-siRNA appeared to have a greater knockdown effect.

In order to test GPx4 knockdown at the protein level, treatments with 20 and 40 nM *GPX4*-siRNA(1) were maintained for 3 days. As shown in Figure 11, groups treated with *GPX4*-siRNA exhibited reduced GPx4 protein expression to various extents when compared to the scrambled negative control group. Significant knockdown of GPx4 protein was observed in both groups treated with 20 and 40 nM siRNA; 40 nM treatment appeared to have greater knock-down effect on GPx4 protein level. Using densitometry, quantification of the protein bands was carried out and levels of GPx4 protein calculated as a ratio of GPx4/B-Actin protein levels, and further normalized as a mean percentage of the scrambled control. GPx4 protein expression was reduced by ~60% and ~85% by treatment with 20 and 40 nM siRNA respectively. Therefore, treatment with 20 nM siRNA was found to achieve a similar knockdown in GPx4 expression (~50-60%) at both mRNA and protein levels, and treatment with 40 nM siRNA was found to result in a greater effect on GPx4 protein expression with knockdown of around 85%.

3.4 Investigating the genome-wide effects of *GPX4* on gene expression

To investigate the function of *GPX4*, direct effects of *GPX4* manipulation (knock-down) on global gene expression was investigated. Microarray-based techniques allowed for the genome-wide effects of *GPX4* manipulation to be probed, profiling global gene expression changes in response to changes in *GPX4* levels. RNA for transcriptome analysis under conditions of *GPX4* knockdown was obtained from cells treated as described in Chapter 2, Section 2.2 to 2.31. RNA for expression analysis was prepared from three independent experiments to produce three biological repeats for each condition (*GPX4* knockdown and corresponding controls), of which all three biological replicates for *GPX4* knock-down and control were hybridised to the expression array. After confirmation that siRNA treatment knocked-down GPx4 protein expression at 72 h following treatment with 20 and 40 nM siRNA, gene expression profiles were measured using the Illumina Gene Expression Service provided by Service XS (Leiden, The Netherlands). Prior to microarray analysis, each RNA sample was subjected to quality and integrity checks before global gene expression. RNA quality was assessed by spectrophotometry and integrity was assessed using Bioanalyser; the integrity output of the Bioanalyser for the samples analysed by microarray hybridisation are shown in Figure 12.

A



B

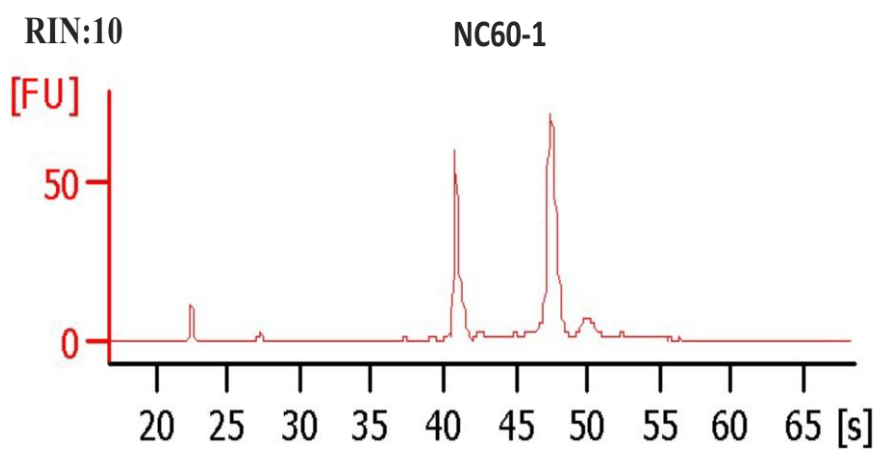


Figure 12. Integrity of RNA used for microarray analysis.

(A) Gel-like electropherogram output image generated from the bioanalyser for 12 samples. (B) Bioanalyser electropherogram output for the samples showing 2 clear bands indicative of good quality RNA. An RNA integrity number (RIN) of 7 or more indicates RNA of sufficient quality.

3.4.1 Microarray hybridisation

The Illumina HumanHT-12 v4 Expression BeadChip comprises 12 identical arrays targeting over 47,000 probes covering genes, gene candidates and splice variants from the 2009 NCBI RefSeq Release 38. RNA samples from 20 and 40 nM siRNA and scrambled negative control treatment were reverse transcribed to produce a cDNA template that was transcribed *in vitro* and amplified to incorporate biotin-labelled nucleotides. Biological triplicates of the RNA samples from cells in which *GPX4* expression was reduced by siRNAs and the corresponding control were hybridised onto individual arrays within the HumanHT-12 v4 Expression BeadChip (Illumina). Signals of the hybridized-labeled sample were developed with Streptavidin-Cy3 and scanned with BeadChip. The intensity value for each probe and gene expression data from the scan images was calculated.

3.4.2 Data analysis

The microarray raw data was supplied electronically and was deposited in GEO (accession GSE40287). Using RankProd analysis (Hong *et al.*, 2006) and visualisation in Genespring GX11 (Agilent) on a quality filtered subset of microarray probes, genes for which expression was up-regulated or down-regulated by a factor of 1.2 fold or greater under conditions of *GPX4* knockdown were identified (Appendices A1 and A2). 795 genes showed a 1.2 fold or greater change in gene expression with p-value of <0.05.

After identification of genes whose expression was reduced or increased, confirmation of changes in biological pathway (s) was deemed necessary. Ingenuity Pathway analysis (IPA) tool was utilised to investigate changes in biological pathways resulting from *GPX4* knock-down. The observed 795 genes were mapped into IPA to generate both pathways and networks. Network eligible molecules were generated from the input microarray data by IPA on the basis of their expression and/or their interaction with other molecules in the Ingenuity Knowledge Base (IKB). In addition, pathway eligible molecules were selected from the microarray dataset by IPA due to their expression values and/or due to having at least one functional annotation or disease association in the IKB. The network eligible molecules then served as “seeds” for generating networks that were overlaid onto available networks to maximize their connectivity with each other relative to all molecules to which they are connected within the IKB.

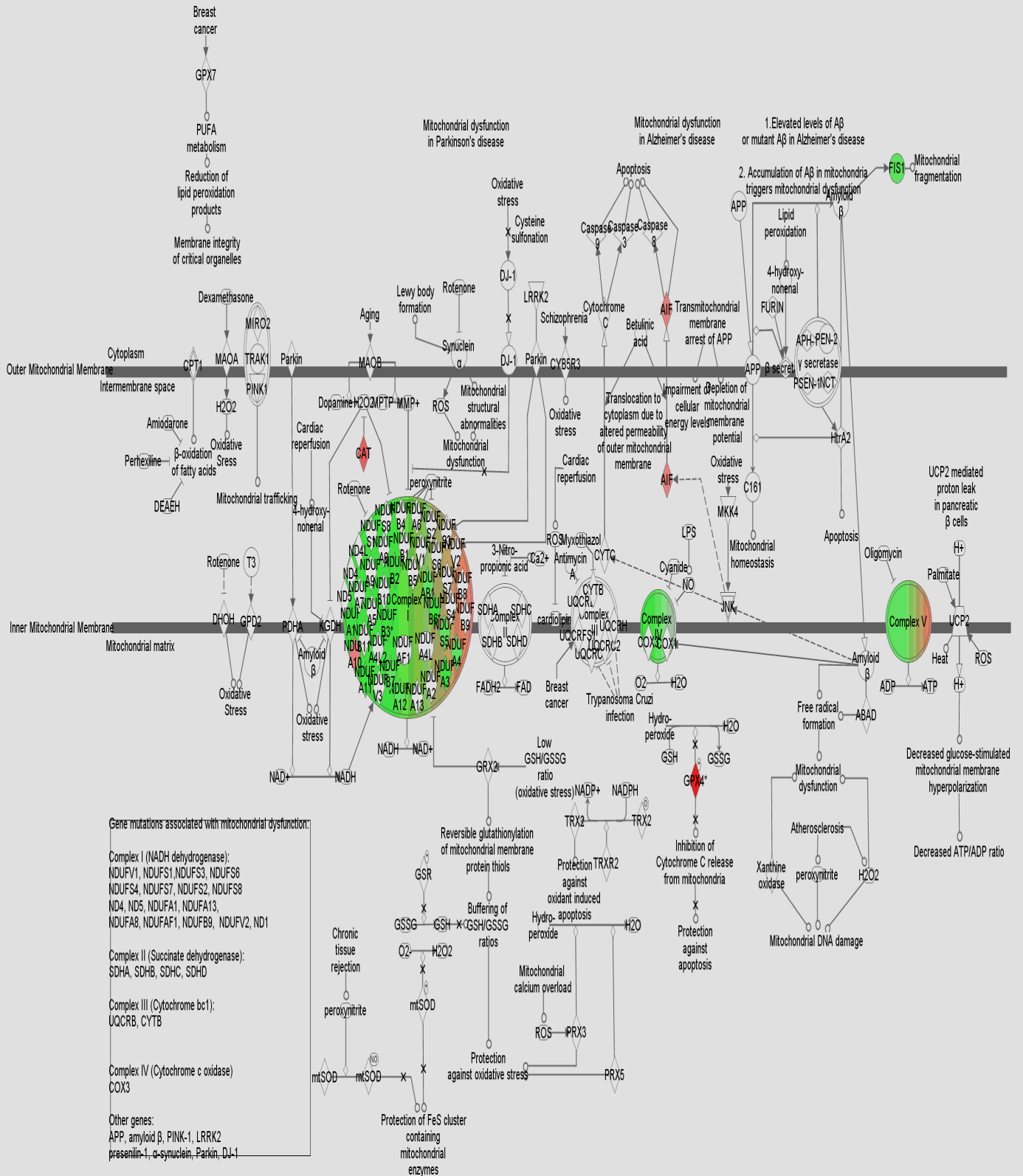
Ingenuity Pathway analysis (IPA) of this dataset showed that the major canonical pathways most significantly affected by *GPX4* knock-down were oxidative phosphorylation, ubiquinone biosynthesis and mitochondrial dysfunction, and the top two toxicological lists were mitochondrial dysfunction and oxidative stress (Table 6). Visualisation of these pathways in a network showed clearly that differentially expressed genes were clustered as those coding for components of mitochondrial complexes I, IV and V (Figure 13); importantly, apoptosis-inducing factor (*AIF*), a key node in the network, was also differentially expressed. Microarray hybridization and data analysis was carried out with both 20 and 40 nM *GPX4* siRNA(1) and negative control siRNA. Changes in gene expression and pathway analysis were the same with both concentrations of siRNA.

CANONICAL PATHWAYS (Already established pathway in IPA)	TOTAL GENES	GENES THAT CHANGED	FOLD CHANGE	P VALUE
OXIDATIVE PHOSPHORYLATION	166	28	1.2-1.7	5.26E-12
UBIQUINONE BIOSYNTHESIS	119	15	1.3-1.7	1.08E-08
MITOCHONDRIAL DYSFUNCTION	172	23	1.3-2.2	1.15E-08
COAGULATION SYSTEMS	37	9	1.3-2.3	7.65E-06
GLYCOSAMINOGLYCAN DEGRADATION	72	7	1.3-2.0	3.6E-04
ARYL HYDROCARBON RECEPTOR SIGNALING	157	15	1.2-1.6	4.43E-04
LPS/IL-1 MEDIATED INHIBITION OF RXR FUNCTION	208	18	1.2-1.6	8026E-04
PURINE METABOLISM	440	25	1.2-1.7	1.07E-04

TOX LIST	TOTAL GENES	GENES THAT CHANGED	FOLD CHANGE	P VALUE
MITOCHONDRIA DYSFUNCTION	125	20	1.3-2.2	1.39E-07
OXIDATIVE STRESS	57	9	1.3-2.4	4.4E-04
LPS/IL-1 MEDIATED INHIBITION OF RXR FUNCTION	187	18	1.2-1.6	6.05E-04

Table 6. Pathway analysis of the transcriptomic data after GPx4 knock-down.

Table show the canonical pathways and toxicological pathway list found to be most significantly affected by IPA analysis of the microarray data after GPX4 knock-down. Core Analysis in Ingenuity Pathway Analysis (IPA) was used to analyse affected pathways of the microarray dataset from the GPX4 knock-down experiment. Ingenuity Pathway Analysis (IPA) highlighted changes in pathways associated with mitochondrial function including oxidative phosphorylation and ubiquinone biosynthesis and oxidative stress.



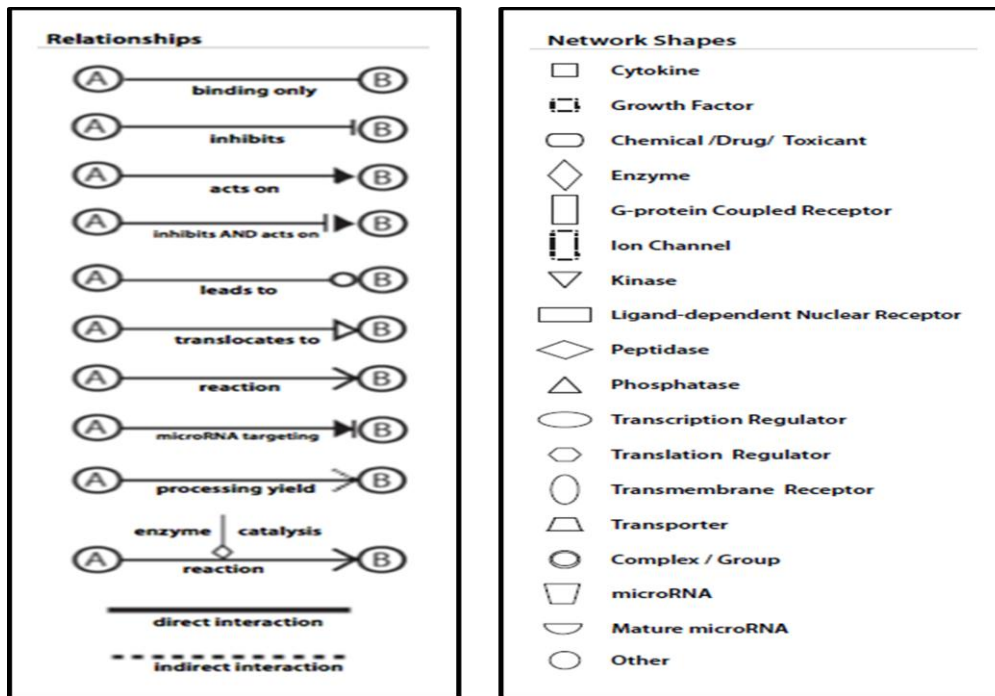


Figure 13. Network analysis of the transcriptomic data.

Network analysis of the transcriptomic data showing changes in genes encoding complex I, IV and V of the mitochondrial electron transport chain following GPX4 knock-down. Both pathway and network analysis of the transcriptomic data indicated alterations in expression of genes encoding components of mitochondria electron chain complexes I, V and IV. The largest circle within the inner mitochondrial membrane is complex I of the mitochondrial electron transport chain, followed by the two highlighted complex IV and V respectively. Up-regulated genes are highlighted in green and down-regulated genes highlighted in red.

3.4.3 Validation of transcriptomic data

To validate the microarray results, quantitative real-time polymerase chain reaction (qRT-PCR) assays were carried out. Remnants of the same RNA extracted from Caco-2 cells treated with *GPX4*-siRNA and scrambled negative control siRNA that was used for the microarray experiment and from a subsequent knockdown were utilised. Validation of the microarray data using qRT-PCR was necessary to confirm that some of the observed changes in gene expression in the microarray data were not by chance and could be reproduced using another technique. qRT-PCR amplifies a gene of interest (target gene) specifically in a given sample and monitors the amplification progress through the utilization of fluorescence technology (Valasek & Repa, 2005).

Since *GPX4* knock-down had major effects on expression of components of complexes I, IV and V, validation of the microarray data by real-time PCR was focussed on specific target genes that code for components of these complexes. The genes selected were: Cytochrome C oxidase copper chaperone (*COX17*), a component of mitochondrial complex IV, which was up-regulated according to the microarray data; NADH dehydrogenase (ubiquinone) 1 alpha subcomplex 6 (*NDUFB6*) a component of complex I and also up-regulated on the microarray; NADH dehydrogenase (ubiquinone) 1 alpha subcomplex 10 (*NDUFA10*), a component of complex I that was down-regulated according to the microarray data; *AIF* and Bcl2 associated X protein (*BAX*), which were down-regulated and up-regulated respectively on the microarray. ATP synthase, H⁺ transporting mitochondrial FO complex, subunit E (*ATP5I*), a component of complex V that was up-regulated according to the microarray data

was investigated with RT-PCR. There was however, enormous difficulty in getting the *ATP5I* primers to amplify hence, the expression of this gene could not be investigated. As shown in (Figure 14) real-time qRTPCR showed that *GPX4* knock-down caused significant down-regulation of *NDUFA10*, and up-regulation of *NDUFB6* and *COX17*, in concordance with the microarray data. Similarly, real-time qRTPCR also confirmed that *GPX4* knock-down led to decreased *AIF* mRNA expression and increased *BAX* expression as found by microarray analysis. *GAPDH* was used as house-keeping genes to normalize the target genes. Although the fold change observed for the up-regulated genes assessed by qRTPCR was higher than that of the microarray experiment and the change in down-regulated genes lower than that of the microarray overall, but the direction of change obtained with the two techniques was the same, so validating the microarray data.

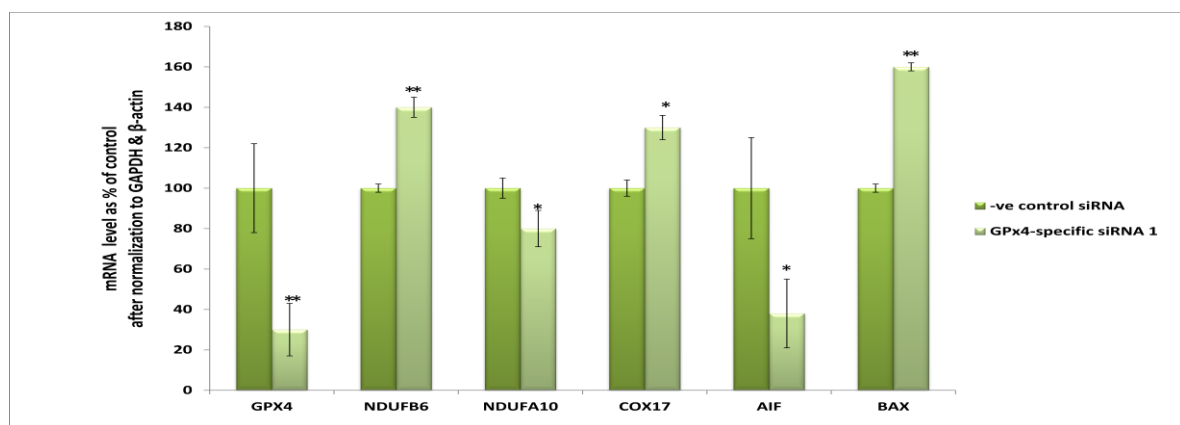


Figure 14. Confirmation of GPX4 knock-down transcriptomic data by quantitative RT-PCR.

*RNA was isolated from Caco-2 cells treated with 20 nM GPX4-siRNA(1) or a scrambled negative control siRNA and target gene expression measure by quantitative RTPCR. Expression was calculated relative to GAPDH and β -actin as the housekeeping control and then as a percentage of the mean value for cells treated with the negative control siRNA. Results confirmed the changes in gene expression observed with the transcriptomic data. Values shown are mean \pm s.e.m. for n=6. Groups were compared using a Mann-Whitney U test, * $p < 0.05$, ** $p < 0.01$*

3.5 Investigation of mitochondrial complex I and IV protein expression following

***GPX4* knock-down**

To investigate if *GPX4* knock-down alters the protein expression of complex I and IV of the mitochondrial electron transport chain, Western blotting was used to analyse levels of major markers of complex I (NADH dehydrogenase (ubiquinone) 1 beta subcomplex 8; NDUFB8) and complex IV function (cytochrome c oxidase subunit II; COX2). Seventy two hours after transfection, cells treated with 20 nM *GPX4*-siRNA(1) were found to have a statistically significantly higher protein expression of both NDUFB8 and COX2 (~150% and 75%) respectively compared to cells treated with the negative control siRNA (Figure 15).

A

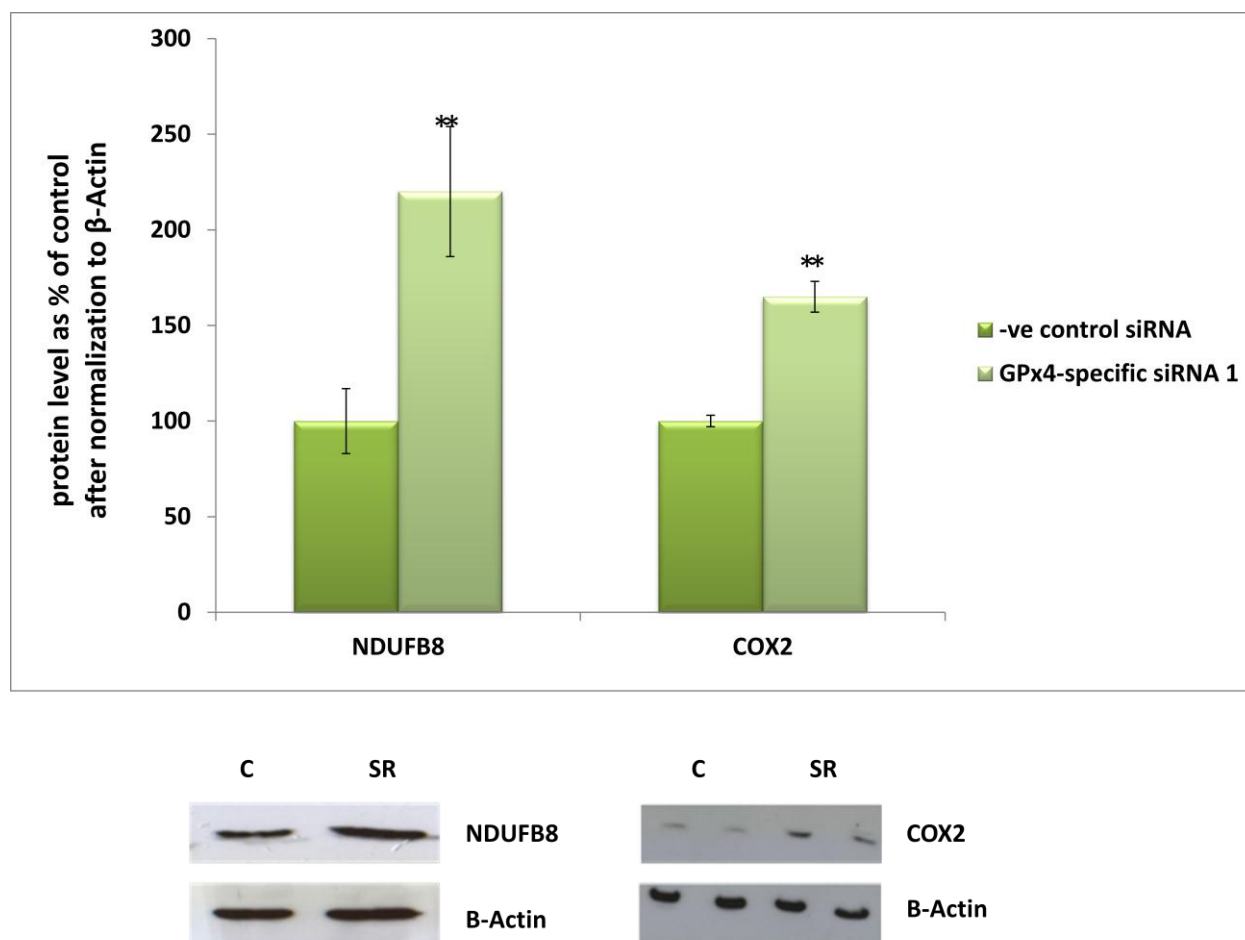
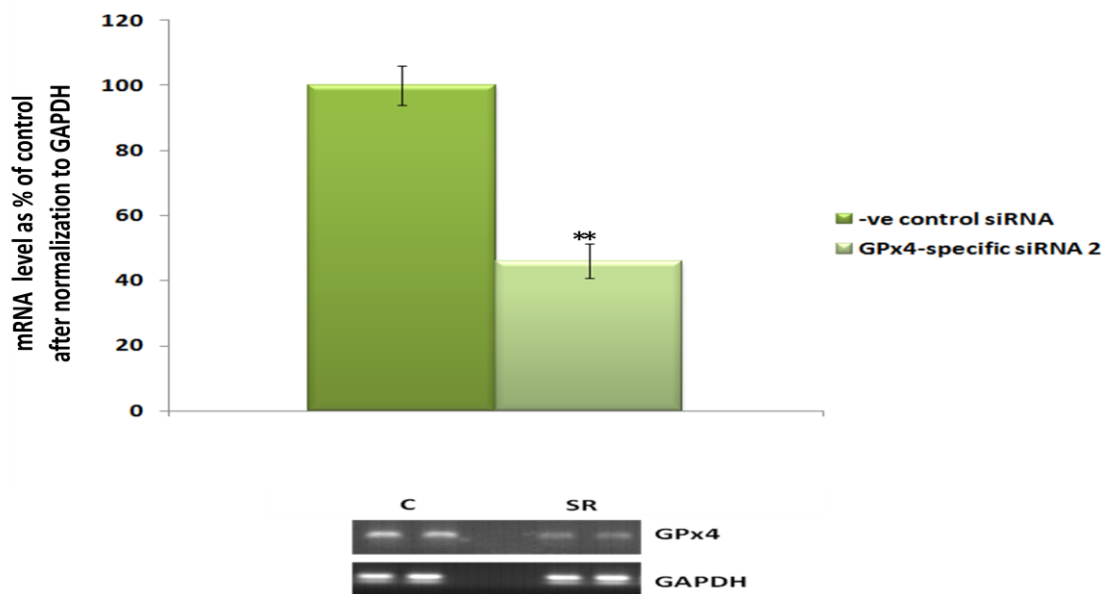


Figure 15. Expression of markers of mitochondrial complexes I and IV after GPX4 knock-down.
*Total protein was extracted from Caco-2 cells treated with GPX4-siRNA (1) or the scrambled negative control for 72 h. Expression of NDUFB8 (mitochondrial complex I indicator) and COX2 (mitochondria complex IV indicator) were measured by western blotting. Protein expression was calculated relative to B-Actin and then as a percentage of the mean value for cells treated with the scrambled control siRNA. Western panels = 2 wells, values shown are mean \pm S.D of n=6. Groups were compared using a Mann-Whitney U test, * $p < 0.05$, ** $p < 0.01$*

3.6 Effects of a second GPX4-specific siRNA on mitochondrial protein expression

As a control, to exclude non-specific off-target effects of the siRNA treatment, measurement of the two mitochondrial components NDUFB8 and COX2 was repeated in cells treated with a second *GPX4*-siRNA. As shown in Figure 16A-B, semi-quantitative RTPCR and Western blotting showed that treatment with this second siRNA for 72 h led to a ~50% decrease in *GPX4* mRNA a ~60% decrease in GPx4 protein expression. This *GPX4* knock-down was accompanied by a 30% increase in NDUFB8 protein expression and a 50% increase in COX2 protein Figure 16C. These results confirm that *GPX4* knock-down with a second siRNA affects expression of components of mitochondrial complexes I and IV, as observed with the first siRNA, indicating that the effects are due to knock-down of *GPX4* and not due to off-target effects.

A



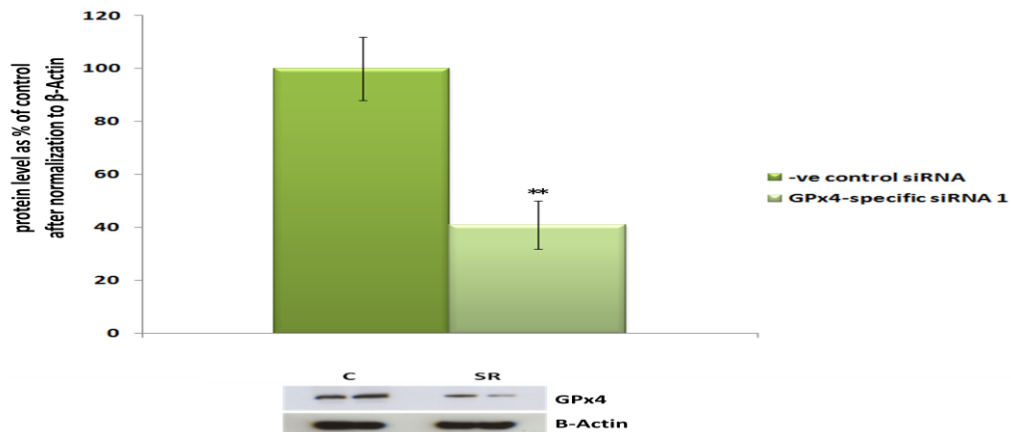
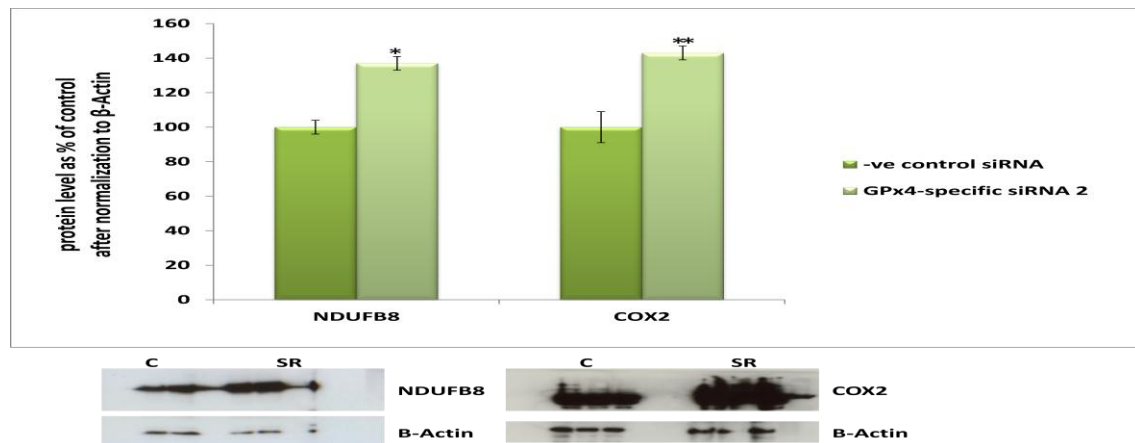
B**C**

Figure 16. Expression of GPx4 mRNA and protein and markers of mitochondrial complexes I and IV after GPX4 knock-down with siRNA (2).

Total RNA and protein was extracted from Caco-2 cells treated with GPX4-siRNA (2) or the scrambled negative control. (A) Percentage expression of GPX4 mRNA following 48 h cell treatment with the second GPX4-siRNA and scrambled negative control mRNA levels were calculated relative to GAPDH as the housekeeping control. (B) Percentage expression of GPx4 protein following 72 h treatment with the second GPX4-siRNA and scrambled negative control. (C) Percentage expression of NDUFB8 and COX2 protein after 72 hours treatment with GPX4-siRNA (2). Protein levels were calculated relative to β-actin as the housekeeping control and then as a percentage of the mean value for cells treated with the negative control siRNA. PCR and western panels = 2 wells, values shown are mean ± S.D of n=6. Groups were compared using a Mann-Whitney U test, * p<0.05, ** p<0.01.

3.6 Discussion

Several selenoproteins such as *GPXI* and *GPX4*, which use glutathione as a substrate, and thioredoxin reductase, which controls the redox state of thioredoxin, are thought to have roles in regulating cellular redox state and intracellular ROS levels. These proteins are often viewed as antioxidants, but their contributions to redox regulation are not fully understood. In order to explore the role of *GPX4* in gut epithelial cell, *GPX4* mRNA and protein expression was knocked-down in Caco-2 cell line and a global gene expression analysis was carried out to study downstream effects.

Previous studies have investigated functions of *GPX4* using transgenic mouse model (Seiler *et al.*, 2008) and cell lines overexpressing an additional mouse or human allele (Imai *et al.*, 2006; Barriere *et al.*, 2004). These studies have suggested roles for *GPX4* in regulation of apoptotic and inflammatory pathways. Gene knock-down approaches using antisense or siRNA approaches provide alternative tools to investigate *GPX4* functions. There are only a few studies in this field using antisense methods to inhibit *GPX4* mRNA expression and these reported different results. Studies on epidermal carcinoma A431 cells reduced *GPX4* expression by 20% in one study (Chen *et al.*, 2000) and 10% in a second study (Chen *et al.*, 2003). Another group used an antisense approach, but in the P4 (MCF-7) cell line, and achieved inhibition of mitochondrial *GPX4* mRNA and protein by 25% approximately (Zhao *et al.*, 2003). Another study on NIH3T3 cells transfected with either PU6-m3 control vector or PU6-M3 vectors containing four different sets of *GPX4*-siRNA achieved 50-80% reduction of *GPX4* mRNA and protein (Yoo *et al.*, 2010).

The use of small interfering RNA (siRNA) has become a technique of choice for lowering gene expression. This method essentially uses a synthesized exogenous small dicer strand RNA (dsRNA) which recognizes and recruits the enzyme complex to a target mRNA. siRNA is ideal for study of dynamic cellular processes because it produces a rapid inhibition of expression in 2-4 days. This compares with long term knock down which takes a longer time and is achieved by stable transfection using a specific short RNA sequence in a vector (e.g. small-hairpin shRNA). In this study, a pre-designed siRNA specific to *GPX4* and a negative control siRNA (-ve control siRNA) designed by mismatching and scrambling the siRNA sequence was used to knock-down the expression of *GPX4* gene in Caco-2 cells. The siRNA matches a 21nt target in exon 4 and optimal prediction was achieved according to various algorithms (Reynolds *et al.*, 2004; Ui-Tei *et al.*, 2006). Additional considerations were applied in order to achieve efficient transfection; (a) cell culture medium used during transfection contained only half the concentration of foetal calf serum so as to minimize the interferon response which could easily occur as a result of interaction between serum and siRNA (according to Ambion user manual), (b) antibiotic was not added to the medium during transfection (according to Ambion user manual), (c) medium was changed 24 h after transfection to minimize cytotoxicity that can be caused by the lipofectamine or the remaining siRNA (as per Ambion user manual).

As judged by semi-quantitative PCR *GPX4* expression was lower following 48 h after transfection with the *GPX4*-siRNA(1) compared with cells transfected with the negative control siRNA. To compensate for any variation in loading and RT efficiency *GPX4* mRNA levels were normalised by calculating the ratio of *GPX4*/*GAPDH* mRNA levels and was further normalized as a mean percentage of the scrambled

control for change in expression. siRNA reduced *GPX4* mRNA by approximately 50-60 % for 20 and 40 nM respectively. The important effect of any siRNA is on the target protein level and in the present work GPx4 protein level was assessed by western blotting 72 h after transfection (protein level is expected to be knocked-down later than the mRNA). Also to compensate for variation in loading GPx4 protein levels were normalised by calculating the ratio of GPx4/ β -actin protein levels and further normalized as a mean percentage of the scrambled control for change in expression. Overall the data indicate knock-down of *GPX4* at both mRNA (2 days) and protein levels (3 days) in agreement with previous findings that siRNA function efficiently 1-3 days post-transfection (Ui-Tei *et al.*, 2006).

The work described in this chapter was a hypothesis-generating genome-wide experiment which aimed to investigate whether reduction in levels of GPx4 protein is sufficient to bring about some consequential effect on a range of biological pathways. Such approaches would detect changes in gene expression as a result of changing the level of *GPX4* expression through all active mechanisms – not only effect on gene expression but also downstream effects on different biological pathways. For example, multiple cellular substrates undergo *GPX4*-mediated ROS or apoptosis induction, including transcription factors and co-regulators that are required for gene expression.

These findings were novel and provide the first transcriptomic evidence to associate reduced *GPX4* expression with dysfunctional mitochondria, particularly in relation to alteration in the mitochondrial oxidative phosphorylation and biosynthesis of ubiquinone in gut epithelial cell. Further investigation into the effects of these altered biological pathways through biological network analysis revealed

changes in mitochondrial electron transport complexes I, IV and V and its components. The mRNA expression of most of the genes within these complexes were up-regulated except for *NDUFA10* which was down-regulated. Validation of the microarray experiment using qRT-PCR confirmed the same pattern of change in gene expression in the selected genes as observed in the microarray data.

Using protein extracted from the GPx4 knock-down experiment using siRNA(1), expression levels of protein encoding components of the mitochondrial electron transport chain complex I and IV were assessed by Western blotting. Depletion of *GPX4* resulted in a significant reduction in protein expression of protein encoding the complex I and IV of the mitochondrial electron transport chain. NDUFB8 and COX2 are strong functional indicators of mitochondrial electron transport chain complex I and IV respectively (Funk & Schnellmann, 2012; Matsumoto *et al.*, 2012). To confirm that these findings with the first siRNA were not by chance, a second siRNA specific to *GPX4* was utilized. Treatment with this second siRNA led to efficient *GPX4* knock-down and this was accompanied by increases in NDUFB8 and COX2 components of mitochondrial complexes I and IV of electron transport chain. Protein expression levels of NDUFB8 and COX2 were increased by ~40% and 50% respectively following *GPX4* knock-down with a second siRNA (Figure 16C), indicating that the previous findings with the first siRNA were not by chance.

Interaction with allosteric effectors allows the rapid regulation of OXOPHOS activity to occur. Non-catalytic binding sites for ADP and ATP in various enzymes and or proteins (Wierenga *et al.* 1986; Rajagopalan *et al.* 1999; Robblee *et al.* 2005; Inoue and Shingyoji 2007), including ATP synthase

(Walker *et al.* 1982), have been identified. The regulatory ability of enzyme activity to bind ADP or ATP to the same site depending on ATP/ADP ratio has been shown for complex IV (COX) subunits. Mammalian OXOPHOS comprises of five enzyme complexes of multiple subunits. Complex I (NADH dehydrogenase) comprises of 45 subunits, 4 subunits in complex II (succinate dehydrogenase), 11 subunits in complex III, 13 subunits in complex IV, and 17 subunits in complex V (ATP synthase) (Carroll *et al.* 2009; McKenzie *et al.* 2009). The complexes must be appropriately encoded, partly on mtDNA and partly by nuclear DNA (except for complex II). Complex formation requires multiple assembly factors and in case of defects, or alterations, may result in various mitochondrial diseases (Kadenbach 2012).

Following ischemia and reperfusion, transgenic mice overexpressing mGPX4 showed reduced levels of lipid peroxide compared to the control group (Dabkowski *et al.*, 2008). These mice also exhibited increased electron transport chain complex I, III, and IV activities in the heart compared with control mice following ischemia reperfusion. The same study showed that overexpression of mGPX4 increased complex I, III, IV activities in subsarcolemmal mitochondria and electron transport chain complex I and III activities in interfibrillar mitochondria. These results from Dabkowski suggested that overexpression of mitochondrial form of GPX4 protects cardiac contractile function and preserves electron transport chain complex activities following ischemia (Dabkowski *et al.*, 2008). These findings complement the work described in this thesis in the sense that reduced GPX4 would result in the loss of function in living organisms, whereas, increased expression of GPX4 would lead to a gain in function. Since the Western blotting data indicate that GPX4 knock-down led to changes in expression of components of

complexes I and IV, findings that correlate with the observed changes in RNA expression of genes expressing components of these complexes, an investigation into mitochondrial integrity and function was carried out, as described in the next Chapter.

Chapter 4: Investigation of mitochondrial function and integrity following *GPX4* knock-down

4.1 Introduction

Deleterious Reactive oxygen species (ROS) modify biological molecules such as nucleic acids, proteins and lipids, and this can result in cell abnormalities (Droge, 2002; Rhaods *et al.*, 2006). On other hand, it has been widely shown that ROS play vital roles in various signaling cascades that regulate the balance between biological processes such as cellular respiration, cell growth, differentiation and death (Brand & Nicholls *et al.*, 2011). Alteration or imbalance in ROS regulation could cause damage in organelles such as the mitochondria (Laloi *et al.*, 2004; Clifton *et al.*, 2005). To maintain normal cell function, a precise balance between ROS generating processes and ROS degrading processes is crucial. Glutathione peroxidases (GPx) are family of selenium dependent enzymes known for their cellular protective function against ROS. At the expense of reduced glutathione, GPx reduces hydroperoxides to the corresponding alcohols. In particular, GPx4 scavenges lipophilic hydroperoxides and in mice, knockdown of this gene leads to abnormal embryonic development and lethal phenotypes in mice (Borchert *et al.*, 2006).

Energy is essential for biological processes and is mostly based on the synthesis of high energy adenosine triphosphate (ATP) by either glycolysis or oxidative phosphorylation (Jezek & Havata 2005). Adenosine diphosphate is converted to ATP through the reduction of nicotinamide adenine dinucleotide (NADH) as electron donor and oxygen as electron acceptor in the electron transport chain (Muller *et al.*,

2004). However, oxidative metabolism is a potential hazard due to ROS and reactive nitrogen species (RNS) being formed as byproducts, particularly the superoxide anion and hydroxyl radical (OH[•]) (Kowaltowski *et al.*, 2009). ROS and RNS have the ability to remove electrons from other molecules and transform them into free radicals and the resulting free radicals are able to modify biological molecules and macromolecules such as polysaccharides (Kaur & Halliwell, 1994), DNA (Richter *et al.*, 1988; LeDoux *et al.*, 1999), RNA (Stadtman & Levine, 2000), proteins (Carney *et al.*, 1991) and lipids (Rubbo *et al.*, 1994) and can alter their function (Sweetlove *et al.*, 2002; Winger *et al.*, 2005).

GPX4 is a unique glutathione peroxidase using phospholipid hydroperoxides as a substrate (Brigelius-Flohe, 1999; Imai & Nakagawa 2003; Bellinger *et al.*, 2009), and in Chapter 3 data is presented to indicate that knock-down of *GPX4* expression leads to changes in expression of components of the mitochondrial electron transport chain complexes. Therefore, one possibility is that the changes in complexes I, IV, and V observed following *GPX4* knock-down may be due to alterations in the mitochondrial membrane, changes in lipid peroxide status and mitochondrial damage as a result of increase in ROS. Such damages would also be expected to possibly lead to alterations in mitochondrial function.

Measurement of mitochondrial respiration is an important tool for understanding regulation of cellular bioenergetics and provides an appropriate indication of the function of mitochondria (Schuh *et al.*, 2012). Hence, experiments were carried out to investigate mitochondrial respiration and parameters of mitochondrial membrane integrity following *GPX4* knock-down in Caco-2 cells. There are different

approaches to investigate mitochondrial function and dysfunction particularly with respect to cellular respiration. Measurements of fluxes by oxygen electrode give information about mitochondrial ability to maintain stable cellular respiration and synthesize ATP (Fernyhough *et al.*, 2010; Ferreira *et al.*, 2010). Cell respiratory control has been shown to be the best approach for the study of cell respiration and this approach reports proton leak rate, coupling efficiency, maximum respiratory rate, respiratory control ratio, spare respiratory capacity and ATP synthesis while measurement of mitochondrial membrane potential provides additional useful information (Fernyhough *et al.*, 2010; Brand & Nicholls, 2011). In the present experiments, respiration was measured using an oxygen electrode (Chapter 2, Section 2.10). In addition, other parameters of mitochondrial function were measured: ATP levels using a recombinant firefly luciferase assay (Chapter 2, Section 2.8), mitochondrial membrane potential using JC-1 (Chapter 2, Section 2.9), lipid peroxide levels using thiobarbituric acid measurements (Chapter 2, Section 2.6), cellular ROS and mitochondria superoxide levels by carboxy-H₂DCFDA and MitoSOX™ Red methods respectively (Chapter 2, Section 2.7 & 2.7.1 respectively). These measurements were made to test the hypothesis that *GPX4* knock-down led to mitochondrial oxidative stress. To address this, levels of both mitochondrial oxidative stress were measured after *GPX4* knock-down. Finally, cell viability was assayed using CellTiter-Blue® array (Chapter 2, Section 2.5).

4.2.1 Impact of *GPX4* knock-down on Lipid peroxides and ROS.

Caco-2 cells were seeded and transfected after 24 h with either *GPX4*-siRNA or a scrambled negative control siRNA. Seventy two hours after transfection, cells were assayed specifically for lipid peroxides and mitochondrial superoxide, *GPX4* knock-down with *GPX4*-siRNA(1) led to a two-fold increase in lipid peroxidation (Figure 17A) and a two-fold increase in mitochondrial superoxide (Figure 17B); the latter may reflect not only increased mitochondrial superoxide levels but also increased activity of other one-electron oxidants such as cytochrome c and H₂O₂ (Lowes & Galley, 2011). Treatment with a second *GPX4*-siRNA also showed increase mitochondrial ROS formation (Figure 18A), confirming that these effects are specifically due to knock-down of *GPX4* and not due to off-target effects.

4.2.2 Impact of *GPX4* knock-down on mitochondrial membrane potential ($\Delta\Psi_m$) and ATP production

Since both superoxide formation and mitochondrial membrane damage have been reported to impair oxidative phosphorylation (Hamanaka & Chandel, 2010) and ATP synthesis (Szeto *et al.*, 2009), measurement of mitochondrial membrane potential and mitochondrial ATP levels were measured after *GPX4* knock-down. *GPX4* knock-down led to a significant reduction in mitochondrial membrane potential a marker of mitochondrial membrane damage by ~ 24% (Figure 19A), and a decrease in mitochondrial ATP by ~30% (Figure 19B). compared with cells treated with the control siRNA

Overall, these results suggest that *GPX4* protects mitochondria from oxidative damage and plays a crucial role in regulating and maintaining the oxidative phosphorylation system and ATP synthesis.

4.2.3 Effects of *GPX4* knock-down on mitochondrial respiration and cellular ROS

To further explore the consequences of *GPX4* knock-down on mitochondrial function, direct measurements of mitochondrial respiration were made in Caco-2 cells treated with either *GPX4*-siRNA(1) or the scrambled negative control siRNA. Oxygen consumption was monitored following addition of metabolic inhibitors and the physiological respiratory control state, uncoupled respiratory capacity, and rotenone+antimycin A sensitive respiration and the uncoupling and respiratory ratios calculated. As shown in Figure 20A, cells depleted of *GPX4* did not show a statistically significant difference in electron transport capacity in routine respiratory state (Cr) compared to control cells. Cells treated with *GPX4* siRNA(1) did not show a statistically significant difference in electron transport capacity related to non-phosphorylating respiration (Cro) compare to control cells. A change in electron transport capacity in relation to non-phosphorylating respiration would have been an indication of proton leak. There was also no statistically significant difference in total uncoupled electron transport capacity related to phosphorylation (Cru & CruRA). Although there was no statistical difference in flux ratios between these cells, it should be noted that small changes in cellular respiration may indicate biologically significant mitochondrial defects (Hutter *et al.*, 2004).

Following cell treatment with *GPX4*-siRNA (1), cellular ROS levels were assessed using carboxy-H2DCFDA. As shown in (Figure 20B), carboxy-H2DCFDA fluorescence showed no significance difference in cellular ROS between cell treated with *GPX4*-siRNA (1) and negative control siRNA, suggesting that *GPX4* knock-down does not affect overall cellular ROS.

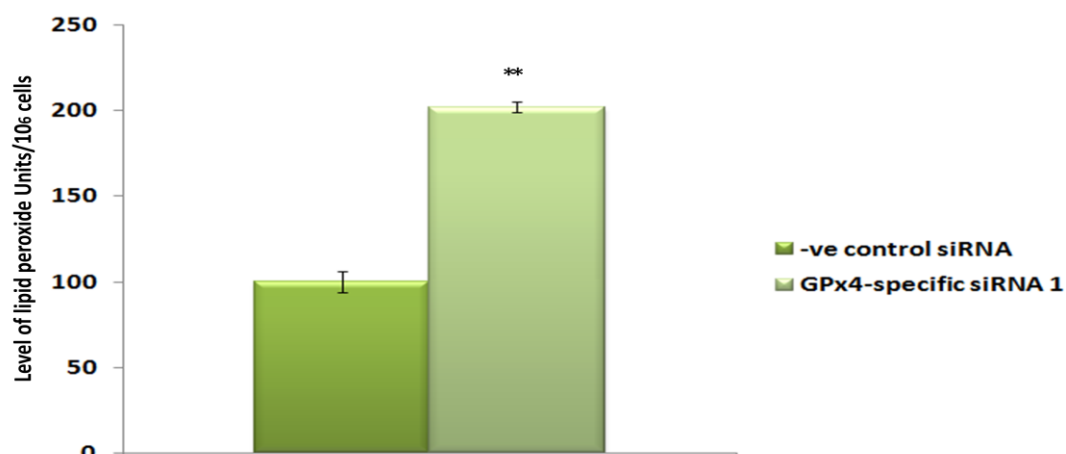
4.2.4 Impact of *GPX4* knock-down on cell Viability

To investigate the possible effect of *GPX4* knock-down on cell viability which could have resulted from changes in lipid peroxide, ATP and mitochondrial membrane potential, effects of *GPX4* knock-down on cells viability was carried out. As shown in Figure 21, no difference in cell viability was observed in *GPX4* knock-down cells compared to cells treated with scrambled negative control siRNA.

4.2.5 Effects of *GPx4* knock-down on mitochondrial superoxide and $\Delta\Psi_m$ with *GPX4*-specific siRNA(2)

Following treatment of cells with the second *GPX4*-siRNA, assessment of mitochondrial superoxide levels and mitochondrial membrane potential was carried out (Figure 18). Treatment with the second *GPX4*-siRNA showed a ~50% increase in mitochondrial superoxide formation and a ~30% decrease in mitochondrial membrane potential indicating, that these effects are due to knock-down of *GPX4* and not off-target effects.

A



B

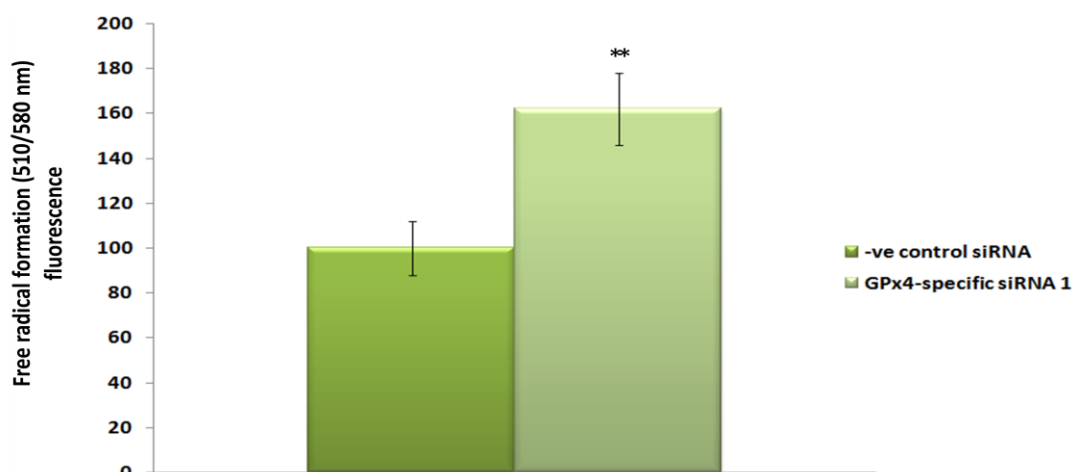
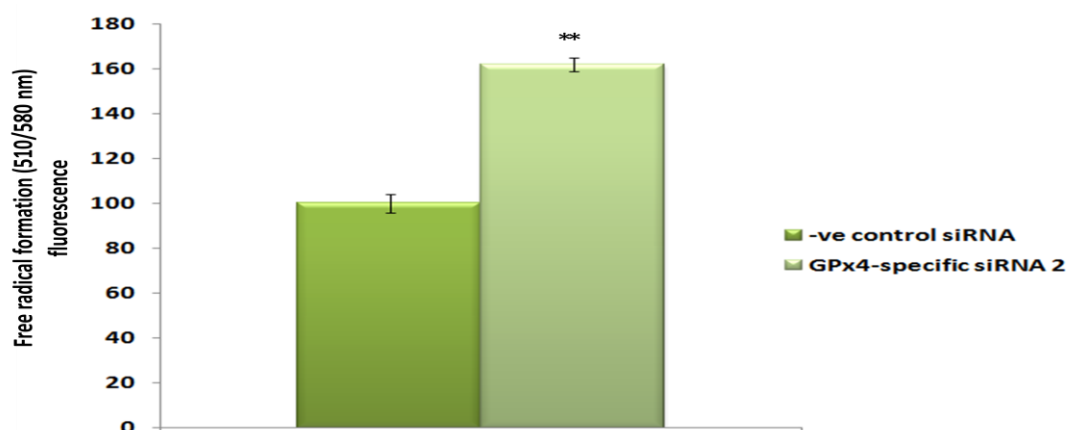


Figure 17. Assessment of lipid peroxide and superoxide level following GPX4 knock-down with GPX4-siRNA(1).

*Caco-2 cells were treated with 20 nM of GPX4-siRNA (1) or a scrambled negative control siRNA. (A) Levels of lipid peroxidation and (B) mitochondrial superoxide were assessed following treatment. Cells treated with negative control siRNA were used as controls and their mean percentage values were used to calculate changes in siRNA treated cells. Values shown are mean \pm s.e.m. $n=6$ for each assay and groups were compared using a Mann-Whitney U test, * $p<0.05$, ** $p<0.01$.*

A



B

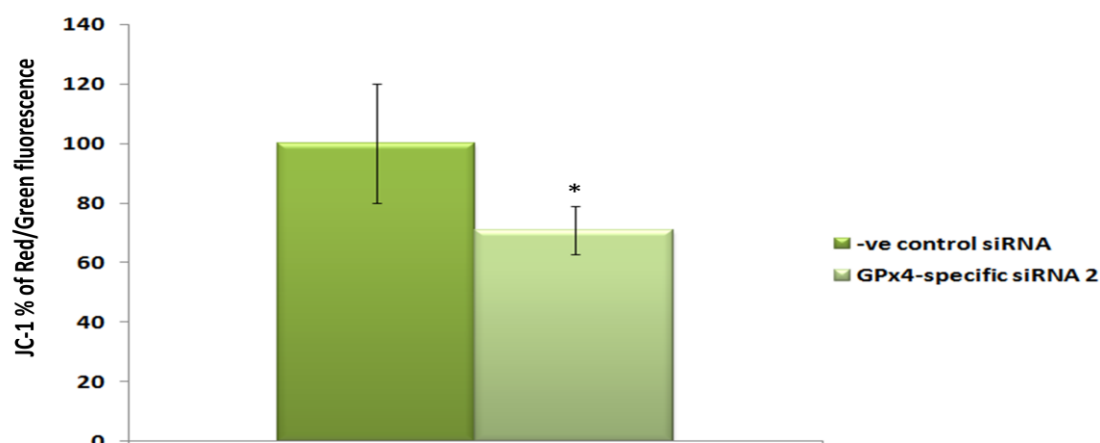
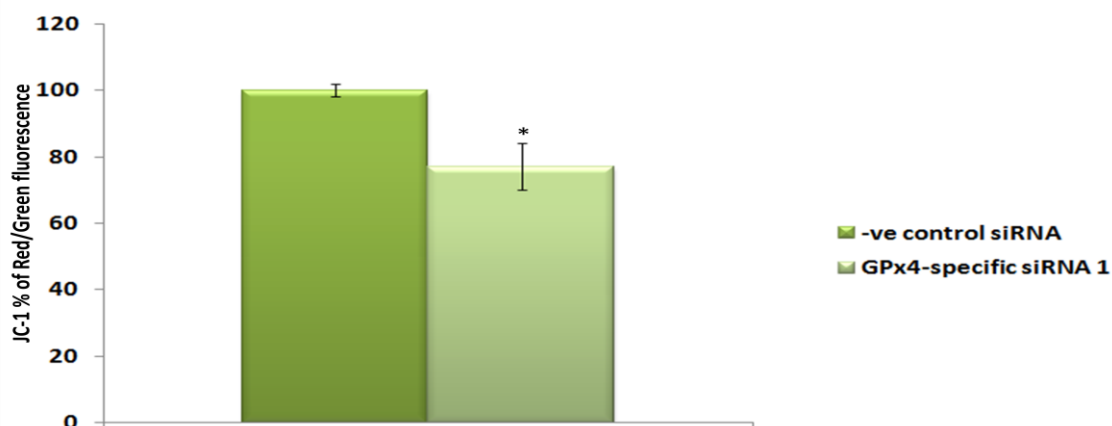


Figure 18. Assessment of mitochondrial membrane integrity and oxidative stress following GPX4 knock-down with siRNA(2).

*Caco-2 cells were treated with 20 nM of GPX4-siRNA (2) or a scrambled negative control siRNA. (A) Levels of mitochondrial superoxide and (B) mitochondrial membrane potential were assessed. (A) Mitosox fluorescence showed increase in ROS (superoxide) levels in cells treated with 20 nM GPX4-siRNA(2) compared with cells treated with a negative control siRNA. (B) Mitochondrial membrane potential (MMP) was lower in cells treated with 20 nM GPX4-siRNA(2) compared with cells treated with a negative control siRNA. Values shown are mean \pm s.e.m. $n=6$ for each assay and groups were compared using a Mann-Whitney U test, * $p<0.05$, ** $p<0.01$*

A



B

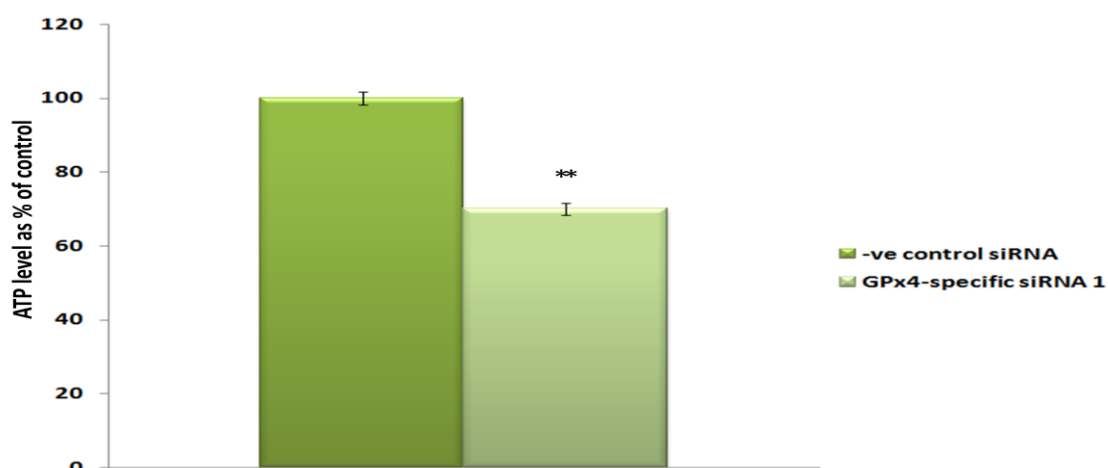
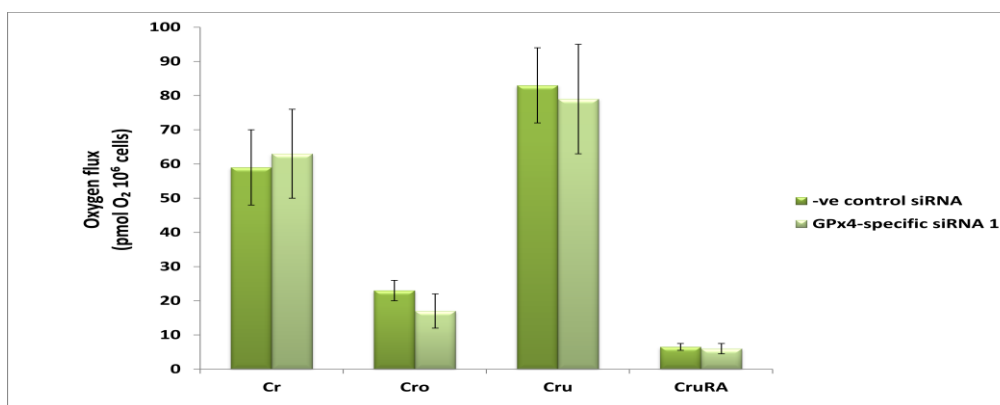


Figure 19. Assessment of mitochondrial membrane potential and mitochondrial ATP following GPX4 knock-down with GPX4-siRNA(1).

*Caco-2 cells were treated with 20 nM of GPX4-siRNA (1) or negative control siRNA. Mitochondrial membrane potential (A) and mitochondrial ATP (B) were assessed following treatment. (A) JC-1 fluorescence showed an approximate 30% decrease in cells treated with 20 nM GPX4-siRNA compared with cells treated with a scrambled negative control siRNA. (B) ATP/ADP ratio were lower in cells treated with 20 nM GPX4-siRNA compared with cells treated with a scrambled negative control siRNA. Cells treated with negative control siRNA were used as controls and their mean percentage values were used to calculate changes in siRNA treated cells. Values shown are mean \pm s.e.m. n=6 for each assay and groups were compared using a Mann-Whitney U test, * $p < 0.05$, ** $p < 0.01$*

A



B



Figure 20. Assessment of mitochondrial respiration and overall cellular ROS following GPX4 knock-down with GPX4 siRNA(1).

Caco-2 cells were treated with 20 nM of the GPX4-siRNA(1) or a scrambled negative control siRNA. (A) Investigation of functional capacity of the mitochondria after GPX4 knock-down. Cellular oxygen consumption was measured in a respirometer by measurement of resting respiration (Cr) successive addition of oligomycin (CrO), carbonyl cyanide *p*-(trifluoromethoxy) (FCCP) (Cru), rotenone and antimycin (CruRA) (inhibitors of mitochondrial complex V, uncoupler, and inhibitor of complex I and III respectively). (B) Cellular ROS were assessed following carboxy-H₂DCFDA treatment. Mean percentage values for cells treated with negative control siRNA were used to calculate changes in siRNA treated cells. Values shown are mean \pm s.e.m. with $n=6$ for cellular oxygen consumption measurements and $n=6$ for cellular ROS measurements. Group (A) were compared using One-way Anova, whereas ROS Groups were compared using a Mann-Whitney U test, * $p<0.05$, ** $p<0.01$.

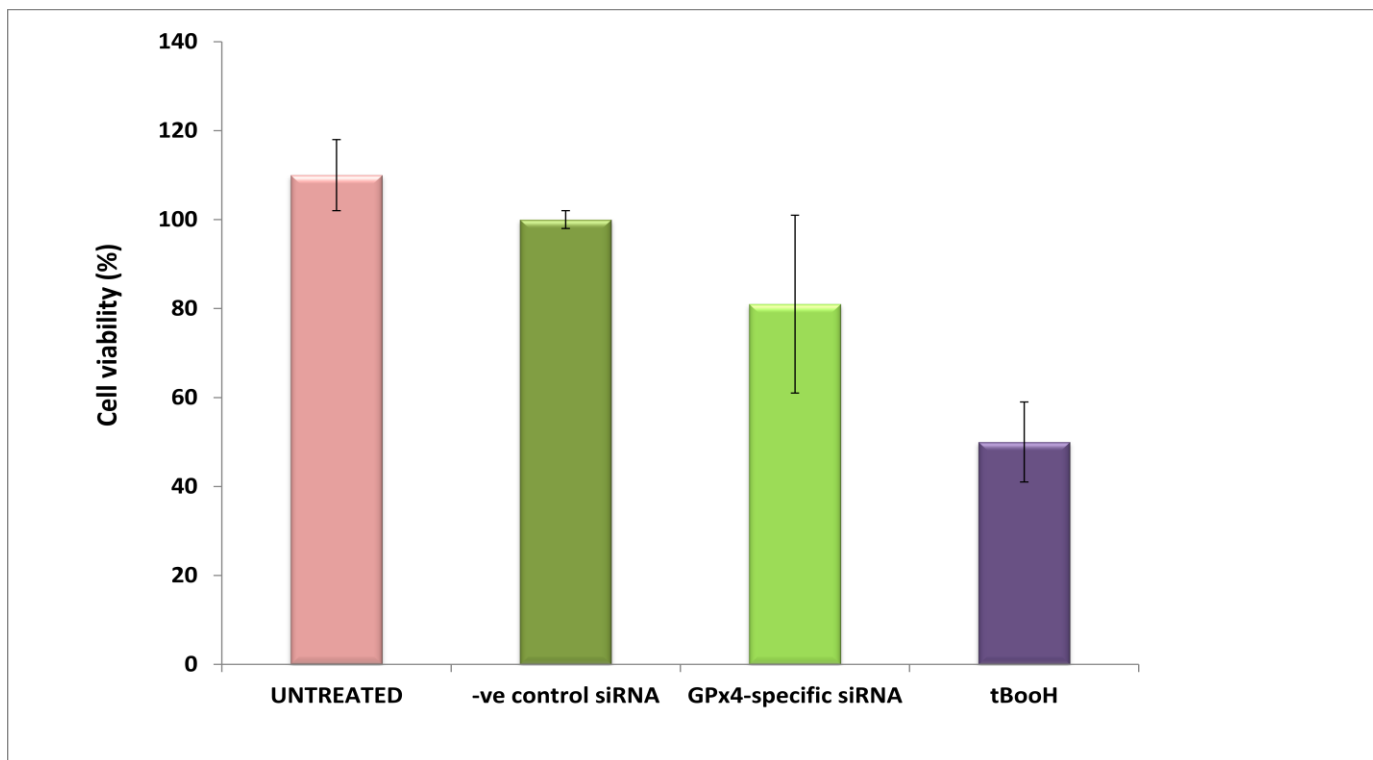


Figure 21. Assessment of cell viability following cell treatment with either GPX4-siRNA(1) or negative control siRNA.

Cells were treated with either siRNA or with tert-butylhydroperoxide (tBooH) as a positive control. tBooH treatment caused a loss of cell viability. There was no difference in levels of viable and non-viable cells between cells treated with GPX4-siRNA(1) and scrambled control group. Cells treated with negative control siRNA were used as controls and their average mean percentage values were used to calculate changes in siRNA treated cells. Values shown are mean \pm S.D for n=6 and groups were compared using a Mann-Whitney U test.

4.3 Discussion

The antioxidant enzyme GPx4 has the ability to reduce complex lipid hydroperoxides in addition to hydrogen peroxide and other organic hydroperoxides (Latchoumycandane *et al.*, 2012). As GPx4 is a ROS scavenger (Ufer & Wang, 2011), *GPX4* depletion is likely to bring about increased levels of ROS in mammalian cells. Previous studies of transgenic *GPX4*^{+/-} mice and fibroblast derived from such mice have shown impairments of responses to oxidative stress (Ran *et al.*, 2003; Garry *et al.*, 2008). Two studies have been carried out since the start of this work and suggested *GPX4* depletion leads to increased ROS production, lipid peroxide production, coupled with reduced mitochondrial integrity and impairment in ATP production (Latchoumycandane *et al.*, 2012; Yoo *et al.*, 2012). Knock-down of *GPX4* in Jurkat cells enhanced phospholipid peroxidation, increased TNF α -stimulated azelaoyl phosphatidylcholine (AZ-PC) formation and increased apoptosis, resulting in mitochondrial damage (Latchoumycandane *et al.*, 2012). Study of transgenic mice in which the *GPX4* gene was ablated by tamoxifen administration showed that the mice exhibited increased mitochondrial damage, increased lipid peroxides (assessed by elevated 4-hydroxynonenal (4-HNE), a strong indicator of lipid peroxide), decreased activity of the mitochondrial electron transport chain and reduced ATP synthesis, supporting the data in this thesis and highlighting the importance of GPx4 in the maintenance of mitochondrial integrity (Yoo *et al.*, 2012).

In another recently published study increased GPx4 activity in selenium supplemented rats was found to protect from elevated thiobarbituric acid formation, a byproduct formed from lipid peroxidation and

observed in selenium depleted rats with low *GPX4* activity (Erkekoglu *et al.*, 2012). In addition, decreased activity of *GPX4* together with decreased level of other antioxidants such as SOD1 and GPx1 resulted in enhanced levels of malondialdehyde (MDA) and oxidative stress in the hippocampus of immature rat brain subjected perinatally, to lead exposure, indicating that disruption of antioxidant balance, including that of *GPX4*, increases oxidative stress (Baranowska-Bosiacka *et al.*, 2012). Knock-down of *GPX4* by siRNA increased *VEGF* and *IL-8* expression resulting in increased linoleic acid peroxide (LOOH) in human HCC cell lines and these findings were further confirmed in a rat hepatocarcinogenesis model. Selenium treatment in these models increased *GPX4* expression and reduced the expression of *VEGF* and *AP-1* (Rohr-Udilova *et al.*, 2012).

Co-overexpression of superoxide dismutase 1 (*SOD1*) with *GPX4* reduced oxidative damage in the retina and slowed the loss of cones in mice deficient of *SOD1*, whereas, increased expression of either *SOD1* or *SOD2* could not rescue these mice from oxidative damage and loss of cones led to Retinitis Pigmentosa (RP). The observations from this study suggest that over-expression of *SOD* must be combined with expression of a peroxide scavenging enzyme such as *GPX4* to combat RP-induced oxidative damage and loss of cone cell function (Usui *et al.*, 2011). Overall the studies outlined above indicate that *GPX4* has an important role in controlling ROS level and limiting mitochondrial damage and the findings described in this thesis (from the *GPX4* knock-down in human gut epithelial cell line (Caco-2)) strongly support the hypothesis that GPx4 has a vital role in protecting cells from ROS and mitochondrial damage.

Mitochondria are the major source of energy in all eukaryotic cells, producing ATP through oxidative phosphorylation and the citric acid cycle. Mitochondria play a role in the modulation of apoptosis through the release of several cell death-inducing molecules (Lenaz *et al.*, 2002; Ravagnan *et al.*, 2002). Many studies have been carried out to elucidate the behaviour and function of mitochondria in most cell lines. Mitochondrial membrane potential is a key indicator of cellular viability due to its reflection of the pumping of hydrogen ions across the inner membrane during the process of electron transport and oxidative phosphorylation which is the driving force behind ATP synthesis. The lipophilic mitochondrial probe JC-1 can be utilized to estimate changes in membrane potential ($\Delta\Psi_m$). JC-1 is a sensitive probe widely used in different cell lines for assessment of $\Delta\Psi_m$ and has been used in to investigate $\Delta\Psi_m$ in mouse (Wilding *et al.*, 2011) and human female germ cells (Van Blerkom *et al.*, 2002).

Following *GPX4* knock-down, JC-1 was used to assess $\Delta\Psi_m$ in both siRNA treated cells and control cells. *GPX4*-siRNA treated cells exhibited a significant reduction in $\Delta\Psi_m$ compared to cells treated with scrambled control siRNA and this result was confirmed with a second *GPX4*-siRNA. Majority of mitochondrial functions such as ATP synthesis and lipid biogenesis depend on the stability and maintenance of $\Delta\Psi_m$ (Voisine *et al.*, 1999). A study comparing wild type mice and transgenic mice overexpressing *GPX4* showed a significant decline in mitochondrial ATP synthesis in livers of wild type mice after exposure to diquat compare to the transgenic mice. The same study observed reduced $\Delta\Psi_m$ in wild type mice following diquat treatment, however $\Delta\Psi_m$ was attenuated in mice overexpressing *GPX4* suggesting that decreased ATP production under oxidative stress is primarily due to reduced $\Delta\Psi_m$ and

that overexpression of *GPX4* maintains $\Delta\Psi_m$ under oxidative stress (Liang *et al.*, 2007). The same group also showed that transgenic mice overexpressing *GPX4* exhibited reduced levels of liver damage and lipid peroxidation induced by diquat concomitant with reduced apoptosis, increased caspase-3 activation and reduced cytochrome c release from mitochondrial (Liang *et al.*, 2004).

Investigation of lipid peroxide levels was carried out in both siRNA treated cells and cells treated with scrambled control siRNA and the data showed increased lipid peroxidation in siRNA treated cells compared with the corresponding controls. Lipid hydroperoxides are primarily produced when lipids are damaged by 1-electron oxidants, such as the tyrosyl radical and nitrogen radical. Advanced products of oxidation such as alkanes, aldehydes and isoprostanes can be generated through peroxidation of lipid (Moore & Roberts, 1998). During the peroxidation of unsaturated fatty acids or tissue lipids, malonaldehyde is produced which reacts with thiobarbituric acid to produce a pink colour that can be measured colorimetrically (Niehaus & Samuelsson, 1968). Malonaldehyde forms through peroxidation of arachidonic acid and is often considered the most accurate way to measure oxidative stress *in vivo* and *in vitro*, and has been used extensively as a biomarker of lipid peroxidation a risk factor for various kinds of diseases (Janero, 1990). Formation of malonaldehyde observed in cells treated with *GPX4*-siRNA was higher than in control cells, suggesting that reduced expression of *GPX4* exposes cells to increase levels of oxidative damage. The increases in lipid peroxidation and ROS are consistent with earlier observations that over-expression of *GPX4* leads to lower levels of mitochondrial cardiolipin peroxidation (Liang *et al.*, 2004). As previously discussed, transgenic mice overexpressing the *GPX4* gene were protected from oxidative damage induced by lipid peroxide (Liang *et al.*, 2007). The study

described in this thesis showed the importance of *GPX4* in protecting human gut epithelial cells from lipid peroxide induced-oxidative damage. This strongly supports the findings of Liang and Colleagues.

Considering the observed changes in lipid peroxide and ATP synthesis, investigations of levels of mitochondrial superoxide formation were also carried out. Increase in mitochondrial ROS has been previously shown to be one of the contributors to mitochondrial oxidative damage, mitochondria DNA damage and reduced mitochondria integrity either through alterations of the mitochondrial electron transport efficiency, mitochondrial oxidative phosphorylation or mitochondrial ATP synthesis (Liang *et al.*, 2007; Tissier *et al.*, 2012; Zhi *et al.*, 2012). To assess mitochondrial superoxide formation, Caco-2 cells were treated with MitoSOX following either siRNA or negative control siRNA treatment. MitoSOX has been widely used to study the presence of superoxide in *vitro* and in *vivo*. A significant increase in superoxide formation was observed in siRNA treated cells compared to control cells. Embryonic fibroblasts lacking the DJ-1 gene exhibited increased mitochondrial damage, reduced mitochondrial ATP production, elevated mitochondrial permeability transition pore and reduced $\Delta\Psi_m$ associated with increased mitochondrial ROS (Giaime *et al.*, 2012), consistent with increased superoxide level leading to mitochondrial damage.

Investigation into cellular oxygen consumption activities was carried out in intact Caco-2 cells treated with siRNA and scrambled control siRNA. To my knowledge, this is the first study of cellular oxygen consumption following *GPX4* knock-down in a human gut epithelial cell line. Mitochondrial functional performance was assessed following *GPX4* knock-down by measuring oxygen utilization using complex

specific substrates. Cells depleted of *GPX4* did not show a statistically significant difference in electron transport capacity in routine respiratory state (Cr) compared to control cells. Compared with control cells, cells treated with *GPX4* siRNA(1) did not show a statistically significant difference in electron transport capacity related to non-phosphorylating respiration (Cro). There was also no statistically significant difference in total uncoupled electron transport capacity related to phosphorylation (Cru & CruRA) between siRNA treated cells and control cells. The intracellular ROS level was measured using 5-(and-6)-carboxy-2',7'-dichlorodihydrofluorescein diacetate (carboxy-H₂DCFDA), a cell membrane permeability indicator that only fluoresces when acetate groups are abolished by intracellular esterases and oxidation takes place in the cell. Carboxy-H₂DCFDA is converted to the fluorescent form DCF irreversibly when oxidized by various kinds of reactive oxygen species (Shimizu *et al.*, 2004) and has been widely used as a general oxidative stress detector (Hansen-Hagge *et al.*, 2008; Naha *et al.*, 2010; Dickie *et al.*, 2012; Kimura *et al.*, 2012; Yang *et al.*, 2012;). As shown in Figure 20B, no change in intracellular ROS was observed in *GPX4*-siRNA treated cells compared with the control group and this finding suggests that although *GPX4* is known to protect cells from oxidative damage, there may be other compensatory factors such as other antioxidants e.g. *GPX1* and Catalase that can limit any increase in oxidative stress when *GPX4* activity is compromised. This finding also suggests that *GPX4* knock-down alone is not enough to bring about changes in overall intracellular ROS.

Changes in membrane permeability and increases reactive oxygen species have been associated with either loss or reduced cell viability (Chen *et al.*, 2012; Fatemi *et al.*, 2012; Kim *et al.*, 2012). Considering the observed changes in $\Delta\Psi_m$, lipid peroxide and superoxide following *GPX4* knock-down

in Caco-2 cells, cell viability was investigated in order to assess the effects of the observed changes in cell growth and stability. As shown in Figure 21, there was no difference in cell viability between Caco-2 cells treated with *GPX4*-siRNA and negative control siRNA. This observation suggests that *GPX4*-siRNA treatment for 72 h does not have any obvious impact on cell viability.

Overall, the data described in this Chapter indicates that reduced expression of *GPX4* alters mitochondrial integrity through altered levels of mitochondrial ROS, lipid peroxide, $\Delta\Psi_m$ and ATP, but not cellular ROS, and that the observed changes do not interfere with cell viability. *GPX4* knock-down led to changes in protein expression of components of complex I and IV of the mitochondrial electron transport chain complexes. These findings correlate with the observed changes in genes expressing components of these complexes, increased lipid peroxide and mitochondrial superoxide, decreased $\Delta\Psi_m$ and ATP synthesis, reflecting changes in mitochondrial metabolism. Overall, the data indicate that *GPX4* knock down altered the functions of Complex I and IV and resulted in increased mitochondrial ROS production and reduced mitochondrial function and integrity. Considering the observed changes in mitochondrial function and integrity, it appears that *GPX4* knock-down also alters mitochondria stability either through increased production of lipid peroxides or through multiple mechanisms. As described in Chapter 3, *GPX4* knock-down led to change in mRNA expression of components of mitochondrial electron transport complexes I, IV and V and changes in protein expression of components of complex I and IV. The microarray data indicated AIF mRNA expression to be altered and network analysis indicated this as a key regulatory component. Since *AIF* has been reported to be a regulator of

expression of complex I and IV, further work was carried out to investigate AIF protein expression following *GPX4* knock-down, as described in the next Chapter.

Chapter 5: Investigation of the impact of *GPX4* knock-down on AIF expression

5.1 Introduction

Microarray data from the *GPX4* knock-down experiment indicated a change in expression of AIF (Figure 15). Inducible inactivation of *GPX4* in mice resulted in 12/15-lipoxygenase-derived lipid peroxidation and activation of AIF (Seiler *et al.*, 2008). AIF is thought both to be part of a mitochondrial apoptotic signalling and to play a role in oxidative phosphorylation by modulating the structure and function of complex I of the respiratory chain (Vahsen *et al.*, 2004; Joza *et al.*, 2009). The observed effects of knock-down on mitochondrial complex I and IV function were followed by measuring levels of the AIF protein. AIF has been reported to regulate complex I and IV activity but also to change expression and activity itself following oxidative stress or activation of apoptosis (Daugas *et al.*, 2000; Vahsen *et al.*, 2004; Joza *et al.*, 2009;). As discussed in Chapter 4, *GPX4* knock-down resulted in altered levels of mitochondrial ROS and lipid peroxide levels, and therefore time-course experiments were also carried out to explore the relationship between ROS and AIF levels following *GPX4* knock-down.

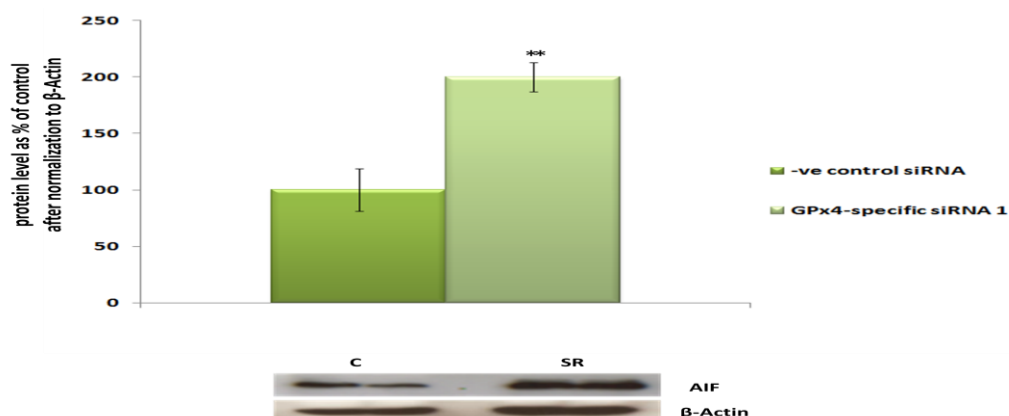
Pro-apoptotic signal molecules induce mitochondrial outer membrane permeability thereby activating the release of mitochondrial proteins (Natarajan & Becker, 2012). AIF is a flavoprotein, which is confined to the mitochondrial intermembrane space of healthy cells (Natarajan & Becker, 2012). AIF has been shown to translocate via the cytosol to the nucleus upon apoptotic signaling and in the nucleus it binds to DNA and induces caspase-independent DNA fragmentation (Natarajan & Becker, 2012;

Wang *et al.*, 2012). AIF has been shown to have oxidoreductase activity and interact electrostatically with double-stranded DNA (Joza *et al.*, 2001). In this chapter, Western blotting was used to assess AIF protein levels after *GPX4* knock-down and a time course experiment carried out to investigate the relationship between changes in AIF, NDUFB8 and COX2.

5.2 Impact of *GPX4* knock-down on AIF protein expression

To study AIF protein expression, Caco-2 cells seeded 24 hours previously at 3.5×10^5 cells/well in a six well plate were transiently transfected with either 20 nM *GPX4*-siRNA(1) or *GPX4*-siRNA(2) or negative control siRNA. Seventy two hours following transfection, cells were lysed, total cell lysate extracted and AIF protein assayed by Western blotting using anti-AIF antibody. As shown in Figure 22A-B, densitometry analysis of the protein band showed that treatment with *GPX4*-siRNA (1) led to ~100% increase in levels of AIF protein and 40% increase following treatment with *GPX4*-siRNA(2).

A



B

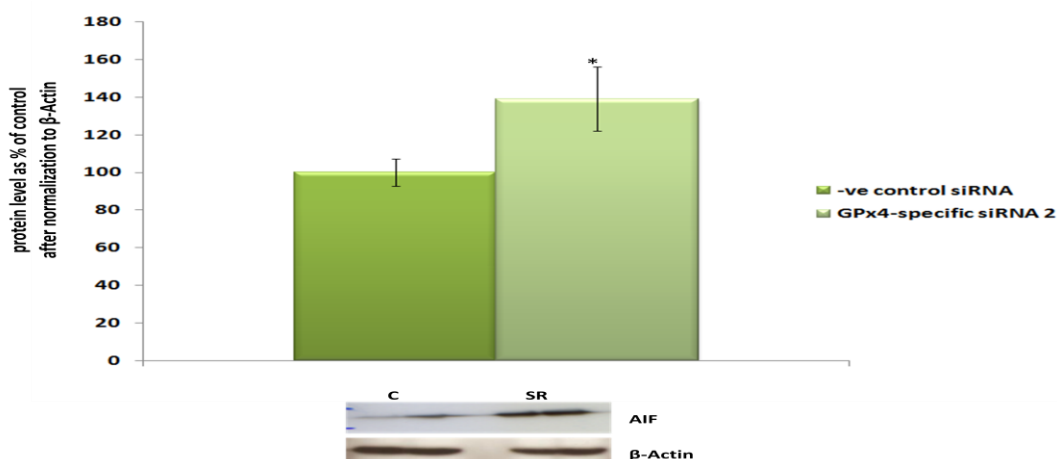


Figure 22. Expression of AIF protein following GPX4 knock-down.

*Caco-2 cells were treated with 20 nM of (A) GPX4-siRNA(1) and (B) GPX4-siRNA(2) and scrambled negative control siRNA. Total protein was extracted following knock-down and AIF protein expression assayed by Western blotting and intensity of the protein bands carried out by densitometry. Protein level was calculated relative to β -actin, and further calculated as a percentage of the mean value for cells treated with the negative control siRNA. Western panels = 2 wells, values shown are mean \pm s.e.m. for n=6. A statistically significant increase in AIF protein expression was observed in cells depleted of GPX4 compared to control cells. Groups were compared using a Mann-Whitney U test, * $p < 0.05$, ** $p < 0.01$*

In further experiments, after knock-down with *GPX4*-siRNA(1) cells were harvested and cytosolic and mitochondrial fraction prepared. After Western blotting, densitometry analysis of the protein bands was carried out and the results showed that *GPX4* knock-down led to an increase in AIF levels in both fractions with the mitochondria fraction showing ~ 58% increase and cytosolic fraction ~38% increase, as shown in Figure 23.

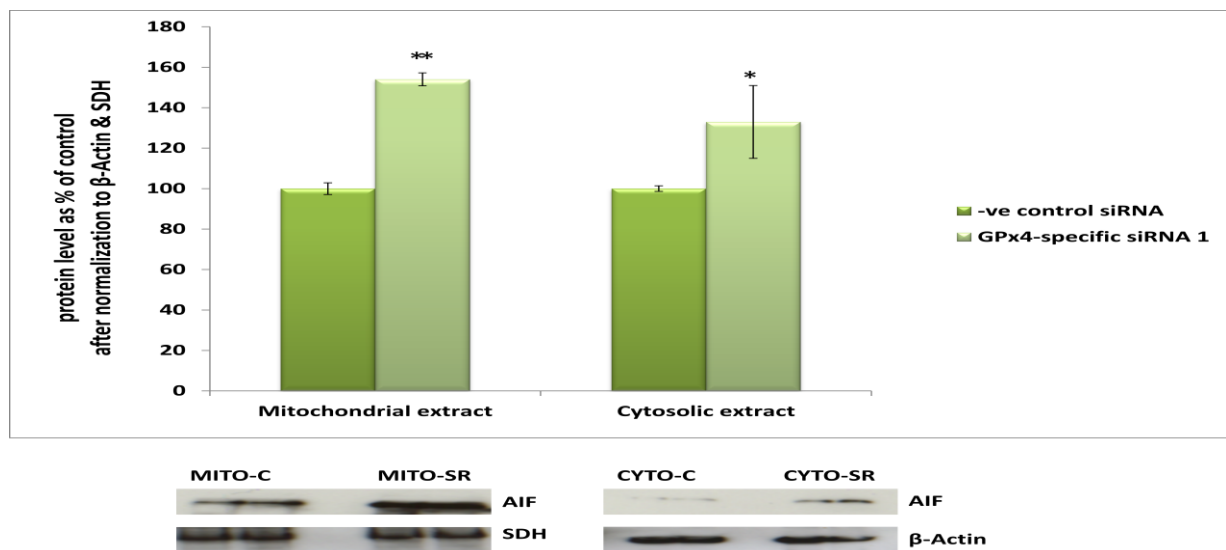


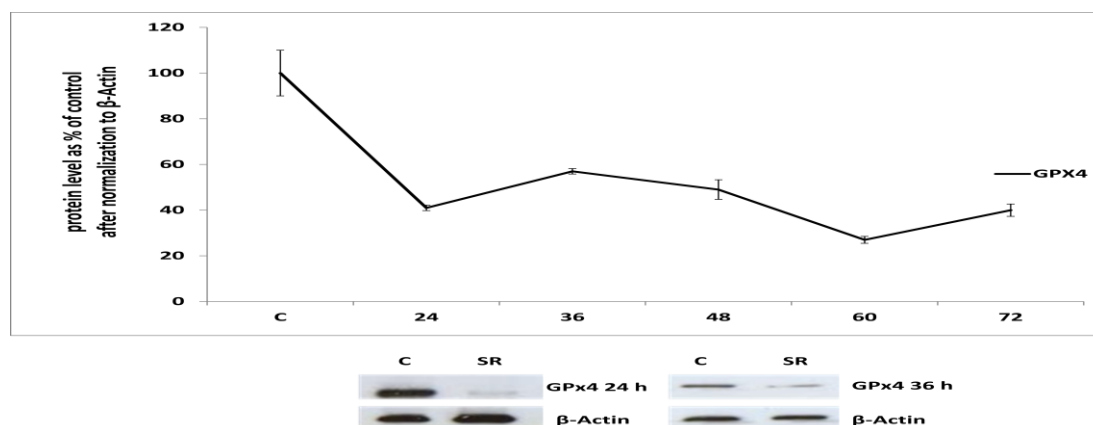
Figure 23. Expression of AIF in mitochondrial and cytosolic fractions following *GPX4* knock-down with siRNA(1).

Caco-2 cells were treated with 20 nM of *GPX4*-siRNA(1) or a scrambled negative control siRNA for 72 h. Mitochondrial and cytosolic fractions prepared following knock-down and AIF protein expression assessed by Western blotting. AIF levels were calculated relative to β -actin for cytosolic fractions and in the case of isolated mitochondria succinate dehydrogenase (SDH) was used as the housekeeping control. Protein expression was then calculated as a percentage of the mean value for cells treated with the negative control siRNA. Western panels = 2 well, values shown are mean \pm s.e.m. for n=4 A statistically significant increase in AIF protein expression was observed in both fractions in cells depleted of *GPX4* compared to control cells. Groups were compared using a Mann-Whitney U test, * $p < 0.05$, ** $p < 0.01$

5.3 A time-Course study to investigate the impact of *GPX4* knock-down on NDUFB8, COX2 and AIF protein expression and on $\Delta\Psi_m$, lipid peroxide and ROS.

To further explore the roles of ROS and AIF in the sequence of events in the mitochondria following *GPX4* knock-down, a time-course experiment was carried out in which GPx4, AIF, NDUFB8 and COX2 levels were measured by Western blotting using Caco-2 protein extracts; levels of lipid peroxide, $\Delta\Psi_m$ and mitochondrial superoxide were also assessed. Caco-2 cells were treated with either *GPX4*-siRNA(1) or negative control siRNA for 24, 36, 48, 60 or 72 h. Cells were lysed and protein extracted from total cell lysate was then used to assess protein expression levels of GPx4, AIF, NDUFB8 and COX2. GPx4 protein at the different time points was monitored by Western blotting. As shown in Figure 24A, GPx4 protein expression was significantly reduced at the different time points investigated. Following confirmation of GPx4 knock-down at protein level, the extracted protein samples from the knock-down experiment were used to monitor the protein levels of AIF, NDUFB8 and COX2 by Western blotting using anti-AIF, NDUFB8 and COX2 antibodies. As shown in Figure 24B, the time-course data showed a 80% increase in level of AIF by 24 h after addition of *GPX4*-siRNA but levels of NDUFB8 and COX2 did not increase until later at 36 h.

A



B

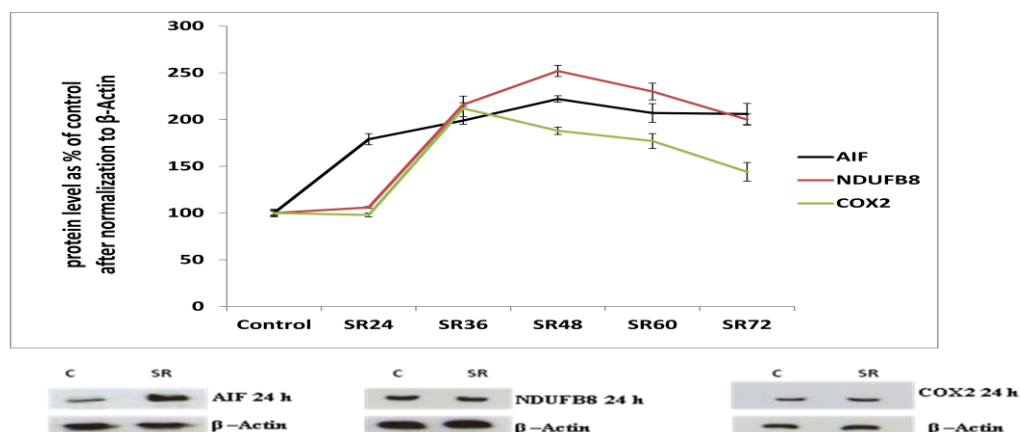
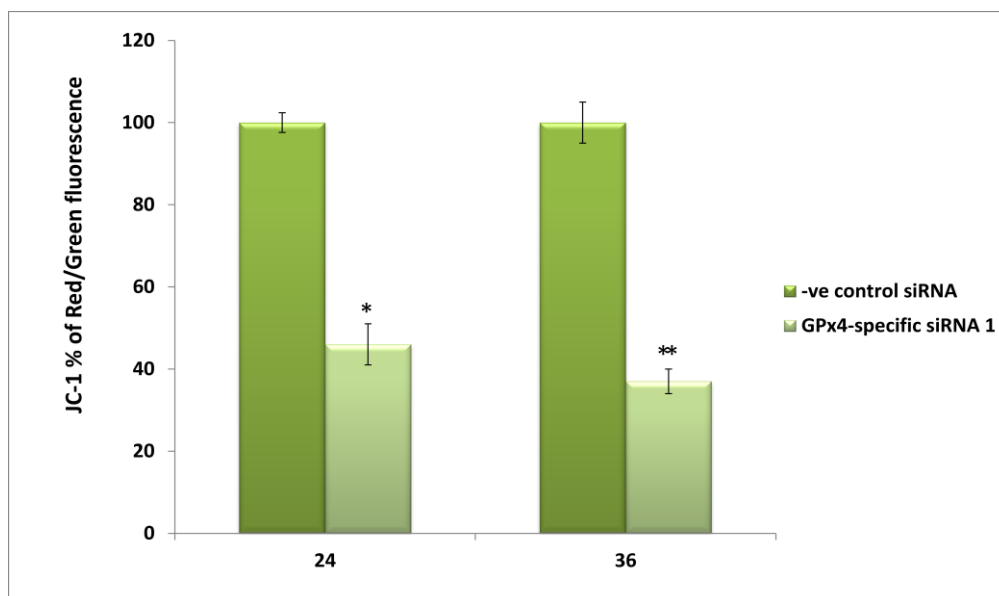


Figure 24. A time-course assessment of GPx4, NDUFB8, COX2 and AIF protein following GPX4 knock-down with siRNA(1).

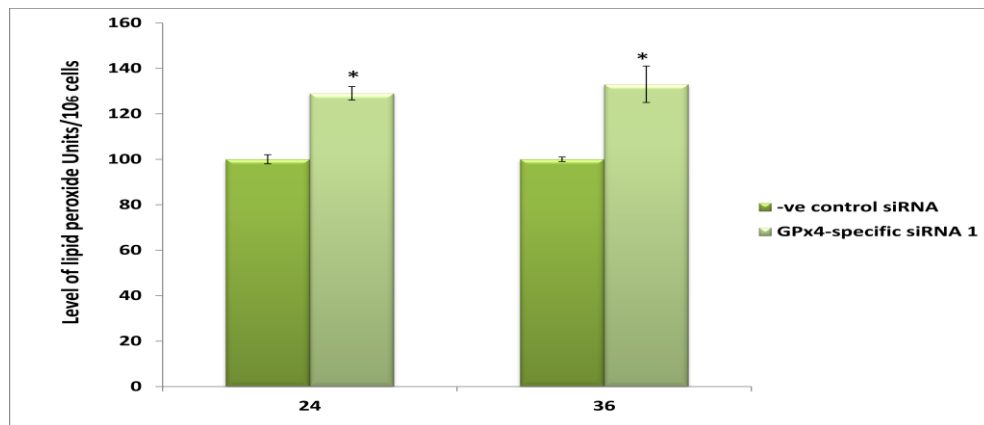
*Caco-2 cells were treated with 20 nM of GPX4-siRNA(1) or a scrambled negative control siRNA. Total protein was extracted 24, 36, 48, 60 and 72 h after knock-down. (A) Expression of GPx4 protein expression at different time points following GPx4 knock-down by Western blotting using anti-GPx4 antibody. (B) Expression of AIF, NDUFB8 and COX2 proteins at 24, 36, 48, 60 and 72 h following GPX4 knock-down. Data shown in figure 24B are from protein extracted 24 h following GPx4 knock-down. Protein expression levels were calculated relative to β -actin as the control and then as a percentage of the mean value for cells treated with the negative control siRNA. Western panels = 1 well for each protein, values shown are mean \pm s.e.m. for $n=4$ for each protein. Groups were compared using a Mann-Whitney U test, * $p<0.05$, ** $p<0.01$.*

Previous experiments described in Chapter 4 showed changes in $\Delta\Psi_m$, lipid peroxide and mitochondrial superoxide following *GPX4* knock-down at 72 h. Investigations of earlier events would help to understand the sequence of events particularly in relation to changes in these parameters. To investigate the sequence of events in relation to mitochondrial integrity following *GPX4* knock-down, a time-course assessment of $\Delta\Psi_m$, lipid peroxide and superoxide production was carried out in Caco-2 cells treated with either *GPX4*-siRNA(1) or the scrambled negative control siRNA. Briefly, cells were seeded in a six well plate and transfected 24 hours later with either *GPX4*-siRNA(1) or negative control siRNA for 24 and 36 h respectively. The time-course data showed that $\Delta\Psi_m$ had decreased by ~56% at 24 h and ~68% at 36 h after addition of *GPX4*-siRNA (Figure 25A) levels of lipid peroxide had increased by ~30% at 24 h and ~37% at 36 h (Figure 25B) and mitochondrial superoxide levels had increased by ~124% at 24 h and ~125% at 36 (Figure 25C) after *GPX4*-siRNA(1) treatment.

A



B



C

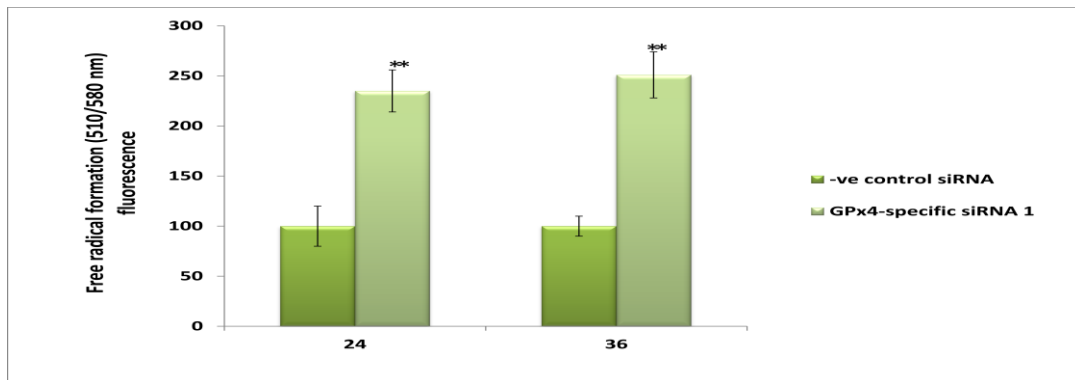


Figure 25. Time-course of mitochondrial integrity, oxidative stress following GPX4 knock-down with siRNA(1)

*Caco-2 cells were subcultured and 42 h later transfected with GPX4-siRNA(1) and scrambled negative control siRNA. Twenty four and 36 h following transfection cells were harvested and assayed for mitochondrial membrane potential, lipid peroxides and superoxide. (A) Assessment of Mitochondrial membrane potential at 24 and 36 h after treatment with either GPX4-siRNA(1) or negative control siRNA. (B) Levels of lipid peroxide were investigated using thiobabituric acid. (C) Assessment of mitochondrial superoxide levels were assayed using MitoSOX 24 and 36 h after treatment with GPX4-siRNA(1) and scrambled negative control siRNA. For all assays cells treated with negative control siRNA were used as controls and their mean percentage values were used to calculate changes in siRNA treated cells. Values shown are mean \pm s.e.m. n=6. Groups were compared using a Mann-Whitney U test, * p<0.05, ** p<0.01.*

5.3 Discussion

The microarray data from the *GPX4* knock-down experiment in Caco-2 cells showed altered expression of *AIF* mRNA as a central component of a mitochondrial network (Figure 17). Altered expression of *AIF* protein was also observed after *GPX4*-siRNA(1) treatment and was further confirmed by the second *GPX4*-siRNA Figure 22B. The change in *AIF* mRNA (down-regulated) and protein (up-regulated) did not complement each other however, both results were consistent throughout the study.

The human *AIF* is a flavoprotein encoding a 67 kDa polypeptide with 613 residues (Sevrioukova, 2009; Sevrioukova, 2011). Flavoproteins are known to catalyse various reactions through the utilization of flavin mononucleotide or flavin adenine dinucleotide as cofactors (Joza *et al.*, 2009). The oxidoreductase properties of *AIF* have been associated with oxidative insult, redox homeostasis and different cellular process such as apoptosis (Ye *et al.*, 2002). *AIF* changes intracellular location by translocating from the inner mitochondria membrane space to the nucleus upon exposure to apoptotic stimuli. *AIF* plays a very important role in the enhancement of mitochondrial bioenergetics and complex I activity/assembly in the maintenance of cellular redox homeostasis (Sevrioukova, 2009).

After *AIF* translocation from the mitochondria to the nucleus, a chromatin degradation complex with other proteins such as cyclophilin A is formed. The translocation is usually triggered by oxidative stress, thereby suggesting the possibility of *AIF* as a redox sensor in the mitochondria (Sevrioukova, 2011). It has also been reported that *AIF* generates superoxide and plays a significant role in mitochondrial function (Miramar *et al.*, 2001).

Previous studies have implicated AIF deficiency or low expression of AIF in reduced oxidative phosphorylation. Although, AIF itself is not a component of mitochondrial complex I, it has been linked strongly with mitochondrial complex I activity as loss of AIF in the mitochondria usually increases oxidative stress (Klein *et al.*, 2002; Vahsen *et al.*, 2004; Pospisilik *et al.*, 2007; Koene *et al.*, 2011). A study in the early mouse embryo after inactivation of AIF showed impaired activity of mitochondrial complex I and increased apoptosis (Brown *et al.*, 2006), suggesting that altered expression of AIF results in impaired mitochondrial bioenergetics including respiration and energy metabolism. A study of Harlequin mice deficient in AIF also implicated AIF involvement in mitochondrial respiratory activity (Klein *et al.*, 2002). Harlequin mice exhibit significant reduction in AIF mRNA expression (~80%-90%) compared to wild type mice and have been considered as an appropriate model for the evaluation of the physiological role of AIF in the mitochondria, including complex I function and oxidative phosphorylation (Klein *et al.*, 2002; Culmsee *et al.*, 2005). Harlequin mice exhibit approximately 50% reduced oxidative phosphorylation and complex I function, increased oxidative stress in brain, heart and cerebellum, and elevated levels of lipid peroxides and mitochondrial damage (Joza *et al.*, 2001; Klein *et al.*, 2002). Additionally, the mice are highly resistant to polyADP-ribose polymerase (PARP) induced cell death (Klein *et al.*, 2002) and T cells extracted from Harlequin mice exhibited increased sensitivity to Fas-ligand induced apoptosis compared with wild type mice (Joza *et al.*, 2001; Joza *et al.*, 2009).

Although AIF has been described as an antioxidant enzyme due to the observation of increased levels of oxidative stress in Harlequin mice, *in vitro* knock-down of AIF has not yet provided substantial evidence to back up the hypothesis that AIF functions as an antioxidant enzyme (Apostolova *et al.*,

2006; Krantic *et al.*, 2007). Cells deficient in AIF exhibited increased loss of cell tumorigenicity as a result of loss of complex I activity. Increased oxidative stress has been shown to induce depolarization of mitochondrial membrane potential in cultured NRK-52E cells, resulting in activation and increased secretion of AIF (Kim *et al.*, 2012). A study investigating the function of GPx4 in photoreceptor cells showed that there was a severe degeneration of rods and cones in GPx4 knock-out cells, and nuclear translocation of AIF and increased apoptosis (Ueta., *et al.*, 2012).

Increased levels of AIF protein in both mitochondrial and cytosolic extracts were observed following *GPX4* knock-down. As discussed previously, AIF translocation involves its migration from the mitochondria to the cytosol and further to the nucleus. Observation of AIF in the cytosol was a strong indication that AIF indeed translocated from the intermembrane space of the mitochondrial into the cytosol and possibly to the nucleus. The presence of AIF in the cytosol of cells treated with *GPX4* siRNA may have been as a result of increased oxidative stress.

The time-course experiment showed increased level of AIF protein at 24 h after knock-down before changes in levels of NDUFB8 and COX2. Also the time course experiment showed decreased $\Delta\Psi_m$ at 24 and 36 h and increased lipid peroxide and mitochondrial superoxide at these time points. These observations were a clear indication that knock-down of *GPX4* did not cause changes in NDUFB8 and COX2 expression which then had secondary effect on superoxide and $\Delta\Psi_m$. Knock-down either resulted in changes in the mitochondrial redox state, which then altered AIF expression or altered expression of AIF first. Altered AIF expression may have changed the mitochondrial redox state

including levels of lipid peroxide, mitochondrial superoxide levels and $\Delta\Psi_m$, resulting in changes in mitochondrial complexes I and IV.

To summarize, the difference in the pattern of AIF expression at mRNA (down-regulated) and protein (up-regulated), is difficult to understand. However, the observed increase in AIF prior to that of NDUF8 is consistent with AIF being a key factor in the regulation of the genes encoding components of complex I in response to *GPX4* knock-down. Taken together these data suggest that following *GPX4* knock-down, mitochondrial membrane damage and decreased membrane potential causes changes in AIF protein which lead to alterations in expression of complex I components. These findings linking lower *GPX4* expression and changes in expression of components of respiratory complex I and AIF strongly suggest that *GPX4* plays an important role in mitochondria function. These findings are complementary to the earlier observation that lower *GPX4* expression leads to altered 12/15 lipoxygenase activity and AIF-mediated cell death (Seiler *et al.*, 2008; Conrad, M., 2009). The study described in this thesis also support earlier observation that absence of *GPX4* affects angiogenesis in murine embryonic fibroblasts through the increase of 12/15 lipooxygenase activity (an enzyme that promotes apoptosis). This finding suggests that *GPX4* controls 12/15-LOX activity, which is an important regulator of tumor angiogenesis (Schneider *et al.*, 2010).

Chapter 6: Investigating the effect of Mitoquinone (MitoQ₁₀) on Caco-2 cells following *GPX4* knock down.

6.1 Introduction

Mitoquinone (MitoQ) is one of the several antioxidants that can be targeted to mitochondria by their conjugation to the triphenylphosphonium (TPP) moiety (Asin-Cayuela *et al.*, 2004) (see Figure 25). As lipid peroxidation is important in many forms of mitochondrial oxidative damage, and because the alkylTPP conjugates strongly associate with the mitochondrial inner membrane (Asin-Cayuela *et al.*, 2004; Green *et al.*, 2004), the effect of an antioxidant that acts against lipid peroxidation, particularly the targeted version of ubiquinol MitoQ₁₀ was further investigated. MitoQ₁₀, when absorbed, accumulates at a 5-10 fold higher concentration in the plasma membrane and 100-500 fold higher concentration in the mitochondrial membrane (Jauslin *et al.*, 2003). As reported in the preceding chapters, mitochondrial superoxide formation seems to be one of the contributors to mitochondrial dysfunction following *GPX4* knock-down in Caco-2 cells; Indeed, results showed changes in ubiquinone biosynthesis pathway, protein expression of components of mitochondrial complex I and IV, AIF and changes in levels of lipid peroxide, $\Delta\Psi_m$, and mitochondrial ATP. I hypothesized that MitoQ₁₀ would interfere with the effects of *GPX4* knock-down, particularly changes in lipid peroxides, since it blocks lipid peroxidation. Additionally, MitoQ₁₀ was selected for this study because it is directly targeted to the mitochondria (Asin-Cayuela *et al.*, 2004), where it is proposed the initiating events or effects of *GPX4* knock-down occurred.

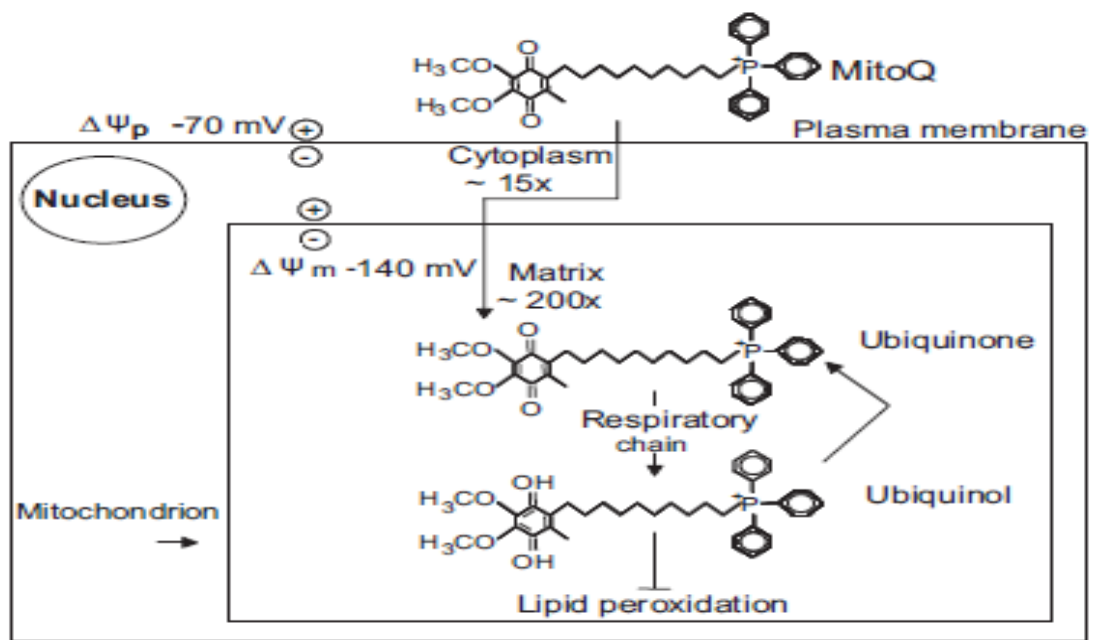


Figure 26. Structure of Mitoquinone and scheme illustrating its uptake into plasma membranes and mitochondrial membranes.

Mitoquinone accumulates 5 to 10-fold within the cell driven by the plasma membrane potential ($\Delta\Psi_p$) and then further accumulates (100 to 500-fold) within the mitochondria driven by the mitochondrial membrane potential ($\Delta\Psi_m$). In the mitochondrial matrix MitoQ10 is reduced to the active antioxidant form ubiquinol by the respiratory chain; this prevents lipid peroxidation. Antioxidant activity produces the ubiquinone form, which is then recycled back to ubiquinol by the respiratory chain (Taken from Doughan & Dikalov, 2007).

6.1.2 Effect of MitoQ10 on *GPX4* mRNA expression in Caco-2 cells.

Experiments were carried out to ascertain if MitoQ₁₀ treatment has any effect on *GPX4* status in Caco-2 cells. Cells were seeded at 3.5×10^5 per well and 24 h later were treated with either 1 μ M MitoQ₁₀ or decyltriphenylphosphonium bromide (DTPP) (a control compound), which has a similar chemical structure to MitoQ₁₀, but without the antioxidant ubiquinol moiety. Seventy two hours following treatment, cells were lysed and total RNA extracted. The RNA was reverse transcribed to cDNA and subjected to RT-PCR using primers specific to *GPX4* and *GAPDH*. As shown in Figure 27, MitoQ₁₀ treatment did not change the mRNA expression of *GPX4*.

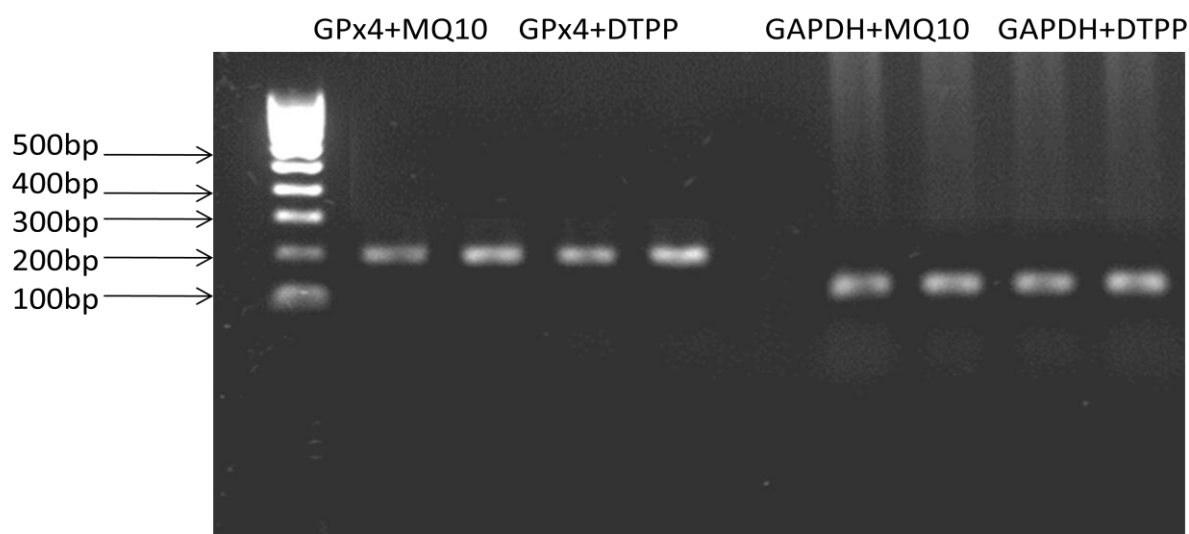


Figure 27. Confirmation of *GPX4* mRNA status following MitoQ₁₀ and DTPP treatment.

*RNA extracted from duplicate culture of Caco-2 cells treated with either MitoQ₁₀ or DTPP, reverse transcribed and PCR carried out using primers specific for *GPX4* to assess *GPX4* mRNA level or *GAPDH* to assess the level of this housekeeping control. By visual observation, there was no difference in *GPX4* mRNA expression following either treatments suggesting that the antioxidant activity of MitoQ does not alter *GPX4* mRNA status.*

6.1.3 Confirmation of GPx4 knock-down at protein level following treatment with *GPX4*-siRNA (1) and MitoQ₁₀.

In a second experiment cells were seeded and transfected 24 h later with either *GPX4*-siRNA or negative control siRNA plus 1 μ M MitoQ₁₀ concentration. Seventy two hours following treatment, cells were lysed and total protein extracted from cell lysate and GPx4 protein assessed by Western blotting using anti-GPx4 antibody. Densitometry analysis of the protein bands showed approximately 70% reduction in GPx4 protein in cells treated with *GPX4*-siRNA(1) plus MitoQ₁₀ indicating that MitoQ₁₀ does not have any impact on the ability of the *GPX4*-siRNA to knock-down GPx4 protein.

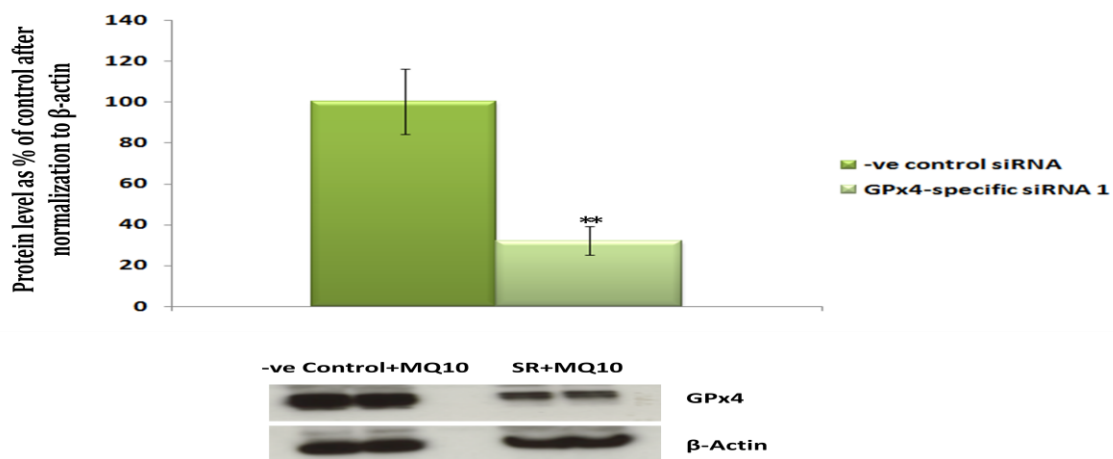


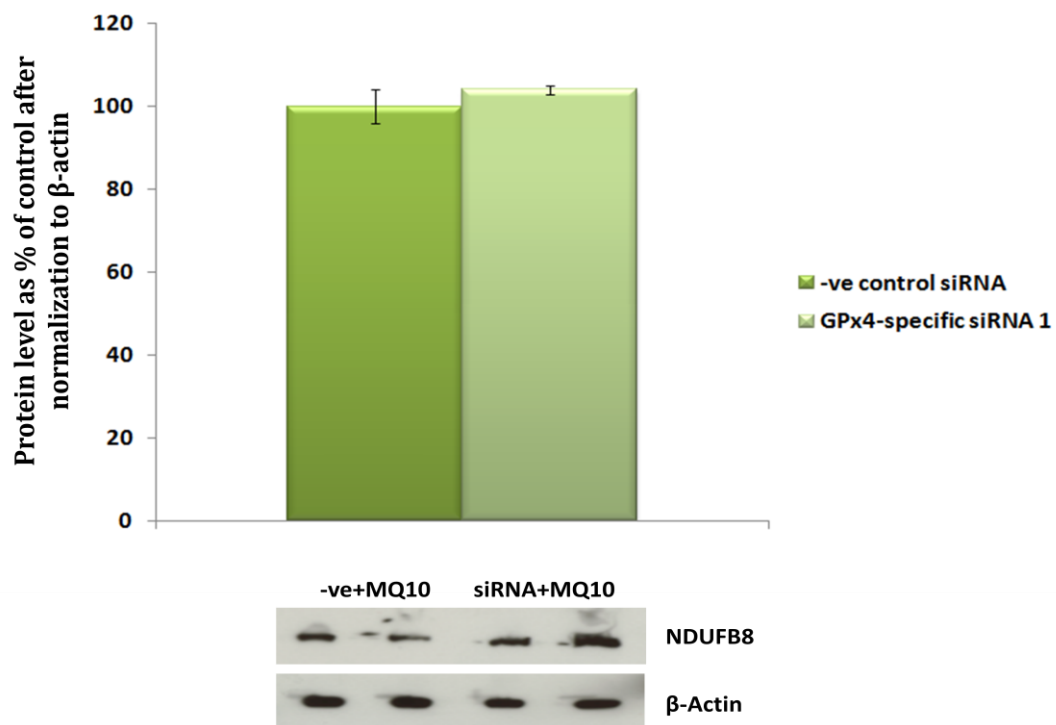
Figure 28. Confirmation of GPX4 knock-down at protein level following siRNA treatment in presence of MitoQ₁₀.

Caco-2 cells were treated for 72 h with *GPX4*-specific siRNA or scrambled negative control in the presence of 1 μ M MitoQ₁₀ concentration, protein was extracted and GPx4 levels assessed by Western blotting. Protein bands were measured by densitometry and GPx4 expression was compared to β -Actin as the control and as a percentage of the mean value for cells treated with the scrambled control siRNA. Western panels = 2 wells, values shown are mean \pm S.D for n=4. Groups were compared using a Mann-Whitney U test, * $p < 0.05$, ** $p < 0.01$.

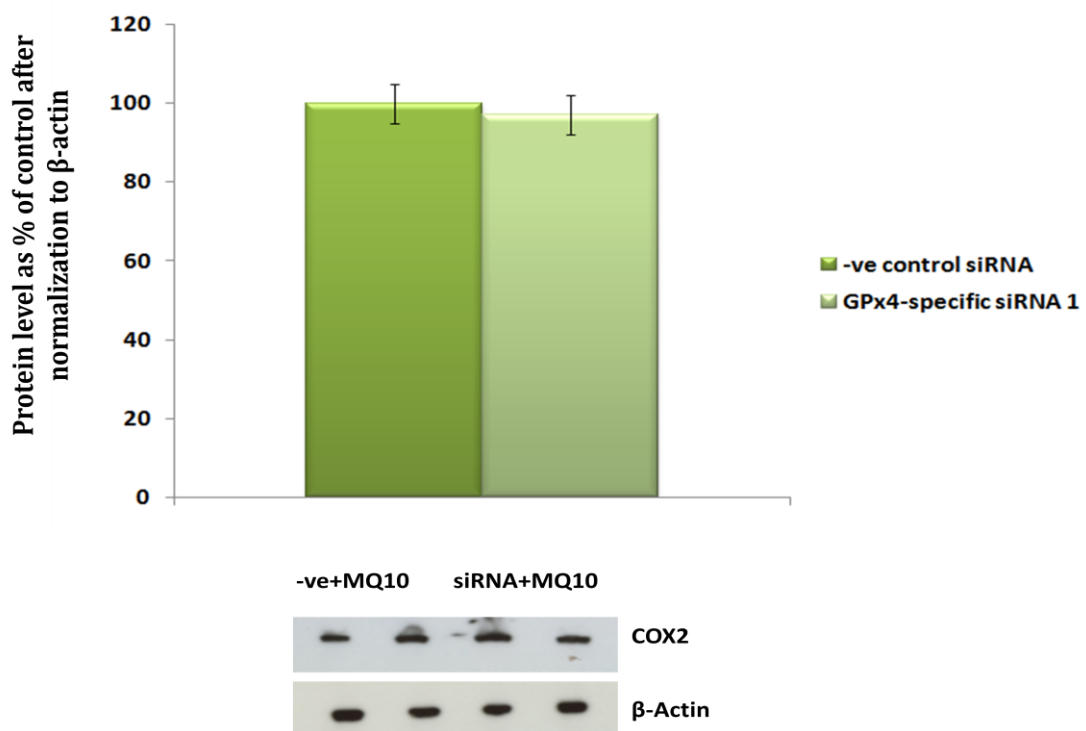
6.1.4 Effect of MitoQ₁₀ treatment on NDUF8, COX2 and AIF protein expression following *GPX4* knock-down in Caco-2 cells.

As discussed in Chapters 4, 5 and 6 of this thesis, *GPX4* knock-down resulted in changes in protein expression of functional markers of complex I and IV of the mitochondrial electron transport chain and AIF. I hypothesized that MitoQ₁₀ treatment abrogates the effects of *GPX4*-siRNA treatment on these proteins in Caco-2 cells. Caco-2 cells were treated with either *GPX4*-siRNA or negative control siRNA with or without 1 μ M MitoQ₁₀ concentration for 72 h. Total protein was extracted from cell lysates and NDUF8 (Figure 29A), COX2 (Figure 29B) and AIF (Figure 29C) measured by Western blotting using antibodies specific to each protein. In the presence of MitoQ₁₀, knock-down of *GPX4* has no significant effect on NDUF8 and COX expression. Indeed, MitoQ₁₀ treatment completely abolished the changes previously observed in NDUF8 and COX2 after *GPX4* knock-down. AIF protein following MitoQ₁₀ treatment and *GPX4* knock-down remained up-regulated as previously observed in the absence of MitoQ₁₀ treatment.

A



B



C

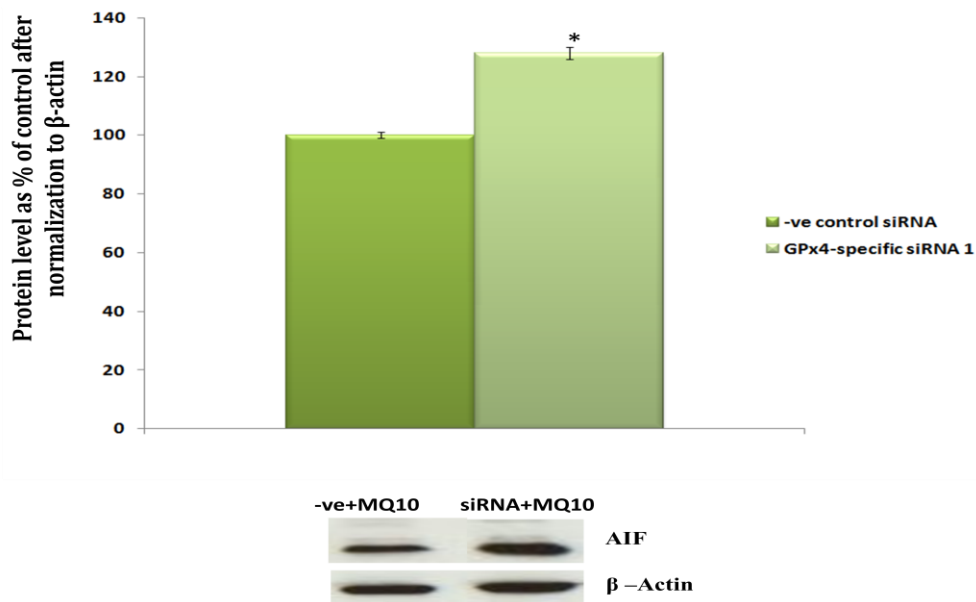
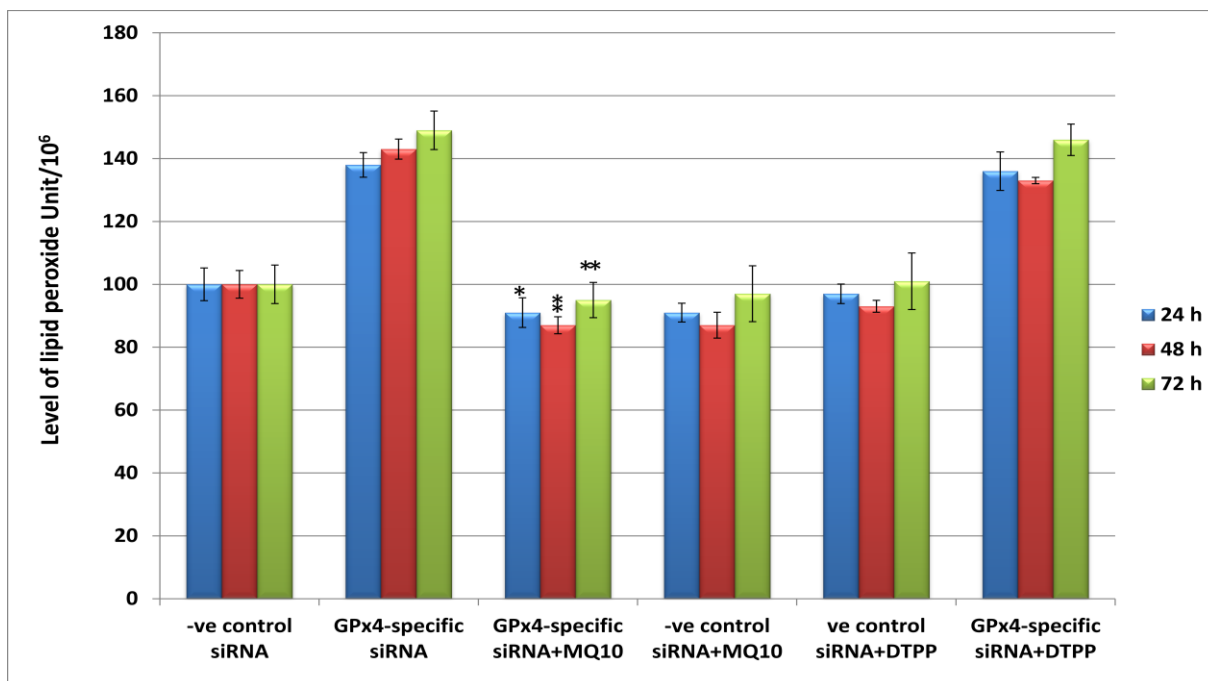


Figure 29. Investigation of the impact of MitoQ10 treatment on the effect of GPX4 knock-down on mitochondrial complex I and IV functional indicators and on AIF

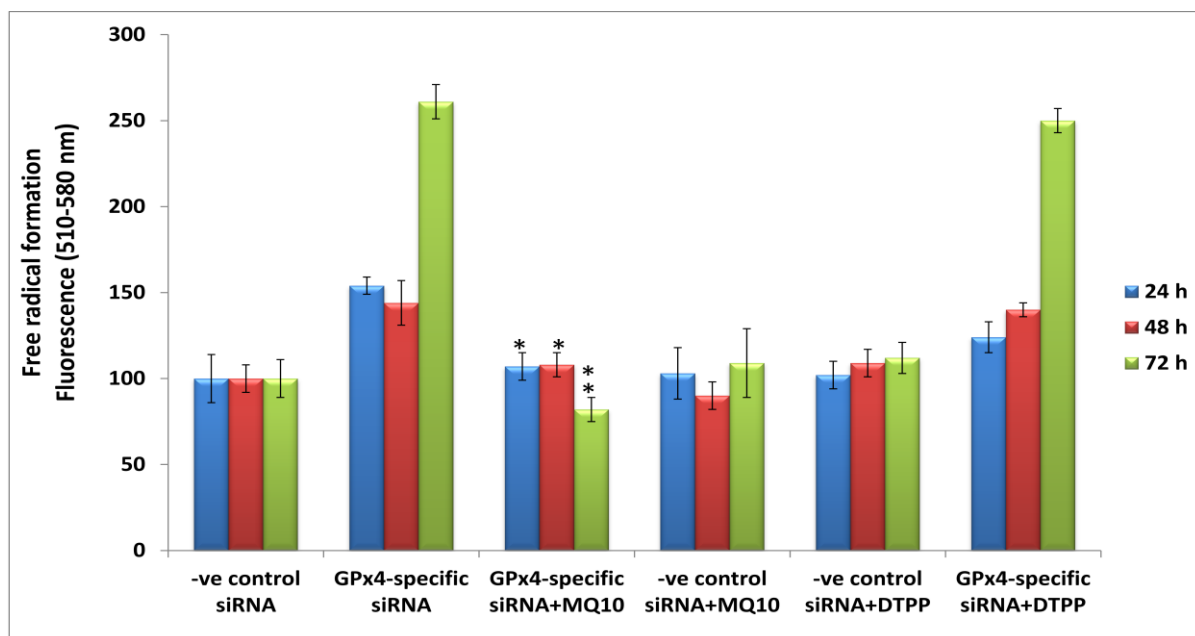
Cells were treated with GPX4-specific siRNA(1) or scrambled negative control in the presence of MitoQ for 72 h. Total cell protein was subjected to Western blotting for analysis of NDUFB8(A), COX2 (B) and AIF (C) (A) Protein expression of NDUFB8 following GPX4 knock-down plus MitoQ₁₀ treatment. (B) Protein expression of COX2 following GPX4 knock-down plus MitoQ₁₀ treatment. (C) Protein expression of AIF following GPX4 knock-down plus MitoQ₁₀. Protein expression levels were calculated relative to β -actin as the housekeeping control and as a percentage of the mean value for cells treated with the negative control siRNA. (Western panels = 2 wells), values shown are mean \pm S.D. n=4 for each protein. Groups were compared using a Mann-Whitney U test, * $p < 0.05$, ** $p < 0.01$.

As previously shown in Chapter 5 of this thesis, *GPX4* knock-down resulted in significant increase in mitochondrial superoxide production and lipid peroxide levels, and reduced mitochondrial membrane potential. To test the effect of MitoQ₁₀ on these parameters following *GPX4* knock-down, cells were seeded in a 96 well plate at 1×10^6 /well and 24 h later transfected with *GPX4*-siRNA(1) or negative control siRNA plus either MitoQ₁₀ or DTPP at 24, 48, and 72 h. Following treatments, cells were washed with PBS and assayed for lipid peroxidation using thiobarbituric acid, superoxide using MitoSOX and mitochondrial membrane potential using JC-1. As shown in Figure 30, MitoQ₁₀ treatment following *GPX4*-siRNA(1) treatment decreased superoxide and lipid peroxide levels, suggesting that MitoQ provided significant protection against oxidative stress (lipid peroxide production, mitochondrial superoxide production). Level of lipid peroxides were three fold higher in cells treated with *GPX4*-siRNA(1) compared with cells treated with both *GPX4*-siRNA and MitoQ₁₀ at three different time points (Figure 30A). Cells treated with DTPP also showed high levels of lipid peroxide (Figure 30A). Additionally, significant reduction of mitochondria superoxide was achieved following treatment with both *GPX4*-siRNA(1) and MitoQ₁₀ at all three time points, compared to cells treated with *GPX4*-siRNA only (Figure 30B). Mitochondrial membrane potential was higher in cells treated with the *GPX4*-siRNA and MitoQ₁₀ compared to cells treated with siRNA alone (Figure 30C).

A



B



C

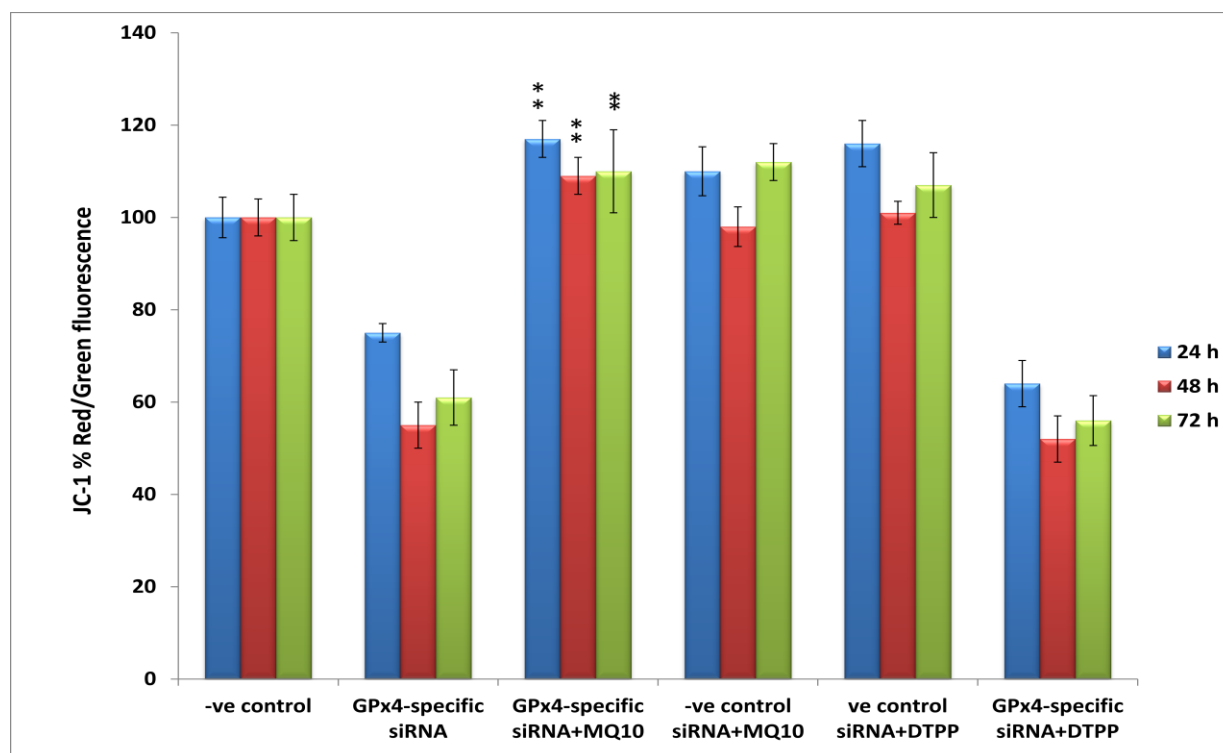


Figure 30. Effects of MitoQ₁₀ on mitochondrial integrity and oxidative stress following GPX4 knock-down with siRNA(1).

Caco-2 cells were treated with 20 nM GPX4-siRNA and either 1µM MitoQ₁₀, 1µM of DecylTPP (at 24, 48, and 72 h) (A) Assessment of lipid peroxide in cells depleted of GPX4 and treated with MitoQ₁₀ and in control cells. (B) Assessment of mitochondria superoxide in cells treated with GPX4-siRNA plus MitoQ₁₀ and in control cells. (C) Assessment of Mitochondrial membrane potential in cells treated with GPX4-siRNA plus MitoQ₁₀ and in control cells. Cells treated with negative control siRNA were used as controls and their mean percentage values were used to calculate changes in siRNA treated cells. Values shown are mean ± S.D for n=6 for each assay and groups were compared using a Mann-Whitney U test, (comparing cells treated with GPX4-siRNA and cells treated with GPX4-siRNA and MitoQ₁₀) p<0.05, ** p<0.01.*

6.2 Discussion

Mitochondria are a major site of reactive oxygen species (ROS) generation within cells, and there is increasing evidence that mitochondrial oxidative stress contributes to a wide range of pathologies, including cardiovascular disease, neurodegeneration and aging (James *et al.*, 2005). Production of ROS by the mitochondrial respiratory chain (complex I through complex III) occurs under normal physiological conditions and is as a result of 1-electron reduction of O₂ to superoxide (O₂⁻) by the respiratory chain, which goes on to produce a range of damaging ROS. Production of ROS lead to nonspecific modification of mitochondrial proteins, lipids, and nucleic acids, thereby altering mitochondrial function (Koopman *et al.*, 2005). Mitochondrial DNA is particularly susceptible to modification by ROS, and this damage can rapidly lead to functional changes in the cell, because it encodes 13 essential polypeptide components of the mitochondrial respiratory chain (Kelso *et al.*, 2000; Koopman *et al.*, 2005; Jing *et al.*, 2011). Mitochondria are normally protected from oxidative damage by a multilayer network of mitochondrial antioxidant systems and these includes the mitochondrial matrix enzyme manganese superoxide dismutase, which converts the O₂⁻ anion to hydrogen peroxide, glutathione peroxidase 4, and peroxiredoxins 3 and 5, which readily convert hydrogen peroxide to water and ultimately prevent mitochondrial oxidative damage such as lipid peroxidation (Ross *et al.*, 2005; James *et al.*, 2007; Murphy, 2008; Smith *et al.*, 2008; Graham *et al.*, 2009). Modification of these antioxidant enzymes resulting from the knockout of manganese superoxide dismutase or glutathione peroxidase 4 gene can significantly influence mitochondrial activity and ROS production (Zhang *et al.*,

2009; García-Fernández *et al.*, 2012). Changes in the mitochondrial antioxidant system may result in a modification of mitochondrial integrity by mitochondria-derived ROS production through increased oxidative stress, which could have confounding effects on mitochondrial membrane potential and ATP production.

A recently developed mitochondria-targeted ubiquinone, MitoQ₁₀, can have important effects on determination of mitochondrial membrane potential and is composed of a lipophilic triphenylphosphonium cation covalently attached to a ubiquinol antioxidant (Nierobisz *et al.*, 2011). Lipophilic cations can easily move through phospholipid bilayers without requiring a specific uptake mechanism; therefore, the triphenylphosphonium cation concentrates MitoQ₁₀ several hundred-fold within the mitochondria. Driven by the large mitochondrial membrane potential MitoQ₁₀ is reduced by the respiratory chain to its active ubiquinol form, which is particularly effective in preventing lipid peroxidation and mitochondrial damage (Smith *et al.*, 2003; Murphy, 2008). Since MitoQ₁₀ has been used in a large range of cell and mitochondrial models (Murphy & Smith, 2010) and has been described as an effective antioxidant against lipid peroxidation (Adlam *et al.*, 2005; Koopman *et al.*, 2005; Murphy, 2008) and is membrane potential dependent (Murphy, 2008), I then hypothesized that cell treatment with MitoQ₁₀ following *GPX4* knock-down may (1) abolish the levels of lipid peroxide and ROS observed previously in siRNA only treated cells and (2) may also retrieve the mitochondrial membrane potential. Experiments described in this Chapter studied whether MitoQ₁₀ could ameliorate effect of *GPX4* knock-down.

GPX4 mRNA status was assessed following cell treatment with MitoQ₁₀ or a control compound DTPP. As shown in Figure 27, *GPX4* mRNA level was similar following either MitoQ₁₀ or DTPP treatment suggesting that MitoQ₁₀ antioxidant activity does not have impact on *GPX4* mRNA expression in Caco-2 cells and can be used as an appropriate compound for further investigation. As also shown in Figure 28, a significant level of *GPX4* knock-down at protein level was achieved in the presence of MitoQ₁₀ indicating that MitoQ₁₀ does not affect *GPX4*-siRNA efficiency.

Protein levels of NDUFB8, COX2 and AIF were also measured following siRNA and MitoQ₁₀ treatment. Effects of MitoQ₁₀ was assessed by comparing MitoQ₁₀ with the control compound decyltriphenylphosphonium (decylTPP). This is composed of the lipophilic triphenylphosphonium cation and aliphatic 10-carbon chain but lacks the ubiquinone moiety and thereby controls for any non-specific effects attributed to the accumulation of lipophilic cations within mitochondria. There was no difference in protein expression between cells treated with siRNA plus MitoQ₁₀ for NDUFB8 (Figure 29A) and COX2 (Figure 29B) compared to the scrambled control siRNA group as observed in the treatment with only *GPX4*-siRNA(1). However, AIF protein expression still remained significantly increased (Figure 29C) in knock-down cells treated with MitoQ₁₀ compared to cells treated with the negative control siRNA.

In addition, MitoQ₁₀ protected cells from *GPX4* knock-down induced lipid peroxide and superoxide, and was able to protect mitochondrial membrane potential. MitoQ₁₀ is orally bio-available and has been shown to accumulate extensively in rat tissues after administration in the drinking water and to protect

against tissue damage (Adlam *et al.*, 2005). MitoQ₁₀ has been shown to be effective against mitochondrial oxidative damage *in vivo* and in rodent models of sepsis and reperfusion injury (Lowe *et al.*, 2008; Supinski *et al.*, 2009; Mukhopadhyay *et al.*, 2012). Cardiovascular diseases such as atherosclerosis had been associated with increased lipid peroxide, combined supplementation of selenium and Coenzyme Q₁₀ resulted to significant reduction of cardiovascular mortality among Swedish citizens aged 70-88 (Alehagen *et al.*, 2012). MitoQ₁₀ protected rat kidney from cold storage injury induced superoxide production, completely prevented mitochondrial dysfunction and significantly improved cell viability in these rats, whereas, these protective effects were not observed in rats treated with DTPP (Mitchell *et al.*, 2010). The protective mechanism observed following MitoQ₁₀ treatment appeared to be attributed to the accumulation of ubiquinol within the mitochondria, because the control substance, decylTPP (DTPP) had no beneficial action. DTPP was used as a control compound because it is known to be taken up in a very similar way to MitoQ₁₀ in cells *in vitro* however lacks the ubiquinol antioxidant moiety as MitoQ₁₀.

In conclusion, the experiments described in this chapter suggest that MitoQ₁₀ in the presence of siRNA increased mitochondrial membrane potential, reduced mitochondrial superoxide and lipid peroxide. Under the same conditions, MitoQ₁₀ prevented increased NDUFB8, COX2 but maintained increase in AIF protein expression. This suggests that increased mitochondrial superoxide is not important for increase in AIF protein expression to occur following *GPX4* knock-down, but increase in superoxide are required for increase NDUFB8 and COX2 protein expression.

Chapter 7: Effect of *GPX4* knock-down on apoptosis signaling in Caco-2 cells.

7.1 Introduction.

Apoptosis, also known as programmed cell death, comprises blebbing of the plasma membrane and fragmentation of DNA (Souza *et al.*, 2012). Cells lose all attachments from the substratum and shrivel during apoptosis. The mechanism of apoptosis involves the release of cytochrome c from the mitochondria into the cytoplasm and activation of a range of other apoptogenic proteins (Souza *et al.*, 2012). Caspases are key enzymes that drive apoptosis and activation of one or more of the Caspases has been widely recognized as an indicator of apoptosis. Activation of other apoptogenic proteins such as Bax, Bak or AIF is also considered as an indication of apoptosis (MacKenzie & Clark 2012).

Following *GPX4* knock-down in Caco-2 cells, the whole genome microarray study described in Chapter 3 indicated changes in mRNA expression of Bax and AIF. It has also been described in Chapter 5 that there were changes in AIF protein level following *GPX4* knock-down. Absence of *GPX4* has been suggested to affect angiogenesis in murine embryonic fibroblasts through the increased activity of 12/15 lipooxygenase, an enzyme that promotes apoptosis, and is an important regulator of tumor angiogenesis (Schneider *et al.*, 2010). Liang and colleagues demonstrated that the cytosolic *GPX4* protected mice from diquat-induced apoptosis (Liang *et al.*, 2009) and reduced *GPX4* expression has been found to increase life-span through increased sensitivity to apoptosis (Ran *et al.*, 2007).

There are two different mechanisms by which apoptosis can occur: the extrinsic apoptotic pathway and the intrinsic mitochondrial-dependent pathway. The extrinsic pathway involves the initiation of extracellular death ligands such as Fas ligand (FasL) through their binding to their corresponding receptors. The extrinsic apoptotic pathway involves activation of Caspase 3 and 7 (known as effector caspases) which leads to a breakdown in cellular components and DNA fragmentation (Zou *et al.*, 1997; Park *et al.*, 2007; Fadeel *et al.*, 2008). Contrary to the extrinsic pathway, the intrinsic pathway (also known as the mitochondrial or AIF-mediated pathway) is regulated by Bcl-2, Bcl-x1, Bax and Bak (Xu *et al.*, 2010). These proteins regulate the permeabilization of the outer membrane of the mitochondria, either positively or negatively, to promote the release of cytochrome c and other apoptotic molecules such as AIF, Smac/DIABLO and Caspase-9 (Fadeel *et al.*, 2008). This results in degradation of cellular components and cell death (Fadeel *et al.*, 2008). Both pathways have been shown to participate in cell apoptosis (Xu *et al.*, 2010). Since microarray analysis following *GPX4* knock-down in Caco-2 cells had shown effects on the expression of AIF and *BAX* mRNA levels and since evidence in the literature has implicated *GPX4* in apoptosis (Liang *et al.*, 2009), a detailed study into the possible link between *GPX4* expression and apoptosis in human intestinal cells was carried out. Activation of apoptosis was assessed by measurement of DNA fragmentation, Caspase-3,-7,-9 protein level and activity, Bax and Bcl-2 protein levels, and levels of phosphatidylserine using Annexin V labeling (an indicator of early stage of apoptosis).

7.2 Results

7.2.1 DNA fragmentation.

Formation of nucleosomal units as a result of nuclear DNA degradation (DNA fragmentation) is one of the hallmarks of apoptotic cell death. Degradation of nuclear DNA occurs in response to different apoptotic stimuli and activation of different apoptogenic proteins in different cell types (Nagata, 2000). Formation of DNA into internucleosomal fragments (fragmented DNA) can be visually observed by the fragments of roughly 180-500 base pairs (Gavrieli *et al.*, 1992). To investigate the effect of *GPX4* knock-down on end stage apoptosis, Caco-2 cells were treated with either *GPX4* siRNA or negative control siRNA and DNA fragmentation assayed as previously described in (Chapter 2 Section 2.11-2.11.1) Cells treated with negative control siRNA did not show any evidence of fragmented nuclear DNA as the DNA remained intact without fragments (Figure 31-NCSIRNA). *GPX4*-siRNA treated cells showed increased level of fragmented DNA (Figure 31-SIRNA) with nuclear DNA fragments of as low as ~200bp. This result is consistent with knock-down of *GPX4* leading to apoptosis.

DNA FRAGMENTATION

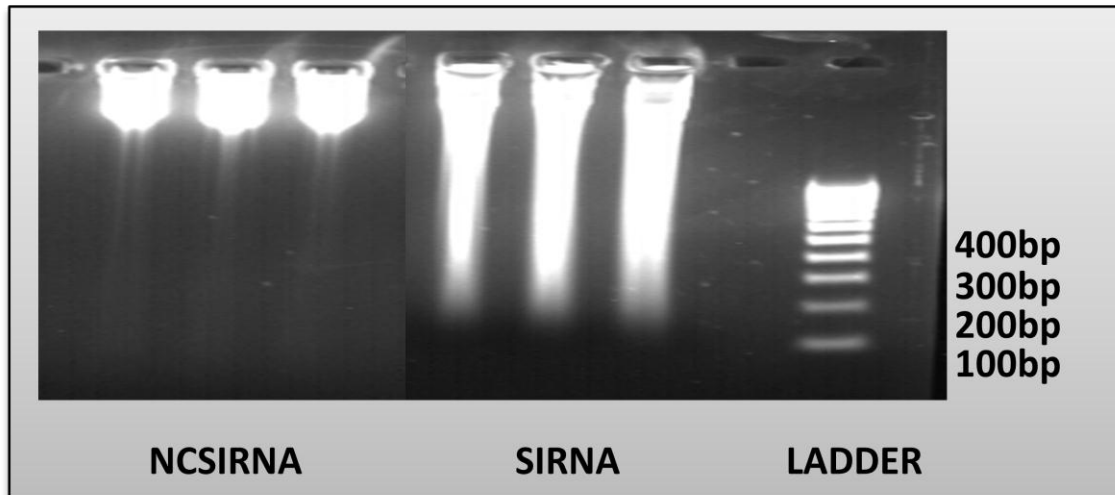


Figure 31. Assessment of DNA fragmentation following treatment with either GPX4-siRNA(1) or scrambled negative control siRNA.

Caco-2 cells were seeded and 24 h later treated with either GPX4-siRNA(SIRNA) or negative control siRNA (NCSIRNA). Seventy two hours following transfection, cells were lysed, nuclear DNA extracted and subjected to electrophoresis along a DNA ladder of 100-1-13bp markers.

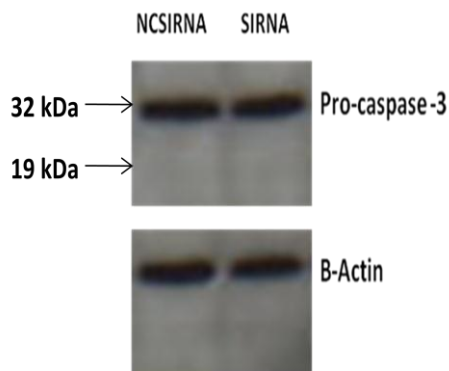
7.2.2 Impact of *GPX4* knock-down on Caspase -3 and -9 protein levels

Caspases play a crucial role in apoptosis and have been shown to play important roles in cell differentiation, survival, proliferation, homeostasis and NFkB activation in different cell types (Sztiller-Sikorska *et al.*, 2009). Since caspases have been implicated in both intrinsic and extrinsic pathways of apoptosis, an investigation of the level of caspase-3 and -9 proteins expression after *GPX4* knock-down was carried out.

Caco-2 cells were seeded and 24 h later transfected with either *GPX4*-siRNA(1) or negative control siRNA. Seventy two hours following transfection cells were washed with cold PBS, lysed and total cell lysate used for protein extraction as described in Chapter 2 Section 2.4-2.4.6. Following protein extraction, caspase-3 and -9 proteins were assessed by Western blotting using specific antibodies. Caspases are zymogens (inactive enzymes precursors) and only become active in the presence of an apoptotic stimulus. Initiator caspases such as caspase-9 cleave the pro-forms of effector caspases such as caspase-3 thereby activating them and caspase-3 then triggers apoptosis by cleaving other protein substrates such as caspase-7 and carbamoyltransferase-dihydroorotase (CAD) within cell. A cleaved caspase-3 can be detected by SDS gel electrophoresis as a ~17-19kDa size protein migrating below the 32 kDa full size protein. As shown in (Figure 31A), there was no cleaved caspase-3 in cells treated with either *GPX4*-siRNA(1) or negative control siRNA suggesting that caspase-3 was not activated following *GPX4* knock-down. Western blotting with an anti-caspase-9 antibody however showed both a full-size

pro-caspase-9 and a cleaved caspase-9 (Figure 32B) following treatment with *GPX4*-siRNA(1), suggesting that *GPX4* knock-down leads to Caspase 9 activation.

A



B

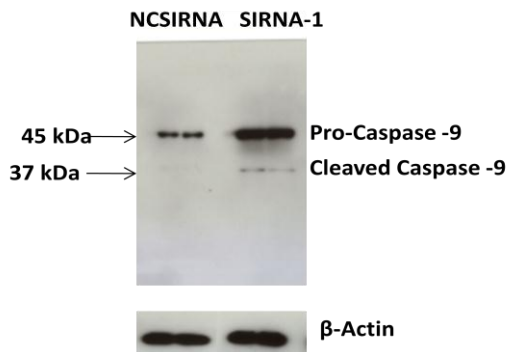


Figure 32. Expression of Caspase-3 and Caspase-9 following *GPX4* knock-down.

Caco-2 cells were treated with either *GPX4*-siRNA (*SIRNA*) or scrambled negative control siRNA (*NCSIRNA*) for 72 h. Cell protein was extracted and caspase 3(A) and caspase-9 (B) assayed by Western blotting. Protein expression was compared to β -actin as a loading control. Note the lower molecular weight caspase-9 band after *GPX4*-siRNA treatment. (Western panels = 2 wells).

7.2.3 Caspase 3/7 enzymatic activity following *GPX4* knock-down

Since no change in cleavage for caspase-3 (an effector caspase for caspase-dependent apoptotic pathway) was observed by Western blotting following *GPX4* knock-down, caspase 3/7 enzymatic activities were measured to verify change in activities of these caspases. Following treatment with *GPX4* siRNA(1) or scrambled negative control siRNA, luminescence-based measurement of caspase activity was carried out at 30, 60, 90 and 120 minutes using Caspase-Glo® 3/7 assay as described in Chapter 2, Section 2.11.2. As shown in Figure 33 there was no statistically significant difference in caspase3/7 activity between cells treated with *GPX4*-siRNA(1) and negative control siRNA, suggesting that neither caspase-3 nor -7 played a role in the apoptosis following *GPX4* knock-down. These observations suggest that apoptosis may possibly be through the alternative intrinsic pathway involving AIF-mediated caspase-9 activation.

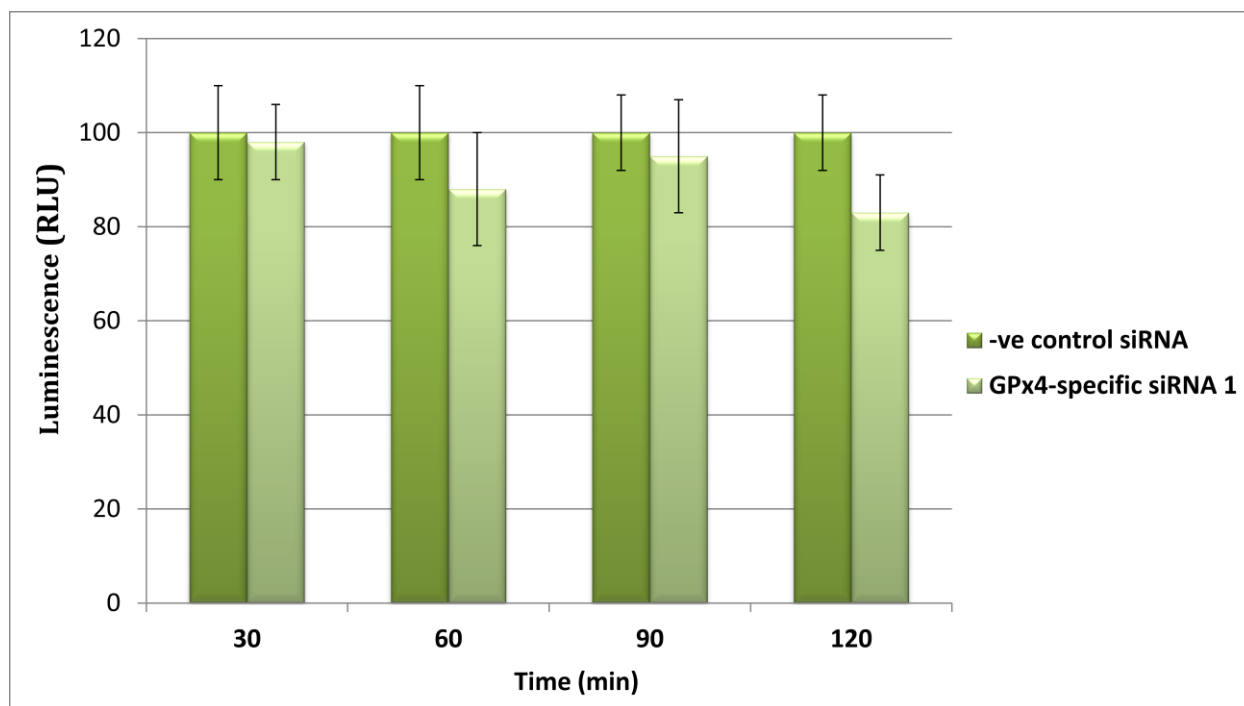


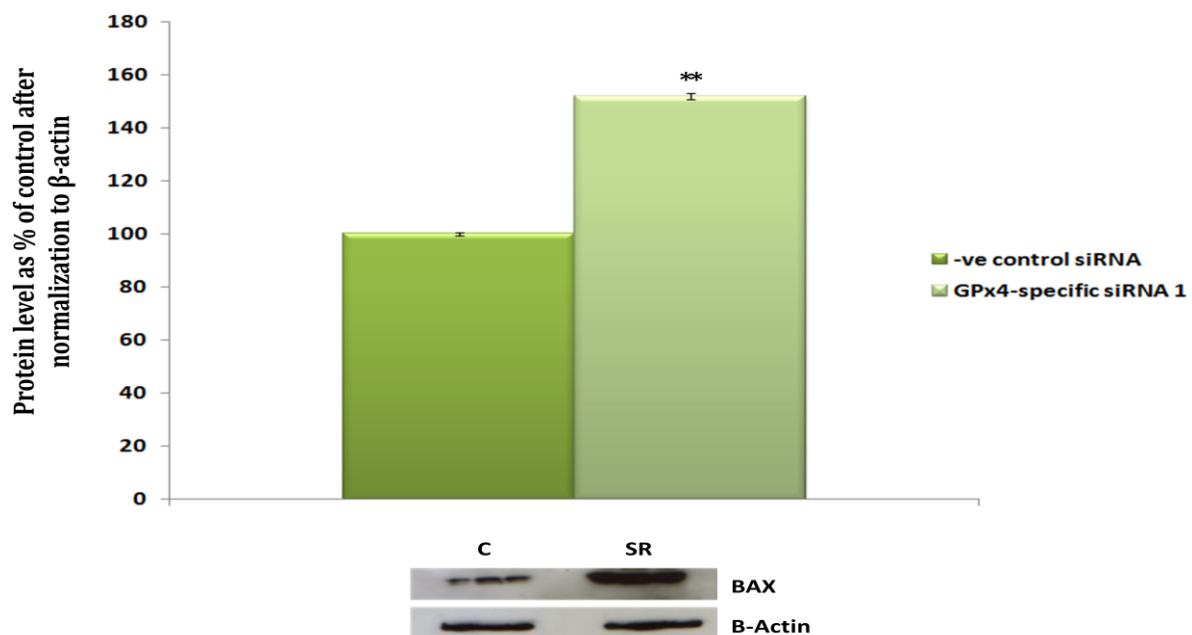
Figure 33. enzymatic activity of caspase-3/7 following treatment with GPX4-siRNA(1) or scrambled negative control siRNA.

*Caco-2 cells were treated with either GPX4-siRNA or scrambled negative control siRNA and then measurement of caspase 3/7 enzyme activities was carried out at different time points. Caspase 3/7 enzyme activity of the GPX4-siRNA treatment group was expressed relative to the level of the control siRNA group, n=4 for each group. Values shown are mean \pm S.D. Groups were compared using a Mann-Whitney U test, * $p < 0.05$, ** $p < 0.01$*

7.2.4 Impact of *GPX4* knock-down on Bax and Bcl-2 protein levels

To test whether *GPX4* knock-down leads to apoptosis through the intrinsic pathway via AIF and caspase-9 activation, measurement of Bax and Bcl-2, markers of the intrinsic pathway of apoptosis, was carried out. Following cell treatment with either *GPX4*-siRNA(1) or negative control siRNA, Western blotting with an anti-Bax and Bcl-2 antibody was used to assess Bax and Bcl-2 protein levels. Bax protein level was increased by 50% (Figure 34A) in *GPX4*-siRNA(1) treated cells compared with control cells, whereas Bcl-2 protein was decreased by 25% (Figure 34B) in *GPX4*-siRNA(1) treated cells. The observed down-regulation of Bcl-2 protein expression and higher levels of Bax following *GPX4* siRNA(1) treatment is consistent with increased activation of apoptosis.

A



B

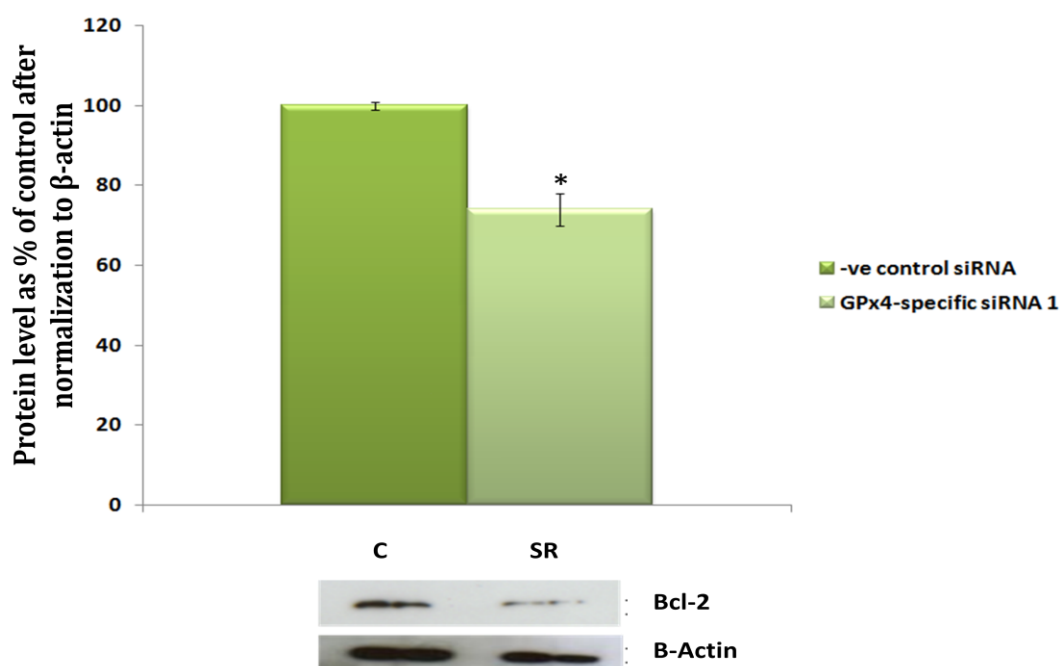


Figure 34. Bax and Bcl-2 protein expression following Caco-2 cell treatment with either GPX4-siRNA(1) or scrambled negative control siRNA.

*Caco-2 cells were treated with GPX4-siRNA (1) or scrambled negative control siRNA for 72 h. Total protein was isolated and Western blotting carried out using anti-Bax (A) and anti-Bcl-2 (B). A significant increase in Bax expression, and a reduction in Bcl-2 were observed following siRNA treatment compared to cells treated with negative control siRNA. Protein bands were measured by densitometry, Bax and Bcl-2 expression normalized to β -Actin as a control and then levels expressed as a percentage of the mean value for cells treated with the scrambled control siRNA. Western panel =3 wells for BAX and 2 wells for Bcl-2, values shown are mean \pm S.D for n=6 Groups were compared using a Mann-Whitney U test, * $p < 0.05$, ** $p < 0.01$*

Since Bax has been strongly linked with apoptosis, further investigation of Bax involvement in *GPX4* knock-down-induced apoptosis was carried out. Caco-2 cells were seeded and 24 h later transfected with either *GPX4* siRNA(1) or negative control siRNA. Seventy two hours following treatment, cells were washed with PBS, lysed and mitochondrial and cytosolic fractions isolated. Bax protein expression was assessed by Western blotting and, as shown in Figure 35, Bax protein was present both in the mitochondrial and cytosol fractions of cells treated with *GPX4*-siRNA(1) and negative control siRNA. Densitometric analysis of the protein bands showed a statistically significant increase of Bax protein in mitochondria fraction of siRNA(1) treated cells compare with control cells. The increased level of Bax protein in the mitochondrial extract of cells treated with *GPX4*-siRNA(1) indicates translocation of Bax from the cytosol into the mitochondria.

Results described in this Chapter have shown *GPX4* knock-down to lead to activation of caspase-9, changes in level of Bax and Bcl-2 protein and DNA fragmentation (marker of end stage apoptosis), all of which point towards activation of the intrinsic apoptotic pathway.

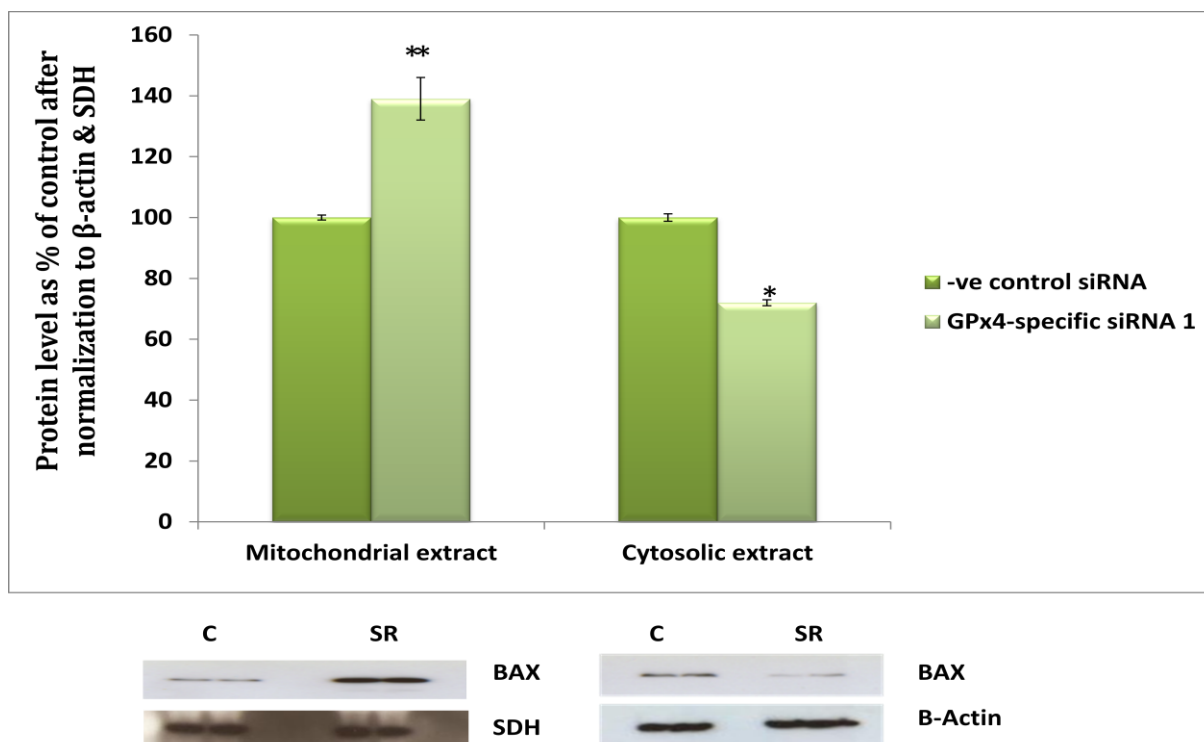


Figure 35. Bax protein levels in mitochondrial and cytosolic fractions expression following treatment with either GPX4 siRNA(1) or scrambled negative control siRNA.

Following treatment of Caco-2 cells with either GPX4-siRNA(1) or scrambled negative control siRNA for 72 h, mitochondrial and cytosolic fractions were isolated. Using anti-Bax antibody, Bax protein was expressed by Western blotting. Bax protein was present in both mitochondrial and cytosolic fractions in both groups. Protein bands were measured by densitometry, cytosolic Bax expression was normalized to β -Actin as the control whereas mitochondrial Bax expression was normalized to SDH as the control and then as a percentage of the mean value for cells treated with the scrambled control siRNA. Western panel = 2 wells, values shown are mean \pm S.D for $n=4$. Groups were compared using a Mann-Whitney U test, * $p<0.05$, ** $p<0.01$

7.2 Flow Cytometric analysis of apoptosis in Caco-2 cells.

Results from previous sections of this chapter have implicated *GPX4* in apoptosis through activation of caspase-9, Bax and Bcl-2 and DNA fragmentation. This section aimed to confirm early stage apoptosis through the release of phosphatidylserine (PS) using Annexin V staining and flow cytometry. In addition, since in Chapter 6 MitoQ10 was shown to influence response of various mitochondrial parameters to *GPX4* knock-down, the effect of MitoQ10 on apoptosis after *GPX4* knock-down was also assessed using Annexin V staining. As described in Chapter 2, section 2.11.3 Caco-2 cells were sub-cultured and left to grow for 24 h before addition of either *GPX4*-siRNA(1) or negative control siRNA and MitoQ10. Seventy two hours following treatment, cells were washed with PBS, harvested and stained with either Annexin V, propidium iodide PI or a combination of Annexin V and PI. Following staining, cells apoptosis were analyzed by flow cytometry.

As shown in Figure 36A and Figure 36B, following cell treatment with either negative control siRNA or both negative control siRNA and MitoQ10, the number of cells undergoing apoptosis appeared low. However, following cell treatment with *GPX4*-siRNA(1) there was a noticeable increase in the number of apoptotic cells (Figure 36C) compared to negative control siRNA treated cells. Quantification of the data (Table 7) confirmed that after *GPX4*-siRNA(1) treatment, there was a greater mean population of apoptotic cells compared to cells treated with the control siRNA however, this difference was not statistically significant. Overall these data suggest that there may be translocation of phosphatidylserine from the inner to the outer plasma membrane in *GPX4*-siRNA(1) treated cells, providing further

evidence that *GPX4* knock-down leads to activation of apoptosis. Additionally, cells treated with *GPX4*-siRNA(1) plus MitoQ₁₀ did not show a statistically significant difference in apoptosis compared to cells treated with the *GPX4*-siRNA only (Figure 36D). This result suggests that lipid peroxidation as a result of *GPX4* knock-down could be one of the causes of changes in DNA fragmentation, caspase 9, Bax and Bcl-2 protein expression, since MitoQ₁₀ has previously been shown in (Chapter 6, Figure 30) to block lipid peroxidation following *GPX4* knock-down.

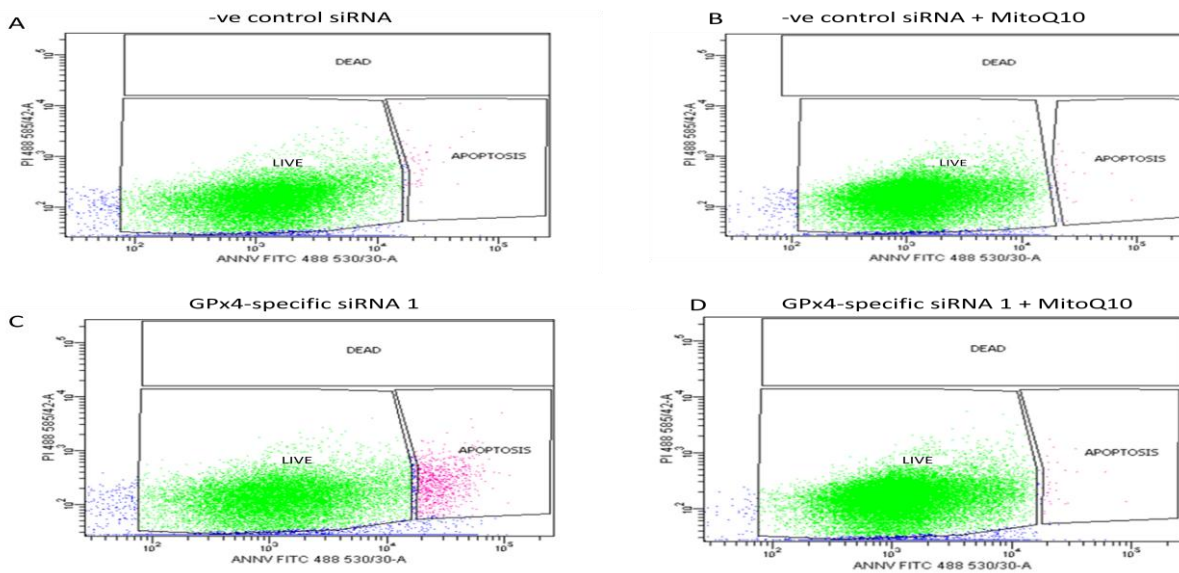


Figure 36. Flow cytometric assessment of apoptosis in Caco-2 cells following GPX4 knockdown.

Caco-2 cells were stained with Annexin V to detect apoptotic cells or PI to detect dead (necrotic) cells. Highlighted in green are vibrant cells (i.e. live cells) and highlighted in pink are apoptotic cells. (A) Cells treated with the *GPX4* negative control siRNA for 72 h (B) Cells treated with a *GPX4* negative control siRNA and MitoQ₁₀ for 72 h (C) Cells treated with *GPX4*-siRNA for 72 h and (D) Cells treated with *GPX4*-siRNA and MitoQ₁₀ for 72 h.

SAMPLE	-ve control siRNA (A)	-ve control +MQ10 (B)	GPX4-siRNA 1 (C)	GPX4-siRNA 1+MQ10 (D)
GROUP	ANNEXIN	ANNEXIN	ANNEXIN	ANNEXIN
%APOPTOSIS	1 ± 0.3	0.9 ± 0.12	3 ± 0.7	0.9 ± 0.1
P-Value		0.6	0.3	0.6

Table 7. Quantification of flow cytometric data to assess apoptosis in Caco-2 cells following GPX4 knockdown.

The percentage of apoptotic cells was calculated from the Annexin V staining. All groups were compared to the percentage of the mean value of cells treated with the negative control siRNA, n=6 for each group. Values shown are mean ± S.D. Groups were compared using Mann-Whiney U test.

7.3 Discussion

Changes in expression of *AIF* and *BAX* mRNA from the microarray data after *GPX4* knock-down led to further investigation of whether *GPX4* knock-down led to cell apoptosis. As shown in Figure 30, fragmented DNA was observed in siRNA(1) treated cells but not in cells treated with negative control siRNA. DNA from siRNA treated cells migrated towards a position suggesting fragments of 100-200bp, which is a typical indication of DNA fragmentation in apoptotic cells (Hotchkiss & Nicholson, 2006).

Generally known as phospholipid-binding protein, Annexin V has a strong binding affinity for phosphatidylserine, a negatively charged phospholipid, known to be localized in the cytosol leaflet of the plasma membrane lipid bilayer, but redistributed from the inner to the outer leaflet in the early phase of apoptosis (Lee *et al.*, 2012). Following Annexin V staining, 3% apoptosis was detected in cells treated with *GPX4*-siRNA(1) compared to cells treated with the negative control siRNA which, showed a 1% apoptosis (Figure 36) although quantification failed to show a statistically significant effect.

Apoptosis can occur through intrinsic (also known as mitochondria or *AIF*-mediated) pathway or extrinsic pathway which involves activation of caspase 3, 7 and 8. To further investigate the mechanism through which the observed DNA fragmentation occurred, caspase-3 and -9 protein expression, caspase 3/7 activities and Bax and Bcl-2 protein expression were investigated. As shown in Figure 31, there was no activation or cleavage of caspase-3 protein in cells treated with either *GPX4*-siRNA(1) or negative control siRNA treated cells. Cleavage to produce a product of approximately 19 kDa would have suggested an activation of pro-caspase-3 which would indicate a caspase-dependent extrinsic pathway

route leading to apoptosis. Increased Caspase 3 and 7 activities have previously been implicated in apoptosis, particularly in the caspase-dependent cell death pathway (Thati *et al.*, 2007). Following *GPX4* knock-down, there was no difference in caspase 3/7 activity in cells treated with siRNA and scrambled control cells (Figure 34) suggesting that the apoptosis observed in the *GPX4* knock-down is independent of caspase-3.

A further study was carried out to explore the protein level of caspase-9 (an initiator caspase linked to mitochondrial death pathway) in cells treated with *GPX4*-siRNA(1) or negative control siRNA. An increase in cleavage of caspase-9 was observed in cells depleted of *GPX4* expression (Figure 32) but not in cells treated with negative control siRNA. This result suggests that the apoptosis observed from the knock-down study may have been through the activation of caspase-9 rather than caspase-3.

The microarray analysis showed *GPX4* knock-down to alter *Bax* mRNA level. Furthermore, a significant increase in Bax protein was observed in cells treated with *GPX4* siRNA(1) compared to negative control siRNA treated cells and this observation was consistent with changes observed from increase in pro-apoptotic *Bax* mRNA (Appendix A1). Increased in *Bax* expression has been widely linked to increased apoptosis (Ekegren *et al.*, 1999; Ismail *et al.*, 2005; Xiao & Zhang, 2008). Generally, Bax is sequestered in the cytosol and is translocated from the cytosol into the mitochondria during apoptosis (Putchá *et al.*, 1999; Bedner *et al.*, 2000; Jia *et al.*, 2001). Translocation of Bax into the mitochondria targets the intermembrane of the mitochondria contact sites and releases cytochrome c (Gao *et al.*, 2001; De Giorgi *et al.*, 2002) which then allows Bax to assemble and package itself within

the mitochondria. Cytochrome c release from the mitochondria cleaves and activates Caspase-9, which sequentially leads to the apoptosis process (Putchá *et al.*, 1999; Gao *et al.*, 2001; Jia *et al.*, 2001).

A study in HeLa cells following Xanthorrhizol (an anti-inflammatory compound that can induce apoptosis) treatment showed increased apoptosis through up-regulation of Bax protein (Ismail *et al.*, 2005). Another study in prenatal fetal brain following exposure to cocaine reported increased Bax protein expression alongside decreased Bcl-2 protein and increased Caspase-9 activity. A study in spinal motor neurons reported increased apoptosis through increased Bax protein expression (Ekegren *et al.*, 1999). In the present work, increased Bax protein was also observed in the isolated mitochondria of cells treated with *GPX4*-siRNA(1) (Figure 35).

Down-regulation of anti-apoptotic protein Bcl-2 expression (Figure 33B) was observed in cells treated with *GPX4*-siRNA(1). Bcl-2 is a crucial regulator of the apoptotic process and an anti-apoptotic protein. Zhang *et al.*, (1999), reported that down-regulation of Bcl-2 mRNA through the use of antisense resulted in increased sensitivity of human gastric adenocarcinoma cell line to phototoxic treatment. A study in human prostate cancer PC3 cells following a delivery of adenoviral ribozyme resulted in down-regulation of Bcl-2 protein expression and increased induction of apoptosis (Dorai *et al.*, 1997a,b; Dorai *et al.*, 1999). Down-regulation of Bcl-2 has been reported as a classical indicator of apoptosis owing to the fact that Bcl-2 function is mainly to inhibit the activation of pro-apoptotic enzymes such as caspases (Cory & Adams, 2002).

These observations suggest that depletion of *GPX4* expression may have acted as an apoptotic stimulus which inhibited expression of anti-apoptotic proteins such as Bcl-2 and activated the expression of pro-apoptotic proteins such as Caspase-9. Bax activation and translocation from the cytosol to the mitochondria, may also have led to a direct activation of intrinsic apoptotic pathway thereby releasing *AIF* from the mitochondrial inter-membrane space to the cytosol. These results are consistent with several studies which suggest that altered *GPX4* leads to effects on apoptosis. For example, overexpression of *GPX4* protected lung fibroblasts from phosphatidylcholine hydroperoxide (PCOOH)-induced loss of mitochondrial membrane potential and blocked apoptosis induced by different apoptotic agents (Garry *et al.*, 2008). During the course of the present work, it was reported that knock-down of *GPX4* with siRNA in Jurkat cells led to enhanced phospholipid peroxidation, increased TNF α -stimulated Az-PC formation and apoptosis (Latchoumycandane *et al.*, 2012). Furthermore, ablation of *GPX4* with tamoxifen administration increased apoptosis in adult mice (Yoo *et al.*, 2012). Previously, Ran *et al* (2007), reported that reduced *GPX4* expression increases life-span in mice through increase sensitivity to apoptosis. Overexpression of *GPX4* in apolipoprotein E-deficient (APOE(-/-)) mice reduced atherosclerotic lesions in aortic tree and aortic sinus suggesting that *GPX4* inhibits the development of atherosclerosis by decreasing lipid peroxidation and inhibits the sensitivity of vascular cells to oxidized lipids (Guo *et al.*, 2008).

Flow cytometry using annexin V antibody showed a non-statistically significant difference in the number of apoptotic cells after *GPX4* knock-down compared to control cells. Additionally, in the presence of MitoQ₁₀ there was also no statistical difference in the the number of apoptotic cells

compared to cells treated with GPX4-siRNA only (Figure 36D). Although MitoQ₁₀ treatment did not show any statistical difference between the two groups, previous studies have implicated MitoQ₁₀ in modulating apoptosis (Wani *et al.*, 2011). MitoQ₁₀ suppressed DNA fragmentation, cytochrome c release and caspase-3 activation against dichlorvos-induced oxidative stress and cell death in rat brain, and MitoQ₁₀ enhanced the activities of MnSOD and glutathione (Wani *et al.*, 2011). MitoQ₁₀ has also been reported to protect pancreatic B-cells against apoptosis and promoted their cell survival and enhanced insulin secretion (Lim *et al.*, 2011). Human fetal liver cells were protected from HOC1-induced cell death by MitoQ₁₀ (Whiteman *et al.*, 2008). An investigation of the mechanism (s) through which cells undergo damage was carried out in cardiomyocyte-like cell line (H9C2) exposed to stimulated ischemia-reperfusion (I/R). This exposure resulted in apoptosis and these cells were found to exhibit increased level of Bax expression. MitoQ₁₀ treatment inhibited further ROS production, protected these cells from apoptosis and enhanced Bcl-2 and Bcl-xl expression (Neuzil *et al.*, 2007).

Chapter 8. Final Discussion

Selenium and selenoproteins have been studied widely in relation to their role in cell physiology and health including antioxidant protection, cancer risk, thyroid hormone metabolism, immune function, inflammation, ER-stress and protein folding, (Sep15 and SelS) (Labunskyy *et al.*, 2009, Shchedrina *et al.*, 2010) and calcium homeostasis (SelN) (Arbogast & Ferreiro, 2010). With regard to intestinal disease, previous studies have implicated Se in protecting the gastrointestinal tract from carcinogenesis and inflammation (Duffield-Lillico *et al.*, 2002, Karp & Koch, 2006). Se intake has been widely linked with reduced risk of colon cancer (Russo *et al.*, 1997, Fairweather-Tait *et al.*, 2011; Rayman, 2012; Meplan & Hesketh, 2012) and has been used to control effects of inflammatory bowel disease (Halliwell *et al.*, 2000). Furthermore, the antioxidant effect of Se is exerted through selenium-dependent enzymes such as the family of GPx, and double knock-out mice of GPx1^{-/-} and GPx2^{-/-} showed increased vulnerability to colitis and colon cancer (Esworthy *et al.*, 2003).

Previous work with knock-out mice has shown that *GPX4* is essential for normal development (Yant *et al.*, 2003). In addition to its essential function in sperm viability and proposed functions in detoxifying lipid hydroperoxides, recent findings suggest a role linked to eicosanoid metabolism and apoptosis (Brigelius, 1999; Imai & Nakagawa, 2003; Seiler *et al.*, 2008; Bellinger *et al.*, 2009; Conrad, 2009). Low *GPX4* expression has been found to lead to higher levels of 12/15 lipoxygenase-derived lipid hydroperoxides and increased AIF-induced apoptosis (Seiler *et al.*, 2008; Conrad, 2009; Conrad *et al.*, 2010). The present findings complement and extend this earlier work by linking *GPX4* and *AIF* to the

mitochondrial respiratory complexes in addition to apoptosis. Interestingly, a common genetic polymorphism has been found in the *GPX4* gene in a region corresponding to the 3' untranslated region (rs713041) (Villette *et al.*, 2002) and this variant has not only been shown to have functional consequences in reporter gene assays and effects on lymphocyte selenoprotein activity (Bernamo *et al.*, 2007; Pagmantidis *et al.*, 2008) but has also been reported to affect susceptibility to CRC risk (Bernamo *et al.*, 2007; Pagmantidis *et al.*, 2008). These results suggest that changes in *GPX4* activity as a result of this variant, possibly in combination with low Se intake, will affect mitochondrial function and apoptosis.

The first aim of the work described in this thesis was to use a gene microarray approach to study the function of *GPX4* in intestinal epithelial cells using siRNA to knock-down *GPX4* expression. In order to carry out this study, two different siRNA specific to *GPX4* were designed using published methods (Reynolds *et al.*, 2004, Ui-Tei *et al.*, 2004) and commercially synthesized as described in Chapter 2, (Section 2.2). Caco-2 cells were used as an appropriate model for this study because they are derived from the human intestinal epithelium where majority of redox process occur. Caco-2 cells are relatively stable model to work with and many studies of antioxidant function (including that of selenoproteins) have been carried out in Caco-2 cell. Recent studies include investigation of the metabolism of linoleic acid (Lengler *et al.*, 2012), glucose uptake (Zheng *et al.* 2012), epigenetic effects of isothiocyanates (Barrera *et al.*, 2012) and *GPX4* induction during enterocytic cell differentiation (Speckmann *et al.*, 2011) was carried ou in Caco-2 cells.

Confirmation of *GPX4* knock-down at both mRNA and protein was determined by PCR and Western blotting respectively. Results obtained following densitometry analysis of mRNA and protein band showed that expression levels of GPx4 both at mRNA and protein were reduced and statistical analysis indicated that the changes were significant.

Following confirmation of *GPX4* knock-down at 72 h, mRNA was isolated and used to study the effects of GPx4 knock-down on global gene expression in Caco-2 cells. The microarray data showed changes in mRNA expression of 795 genes including subunit genes of mitochondrial complexes I, V and IV, and genes involve in apoptosis (Appendix A1 and A2).

Pathway analysis of the genes whose expression changed as a result of *GPX4* knock-down was carried out. Ingenuity Pathway Analysis (IPA) showed that the major canonical pathways affected were mitochondrial pathways including oxidative phosphorylation pathway, ubiquinone pathway and mitochondrial dysfunctional pathway. Toxicology list analysis with IPA also showed increased in oxidative stress in cells treated with *GPX4*-siRNA (Table 6). Network analysis with IPA showed that the major effect of knock-down of *GPX4* in the intestinal epithelial Caco-2 cell line was changes in mitochondrial complexes I, IV and V and their subunits (Figure 13) and also altered mRNA expression of AIF, a key regulator of mitochondrial complex I and IV electron transport chain complexes.

Real-time RT-PCR and Western blotting measurements confirmed that knock-down of *GPX4* led to changes in the respiratory chain complexes (Figure 14 and 15) respectively. Furthermore, although no statistically significant changes in cellular in respiration and cellular ROS were observed in cells treated

with *GPX4*-siRNA (Figure 20), the changes in gene expression were accompanied by increased mitochondrial ROS levels, increased lipid peroxidation, loss of mitochondrial membrane potential and lower ATP levels (Figures 19). Mice over-expressing *GPX4* show changes in response to the oxidant diquat, with lower cardiolipin peroxidation and lower loss of mitochondrial membrane potential and increased apoptosis (Liang *et al.*, 2007; Liang *et al.*, 2009). The present data extend these earlier studies not only by showing that *GPX4* knock-down has complementary effects on mitochondrial lipid peroxidation and membrane potential, but by also showing that *GPX4* knock-down alters expression of components of complexes I, IV and V and, mitochondrial integrity and *AIF* expression.

Additionally, Caco-2 cells were treated with a mitochondria-targeting antioxidant Mitoquinone 10 (MitoQ₁₀) following the observation that *GPX4* knock-down altered mitochondrial ubiquinone biosynthesis pathway. The objective was to investigate if MitoQ₁₀ would modulate some of the effects of *GPX4* knock-down. Indeed MitoQ₁₀ repressed the changes in lipid peroxide, ROS, and elevated mitochondrial membrane potential in cells treated with *GPX4*-siRNA (Figure 30) and prevented the change in protein expression observed in NDUFB8 and COX2 but not the changes in *AIF* (Figure 29). These observations suggest that *GPX4* knock-down may cause the oxidation of ubiquinone (Q₁₀), and preliminary data obtained using mass spectrometry to measure Q₁₀ suggests that knock-down of *GPX4* results in lower Q₁₀ level (data not shown).

MitoQ has recently been used as a therapeutic intervention for ROS and mitochondrial oxidative damage induced pathologies. Combined supplementation of selenium and Coenzyme Q₁₀ resulted in

significant reduction of cardiovascular mortality among Swedish citizens aged 70-88 (Alehagen *et al.*, 2012), supplementation of Coenzyme Q₁₀ reduced oxidative stress and increased antioxidant enzyme activity in patient with coronary artery diseases (Lee *et al.*, 2012). In addition supplementation of soluble MQ₁₀ improves intracellular distribution and promotes mitochondrial respiration in T67 and H9c2 cell lines (Bergamini *et al.*, 2012).

This is the first transcriptomic study of effects of changes in *GPX4* expression and the results emphasise a major role for *GPX4* in AIF/mitochondrial pathways. Indeed the present results suggest that AIF plays a key role in the regulation of the mitochondrial oxidative phosphorylation system following *GPX4* knock-down. First, pathway analysis of the present transcriptomic analysis highlights changes in AIF as being a potential central regulator of the expression changes in complexes I, IV and V. Secondly, confirmation of mRNA data by Western blotting shows changes in NDUFB8, COX2 and AIF levels following *GPX4* knock-down. However the contradiction between change in AIF mRNA and protein has been difficult to understand and this allows room for future investigation. The time course experiment shows that the increased AIF protein expression is an early event, occurring before alterations in NDUFB8 expression (Figure 24). This is consistent with recent studies suggesting that AIF regulates activity of complex I (Daugas *et al.*, 2000; Joza *et al.*, 2009; Hangen *et al.*, 2010).

The findings of this study following *GPX4* knock-down in human gut epithelial cell suggest that the function of *GPX4* is not only restricted to protecting cells against oxidative stress such as hydroperoxides, but can also play a role in either maintaining or regulating functional mitochondria and

protecting cell from apoptosis. Reduced *GPX4* expression also resulted in DNA fragmentation (Figure 32), activation of cleaved caspase-9 protein (Figure 33) and changes in protein expressions of Bax and Bcl-2 (Figure 35). Western blotting showed increased expression of Bax in the mitochondria fraction of siRNA treated cells (Figure 36), which support reports that Bax dimerization as a result of apoptosis stimulus leads to Bax translocation from the cytosol into the mitochondria. These observations strongly suggest *GPX4* involvement in apoptosis. Also a translocation of AIF from the mitochondria into the cytosol was observed in isolated cytosol following siRNA treatment.

Age-related mitochondrial DNA mutations lead to changes in colonic cell apoptosis (Nooteboom *et al.*, 2010), suggesting that changes in mitochondrial oxidative function as a result of altered *GPX4* activity may influence colonic cell proliferation. However, further studies are needed to define whether this is the case, how such effects are related to overall gut epithelial cell function, and whether they influence risk of colorectal cancer.

During the course of the study described in this thesis, a whole genome gene expression and pathway study in fibroblasts of a homogenous group of patients deficient in mitochondrial complex I with defect in one of the nuclear encoded structural subunits, showed increased expression of oxidative stress pathway and decreased selenium metabolism and selenoprotein pathway (Voets *et al.*, 2011). This observation by Voets and colleagues implicated low selenium and selenoproteins in mitochondrial complex I deficiency. A second study in mice photoreceptor cells lacking *GPX4* showed significant decrease in mitochondrial biomass, elevation of cell death associated with the translocation of AIF (also

an important regulator of mitochondrial electron transport chain complexes I and IV), suggesting the critical role of *GPX4* in AIF-mediated cell death (Ueta *et al.*, 2012). Thirdly, a study on *GPX4* ablated mouse (*GPX4*(f/f)) with a flanked *GPX4* exon 2-4 at loxP sites, and further cross-bred with a tamoxifen (tam)-inducible Cre transgenic mouse (R26CreER mice), showed a significant reduction (75-85%) of *GPX4* levels in brain, liver, lung and kidney tissue of adult *GPX4* mice. These mice died within 2 weeks of treatment, but prior to death, exhibited increased mitochondrial damage, increased levels of 4-hydroxynonenal levels, decreased activities of mitochondrial electron transport chains complexes I and IV, decreased ATP synthesis in the liver and increased apoptosis (Yoo *et al.*, 2012). Fourthly, siRNA knock-down of GPx4 in Jurkat cells has been found to lead to increased phospholipid hydroperoxides and TNF α -stimulated Az-PC formation, mitochondrial damage and apoptosis (Latchoumycandane *et al.*, 2012).

This study has reported that in undifferentiated Caco-2 gut epithelial cells changes in *GPX4* activity lead to altered expression of 795 genes of which some are involved in mitochondrial metabolism and some in apoptosis. Interestingly, it has recently been observed that *GPX4* expression is increased during Caco-2 cell differentiation and that there is higher expression in upper villus enterocytes which are fully differentiated (Speckmann *et al.*, 2011). AIF has played a central role in the entire study of this project namely; in the microarray and time course experiment suggesting that the AIF-related protective role of *GPX4* may be particularly important in differentiated enterocytes. Future work should involve investigating the role of GPx4 in other intestinal cell lines and in differentiated Caco-2.

In this study, the siRNA used were expected to knock-down both the cytosolic and mitochondria forms of GPx4, and it was not possible to distinguish between the extent of knock-down of the two forms. However, in control cells expression of mGPx4 was barely detectable by RTPCR and much lower than expression of cGPx4. Thus, the observed effect of the siRNA on mitochondrial parameters suggests that cGPx4 is also important in maintaining mitochondria function. Various studies on GPx4 such as Barriere *et al.* (2004), Ran *et al.*, (2004), Ran *et al.*, (2006), Liang *et al.*, (2007), Garry *et al.*, (2008), Guo *et al.*, (2008), Ufer *et al.*, (2008), and Rubio *et al.*, (2012) have overexpressed both isoforms of GPx4 (mitochondria GPx4 (mGPx4) and cytosolic GPx4 (cGPx4)). On the other hand, Dabkowski *et al.*, (2008), investigated overexpressed GPx4 solely in the mitochondrion (mGPx4). Interestingly, none of these studies was conclusive on the effects of two GPx4 isoforms for mitochondrial function and this presents an opportunity for further study of the relative importance of cGPx4 and mGPx4.

In conclusion, I hypothesise that in Caco-2 gut epithelial cells *GPX4* protects mitochondria from oxidative damage and plays a crucial role in regulating and maintaining the redox state, a functional oxidative phosphorylation system and ATP synthesis possibly through AIF (Figure 37). The Mito₁₀ experiment showed that the antioxidant lessened the effects of *GPX4* knock-down on mitochondrial membrane potential, mitochondrial superoxide and mitochondrial Complex I and IV but not AIF. This suggests that *GPX4* knock-down alters lipid peroxide and changes CoQ₁₀ levels, which in turn affects mitochondrial membrane potential and Complex I and IV (Figure 37). This is also compatible with the time-course data showing *GPX4* knock-down affecting lipid peroxide, mitochondrial membrane potential before expression of complex I and IV. However, *GPX4* knock-down also affects AIF and I

suggest that this may be a result of change in mitochondrial ROS or a result of changes in regulation of complex I and IV.

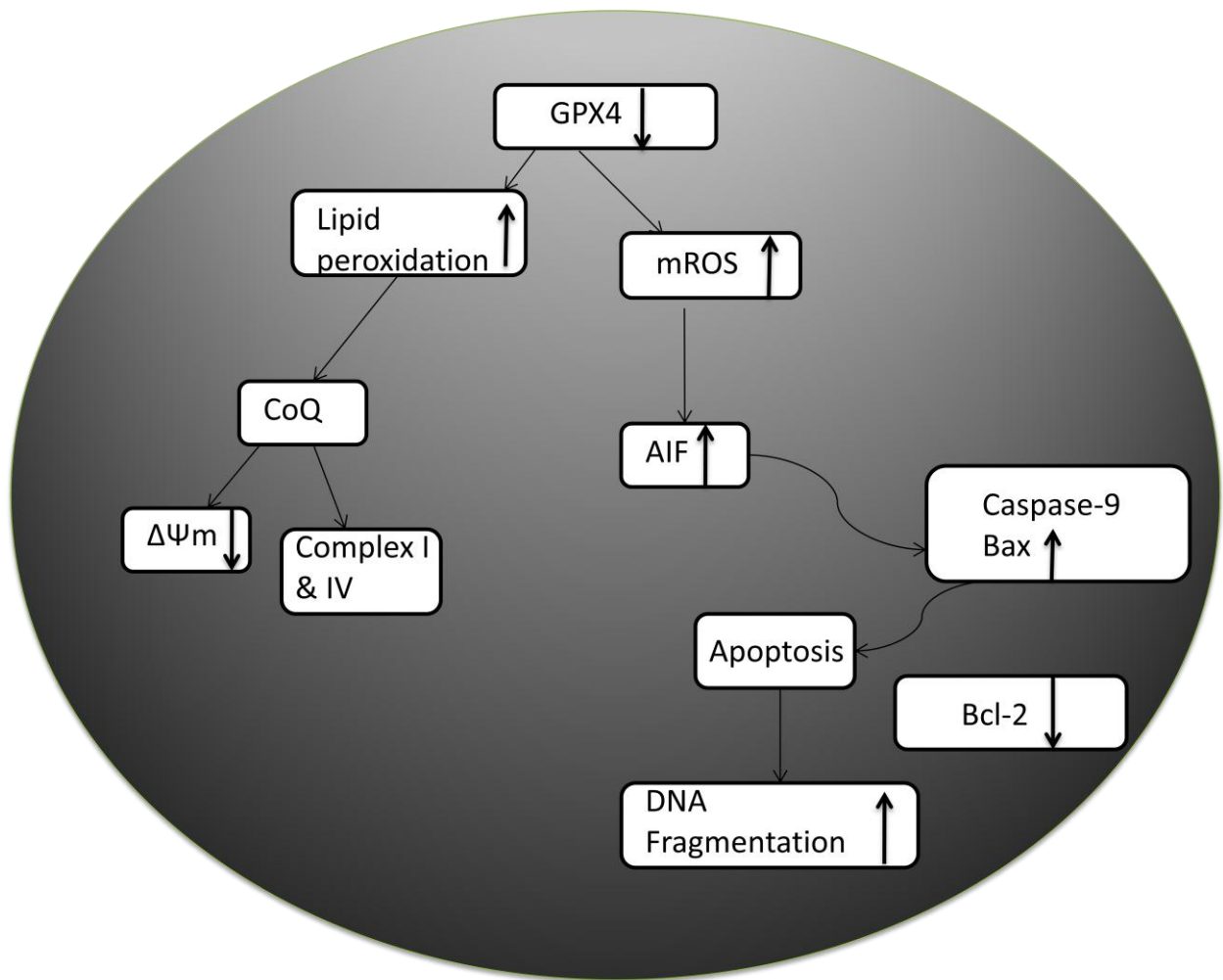


Figure 37. A hypothetical model of the role of GPX4 in Caco-2 cells

The hypothetical model is based on the findings described in this thesis and observed increase (↑) and decrease (↓) are indicated. In the model, oxidized lipids and ROS increase as a result of reduced GPX4 expression, and their changes are proposed to have two sets of consequences. First, activation of mitochondrial apoptogenic proteins such as AIF, Caspase-9 and Bax. Activation of Bax inhibits anti-apoptotic Bcl-2 expression and induction of DNA fragmentation. Second, increased lipid peroxides following GPX4 knock-down also affect ubiquinone (CoQ) biosynthesis which in turn affects mitochondrial membrane potential ($\Delta\Psi_m$) and mitochondria complex I and IV.

Chapter 9. References

- ABE, M., XIE, W., REGAN, M. M., KING, I. B., STAMPFER, M. J., KANTOFF, P. W., OH, W. K. & CHAN, J. M. 2011. Single-nucleotide polymorphisms within the antioxidant defence system and associations with aggressive prostate cancer. *BJU International*, 107, 126-134.
- ABRAHAMSEN, M. S., TEMPLETON, T. J., ENOMOTO, S., ABRAHANTE, J. E., ZHU, G., LANCTO, C. A., DENG, M., LIU, C., WIDMER, G., TZIPORI, S., BUCK, G. A., XU, P., BANKIER, A. T., DEAR, P. H., KONFORTOV, B. A., SPRIGGS, H. F., IYER, L., ANANTHARAMAN, V., ARAVIND, L. & KAPUR, V. 2004. Complete genome sequence of the apicomplexan, *Cryptosporidium parvum*. *Science*, 304, 441 - 445.
- ABRAMOV, A. Y., SMULDERS-SRINIVASAN, T. K., KIRBY, D. M., ACIN-PEREZ, R., ENRIQUEZ, J. A., LIGHTOWLERS, R. N., DUCHEN, M. R. & TURNBULL, D. M. 2010. Mechanism of neurodegeneration of neurons with mitochondrial DNA mutations. *Brain*, 133, 797-807.
- ADLAM, V. J., HARRISON, J. C., PORTEOUS, C. M., JAMES, A. M., SMITH, R. A. J., MURPHY, M. P. & SAMMUT, I. A. 2005. Targeting an antioxidant to mitochondria decreases cardiac ischemia-reperfusion injury. *The FASEB Journal*, 19, 1088-1095.
- AHN, J. H., CHOI, J. H., SONG, J. M., LEE, C. H., YOO, K.-Y., HWANG, I. K., KIM, J. S., SHIN, H.-C. & WON, M.-H. 2011. Increase in Trx2/Prx3 redox system immunoreactivity in the spinal cord and hippocampus of aged dogs. *Experimental Gerontology*, 46, 946-952.
- AITKEN, R. J. 1989. The role of free oxygen radicals and sperm function. *Int J Androl*, 12, 95-7.
- AITKEN, R. J. 1999. The Amoroso Lecture The human spermatozoon – a cell in crisis? *Journal of Reproduction and Fertility*, 115, 1-7.
- AKBARALY, T., HININGER-FAVIER, I., CARRIERE, I., ARNAUD, J., GOURLET, V., ROUSSEL, A. & BERR, C. 2007. Plasma selenium over time and cognitive decline in the elderly. *Epidemiology*, 18, 52-8.
- AKEMATSU, T. & MATSUOKA, T. 2008. Chromatin extrusion in resting encystment of Colpoda cucullus: a possible involvement of apoptosis-like nuclear death. *Cell Biol Int*, 32, 31 - 38.
- AKEMATSU, T. & ENDOH, H. 2010. Role of apoptosis-inducing factor (AIF) in programmed nuclear death during conjugation in *Tetrahymena thermophila*. *BMC Cell Biology*, 11, 13.
- ALBERICI, L. C., OLIVEIRA, H. C. F., PAIM, B. A., MANTELLO, C. C., AUGUSTO, A. C., ZECCHIN, K. G., GURGUEIRA, S. A., KOWALTOWSKI, A. J. & VERCESI, A. E. 2009. Mitochondrial ATP-sensitive K⁺ channels as redox signals to liver mitochondria in response to hypertriglyceridemia. *Free Radical Biology and Medicine*, 47, 1432-1439.
- ALEHAGEN, U., JOHANSSON, P., BJÖRNSTEDT, M., ROSÉN, A. & DAHLSTRÖM, U. 2012. Cardiovascular mortality and N-terminal-proBNP reduced after combined selenium and coenzyme Q10 supplementation: A 5-year prospective randomized double-blind placebo-controlled trial among elderly Swedish citizens. *International Journal of Cardiology*.
- ALLAN, C. B., LACOURCIERE, G. M. & STADTMAN, T. C. 1999. Responsiveness of selenoproteins to dietary selenium 1, 2 *Annual Review of Nutrition*, 19, 1-16.
- ALVAREZ, J. G. & STOREY, B. T. 1982. Spontaneous lipid peroxidation in rabbit epididymal spermatozoa: its effect on sperm motility. *Biology of Reproduction*, 27, 1102-1108.
- AMBROSE, M., RYAN, A., O'SULLIVAN, G. C., DUNNE, C. & BARRY, O. P. 2006. Induction of Apoptosis in Renal Cell Carcinoma by Reactive Oxygen Species: Involvement of Extracellular Signal-Regulated Kinase 1/2, p38 δ/γ , Cyclooxygenase-2 Down-Regulation, and Translocation of Apoptosis-Inducing Factor. *Molecular Pharmacology*, 69, 1879-1890.
- AMIRI, M., FARZIN, L., MOASSESI, M. & SAJADI, F. 2010. Serum trace element levels in febrile convulsion. *Biol Trace Elem Res*, 135, 38-44.

- ANDREASSON, K. I., SAVONENKO, A., VIDENSKY, S., GOELLNER, J. J., ZHANG, Y., SHAFFER, A., KAUFMANN, W. E., WORLEY, P. F., ISAKSON, P. & MARKOWSKA, A. L. 2001. Age-Dependent Cognitive Deficits and Neuronal Apoptosis in Cyclooxygenase-2 Transgenic Mice. *J Neurosci*, 21, 8198 - 8209.
- ANTHONY, G., STROH, A., LOTTSPREICH, F. & KADENBACH, B. 1990. Different isozymes of cytochrome c oxidase are expressed in bovine smooth muscle and skeletal or heart muscle. *FEBS Letters*, 277, 97-100.
- APOSTOLOVA, N., CERVERA, A. M., VICTOR, V. M., CADENAS, S., SANJUAN-PLA, A., ALVAREZ-BARRIENTOS, A., ESPLUGUES, J. V. & MCCREATH, K. J. 2005. Loss of apoptosis-inducing factor leads to an increase in reactive oxygen species, and an impairment of respiration that can be reversed by antioxidants. *Cell Death Differ*, 13, 354-357.
- ARAI, M., IMAI, H., KOUMURA, T., YOSHIDA, M., EMOTO, K., UMEDA, M., CHIBA, N. & NAKAGAWA, Y. 1999. Mitochondrial Phospholipid Hydroperoxide Glutathione Peroxidase Plays a Major Role in Preventing Oxidative Injury to Cells. *Journal of Biological Chemistry*, 274, 4924-4933.
- ARAI, M., IMAI, H., SUMI, D., IMANAKA, T., TAKANO, T., CHIBA, N. & NAKAGAWA, Y. 1996. Import into Mitochondria of Phospholipid Hydroperoxide Glutathione Peroxidase Requires a Leader Sequence. *Biochemical and Biophysical Research Communications*, 227, 433-439.
- ARAKAWA, H., LOTVALL, J., KAWIKOVA, I., TOKUYAMA, K., LOFDAHI, C. & SKOOGH, B. 1994. Effect of maturation on airway plasma exudation induced by eicosanoids in guinea pig. *Eur J Pharmacol*, 259, 251-7.
- ARBOGAST, S. & FERREIRO, A. 2010. Selenoproteins and protection against oxidative stress: selenoprotein N as a novel player at the crossroads of redox signaling and calcium homeostasis. *Antioxid Redox Signal*, 12, 893-904.
- ARNOULT, D., TATISCHEFF, I., ESTAQUIER, J., GIRARD, M., SUREAU, F., TISSIER, J. P., GRODET, A., DELLINGER, M., TRAINCARD, F., KAHN, A., AMEISEN, J. C. & PETIT, P. X. 2001. On the evolutionary conservation of the cell death pathway: mitochondrial release of an apoptosis-inducing factor during Dictyostelium discoideum cell death. *Mol Biol Cell*, 12, 3016 - 3030.
- ASHRAFI, M. R., SHABANIAN, R., ABBASKHANIAN, A., NASIRIAN, A., GHOFRANI, M., MOHAMMADI, M., ZAMANI, G. R., KAYHANIDOOST, Z., EBRAHIMI, S. & POURPAK, Z. 2007a. Selenium and Intractable Epilepsy: Is There Any Correlation? *Pediatric Neurology*, 36, 25-29.
- ASHRAFI, M. R., SHAMS, S., NOURI, M., MOHSENI, M., SHABANIAN, R., YEKANINEJAD, M. S., CHEGINI, N., KHODADAD, A. & SAFARALIZADEH, R. 2007b. A Probable Causative Factor for an Old Problem: Selenium and Glutathione Peroxidase Appear to Play Important Roles in Epilepsy Pathogenesis. *Epilepsia*, 48, 1750-1755.
- ASIN-CAYUELA, J., MANAS, A.-R. B., JAMES, A. M., SMITH, R. A. J. & MURPHY, M. P. 2004. Fine-tuning the hydrophobicity of a mitochondria-targeted antioxidant. *FEBS Letters*, 571, 9-16.
- AUMANN, K. D., BEDORF, N., B., BRIGELIUS-FLOHÄ, R., SCHOMBURG, D. & FLOHE, L. 1997. Glutathione peroxidase revisited--simulation of the catalytic cycle by computer-assisted molecular modelling. *Biomed Environ Sci.*, 10, 136-55.
- AVISSAR, N., ORNT, D. B., YAGIL, Y., HOROWITZ, S., WATKINS, R. H., KERL, E. A., TAKAHASHI, K., PALMER, I. S. & COHEN, H. J. 1994. Human kidney proximal tubules are the main source of plasma glutathione peroxidase. *American Journal of Physiology - Cell Physiology*, 266, C367-C375.
- BACHELERIE, F., ALCAMI, J., ARENZANA-SEISDEDOS, F. & VIRELIZIER, J. L. 1991. HIV enhancer activity perpetuated by NF-kappaB induction on infection of monocytes. *Nature*, 350, 709 - 712.

- BAEK, I., YON, J., LEE, S., JIN, Y., KIM, M., AHN, B., HONG, J., CHOO, Y., LEE, B., YUN, Y. & NAM, S. 2007. Effects of endocrine disrupting chemicals on expression of phospholipid hydroperoxide glutathione peroxidase mRNA in rat testes. *J Vet Sci*, 8, 213-8.
- BAEUERLE, P. A. & BALTIMORE, D. 1988. Activation of DNA-binding activity in an apparently cytoplasmic precursor of the NF-kappaB transcription factor. *Cell*, 53, 211 - 217.
- BAIN, P. A. & SCHULLER, K. A. 2012. A glutathione peroxidase 4 (GPx4) homologue from southern bluefin tuna is a secreted protein: First report of a secreted GPx4 isoform in vertebrates. *Comparative Biochemistry and Physiology Part B: Biochemistry and Molecular Biology*, 161, 392-397.
- BAJT, M., HO, Y., VONDERFECHT, S. & JAESCHKE, H. 2002. Reactive oxygen as modulator of TNF and fas receptor-mediated apoptosis in vivo: studies with glutathione peroxidase-deficient mice. *Antioxid Redox Signal*, 4, 733-40.
- BAKER, D. J. & HEPPLER, R. T. 2006. Elevated caspase and AIF gene expression correlate with progression of sarcopenia during aging in male F344BN rats. *Experimental Gerontology*, 41, 1149-1156.
- BALDWIN, A. J. 1996. The NF-kappaB and IkappaB proteins: new discoveries and insights. *An Rev Immunol*, 14, 649 - 683.
- BANERJEE, S., YANG, S. & FOSTER, C. B. 2011. A luciferase reporter assay to investigate the differential selenium-dependent stability of selenoprotein mRNAs. *The Journal of Nutritional Biochemistry*.
- BANNING, A., SCHNURR, K., BÖL, G.-F., KUPPER, D., MÜLLER-SCHMEHL, K., VIITA, H., YLÄ-HERTTUALA, S. & BRIGELIUS-FLOHÉ, R. 2004. Inhibition of basal and interleukin-1-induced VCAM-1 expression by phospholipid hydroperoxide glutathione peroxidase and 15-lipoxygenase in rabbit aortic smooth muscle cells. *Free Radical Biology and Medicine*, 36, 135-144.
- BANNING, A., KIPP, A., SCHMITMEIER, S., LÖWINGER, M., FLORIAN, S., KREHL, S., THALMANN, S., THIERBACH, R., STEINBERG, P. & BRIGELIUS-FLOHÉ, R. 2008. Glutathione Peroxidase 2 Inhibits Cyclooxygenase-2-Mediated Migration and Invasion of HT-29 Adenocarcinoma Cells but Supports Their Growth as Tumors in Nude Mice. *Cancer Research*, 68, 9746-9753.
- BAO, Y., JEMTH, P., MANNERNVIK, B. & WILLIAMSON, G. 1997. Reduction of thymine hydroperoxide by phospholipid hydroperoxide glutathione peroxidase and glutathione transferases. *FEBS Letters*, 410, 210-212.
- BAO, Y., & WILLIAMSON, G. 2006. Metabolism of hydroperoxy-phospholipids in human hepatoma HepG2 cells. *Journal of lipid research*, 37, 2351-60.
- BARANOWSKA-BOSIACKA, I., GUTOWSKA, I., MARCHLEWICZ, M., MARCHETTI, C., KURZAWSKI, M., DZIEDZIEJKO, V., KOLASA, A., OLSZEWSKA, M., RYBICKA, M., SAFRANOW, K., NOWACKI, P., WISZNIEWSKA, B. & CHLUBEK, D. 2012. Disrupted pro- and antioxidative balance as a mechanism of neurotoxicity induced by perinatal exposure to lead. *Brain Research*, 1435, 56-71.
- BARGER, S. W., HORSTER, D., FURUKAWA, K., GOODMAN, Y., KRIEGLSTEIN, J. & MATTSON, M. P. 1995. Tumor necrosis factors alpha and beta protect neurons against amyloid beta-peptide toxicity: evidence for involvement of a kappa B-binding factor and attenuation of peroxide and Ca²⁺ accumulation. *Proc Natl Acad Sci U S A*, 92, 9328 - 9332.
- BARRERA, L. N., CASSIDY, A., JOHNSON, I. T., BAO, Y. & BELSHAW, N. J. 2012. Epigenetic and antioxidant effects of dietary isothiocyanates and selenium: potential implications for cancer chemoprevention. *Proceedings of the Nutrition Society*, 71, 237-245.

- BARRIÈRE, G., RABINOVITCH-CHABLE, H., COOK-MOREAU, J., FAUCHER, K., RIGAUD, M. & STURTZ, F. 2004. PHGPx Overexpression Induces an Increase in COX-2 Activity in Colon Carcinoma Cells. *Anticancer Research*, 24, 1387-1392.
- BARTSCH, H., NAIR, J. & OWEN, R. 2002. Exocyclic DNA adducts as oxidative stress markers in colon carcinogenesis: potential role of lipid peroxidation, dietary fat and antioxidants. *Biol Chem*, 383, 915-21.
- BASELER, W. A., WILLIAMSON, C. L., DABKOWSKI, E. R., CROSTON, T. L. & HOLLANDER, J. M. 2010. Mitochondria-specific overexpression of phospholipid hydroperoxide glutathione peroxidase (GPx4) attenuates ischemia/reperfusion (I/R) associated apoptosis. *FASEB J.*, 24, 1b560-.
- BAUM, M., SHOR-POSNER, G., LAI, S., ZHANG, G., LAI, H., FLETCHER, R. M., SAUBERLICH, H. & PAGE, J. 1997. High risk of HIV-related mortality is associated with selenium deficiency. *J Acquir Immune Defic Syndr Hum Retroviro*, 370-4.
- BAZAN, N. G. 2001. COX-2 as a multifunctional neuronal modulator. *Nat Med*, 7, 414 - 415.
- BECK, M. A., SHI, Q., MORRIS, V. & LEVANDER, O. 1995. Rapid genomic evolution of a non-virulent coxsackievirus B3 in selenium-deficient mice results in selection of identical virulent isolates. *Nat Med*, 433-6.
- BECK, M. A. 1997a. Increased Virulence of Coxsackievirus B3 in Mice Due to Vitamin E or Selenium Deficiency. *The Journal of Nutrition*, 127, 966S-970S.
- BECK, M. A. 1997b. Rapid genomic evolution of a non-virulent coxsackievirus B3 in selenium-deficient mice. *Biomed Environ Sci.*, 307-15.
- BECK, M. A., ESWORTHY, R. S., HO, Y. & CHU, F. 1998. Glutathione peroxidase protects mice from viral-induced myocarditis. *The FASEB Journal*, 12, 1143-1149.
- BECK, M. A. 1999. Selenium and host defence towards viruses. *Proceedings of the Nutrition Society*, 58, 707-711.
- BECK, M. A., NELSON, H. K., SHI, Q., VAN DAEL, P., SCHIFFRIN, E. J., BLUM, S., BARCLAY, D. & LEVANDER, O. A. 2001. Selenium deficiency increases the pathology of an influenza virus infection. *The FASEB Journal*.
- BECKETT, G. J. & ARTHUR, J. R. 2005. Selenium and endocrine systems. *Journal of Endocrinology*, 184, 455-465.
- BEDNER, E., LI, X., KUNICKI, J. & DARZYNKIEWICZ, Z. 2000. Translocation of Bax to mitochondria during apoptosis measured by laser scanning cytometry. *Cytometry*, 41, 83-88.
- BELLINGER, F. P., RAMAN, A. V., REEVES, M. A. & BERRY, M. J. 2009. Regulation and function of selenoproteins in human disease. *Biochemical Journal*, 422, 11-22.
- BELLINGER, F.P., BELLINGER, M., SEALE, L., TAKEMOTO, A., RAMAN, A., MIKI, T., MANNING-BOG, A., BERRY, M., WHITE, L. & ROSS, G. 2011. Glutathione Peroxidase 4 is associated with Neuromelanin in Substantia Nigra and Dystrophic Axons in Putamen of Parkinson's brain. *Molecular Neurodegeneration*, 6, 8.
- BERGAMINI, C., MORUZZI, N., SBLENDIDO, A., LENAIZ, G. & FATO, R. 2012. A Water Soluble CoQ₁₀ Formulation Improves Intracellular Distribution and Promotes Mitochondrial Respiration in Cultured Cells. *PLoS ONE*, 7, e33712.
- BERMANO, G., NICOL, F., JA, D., SUNDE, R. A., BECKETT, G. J., ARTHUR, J. & HESKETH, J. 1995. Tissue-specific regulation of selenoenzyme gene expression during selenium deficiency in rats. *Biochem J*, 311, 425-30.
- BERMANO, G., ARTHUR, J. & HESKETH, J. 1996a. A cell culture model to study regulation of selenoprotein gene expression of selenium. *Biochem Soc Trans*, 24, 224.
- BERMANO, G., ARTHUR, J. R. & HESKETH, J. E. 1996b. Role of the 3' untranslated region in the regulation of cytosolic glutathione peroxidase and phospholipid-hydroperoxide glutathione peroxidase gene expression by selenium supply. *Biochem. J.*, 320, 891-895.

- BERMANO, G., ARTHUR, J. R. & HESKETH, J. E. 1996c. Selective control of cytosolic glutathione peroxidase and phospholipid hydroperoxide glutathione peroxidase mRNA stability by selenium supply. *FEBS Letters*, 387, 157-160.
- BERMANO, G., PAGMANTIDIS, V., HOLLOWAY, N., KADRI, S., MOWAT, N., SHIEL, R., ARTHUR, J., MATHERS, J., DALY, A., BROOM, J. & HESKETH, J. 2007. Evidence that a polymorphism within the 3'UTR of glutathione peroxidase 4 is functional and is associated with susceptibility to colorectal cancer. *Genes & Nutrition*, 2, 225-232.
- BERMANO, G., SMYTH, E., GOUA, M., HEYS, S. D. & WAHLE, K. W. J. 2010. Impaired expression of glutathione peroxidase-4 gene in peripheral blood mononuclear cells: A biomarker of increased breast cancer risk. *Cancer Biomarkers*, 7, 39-46.
- BERRY, M. J. 2005. Insights into the hierarchy of selenium incorporation. *Nat Genet*, 37, 1162-1163.
- BIANCHI, P., PIMENTEL, D. R., MURPHY, M. P., COLUCCI, W. S. & PARINI, A. 2005. A new hypertrophic mechanism of serotonin in cardiac myocytes: receptor-independent ROS generation. *The FASEB Journal*, 19, 641-643.
- BIDÈRE, N., LORENZO, H. K., CARMONA, S., LAFORGE, M., HARPER, F., DUMONT, C. & SENIK, A. 2003. Cathepsin D Triggers Bax Activation, Resulting in Selective Apoptosis-inducing Factor (AIF) Relocation in T Lymphocytes Entering the Early Commitment Phase to Apoptosis. *Journal of Biological Chemistry*, 278, 31401-31411.
- GEERLING, B. J., BADART-SMOOK A., STOCKBRUGGER, R. W., S. & BRUMMER, R. J. 2000. Comprehensive nutritional status in recently diagnosed patients with inflammatory bowel disease compared with population controls. *Eur J Clin Nutr*, 54, 14-21.
- BJELAKOVIC, G., NIKOLOVA, D., SIMONETTI, R. G. & GLUUD, C. 2008. Systematic review: primary and secondary prevention of gastrointestinal cancers with antioxidant supplements. *Alimentary Pharmacology & Therapeutics*, 28, 689-703.
- BJÖRNSTEDT, M., XUE, J., HUANG, W., AKESSON, B. & HOLMGREN, A. 1994. The thioredoxin and glutaredoxin systems are efficient electron donors to human plasma glutathione peroxidase. *Journal of Biological Chemistry*, 269, 29382-29384.
- BLOT, W. J., LI, J. Y., TAYLOR, P. R., GUO, W., DAWSEY, S. M. & LI, B. 1995. The Linxian trials: mortality rates by vitamin-mineral intervention group. *The American Journal of Clinical Nutrition*, 62, 1424S-1426S.
- BOITANI, C. & PUGLISI, R. 2009. Selenium, a Key Element in Spermatogenesis and Male Fertility Molecular Mechanisms in Spermatogenesis. In: CHENG, C. Y. (ed.). Springer New York.
- BONNE, G., SEIBEL, P., POSSEKEL, S., MARSAC, C. & KADENBACH, B. 1993. Expression of human cytochrome c, oxidase subunits during fetal development. *European Journal of Biochemistry*, 217, 1099-1107.
- BORCHERT, A., WANG, C. C., UFER, C., SCHIEBEL, H., SAVASKAN, N. E. & KUHN, H. 2006. The Role of Phospholipid Hydroperoxide Glutathione Peroxidase Isoforms in Murine Embryogenesis. *Journal of Biological Chemistry*, 281, 19655-19664.
- BOSEDASGUPTA, S., DAS, B. B., SENGUPTA, S., GANGULY, A., ROY, A., DEY, S., TRIPATHI, G., DINDA, B. & MAJUMDER, H. K. 2008. The caspase-independent algorithm of programmed cell death in Leishmania induced by baicalin: the role of LdEndoG, LdFEN-1 and LdTatD as a DNA 'degradesome'. *Cell Death Differ*, 15, 1629 - 1640.
- BÖSL, M. R., TAKAKU, K., OSHIMA, M., NISHIMURA, S. & TAKETO, M. M. 1997. Early embryonic lethality caused by targeted disruption of the mouse selenocysteine tRNA gene (Trsp). *Proceedings of the National Academy of Sciences*, 94, 5531-5534.
- BOURGERON, T. 2000. Mitochondrial function and male infertility. *Results Probl Cell Differ*, 28, 187-210.
- BRAND, M. D. & NICHOLLS, D. 2011. Assessing mitochondrial dysfunction in cells. *Biochem J*, 435, 297-312.

- BREDER, C. D., DEWITT, D. & KRAIG, R. P. 1995. Characterization of inducible cyclooxygenase in rat brain. *J Comp Neurol*, 355, 296 - 315.
- BRIGELIUS-FLOHÉ, R. 1999. Tissue-specific functions of individual glutathione peroxidases. *Free Radical Biology and Medicine*, 27, 951-965.
- BRIGELIUS-FLOHÉ, R., MAURER, S., LÖTZER, K., BÖL, G.-F., KALLIONPÄÄ, H., LEHTOLAINEN, P., VIITA, H. & YLÄ-HERTTUALA, S. 2000. Overexpression of PHGPx inhibits hydroperoxide-induced oxidation, NFκB activation and apoptosis and affects oxLDL-mediated proliferation of rabbit aortic smooth muscle cells. *Atherosclerosis*, 152, 307-316.
- BRIGELIUS-FLOHÉ, R. 2006. Glutathione peroxidases and redox-regulated transcription factors. *Biol Chem*, 387, 1329-35.
- BRIGELIUS-FLOHÉ, R. 2008. Selenium Compounds and Selenoproteins in Cancer. *Chemistry & Biodiversity*, 5, 389-395.
- BRIGELIUS-FLOHÉ, R. & KIPP, A. 2009. Glutathione peroxidases in different stages of carcinogenesis. *Biochimica et Biophysica Acta (BBA) - General Subjects*, 1790, 1555-1568.
- BROWN, D., YU, B. D., JOZA, N., BÉNIT, P., MENESES, J., FIRPO, M., RUSTIN, P., PENNINGER, J. M. & MARTIN, G. R. 2006. Loss of Aif function causes cell death in the mouse embryo, but the temporal progression of patterning is normal. *Proceedings of the National Academy of Sciences*, 103, 9918-9923.
- BROWN KM, A. J. 2001. Selenium, selenoproteins and human health: a review. *Public Health Nutr.*, 4, 593-9.
- BUHRKE, T., MERKEL, R., LENGLER, I. & LAMPEN, A. 2012. Absorption and Metabolism of <i>trans</i>-9,<i>trans</i>-11-CLA and of Its Oxidation Product 9,11-Furan Fatty Acid by Caco-2 Cells. *Lipids*, 47, 435-442.
- BURK, R. F. & HILL, K. E. 2009. Selenoprotein P—Expression, functions, and roles in mammals. *Biochimica et Biophysica Acta (BBA) - General Subjects*, 1790, 1441-1447.
- BURTON, T. R., EISENSTAT, D. D. & GIBSON, S. B. 2009. BNIP3 (Bcl-2 19 kDa Interacting Protein) Acts as Transcriptional Repressor of Apoptosis-Inducing Factor Expression Preventing Cell Death in Human Malignant Gliomas. *The Journal of Neuroscience*, 29, 4189-4199.
- CAMPA, A., SHOR-POSNE, R. G., INDACOCHEA, F., ZHANG, G., H, L., ASTHANA, D., SCOTT, G. & BAUM, M. 1999. Mortality risk in selenium-deficient HIV-positive children. *J Acquir Immune Defic Syndr Hum Retrovirol*, 508-13.
- CANDÉ, C., CECCONI, F., DESSEN, P. & KROEMER, G. 2002a. Apoptosis-inducing factor (AIF): key to the conserved caspase-independent pathways of cell death? *Journal of Cell Science*, 115, 4727-4734.
- CANDE, C., COHEN, I., DAUGAS, E., RAVAGNAN, L., LAROCLETTE, N., ZAMZAMI, N. & KROEMER, G. 2002b. Apoptosis-inducing factor (AIF): a novel caspase-independent death effector released from mitochondria. *Biochimie*, 84, 215 - 222.
- CANDE, C., VAHSEN, N., KOURANTI, I., SCHMITT, E., DAUGAS, E., SPAHR, C., LUBAN, J., KROEMER, R. T., GIORDANETTO, F., GARRIDO, C., PENNINGER, J. M. & KROEMER, G. 2004. AIF and cyclophilin A cooperate in apoptosis-associated chromatinolysis. *Oncogene*, 23, 1514-1521.
- CARNEY, J. M., STARKE-REED, P. E., OLIVER, C. N., LANDUM, R. W., CHENG, M. S., WU, J. F. & FLOYD, R. A. 1991. Reversal of age-related increase in brain protein oxidation, decrease in enzyme activity, and loss in temporal and spatial memory by chronic administration of the spin-trapping compound N-tert-butyl-alpha-phenylnitron. *Proceedings of the National Academy of Sciences*, 88, 3633-3636.
- CARROLL, R. & RACKER, E. 1977. Preparation and characterization of cytochrome c oxidase vesicles with high respiratory control. *J Biol Chem*, 252, 6981-90.

- CASTAGNE, V., GAUTSCHI, M., LEFEVRE, K., POSADA, A. & CLARKE, P. G. H. 1999. Relationships between neuronal death and the cellular redox status. Focus on the developing nervous system. *Progress in Neurobiology*, 59, 397-423.
- CEBRIAN, A., PHAROAH, P. D., AHMED, S., SMITH, P. L., LUCCARINI, C., LUBEN, R., REDMAN, K., MUNDAY, H., EASTON, D. F., DUNNING, A. M. & PONDER, B. A. J. 2006. Tagging Single-Nucleotide Polymorphisms in Antioxidant Defense Enzymes and Susceptibility to Breast Cancer. *Cancer Research*, 66, 1225-1233.
- CHABORY, E., DAMON, C., LENOIR, A., HENRY-BERGER, J., VERNET, P., CADET, R., SAEZ, F. & DREVET, J. R. 2010. Mammalian glutathione peroxidases control acquisition and maintenance of spermatozoa integrity. *Journal of Animal Science*, 88, 1321-1331.
- CHEN, C. J., HUANG, H. S., LIN, S. B. & CHANG, W. C. 2000. Regulation of cyclooxygenase and 12-lipoxygenase catalysis by phospholipid hydroperoxide glutathione peroxidase in A431 cells. *Prostaglandins, Leukotrienes and Essential Fatty Acids*, 62, 261-268.
- CHEN, C., HUANG, H. & CHANG, W. 2002. Inhibition of arachidonate metabolism in human epidermoid carcinoma a431 cells overexpressing phospholipid hydroperoxide glutathione peroxidase. *J Biomed Sci*, 9, 453-9.
- CHEN, C.-J., HUANG, H.-S. & CHANG, W.-C. 2003. Depletion of phospholipid hydroperoxide glutathione peroxidase up-regulates arachidonate metabolism by 12(S)-lipoxygenase and cyclooxygenase 1 in human epidermoid carcinoma A431 cells. *The FASEB Journal*.
- CHEN, K., THOMAS, S. R., ALBANO, A., MURPHY, M. P. & KEANEY, J. F. 2004. Mitochondrial Function Is Required for Hydrogen Peroxide-induced Growth Factor Receptor Transactivation and Downstream Signaling. *Journal of Biological Chemistry*, 279, 35079-35086.
- CHEN, Y.-C., TSAI, S.-H., LIN-SHIAU, S.-Y. & LIN, J.-K. 1999. Elevation of apoptotic potential by anoxia-hyperoxia shift in NIH3T3 cells. *Molecular and Cellular Biochemistry*, 197, 147-159.
- CHEN, Y., CAI, J. & JONES, D. P. 2006. Mitochondrial thioredoxin in regulation of oxidant-induced cell death. *FEBS Letters*, 580, 6596-6602.
- CHOPRA, H., TIMAR, J., RONG, X., GROSSI, I., HATFIELD, J., FRIGIEL, S., FINCH, C., TAYLOR, J. & HONN, K. 1992. Is there a role for the tumor cell integrin alpha IIb beta 3 and cytoskeleton in tumor cell-platelet interaction? *Clin Exp Metastasis*, 10, 152-37.
- CHRISTOPH UFER, C. C. W., MICHAEL FAHLING, HEIKE SCHIEBEL, BERND J. THIELE, E. ELLEN BILLET, HARTMUT KUHN, AND ASTRID BORCHERT 2008. Translational regulation of glutathione peroxidase 4 expression through guanine-rich sequence-binding factor 1 is essential for embryonic brain development. *Genes Dev*, 22, 18350-50.
- CHRISTOS, C. & VERA, A.-V. 2001. Mitochondria deficient in complex I activity are depolarized by hydrogen peroxide in nerve terminals: relevance to Parkinson's disease. *Journal of Neurochemistry*, 76, 302-306.
- CHU, F. F., DOROSHOW, J. H. & ESWORTHY, R. S. 1993. Expression, characterization, and tissue distribution of a new cellular selenium-dependent glutathione peroxidase, GSHPx-GI. *Journal of Biological Chemistry*, 268, 2571-6.
- CLARK, L. C., COMBS, G. F. Jr., TURNBULL, B. W., SLATE, E. H., CHALKER, D. K., CHOW, J., DAVIS, L. S., GLOVER, R. A., GRAHAM, G. F., GROSS, E. G., KRONGRAD, A., LESHER, J. L. Jr., PARK, H. K., SANDERS, B. B. Jr., SMITH, C. L., TAYLOR, J. R. 1996. Effects of selenium supplementation for cancer prevention in patients with carcinoma of the skin: A randomized controlled trial. *JAMA: The Journal of the American Medical Association*, 276, 1957-1963.
- CLIFTON, R., LISTER, R., PARKER, K., SAPPL, P., ELHAFEZ, D., MILLAR, A., DAY, D. & WHELAN, J. 2005. Stress-induced co-expression of alternative respiratory chain components in *Arabidopsis thaliana*. *Plant Molecular Biology*, 58, 193-212.

- COMBS, G. F Jr. 2000. Food system-based approaches to improving micronutrient nutrition: the case for selenium. *Biofactors*, 39-43.
- CONRAD, M., M. S., SEILER, A. & BORNKAMM, G. W. 2007. Physiological role of phospholipid hydroperoxide glutathione peroxidase in mammals. *Biol Chem*, 388.
- CONRAD, M. 2009. Transgenic mouse models for the vital selenoenzymes cytosolic thioredoxin reductase, mitochondrial thioredoxin reductase and glutathione peroxidase 4. *Biochimica et Biophysica Acta (BBA) - General Subjects*, 1790, 1575-1585.
- COPELAND, P. R., FLETCHER, J. E., CARLSON, B. A., HATFIELD, D. L. & DRISCOLL, D. M. 2000. A novel RNA binding protein, SBP2, is required for the translation of mammalian selenoprotein mRNAs. *EMBO J*, 19, 306-314.
- COPELAND, P. R., DONOVAN, J. 2010. Threading the Needle: Getting Selenocysteine Into Proteins. *Antioxidant and redox signalling*, 12, 881.
- CORY, S. & ADAMS, J. M. 2002. The Bcl2 family: regulators of the cellular life-or-death switch. *Nat Rev Cancer*, 2, 647-656.
- COURTOIS, G., SMAHI, A. & ISRAEL, A. 2001. NEMO/IKK gamma: linking NF-kappaB to human disease. *Trends Mol Med*, 7, 427 - 430.
- CRACK, P. J., TAYLOR, J. M., FLENTJAR, N. J., DE HAAN, J., HERTZOG, P., IANNELLO, R. C. & KOLA, I. 2001. Increased infarct size and exacerbated apoptosis in the glutathione peroxidase-1 (Gpx-1) knockout mouse brain in response to ischemia/reperfusion injury. *Journal of Neurochemistry*, 78, 1389-1399.
- CRANE, M. S., HOWIE, A. F., ARTHUR, J. R., NICOL, F., CROSLEY, L. K. & BECKETT, G. J. 2009. Modulation of thioredoxin reductase-2 expression in EAhy926 cells: Implications for endothelial selenoprotein hierarchy. *Biochimica et Biophysica Acta (BBA) - General Subjects*, 1790, 1191-1197.
- CULMSEE C, Z. C., LANDSHAMER S, BECATTINI B, WAGNER E, PELLECCIA M, BLOMGREN K, PLESNILA N. 2005. Apoptosis-inducing factor triggered by poly(ADP-ribose) polymerase and Bid mediates neuronal cell death after oxygen-glucose deprivation and focal cerebral ischemia. *J Neurosci*, 25, 10262-72.
- CURRAN, J. E., JOWETT, J. B. M., ELLIOTT, K. S., GAO, Y., GLUSCHENKO, K., WANG, J., AZIM, D. M. A., CAI, G., MAHANEY, M. C., COMUZZIE, A. G., DYER, T. D., WALDER, K. R., ZIMMET, P., MACCLUER, J. W., COLLIER, G. R., KISSEBAH, A. H. & BLANGERO, J. 2005. Genetic variation in selenoprotein S influences inflammatory response. *Nat Genet*, 37, 1234-1241.
- DABKOWSKI, E. R., WILLIAMSON, C. L. & HOLLANDER, J. M. 2008. Mitochondria-specific transgenic overexpression of phospholipid hydroperoxide glutathione peroxidase (GPx4) attenuates ischemia/reperfusion-associated cardiac dysfunction. *Free Radical Biology and Medicine*, 45, 855-865.
- DAS, A., BYRD, D. & BRODEHL, H. 1994. Regulation of the mitochondrial ATP-synthase in human fibroblasts. *Clin Chim Acta*, 231, 61-8.
- DAS, J., MILLER, S. T. & STERN, D. L. 2004. Comparison of Diverse Protein Sequences of the Nuclear-Encoded Subunits of Cytochrome C Oxidase Suggests Conservation of Structure Underlies Evolving Functional Sites. *Molecular Biology and Evolution*, 21, 1572-1582.
- DAUGAS, E., NOCHY, D., RAVAGNAN, L., LOEFFLER, M., SUSIN, S. A., ZAMZAMI, N. & KROEMER, G. 2000a. Apoptosis-inducing factor (AIF): a ubiquitous mitochondrial oxidoreductase involved in apoptosis. *FEBS Letters*, 476, 118-123.
- DAUGAS, E., SUSIN, S. A., ZAMZAMI, N., FERRI, K. F., IRINOPOULOU, T., LAROCLETTE, N., PRÉVOST, M.-C., LEBER, B., ANDREWS, D., PENNINGER, J. & KROEMER, G. 2000b.

- Mitochondrio-nuclear translocation of AIF in apoptosis and necrosis. *The FASEB Journal*, 14, 729-739.
- DAVIS, M. C., WARD, J. G., HERRICK, G. & ALLIS, C. D. 1992. Programmed nuclear death: apoptotic-like degradation of specific nuclei in conjugating Tetrahymena. *Dev Biol*, 154, 419 - 432.
- DE GIORGI, F., LARTIGUE, L., BAUER, M. K. A., SCHUBERT, A., GRIMM, S., HANSON, G. T., REMINGTON, S. J., YOULE, R. J. & ICHAS, F. 2002. The permeability transition pore signals apoptosis by directing Bax translocation and multimerization. *The FASEB Journal*.
- DEWET, J. R., WOOD, K. V., DELUCA, M., HELINSKI, D. R. & SUBRAMANI, S. 1987. Firefly luciferase gene: structure and expression in mammalian cells. *Mol Cell Biol*, 7, 725 - 737.
- DELHASE, M. & KARIN, M. 1999. The I κ B kinase: a master regulator of NF- κ B, innate immunity, and epidermal differentiation. *Cold Spring Harb Symp Quant Biol*, 64, 491 - 503.
- DERUMEAUX, H., VALEIX, P., CASTETBON, K., BENSIMON, M., BOUTRON-RUAULT, M. C., ARNAUD, J. & HERCBERG, S. 2003. Association of selenium with thyroid volume and echostructure in 35- to 60-year-old French adults. *European Journal of Endocrinology*, 148, 309-315.
- DIAZ, G., SETZU, M. D., ZUCCA, A., ISOLA, R., DIANA, A., MURRU, R., SOGOS, V. & GREMO, F. 1999. Subcellular heterogeneity of mitochondrial membrane potential: relationship with organelle distribution and intercellular contacts in normal, hypoxic and apoptotic cells. *Journal of Cell Science*, 112, 1077-1084.
- DICKIE, L. J., AZIZ, A. M., SAVIC, S., LUCHERINI, O. M., CANTARINI, L., GEILER, J., WONG, C. H., COUGHLAN, R., LANE, T., LACHMANN, H. J., HAWKINS, P. N., ROBINSON, P. A., EMERY, P., MCGONAGLE, D. & MCDERMOTT, M. F. 2012. Involvement of X-box binding protein 1 and reactive oxygen species pathways in the pathogenesis of tumour necrosis factor receptor-associated periodic syndrome. *Annals of the Rheumatic Diseases*.
- DIKIY, A., NOVOSELOV, S. V., FOMENKO, D. E., SENGUPTA, A., CARLSON, B. A., CERNY, R. L., GINALSKI, K., GRISHIN, N. V., HATFIELD, D. L. & GLADYSHEV, V. N. 2007. SelT, SelW, SelH, and Rdx12: Genomics and Molecular Insights into the Functions of Selenoproteins of a Novel Thioredoxin-like Family†. *Biochemistry*, 46, 6871-6882.
- DJAFARZADEH, S., VUDA, M., TAKALA, J., OCHS, M. & JAKOB, S. M. 2011. Toll-like receptor-3-induced mitochondrial dysfunction in cultured human hepatocytes. *Mitochondrion*, 11, 83-88.
- DORAI, T., OLSSON, C. A., KATZ, A. E. & BUTTYAN, R. 1997a. Development of a hammerhead ribozyme against bcl-2. I. Preliminary evaluation of a potential gene therapeutic agent for hormone-refractory human prostate cancer. *The Prostate*, 32, 246-258.
- DORAI, T., GOLUBOFF, E. T., OLSSON, C. A., BUTTYAN, R. 1997b. Development of a hammerhead ribozyme against BCL-2. II. Ribozyme treatment sensitizes hormone-resistant prostate cancer cells to apoptotic agents. *Anticancer Research*, 17, 3307-12.
- DORAI, T., PERLMAN, H., WALSH, K., SHABSIGH, A., GOLUBOFF, E. T., OLSSON, C. A. & BUTTYAN, R. 1999. A recombinant defective adenoviral agent expressing anti-bcl-2 ribozyme promotes apoptosis of bcl-2-expressing human prostate cancer cells. *International Journal of Cancer*, 82, 846-852.
- DOUGHAN, AK, DIKALOV, S. I. 2007. Mitochondrial redox cycling of mitoquinone leads to superoxide production and cellular apoptosis. *Antioxid Redox Signal*, 9, 1825-36.
- DRAKEW, A., MULLER, M., GAHWILER, B. H., THOMPSON, S. M. & FROTSCHER, M. 1996. Spine loss in experimental epilepsy: quantitative light and electron microscopic analysis of intracellularly stained CA3 pyramidal cells in hippocampal slice cultures. *Neuroscience*, 70, 31 - 45.
- DRANKA, B. P., BENAVIDES, G. A., DIERS, A. R., GIORDANO, S., ZELICKSON, B. R., REILY, C., ZOU, L., CHATHAM, J. C., HILL, B. G., ZHANG, J., LANDAR, A. & DARLEY-USMAR,

- V. M. 2011. Assessing bioenergetic function in response to oxidative stress by metabolic profiling. *Free Radical Biology and Medicine*, 51, 1621-1635.
- DRÖGE, W. 2002a. Aging-related changes in the thiol/disulfide redox state: implications for the use of thiol antioxidants. *Experimental Gerontology*, 37, 1333-1345.
- DRÖGE, W. 2002b. Free Radicals in the Physiological Control of Cell Function. *Physiological Reviews*, 82, 47-95.
- DU, X. H., DAI, X. X., XIA, S. R., ZOU, X. Z., YAN, S. W., MO, X. Y., LU, B. G. & Xiong Y. M. 2012. SNP and mRNA expression for glutathione peroxidase 4 in Kashin-Beck disease. *British Journal of Nutrition*, 23, 1-6.
- DUBOIS, R. N., ABRAMSON, S. B., CROFFORD, L., GUPTA, R. A., SIMON, L. S., VAN DE PUTTE, L. B. & LIPSKY, P. E. 1998. Cyclooxygenase in biology and disease. *FASEB J*, 12, 1063 - 1073.
- DUCHEN, M. R. 2004. Mitochondria in health and disease: perspectives on a new mitochondrial biology. *Molecular Aspects of Medicine*, 25, 365-451.
- DUFFIELD-LILLICO, A. J., REID, M. E., TURNBULL, B. W., COMBS, G. F., SLATE, E. H., FISCHBACH, L. A., MARSHALL, J. R. & CLARK, L. C. 2002. Baseline Characteristics and the Effect of Selenium Supplementation on Cancer Incidence in a Randomized Clinical Trial. *Cancer Epidemiology Biomarkers & Prevention*, 11, 630-639.
- EFREMOV, R. G. & SAZANOV, L. A. 2011a. Respiratory complex I: 'steam engine' of the cell? *Current Opinion in Structural Biology*, 21, 532-540.
- EFREMOV, R. G. & SAZANOV, L. A. 2011b. Structure of the membrane domain of respiratory complex I. *Nature*, 476, 414-420.
- EISINGER, A. L., NADAULD, L. D., SHELTON, D. N., PRESCOTT, S. M., STAFFORINI, D. M. & JONES, D. A. 2007. Retinoic Acid Inhibits β -Catenin through Suppression of Cox-2. *Journal of Biological Chemistry*, 282, 29394-29400.
- EISINGER, A. L., PRESCOTT, S. M., JONES, D. A. & STAFFORINI, D. M. 2007. The role of cyclooxygenase-2 and prostaglandins in colon cancer. *Prostaglandins & Other Lipid Mediators*, 82, 147-154.
- EKEGREN T, G. E., LINDHOLM D, AQUILONIUS SM. 1999. Upregulation of Bax protein and increased DNA degradation in ALS spinal cord motor neurons. *Acta Neurol Scand*, 100, 317-21.
- ENDO, H. & KOBAYASHI, T. 2006. Death harmony played by nucleus and mitochondria: nuclear apoptosis during conjugation of Tetrahymena. *Autophagy*, 2, 129 - 131.
- ERKEKOGLU, P., GIRAY, B. K., KIZILGÜN, M., RACHIDI, W., HININGER-FAVIER, I., ROUSSEL, A.-M., FAVIER, A. & HINCAL, F. 2012. Di(2-ethylhexyl)phthalate-induced renal oxidative stress in rats and protective effect of selenium. *Toxicology Mechanisms and Methods*, 22, 415-23.
- ESWORTHY, R. S., SW, B., DOROSHOW, J. H. & FF, C. 2003. Microflora trigger colitis in mice deficient in selenium-dependent glutathione peroxidase and induce Gpx2 gene expression. *Biol Chem*, 384, 597-607.
- FADEEL, B., OTTOSSON, A. & PERVAIZ, S. 2007. Big wheel keeps on turning: apoptosome regulation and its role in chemoresistance. *Cell Death Differ*, 15, 443-452.
- FAIRWEATHER-TAIT, S., BAO, Y., BROADLEY, M., COLLINGS, R., FORD, D., HESKETH, J. E. & HURST, R. 2011. Selenium in human health and disease. *Antioxid Redox Signal*, 1337-83.
- FATEMI, N., SANATI, M., ZAVAREHEI, M., AYAT, H., ESMAEILI, V., GOLKAR-NARENJI, A., ZARABI, M. & GOURABI, H. 2012. Effect of tertiary-butyl hydroperoxide (TBHP)-induced oxidative stress on mice sperm quality and testis histopathology. *Andrologia*, 10.
- FAWZI, W., MSAMANGA, G., SPIEGELMAN, D. & HUNTER, D. J. 2005. Studies of Vitamins and Minerals and HIV Transmission and Disease Progression. *The Journal of Nutrition*, 135, 938-944.

- FENG GAO, C., REN, S., ZHANG, L., NAKAJIMA, T., ICHINOSE, S., HARA, T., KOIKE, K. & TSUCHIDA, N. 2001. Caspase-Dependent Cytosolic Release of Cytochrome c and Membrane Translocation of Bax in p53-Induced Apoptosis. *Experimental Cell Research*, 265, 145-151.
- FERGUSON, J. F., PHILLIPS, C. M., TIERNEY, A. C., PÉREZ-MARTÍNEZ, P., DEFOORT, C., HELAL, O., LAIRON, D., PLANELLS, R., SHAW, D. I., LOVEGROVE, J. A., GJELSTAD, I. M. F., DREVON, C. A., BLAAK, E. E., SARIS, W. H. M., LESZCZYŃSKA-GOŁĄBEK, I., KIEC-WILK, B., RISÉRUS, U., KARLSTRÖM, B., MIRANDA, J. L. & ROCHE, H. M. 2010. Gene-nutrient interactions in the metabolic syndrome: single nucleotide polymorphisms in ADIPOQ and ADIPOR1 interact with plasma saturated fatty acids to modulate insulin resistance. *The American Journal of Clinical Nutrition*, 91, 794-801.
- FERGUSON, L. R., KARUNASINGHE, N., ZHU, S. & WANG, A. H. 2012. Selenium and its' role in the maintenance of genomic stability. *Mutation Research/Fundamental and Molecular Mechanisms of Mutagenesis*, 733, 100-10.
- FERNYHOUGH, P., ROY CHOWDHURY, S. & SCHMIDT, R. 2010. Mitochondrial stress and the pathogenesis of diabetic neuropathy. *Expert Rev Endocrinol Metab*, 5, 39-49.
- FERREIRA, R., XAPELLI, S., SANTOS, T., SILVA, A. P., CRISTÓVÃO, A., CORTES, L. & MALVA, J. O. 2010. Neuropeptide Y Modulation of Interleukin-1 β (IL-1 β)-induced Nitric Oxide Production in Microglia. *Journal of Biological Chemistry*, 285, 41921-41934.
- FISSORE, R. A., KUROKAWA, M., KNOTT, J., ZHANG, M. & SMYTH, J. 2002. Mechanisms underlying oocyte activation and postovulatory ageing. *Reproduction*, 124, 745-754.
- FLOHÉ, L. 2007. Selenium in mammalian spermiogenesis. *Biol Chem*, 388, 987-95.
- FOLGERØ, T., BERTHEUSSEN, K., LINDAL, S., TORBERGSEN, T. & ØIAN, P. 1993. Andrology: Mitochondrial disease and reduced sperm motility. *Human Reproduction*, 8, 1863-1868.
- FORSTERMANN, U., HELDT, R., KNAPPEN, F. & HERTTING, G. 1982. Potential anticonvulsive properties of endogenous prostaglandins formed in mouse brain. *Brain Res*, 240, 303 - 310.
- FROTSCHER, M. & HEIMRICH, B. 1993. Formation of layer-specific fiber projections to the hippocampus in vitro. *Proc Natl Acad Sci U S A*, 90, 10400 - 10403.
- FUKUI, M., CHOI, H. J. & ZHU, B. T. 2012. Rapid generation of mitochondrial superoxide induces mitochondrion-dependent but caspase-independent cell death in hippocampal neuronal cells that morphologically resembles necroptosis. *Toxicology and Applied Pharmacology*, 262, 156-166.
- FUNK, J. A. & SCHNELLMANN, R. G. 2012. Persistent disruption of mitochondrial homeostasis after acute kidney injury. *American Journal of Physiology - Renal Physiology*, 302, F853-F864.
- GAIDO, M. L. & CIDLOWSKI, J. A. 1991. Identification, purification, and characterization of a calcium-dependent endonuclease (NUC18) from apoptotic rat thymocytes. NUC18 is not histone H2B. *J Biol Chem*, 266, 18580 - 18585.
- GALLUZZI, L., JOZA, N., TASDEMIR, E., MAIURI, M. C., HENGARTNER, M., ABRAMS, J. M., TAVERNARAKIS, N., PENNINGER, J., MADEO, F. & KROEMER, G. 2008. No death without life: vital functions of apoptotic effectors. *Cell Death Differ*, 15, 1113 - 1123.
- GANNAVARAM, S., VEDVYAS, C. & DEBRABANT, A. 2008. Conservation of the pro-apoptotic nuclease activity of endonuclease G in unicellular trypanosomatid parasites. *J Cell Sci*, 121, 99 - 109.
- GANTHER, H. E. 1999. Selenium metabolism, selenoproteins and mechanisms of cancer prevention: complexities with thioredoxin reductase. *Carcinogenesis*, 20, 1657-1666.
- GAO, H., YIN, Z., ZHOU, N., FENG, X., GAO, F. & WANG, H. 2008. Glycogen synthase kinase 3 inhibition protects the heart from acute ischemia-reperfusion injury via inhibition of inflammation and apoptosis. *J Cardiovasc Pharmacol*, 52, 286-92.
- GAO, L.-P., CHENG, M.-L., CHOU, H.-J., YANG, Y.-H., HO, H.-Y. & CHIU, D. T.-Y. 2009. Ineffective GSH regeneration enhances G6PD-knockdown Hep G2 cell sensitivity to diamide-induced oxidative damage. *Free Radical Biology & Medicine*, 47, 529-35.

- GAO, S., JIN, Y., HALL, K. S., LIANG, C., UNVERZAGT, F. W., JI, R., MURRELL, J. R., CAO, J., SHEN, J., MA, F., MATESAN, J., YING, B., CHENG, Y., BIAN, J., LI, P. & HENDRIE, H. C. 2007. Selenium Level and Cognitive Function in Rural Elderly Chinese. *American Journal of Epidemiology*, 165, 955-965.
- GARCÍA-FERNÁNDEZ, M., CASTILLA-ORTEGA, E., PEDRAZA, C., BLANCO, E., HURTADO-GUERRERO, I., BARBANCHO, M. A., CHUN, J., RODRÍGUEZ-DE-FONSECA, F., ESTIVILL-TORRÚS, G. & NÚÑEZ, L. J. S. Chronic Immobilization in the malpar1 Knockout Mice Increases Oxidative Stress in the Hippocampus. *International Journal of Neuroscience*, 0, null.
- GARRY, M. R., KAVANAGH, T. J., FAUSTMAN, E. M., SIDHU, J. S., LIAO, R., WARE, C., VLIET, P. A. & DEEB, S. S. 2008. Sensitivity of mouse lung fibroblasts heterozygous for GPx4 to oxidative stress. *Free Radical Biology and Medicine*, 44, 1075-1087.
- GAUTREY, H., NICOL, F., SNEDDON, A. A., HALL, J. & HESKETH, J. 2011. A T/C polymorphism in the GPX4 3'UTR affects the selenoprotein expression pattern and cell viability in transfected Caco-2 cells. *Biochimica et Biophysica Acta (BBA) - General Subjects*, 1810, 284-291.
- GAVRIELI, Y., SHERMAN, Y. & BEN-SASSON, S. A. 1992. Identification of programmed cell death in situ via specific labeling of nuclear DNA fragmentation. *The Journal of Cell Biology*, 119, 493-501.
- GIAIME, E., YAMAGUCHI, H., GAUTIER, C. A., KITADA, T. & SHEN, J. 2012. Loss of DJ-1 Does Not Affect Mitochondrial Respiration but Increases ROS Production and Mitochondrial Permeability Transition Pore Opening. *PLoS ONE*, 7, e40501.
- GLATTRE, E., THOMASSEN, Y., THORESEN, S. Ø., HALDORSEN, T., LUND-LARSEN, P. G., THEODORSEN, L. & AASETH, J. 1989. Prediagnostic Serum Selenium in a Case-Control Study of Thyroid Cancer. *International Journal of Epidemiology*, 18, 45-49.
- GODEAS, C., TRAMER, F., MICALI, F., SORANZO, M., SANDRI, G. & PANFILI, E. 1997. Distribution and possible novel role of phospholipid hydroperoxide glutathione peroxidase in rat epididymal spermatozoa. *Biology of Reproduction*, 57, 1502-1508.
- GONG, M., HAY, S., MARSHALL, K. R., MUNRO, A. W. & SCRUTTON, N. S. 2007. DNA Binding Suppresses Human AIF-M2 Activity and Provides a Connection between Redox Chemistry, Reactive Oxygen Species, and Apoptosis. *Journal of Biological Chemistry*, 282, 30331-30340.
- GORDEEVA, A. V., LABAS, Y. A. & ZVYAGILSKAYA, R. A. 2004. Apoptosis in unicellular organisms: mechanisms and evolution. *Biochemistry (Mosc)*, 69, 1055 - 1066.
- GRAHAM, D., HUYNH, N. N., HAMILTON, C. A., BEATTIE, E., SMITH, R. A. J., COCHEMÉ, H. M., MURPHY, M. P. & DOMINICZAK, A. F. 2009. Mitochondria-Targeted Antioxidant MitoQ10 Improves Endothelial Function and Attenuates Cardiac Hypertrophy. *Hypertension*, 54, 322-328.
- GRAHAM, L. S., PARHAMI, F., TINTUT, Y., KITCHEN, C. M. R., DEMER, L. L. & EFFROS, R. B. 2009. Oxidized lipids enhance RANKL production by T lymphocytes: Implications for lipid-induced bone loss. *Clinical Immunology*, 133, 265-275.
- GREEN, K., BRAND, M. D. & MURPHY, M. P. 2004. Prevention of Mitochondrial Oxidative Damage as a Therapeutic Strategy in Diabetes. *Diabetes*, 53, S110-S118.
- GRILLI, M., PIZZI, M., MEMO, M. & SPANO, P. 1996. Neuroprotection by aspirin and sodium salicylate through blockade of NF-kappaB activation. *Science*, 274, 1383 - 1385.
- GRISHKO, V. I., DRUZHYNA, N., LEDOUX, S. P. & WILSON, G. L. 1999. Nitric oxide-induced damage to mtDNA and its subsequent repair. *Nucleic Acids Research*, 27, 4510-4516.
- GROSS, A., JOCKEL, J., WEI, M. C. & KORSMEYER, S. J. 1998. Enforced dimerization of BAX results in its translocation, mitochondrial dysfunction and apoptosis. *EMBO J*, 17, 3878-3885.

- GROSSMANN, A. & WENDEL, A. 1983. Non-reactivity of the selenoenzyme glutathione peroxidase with enzymatically hydroperoxidized phospholipids. *European Journal of Biochemistry*, 135, 549-552.
- GUERRINI, L., BLASI, F. & DENIS, D. S. 1995. Synaptic activation of NF-kappaB by glutamate in cerebellar granule neurons in vitro. *Proc Natl Acad Sci USA*, 92, 9077 - 9081.
- GUERRINI, L., MOLteni, A., WIRTH, T., KISTLER, B. & BLASI, F. 1997. Glutamate-dependent activation of NF-kappaB during mouse cerebellum development. *J Neurosci*, 17, 6057 - 6063.
- GUO, Q., ROBINSON, N. & MATTSON, M. P. 1998. Secreted beta-amyloid precursor protein counteracts the proapoptotic action of mutant presenilin-1 by activation of NF-kappaB and stabilization of calcium homeostasis. *J Biol Chem*, 273, 12341 - 12351.
- GUO, Z., RAN, Q., ROBERTS II, L. J., ZHOU, L., RICHARDSON, A., SHARAN, C., WU, D. & YANG, H. 2008. Suppression of atherosclerosis by overexpression of glutathione peroxidase-4 in apolipoprotein E-deficient mice. *Free Radical Biology and Medicine*, 44, 343-352.
- GURBUXANI, S., SCHMITT, E., CANDE, C., PARCELLIER, A., HAMMANN, A., DAUGAS, E., KOURANTI, I., SPAHR, C., PANCE, A., KROEMER, G. & GARRIDO, C. 0000. Heat shock protein 70 binding inhibits the nuclear import of apoptosis-inducing factor. *Oncogene*, 22, 6669-6678.
- HADLEY, K. B. & SUNDE, R. A. 2001. Selenium regulation of thioredoxin reductase activity and mRNA levels in rat liver. *The Journal of Nutritional Biochemistry*, 12, 693-702.
- HAHN, M. A., HAHN, T., LEE, D.-H., ESWORTHY, R. S., KIM, B.-W., RIGGS, A. D., CHU, F.-F. & PFEIFER, G. P. 2008. Methylation of Polycomb Target Genes in Intestinal Cancer Is Mediated by Inflammation. *Cancer Research*, 68, 10280-10289.
- HALLIWELL, B., K, Z. & WHITEMAN, M. 2000. The gastrointestinal tract: a major site of antioxidant action? *Free Radical Research*, 819-30.
- HAMANAKA, R. B. & CHANDEL, N. S. 2010. Mitochondrial reactive oxygen species regulate cellular signaling and dictate biological outcomes. *Trends in Biochemical Sciences*, 35, 505-513.
- HANGEN, E., BLOMGREN, K., BÉNIT, P., KROEMER, G. & MODJTAHEDI, N. 2010a. Life with or without AIF. *Trends in Biochemical Sciences*, 35, 278-287.
- HANGEN, E., DE ZIO, D., BORDI, M., ZHU, C., DESSEN, P., CAFFIN, F., LACHKAR, S., PERFETTINI, J. L., LAZAR, V., BENARD, J., FIMIA, G. M., PIACENTINI, M., HARPER, F., PIERRON, G., VICENCIO, J. M., BENIT, P., DE ANDRADE, A., HOGLINGER, G., CULMSEE, C., RUSTIN, P., BLOMGREN, K., CECCONI, F., KROEMER, G. & MODJTAHEDI, N. 2010b. A brain-specific isoform of mitochondrial apoptosis-inducing factor: AIF2. *Cell Death Differ*, 17, 1155-1166.
- HANSEN, J. M., ZHANG, H. & JONES, D. P. 2006. Mitochondrial Thioredoxin-2 Has a Key Role in Determining Tumor Necrosis Factor- α -Induced Reactive Oxygen Species Generation, NF- κ B Activation, and Apoptosis. *Toxicological Sciences*, 91, 643-650.
- HANSEN-HAGGE, T. E., BAUMEISTER, E., BAUER, T., SCHMIEDEKE, D., RENNÉ, T., WANNER, C. & GALLE, J. 2008. Transmission of oxLDL-derived lipid peroxide radicals into membranes of vascular cells is the main inducer of oxLDL-mediated oxidative stress. *Atherosclerosis*, 197, 602-611.
- HATTORI, H., IMAI, H., FURUHAMA, K., SATO, O. & NAKAGAWA, Y. 2005a. Induction of phospholipid hydroperoxide glutathione peroxidase in human polymorphonuclear neutrophils and HL60 cells stimulated with TNF- α . *Biochemical and Biophysical Research Communications*, 337, 464-473.
- HATTORI, H., IMAI, H., HANAMOTO, A., FURUHAMA, K. & NAKAGAWA, Y. 2005b. Up-regulation of phospholipid hydroperoxide glutathione peroxidase in rat casein-induced polymorphonuclear neutrophils. *Biochem. J.*, 389, 279-287.

- HEIRMAN, I., GINNEBERGE, D., BRIGELIUS-FLOHÉ, R., HENDRICKX, N., AGOSTINIS, P., BROUCKAERT, P., ROTTIERS, P. & GROOTEN, J. 2006. Blocking tumor cell eicosanoid synthesis by GPx4 impedes tumor growth and malignancy. *Free Radical Biology and Medicine*, 40, 285-294.
- HENDERSON, A. 1994. Endothelial control of myocardial function. *Arzneimittelforschung*, 44, 462-4.
- HERMESZ, E. & FERENCZ, Á. 2009. Identification of two phospholipid hydroperoxide glutathione peroxidase (gpx4) genes in common carp. *Comparative Biochemistry and Physiology Part C: Toxicology & Pharmacology*, 150, 101-106.
- HESKETH, J. 2008. Nutrigenomics and selenium: gene expression patterns, physiological targets, and genetics. *Annual Review of Nutrition*, 28, 157-77.
- HIROTAKA IMAI, N. H., ‡ RYO IWAMOTO,‡ JYUNKO SUZUKI,‡ TOSHIYUKI SUZUKI,‡ YOKO TAJIMA,‡ KUMIKO KONISHI,‡ SHINTARO MINAMI,‡ SHIZUKO ICHINOSE,¶ KAZUHIRO ISHIZAKA,|| SEIJI SHIODA,** SATORU ARATA,‡‡ MASUHIRO NISHIMURA,§§ SHINSAKU NAITO,§§ AND YASUHIITO NAKAGAWA 2009. Depletion of Selenoprotein GPx4 in Spermatocytes Causes Male Infertility in Mice. *J Biol Chem*, 284, 32522-32532.
- HISAMATSU, T., OGATA, H. & HIB, I. T. 2008. Innate immunity in inflammatory bowel disease: state of the art. *Curr Opin Gastroenterol*, 448-54.
- HO, Y.-S., MAGNENAT, J.-L., BRONSON, R. T., CAO, J., GARGANO, M., SUGAWARA, M. & FUNK, C. D. 1997. Mice Deficient in Cellular Glutathione Peroxidase Develop Normally and Show No Increased Sensitivity to Hyperoxia. *Journal of Biological Chemistry*, 272, 16644-16651.
- HOFFMANN, F. W., HASHIMOTO, A. S., LEE, B. C., ROSE, A. H., SHOHET, R. V. & HOFFMANN, P. R. 2011. Specific antioxidant selenoproteins are induced in the heart during hypertrophy. *Archives of Biochemistry and Biophysics*, 512, 38-44.
- HOFFMANN, P. R., HÖGE, S. C., LI, P.-A., HOFFMANN, F. W., HASHIMOTO, A. C. & BERRY, M. J. 2007. The selenoproteome exhibits widely varying, tissue-specific dependence on selenoprotein P for selenium supply. *Nucleic Acids Research*, 35, 3963-3973.
- HOFSTAD, B., ALMENDINGEN, K., VATN, M., ANDERSEN, S., OWEN, R., LARSEN, S. & OSNES, M. 1998. Growth and recurrence of colorectal polyps: a double-blind 3-year intervention with calcium and antioxidants. *Digestion*, 148-56.
- HONG, F., BREITLING, R., MCENTEE, C. W., WITTNER, B. S., NEMHAUSER, J. L. & CHORY, J. 2006. RankProd: a bioconductor package for detecting differentially expressed genes in meta-analysis. *Bioinformatics*, 22, 2825-2827.
- YE, H., CANDE, C., STEPHANOU, N.C., JIANG, S., GURBUXANI, S., LAROCLETTE, N., DAUGAS, E., GARRIDO, C., KROEMER, G. & HAO WU 2002. DNA binding is required for the apoptogenic action of apoptosis inducing factor. *Nat Struct Biol*, 9, 680-684.
- HOTCHKISS, R. S. & NICHOLSON, D. W. 2006. Apoptosis and caspases regulate death and inflammation in sepsis. *Nat Rev Immunol*, 6, 813-822.
- HU, Z., LEE, K. S., CHOO, Y. M., YOON, H. J., KIM, I., WEI, Y. D., GUI, Z. Z., ZHANG, G. Z., SOHN, H. D. & JIN, B. R. 2010. Molecular characterization of a phospholipid-hydroperoxide glutathione peroxidase from the bumblebee *Bombus ignitus*. *Comparative Biochemistry and Physiology Part B: Biochemistry and Molecular Biology*, 155, 54-61.
- HUANG, H.-S., CHEN, C.-J., LU, H. S. & CHANG, W.-C. 1998. Identification of a lipoxygenase inhibitor in A431 cells as a phospholipid hydroperoxide glutathione peroxidase. *FEBS Letters*, 424, 22-26.
- HUANG, H.-S., CHEN, C., SUZUKI, H., YAMAMOTO, S. & CHANG, W. 1999. Inhibitory effect of phospholipid hydroperoxide glutathione peroxidase on the activity of lipoxygenases and cyclooxygenases. *Prostaglandins Other Lipid Mediat*, 58, 65-75.

- HUANG, J., GAO, J., LV, X., LI, G., HAO, D., YAO, X., ZHOU, L., LIU, D. & WANG, R. 2010. Target gene therapy of glioma: overexpression of BAX gene under the control of both tissue-specific promoter and hypoxia-inducible element. *Acta Biochim Biophys Sin*, 42, 274-280.
- HUANG, J.-Q., LI, D.-L., ZHAO, H., SUN, L.-H., XIA, X.-J., WANG, K.-N., LUO, X. & LEI, X. G. 2011. The Selenium Deficiency Disease Exudative Diathesis in Chicks Is Associated with Downregulation of Seven Common Selenoprotein Genes in Liver and Muscle. *The Journal of Nutrition*, 141, 1605-1610.
- HUANG, Y.-T., CHUEH, S.-C., TENG, C.-M. & GUH, J.-H. 2004. Investigation of ouabain-induced anticancer effect in human androgen-independent prostate cancer PC-3 cells. *Biochemical Pharmacology*, 67, 727-733.
- HURST, R., KORYTOWSKI, W., KRISKA, T., ESWORTHY, R. S., CHU, F.-F. & GIROTTI, A. W. 2001. Hyperresistance to cholesterol hydroperoxide-induced peroxidative injury and apoptotic death in a tumor cell line that overexpresses glutathione peroxidase isotype-4. *Free Radical Biology and Medicine*, 31, 1051-1065.
- HÜTTEMANN, M., KADENBACH, B. & GROSSMAN, L. I. 2001. Mammalian subunit IV isoforms of cytochrome c oxidase. *Gene*, 267, 111-123.
- HÜTTEMANN, M., JARADAT, S. & GROSSMAN, L. I. 2003a. Cytochrome c oxidase of mammals contains a testes-specific isoform of subunit VIb—the counterpart to testes-specific cytochrome c? *Molecular Reproduction and Development*, 66, 8-16.
- HÜTTEMANN, M., SCHMIDT, T. R. & GROSSMAN, L. I. 2003b. A third isoform of cytochrome c oxidase subunit VIII is present in mammals. *Gene*, 312, 95-102.
- HUTTER, E., RENNER, K., PFISTER, G., STÖCKL, P., JANSEN-DÜRR, P. & GNAIGER, E. 2004. Senescence-associated changes in respiration and oxidative phosphorylation in primary human fibroblasts. *Biochem. J.*, 380, 919-928.
- HWANG, P. M., BUNZ, F., YU, J., RAGO, C., CHAN, T. A., MURPHY, M. P., KELSO, G. F., SMITH, R. A. J., KINZLER, K. W. & VOGELSTEIN, B. 2001. Ferredoxin reductase affects p53-dependent, 5-fluorouracil-induced apoptosis in colorectal cancer cells. *Nat Med*, 7, 1111-1117.
- HYDE, C. A. C. & MISSAILIDIS, S. 2009. Inhibition of arachidonic acid metabolism and its implication on cell proliferation and tumour-angiogenesis. *International Immunopharmacology*, 9, 701-715.
- IMAI, H., SUMI, D., HANAMOTO, A., ARAI, M., SUGIYAMA, A., CHIBA, N., KUCHINO, Y. & NAKAGAWA, Y. 1995. Molecular Cloning and Functional Expression of a cDNA for Rat Phospholipid Hydroperoxide Glutathione Peroxidase: 3'-Untranslated Region of the Gene Is Necessary for Functional Expression. *Journal of Biochemistry*, 118, 1061-1067.
- IMAI, H., SUMI, D., SAKAMOTO, H., HANAMOTO, A., ARAI, M., CHIBA, N. & NAKAGAWA, Y. 1996. Overexpression of Phospholipid Hydroperoxide Glutathione Peroxidase Suppressed Cell Death Due to Oxidative Damage in Rat Basophile Leukemia Cells (RBL-2H3). *Biochemical and Biophysical Research Communications*, 222, 432-438.
- IMAI, H., NARASHIMA, K., ARAI, M., SAKAMOTO, H., CHIBA, N. & NAKAGAWA, Y. 1998. Suppression of Leukotriene Formation in RBL-2H3 Cells That Overexpressed Phospholipid Hydroperoxide Glutathione Peroxidase. *Journal of Biological Chemistry*, 273, 1990-1997.
- IMAI, H., SUZUKI, K., ISHIZAKA, K., ICHINOSE, S., OSHIMA, H., OKAYASU, I., EMOTO, K., UMEDA, M. & NAKAGAWA, Y. 2001. Failure of the Expression of Phospholipid Hydroperoxide Glutathione Peroxidase in the Spermatozoa of Human Infertile Males. *Biology of Reproduction*, 64, 674-683.
- IMAI, H. & NAKAGAWA, Y. 2003a. Biological significance of phospholipid hydroperoxide glutathione peroxidase (PHGPx, GPx4) in mammalian cells. *Free Radical Biology and Medicine*, 34, 145-169.

- IMAI, H., HIRAO, F., SAKAMOTO, T., SEKINE, K., MIZUKURA, Y., SAITO, M., KITAMOTO, T., HAYASAKA, M., HANAOKA, K. & NAKAGAWA, Y. 2003b. Early embryonic lethality caused by targeted disruption of the mouse PHGPx gene. *Biochemical and Biophysical Research Communications*, 305, 278-286.
- IMAI, H. 2004. Biological significance of lipid hydroperoxide and its reducing enzyme, phospholipid hydroperoxide glutathione peroxidase, in mammalian cells]. *Yakugaku Zasshi.*, 124, 937-57.
- IMAI, H., SAITO, M., KIRAI, N., HASEGAWA, J., KONISHI, K., HATTORI, H., NISHIMURA, M., NAITO, S. & NAKAGAWA, Y. 2006. Identification of the Positive Regulatory and Distinct Core Regions of Promoters, and Transcriptional Regulation in Three Types of Mouse Phospholipid Hydroperoxide Glutathione Peroxidase. *Journal of Biochemistry*, 140, 573-590.
- IMAI, H. 2010. New Strategy of Functional Analysis of PHGPx Knockout Mice Model Using Transgenic Rescue Method and Cre-LoxP System. *Journal of Clinical Biochemistry and Nutrition*, 46, 1-13.
- INOUE, Y. & SHINGYOJI, C. 2007. The roles of noncatalytic ATP binding and ADP binding in the regulation of dynein motile activity in flagella. *Cell Motility and the Cytoskeleton*, 64, 690-704.
- ISMAIL, N., PIHIE, A. H. L. & NALLAPAN, M. 2005. Xanthorrhizol Induces Apoptosis Via the Up-regulation of Bax and p53 in HeLa Cells. *Anticancer Research*, 25, 2221-2227.
- JABLONSKA, E., GROMADZINSKA, J., SOBALA, W., RESZKA, E. & WASOWICZ, W. 2008. Lung cancer risk associated with selenium status is modified in smoking individuals by <i>Sep15 polymorphism. *European Journal of Nutrition*, 47, 47-54.
- JACOBSON, M. D., WEIL, M. & RAFF, M. C. 1997. Programmed cell death in animal development. *Cell*, 88, 347 - 354.
- JAMES, A. M., COCHEMÉ, H. M. & MURPHY, M. P. 2005a. Mitochondria-targeted redox probes as tools in the study of oxidative damage and ageing. *Mechanisms of Ageing and Development*, 126, 982-986.
- JAMES, A. M., COCHEMÉ, H. M., SMITH, R. A. J. & MURPHY, M. P. 2005b. Interactions of Mitochondria-targeted and Untargeted Ubiquinones with the Mitochondrial Respiratory Chain and Reactive Oxygen Species. *Journal of Biological Chemistry*, 280, 21295-21312.
- JAMES, A. M., SHARPLEY, M. S., MANAS, A.-R. B., FRERMAN, F. E., HIRST, J., SMITH, R. A. J. & MURPHY, M. P. 2007. Interaction of the Mitochondria-targeted Antioxidant MitoQ with Phospholipid Bilayers and Ubiquinone Oxidoreductases. *Journal of Biological Chemistry*, 282, 14708-14718.
- JAMES, D., PARONE, P. A., TERRADILLOS, O., LUCKEN-ARDJOMANDE, S., MONTESSUIT, S., & MARTINOU, J. C. 2007. Mechanisms of mitochondrial outer membrane permeabilization. *Novartis Found Symp*, 287, 170-6.
- JANSSEN, R., NIJTMANS, L., HEUVEL, L. & SMEITINK, J. 2006. Mitochondrial complex I: Structure, function and pathology. *Journal of Inherited Metabolic Disease*, 29, 499-515.
- JASPERS, I., ZHANG, W., BRIGHTON, L. E., CARSON, J. L., STYBLO, M. & BECK, M. A. 2007. Selenium deficiency alters epithelial cell morphology and responses to influenza. *Free Radical Biology and Medicine*, 42, 1826-1837.
- JAUSLIN, M. L., MEIER, T., SMITH, R. A. J. & MURPHY, M. P. 2003. Mitochondria-targeted antioxidants protect Friedreich Ataxia fibroblasts from endogenous oxidative stress more effectively than untargeted antioxidants. *The FASEB Journal*.
- JEŽEK, P. & HLAVATÁ, L. 2005. Mitochondria in homeostasis of reactive oxygen species in cell, tissues, and organism. *The International Journal of Biochemistry & Cell Biology*, 37, 2478-2503.

- JIA, L., PATWARI, Y., SRINIVASULA S. M., NEWLAND, A. C., FERNANDES-ALNEMRI, T., ALNEMRI, E. S., & KELSEY, S. M. 2001. Bax translocation is crucial for the sensitivity of leukaemic cells to etoposide-induced apoptosis. *Oncogene*, 20, 4817-26.
- JING L, K. S., MENDELEV N, LI PA 2011. Coenzyme q10 ameliorates ultraviolet B irradiation induced cell death through inhibition of mitochondrial intrinsic cell death pathway. *Int J Mol Sci*, 12, 8302-15.
- JONES, R. & MANN, T. 1973. Lipid peroxidation in spermatozoa. *Proc R Soc Lond B Biol Sci*, 184, 103-7.
- JOZA, N., SUSIN, S. A., DAUGAS, E., STANFORD, W. L., CHO, S. K., LI, C. Y. J., SASAKI, T., ELIA, A. J., CHENG, H. Y. M., RAVAGNAN, L., FERRI, K. F., ZAMZAMI, N., WAKEHAM, A., HAKEM, R., YOSHIDA, H., KONG, Y.-Y., MAK, T. W., ZUNIGA-PFLUCKER, J. C., KROEMER, G. & PENNINGER, J. M. 2001. Essential role of the mitochondrial apoptosis-inducing factor in programmed cell death. *Nature*, 410, 549-554.
- JOZA, N., POSPISILIK, J. A., EMILIE, H., TOSHIKATSU, H., NAZANINE, M., JOSEF, M. P. & GUIDO, K. 2009. AIF: Not Just an Apoptosis-Inducing Factor. *Annals of the New York Academy of Sciences*, 1171, 2-11.
- KADENBACH, B. 2012. Introduction to Mitochondrial Oxidative Phosphorylation Mitochondrial Oxidative Phosphorylation. In: KADENBACH, B. (ed.). Springer New York.
- KALANTARI, P., NARAYAN, V., NATARAJAN, S. K., MURALIDHAR, K., GANDHI, U. H., VUNTA, H., HENDERSON, A. J. & PRABHU, K. S. 2008. Thioredoxin Reductase-1 Negatively Regulates HIV-1 Transactivating Protein Tat-dependent Transcription in Human Macrophages. *Journal of Biological Chemistry*, 283, 33183-33190.
- KALTSCHMIDT, B., UHEREK, M., VOLK, B., BAEUERLE, P. A. & KALTSCHMIDT, C. 1997. Transcription factor NF-kappaB is activated in primary neurons by amyloid beta peptides and in neurons surrounding early plaques from patients with Alzheimer disease. *Proc Natl Acad Sci U S A*, 94, 2642 - 2647.
- KALTSCHMIDT, B., UHEREK, M., WELLMANN, H., VOLK, B. & KALTSCHMIDT, C. 1999. Inhibition of NF-kappaB potentiates amyloid-beta-mediated neuronal apoptosis. *Proc Natl Acad Sci USA*, 96, 9409 - 9414.
- KALTSCHMIDT, B., DELLER, T., FROTSCHER, M. & KALTSCHMIDT, C. 2000. Ultrastructural localization of activated NF-kappaB in granule cells of the rat fascia dentata. *Neuroreport*, 11, 839 - 844.
- KALTSCHMIDT, B., LINKER, R., DENG, J. & KALTSCHMIDT, C. 2002. Cyclooxygenase-2 is a neuronal target gene of NF-kappaB. *BMC Molecular Biology*, 3, 16.
- KALTSCHMIDT, C., KALTSCHMIDT, B. & BAEUERLE, P. A. 1993. Brain synapses contain inducible forms of the transcription factor NF-kappaB. *Mech Dev*, 43, 135 - 147.
- KALTSCHMIDT, C., KALTSCHMIDT, B., NEUMANN, H., WEKERLE, H. & BAEUERLE, P. A. 1994. Constitutive NF-kappaB activity in neurons. *Mol Cell Biol*, 14, 3981 - 3992.
- KALTSCHMIDT, C., KALTSCHMIDT, B. & BAEUERLE, P. A. 1995a. Stimulation of ionotropic glutamate receptors activates transcription factor NF-kappaB in primary neurons. *Proc Natl Acad Sci USA*, 92, 9618 - 9622.
- KALTSCHMIDT, C., KALTSCHMIDT, B., HENKEL, T., STOCKINGER, H. & BAEUERLE, P. A. 1995b. Selective recognition of the activated form of transcription factor NF-kappaB by a monoclonal antibody. *Biol Chem Hoppe Seyler*, 376, 9 - 16.
- KANDOUZ, M., NIE, D., PIDGEON, G., KRISHNAMOORTHY, S., MADDIPATI, K. & HONN, K. 2003. Platelet-type 12-lipoxygenase activates NF-kappaB in prostate cancer cells. *Prostaglandins & Other Lipid Mediators*, 71, 189-204.
- KARIN, M. & BEN-NERIAH, Y. 2000. Phosphorylation meets ubiquitination: the control of NF-kappaB activity. *Annu Rev Immunol*, 18, 621 - 663.

- KARP, S. M. & KOCH, T. R. 2006. Mechanisms of Macronutrient Deficiency and Associated Clinical Conditions. *Disease-a-Month*, 52, 164-169.
- KARP, S. M. & KOCH, T. R. 2006a. Mechanisms of Micronutrient Deficiency. *Disease-a-Month*, 52, 208-210.
- KARP, S. M. & KOCH, T. R. 2006b. Micronutrient Supplements in Inflammatory Bowel Disease. *Disease-a-Month*, 52, 211-220.
- KARP, S. M. & KOCH, T. R. 2006c. Nutrient Supplements in Inflammatory Bowel Disease. *Disease-a-Month*, 52, 170-175.
- KARP, S. M. & KOCH, T. R. 2006d. Oxidative Stress and Antioxidants in Inflammatory Bowel Disease. *Disease-a-Month*, 52, 199-207.
- KATO, T., READ, R., ROZGA, J. & BURK, R. F. 1992. Evidence for intestinal release of absorbed selenium in a form with high hepatic extraction. *American Journal of Physiology - Gastrointestinal and Liver Physiology*, 262, G854-G858.
- KAUFMANN, W. E., WORLEY, P. F., PEGG, J., BREMER, M. & ISAKSON, P. 1996. COX-2, a synaptically induced enzyme, is expressed by excitatory neurons at postsynaptic sites in rat cerebral cortex. *Proc Natl Acad Sci U S A*, 93, 2317 - 2321.
- KAUR, H. & HALLIWELL, B. 1994. Aromatic Hydroxylation of Phenylalanine as an Assay for Hydroxyl Radicals: Measurement of Hydroxyl Radical Formation from Ozone and in Blood from Premature Babies Using Improved HPLC Methodology. *Analytical Biochemistry*, 220, 11-15.
- KELSO, G. F., PORTEOUS, C. M., COULTER, C. V., HUGHES, G., PORTEOUS, W. K., LEDGERWOOD, E. C., SMITH, R. A. J. & MURPHY, M. P. 2001. Selective Targeting of a Redox-active Ubiquinone to Mitochondria within Cells. *Journal of Biological Chemistry*, 276, 4588-4596.
- KIERMAYER, C., MICHALKE, B., SCHMIDT, J. & BRIELMEIER, M. 2007. Effect of selenium on thioredoxin reductase activity in Txnrd1 or Txnrd2 hemizygous mice. *Biological Chemistry*, 388, 1091-1097.
- KIM, A., MURPHY, M. P. & OBERLEY, T. D. 2005. Mitochondrial redox state regulates transcription of the nuclear-encoded mitochondrial protein manganese superoxide dismutase: a proposed adaptive response to mitochondrial redox imbalance. *Free Radical Biology and Medicine*, 38, 644-654.
- KIM, G. S., JUNG, J. E., NARASIMHAN, P., SAKATA, H., YOSHIOKA, H., SONG, Y. S., OKAMI, N. & CHAN, P. H. 2012. Release of mitochondrial apoptogenic factors and cell death are mediated by CK2 and NADPH oxidase. *J Cereb Blood Flow Metab*, 32, 720-730.
- KIM, J. & PARTHASARATHY, S. 1998. Oxidation and the spermatozoa. *Semin Reprod Endocrinol*, 16, 235-9.
- KIM, S. H., CAI, G. B., BAE, Y. A., LEE, E. G., LEE, Y. S. & KONG, Y. 2009. Two novel phospholipid hydroperoxide glutathione peroxidase genes of *Paragonimus westermani* induced by oxidative stress. *Parasitology*, 136, 553-565.
- KIM, S.-M., KIM, Y.-G., JEONG, K.-H., LEE, S.-H., LEE, T.-W., IHM, C.-G. & MOON, J.-Y. 2012. Angiotensin II-Induced Mitochondrial Nox4 Is a Major Endogenous Source of Oxidative Stress in Kidney Tubular Cells. *PLoS ONE*, 7, e39739.
- KIMURA, T., TAKABATAKE, Y., TAKAHASHI, A., KAIMORI, J.-Y., MATSUI, I., NAMBA, T., KITAMURA, H., NIIMURA, F., MATSUSAKA, T., SOGA, T., RAKUGI, H. & ISAKA, Y. 2011. Autophagy Protects the Proximal Tubule from Degeneration and Acute Ischemic Injury. *Journal of the American Society of Nephrology*, 22, 902-913.
- KING, A., GOTTLIEB, E., BROOKS, D. G., MURPHY, M. P. & DUNAIEF, J. L. 2004. Mitochondria-derived Reactive Oxygen Species Mediate Blue Light-induced Death of Retinal Pigment Epithelial Cells. *Photochemistry and Photobiology*, 79, 470-475.

- KIPP, A., BANNING, A., VAN SCHOTHORST, E. M., MÉPLAN, C., SCHOMBURG, L., EVELO, C., COORT, S., GAJ, S., KEIJER, J., HESKETH, J. & BRIGELIUS-FLOHÉ, R. 2009. Four selenoproteins, protein biosynthesis, and Wnt signalling are particularly sensitive to limited selenium intake in mouse colon. *Molecular Nutrition & Food Research*, 53, 1561-1572.
- KLEIN, J. A., LONGO-GUESS, C. M., ROSSMANN, M. P., SEBURN, K. L., HURD, R. E., FRANKEL, W. N., BRONSON, R. T. & ACKERMAN, S. L. 2002. The harlequin mouse mutation downregulates apoptosis-inducing factor. *Nature*, 419, 367-374.
- KOBAYASHI, T. & ENDOH, H. 2003. Caspase-like activity in programmed nuclear death during conjugation of *Tetrahymena thermophila*. *Cell Death Differ*, 10, 634 - 640.
- KOBAYASHI, T. & ENDOH, H. 2005. A possible role of mitochondria in the apoptotic-like programmed nuclear death of *Tetrahymena thermophila*. *FEBS J*, 272, 5378 - 5387.
- KOENE, S. & SMEITINK, J. 2011. Metabolic manipulators: a well founded strategy to combat mitochondrial dysfunction. *J Inherit Metab Dis*, 34, 315-25.
- KOHRLE, J. 2000. The deiodinase family: selenoenzymes regulating thyroid hormone availability and action. *Cell Mol Life Sci*, 57, 1853-63.
- KOONIN, E. V. & ARAVIND, L. 2002. Origin and evolution of eukaryotic apoptosis: the bacterial connection. *Cell Death Differ*, 9, 394 - 404.
- KOOPMAN, W. J. H., VERKAART, S., VISCH, H.-J., VAN DER WESTHUIZEN, F. H., MURPHY, M. P., VAN DEN HEUVEL, L. W. P. J., SMEITINK, J. A. M. & WILLEMS, P. H. G. M. 2005. Inhibition of complex I of the electron transport chain causes O₂⁻-mediated mitochondrial outgrowth. *American Journal of Physiology - Cell Physiology*, 288, C1440-C1450.
- KOOPMAN, W. J. H., VERKAART, S., VISCH, H.-J., VAN DER WESTHUIZEN, F. H., MURPHY, M. P., VAN DEN HEUVEL, L. W. P. J., SMEITINK, J. A. M. & WILLEMS, P. H. G. M. 2005a. Inhibition of complex I of the electron transport chain causes O₂⁻-mediated mitochondrial outgrowth. *American Journal of Physiology - Cell Physiology*, 288, C1440-C1450.
- KOOPMAN, W. J. H., VISCH, H.-J., VERKAART, S., VAN DEN HEUVEL, L. W. P. J., SMEITINK, J. A. M. & WILLEMS, P. H. G. M. 2005b. Mitochondrial network complexity and pathological decrease in complex I activity are tightly correlated in isolated human complex I deficiency. *American Journal of Physiology - Cell Physiology*, 289, C881-C890.
- KOPP, E. & GHOSH, S. 1994. Inhibition of NF-kappaB by sodium salicylate and aspirin. *Science*, 265, 956 - 959.
- KRANTIC, S., MECHAWAR, N., REIX, S. & QUIRION, R. 2007. Apoptosis-inducing factor: A matter of neuron life and death. *Progress in Neurobiology*, 81, 179-196.
- KRISKA, T., KORYTOWSKI, W. & GIROTTI, A. W. 2002. Hyperresistance to photosensitized lipid peroxidation and apoptotic killing in 5-aminolevulinate-treated tumor cells overexpressing mitochondrial GPX4. *Free Radical Biology and Medicine*, 33, 1389-1402.
- KRISKA, T., KORYTOWSKI, W. & GIROTTI, A. W. 2005. Role of mitochondrial cardiolipin peroxidation in apoptotic photokilling of 5-aminolevulinate-treated tumor cells. *Archives of Biochemistry and Biophysics*, 433, 435-446.
- KRISKA, T., LEVCHENKO, V. V., CHU, F.-F., ESWORTHY, R. S. & GIROTTI, A. W. 2008. Novel enrichment of tumor cell transfectants expressing high levels of type 4 glutathione peroxidase using 7 α -hydroperoxycholesterol as a selection agent. *Free Radical Biology and Medicine*, 45, 700-707.
- KIRKENGAARD, K. G., HAGGLUND, P., FINNIE, C., SVENSSON, B. & HENRIKSEN, A. 2009. Structure of *Hordeum vulgare* NADPH-dependent thioredoxin reductase 2. Unwinding the reaction mechanism. *Acta Crystallogr D Biol Crystallogr*, 65, 932-941.
- KROEMER, G., DALLAPORTA, B. & RESCHE-RIGON, M. 1998. The mitochondrial death/life regulator in apoptosis and necrosis. *Annu Rev Physiol*, 60, 619-42.

- KRYUKOV, G. V., CASTELLANO, S., NOVOSELOV, S. V., LOBANOV, A. V., ZEHTAB, O., GUIGÓ, R. & GLADYSHEV, V. N. 2003. Characterization of Mammalian Selenoproteomes. *Science*, 300, 1439-1443.
- KUMARASWAMY, E., MALYKH, A., KOROTKOV, K. V., KOZYAVKIN, S., HU, Y., KWON, S. Y., MOUSTAFA, M. E., CARLSON, B. A., BERRY, M. J., LEE, B. J., HATFIELD, D. L., DIAMOND, A. M. & GLADYSHEV, V. N. 2000. Structure-Expression Relationships of the 15-kDa Selenoprotein Gene. *Journal of Biological Chemistry*, 275, 35540-35547.
- KUNSCH, C., RUBEN, S. M. & ROSEN, C. A. 1992. Selection of optimal kappaB/Rel DNA-binding motifs: interaction of both subunits of NF-kappaB with DNA is required for transcriptional activation. *Mol Cell Biol*, 12, 4412 - 4421.
- LABUNSKYY, V. M., YOO, M.-H., HATFIELD, D. L. & GLADYSHEV, V. N. 2009. Sep15, a Thioredoxin-like Selenoprotein, Is Involved in the Unfolded Protein Response and Differentially Regulated by Adaptive and Acute ER Stresses. *Biochemistry*, 48, 8458-8465.
- LALOI, C., APEL, K. & DANON, A. 2004. Reactive oxygen signalling: the latest news. *Current Opinion in Plant Biology*, 7, 323-328.
- LATCHOUMYCADANE, C., MARATHE, G. K., ZHANG, R. & MCINTYRE, T. M. 2012. Oxidatively Truncated Phospholipids Are Required Agents of Tumor Necrosis Factor α (TNF α)-induced Apoptosis. *Journal of Biological Chemistry*, 287, 17693-17705.
- LEE, B.-J., HUANG, Y.-C., CHEN, S.-J. & LIN, P.-T. 2012. Coenzyme Q10 supplementation reduces oxidative stress and increases antioxidant enzyme activity in patients with coronary artery disease. *Nutrition*, 28, 250-255.
- LEE, D.-H., ESWORTHY, R. S., CHU, C., PFEIFER, G. P. & CHU, F.-F. 2006. Mutation Accumulation in the Intestine and Colon of Mice Deficient in Two Intracellular Glutathione Peroxidases. *Cancer Research*, 66, 9845-9851.
- LEE, S. H., MENG, X. W., FLATTEN, K. S., LOEGERING, D. A. & KAUFMANN, S. H. 2012. Phosphatidylserine exposure during apoptosis reflects bidirectional trafficking between plasma membrane and cytoplasm. *Cell Death Differ*.
- LEE, S. O., YEON CHUN, J., NADIMINTY, N., TRUMP, D. L., IP, C., DONG, Y. & GAO, A. C. 2006. Monomethylated selenium inhibits growth of LNCaP human prostate cancer xenograft accompanied by a decrease in the expression of androgen receptor and prostate-specific antigen (PSA). *The Prostate*, 66, 1070-1075.
- LEE, W., MITCHELL, P. & TJIAN, R. 1987. Purified transcription factor AP-1 interacts with TPA-inducible enhancer elements. *Cell*, 49, 741 - 752.
- LEMIEUX, H., SEMSROTH, S., ANTRETTTER, H., HÖFER, D. & GNAIGER, E. 2011. Mitochondrial respiratory control and early defects of oxidative phosphorylation in the failing human heart. *The International Journal of Biochemistry & Cell Biology*, 43, 1729-1738.
- LENAZ, G., BOVINA, C., D'AURELIO, M., FATO, R., FORMIGGINI, G., GENOVA, M. L., GIULIANO, G., PICH, M. M., PAOLUCCI, U. G. O., CASTELLI, G. P. & VENTURA, B. 2002. Role of Mitochondria in Oxidative Stress and Aging. *Annals of the New York Academy of Sciences*, 959, 199-213.
- LESAGE, S., ZOULALI, H., COLOMBEL, J. F., BELAICHE, J., CÉZARD, J. P., TYSK, C., ALMER, S., GASSULL, M., BINDER, V., CHAMAILLARD, M., LE GALL, I., THOMAS, G. & HUGOT, J. P. 2000. Genetic analyses of chromosome 12 loci in Crohn's disease. *Gut*, 47, 787-791.
- LI, H., LI, H., WANG, Y., XU, H., FAN, W., WANG, M., SUN, P. & XIE, X. 2004. An intervention study to prevent gastric cancer by micro-selenium and large dose of allitridum. *Chin Med J(Engl)*, 1155-60.
- LI, L. Y., LUO, X. & WANG, X. 2001. Endonuclease G is an apoptotic DNase when released from mitochondria. *Nature*, 412, 95-99.

- LI, P., NIJHAWAN, D., BUDIHARDJO, I., SRINIVASULA, S. M., AHMAD, M., ALNEMRI, E. S. & WANG, X. 1997. Cytochrome c and dATP-Dependent Formation of Apaf-1/Caspase-9 Complex Initiates an Apoptotic Protease Cascade. *Cell*, 91, 479-489.
- LIANG, H., REMMEN, H. V., FROHLICH, V., LECHLEITER, J., RICHARDSON, A. & RAN, Q. 2007. Gpx4 protects mitochondrial ATP generation against oxidative damage. *Biochemical and Biophysical Research Communications*, 356, 893-898.
- LIANG, H., RAN, Q., JANG, Y. C., HOLSTEIN, D., LECHLEITER, J., MCDONALD-MARSH, T., MUSATOV, A., SONG, W., VAN REMMEN, H. & RICHARDSON, A. 2009a. Glutathione peroxidase 4 differentially regulates the release of apoptogenic proteins from mitochondria. *Free Radical Biology and Medicine*, 47, 312-320.
- LIANG, H., YOO, S.-E., NA, R., WALTER, C. A., RICHARDSON, A. & RAN, Q. 2009b. Short Form Glutathione Peroxidase 4 Is the Essential Isoform Required for Survival and Somatic Mitochondrial Functions. *Journal of Biological Chemistry*, 284, 30836-30844.
- LIETZ G, H. J. 2009. A network approach to micronutrient genetics: interactions with lipid metabolism. *Curr Opin Lipidol.*, 20, 112-20.
- LILI LU, B. C. O., YOUNG-JOON JO, THOMAS W. LAUER, SHINICHI USUI, KEIICHI KOMEIMA, BING XIE, AND PETER A. CAMPOCHIARO 2009. Increased Expression of Glutathione Peroxidase 4 Strongly Protects Retina from Oxidative Damage. *Antioxid Redox Signal*, 11, 715-724.
- LIM, S., RASHID, M. A., JANG, M., KIM, Y., WON, H., LEE, J., WOO, J. T., KIM, J. S., MURPHY, M. P., ALI, L., HA, J. & KIM, S. S. 2011. Mitochondria-targeted Antioxidants Protect Pancreatic β -cells against Oxidative Stress and Improve Insulin Secretion in Glucotoxicity and Glucolipotoxicity. *Cellular Physiology and Biochemistry*, 28, 873-886.
- LINDER, D., FREUND, R. & KADENBACH, B. 1995. Species-specific expression of cytochrome c oxidase isozymes. *Comparative Biochemistry and Physiology Part B: Biochemistry and Molecular Biology*, 112, 461-9.
- LIU, H. C., SHA, W. C., SCOTT, M. L. & BALTIMORE, D. 1994. Sequential induction of NF-kappaB/Rel family proteins during B-cell terminal differentiation. *Mol Cell Biol*, 14, 5349 - 5359.
- LIU, H., NISHITOH, H., ICHIJO, H. & KYRIAKIS, J. M. 2000. Activation of Apoptosis Signal-Regulating Kinase 1 (ASK1) by Tumor Necrosis Factor Receptor-Associated Factor 2 Requires Prior Dissociation of the ASK1 Inhibitor Thioredoxin. *Molecular and Cellular Biology*, 20, 2198-2208.
- LIU, L. & KEEFE, D. L. 2000. Cytoplasm Mediates Both Development and Oxidation-Induced Apoptotic Cell Death in Mouse Zygotes. *Biology of Reproduction*, 62, 1828-1834.
- LIU, R., LI, B., FLANAGAN, S. W., OBERLEY, L. W., GOZAL, D. & QIU, M. 2002. Increased mitochondrial antioxidative activity or decreased oxygen free radical propagation prevent mutant SOD1-mediated motor neuron cell death and increase amyotrophic lateral sclerosis-like transgenic mouse survival. *Journal of Neurochemistry*, 80, 488-500.
- LIWEI, L., WEI, Z., RUIFA, H. & CHUNYU, L. 2012. Association between genetic variants in glutathione peroxidase 1 gene and risk of prostate cancer: a meta-analysis. *Molecular Biology Reports*, 1-5.
- LOEFFLER, M., DAUGAS, E., SUSIN, S. A., ZAMZAMI, N., MÉTIVIER, D., NIEMINEN, A.-L., BROTHERS, G., PENNINGER, J. M. & KROEMER, G. 2001. Dominant cell death induction by extramitochondrially targeted apoptosis-inducing factor. *The FASEB Journal*, 15, 758-767.
- LOH, K., DENG, H., FUKUSHIMA, A., CAI, X., BOIVIN, B., GALIC, S., BRUCE, C., SHIELDS, B. J., SKIBA, B., OOMS, L. M., STEPTO, N., WU, B., MITCHELL, C. A., TONKS, N. K., WATT, M. J., FEBBRAIO, M. A., CRACK, P. J., ANDRIKOPOULOS, S. & TIGANIS, T. 2009. Reactive Oxygen Species Enhance Insulin Sensitivity. *Cell Metabolism*, 10, 260-272.

- LORENZO, H. K., SUSIN, S. A., PENNINGER, J. & KROEMER, G. 1999. Apoptosis inducing factor (AIF): a phylogenetically old, caspase-independent effector of cell death. *Cell Death Differ*, 6, 516 - 524.
- LORENZO, H. K. & SUSIN, S. A. 2007. Therapeutic potential of AIF-mediated caspase-independent programmed cell death. *Drug Resist Updat*, 10, 235 - 255.
- LOTHROP, A. P., RUGGLES, E. L. & HONDAL, R. J. 2009. No Selenium Required: Reactions Catalyzed by Mammalian Thioredoxin Reductase That Are Independent of a Selenocysteine Residue. *Biochemistry*, 48, 6213-6223.
- LOWES, D. A., THOTTAKAM, B. M. V., WEBSTER, N. R., MURPHY, M. P. & GALLEY, H. F. 2008. The mitochondria-targeted antioxidant MitoQ protects against organ damage in a lipopolysaccharide-peptidoglycan model of sepsis. *Free Radical Biology and Medicine*, 45, 1559-1565.
- LOWES, D. A. & GALLEY, H. F. 2011. Mitochondrial protection by the thioredoxin-2 and glutathione systems in an in vitro endothelial model of sepsis. *Biochemical Journal*, 436, 123-132.
- LU, C., QIU, F., ZHOU, H., PENG, Y., HAO, W., XU, J., YUAN, J., WANG, S., QIANG, B., XU, C. & PENG, X. 2006a. Identification and characterization of selenoprotein K: An antioxidant in cardiomyocytes. *FEBS Letters*, 580, 5189-5197.
- LU, C., ZHU, F., CHO, Y. Y., TANG, F., ZYKOVA, T., MA, W. Y., BODE, A. M. & DONG, Z. 2006b. Cell apoptosis: requirement of H2AX in DNA ladder formation, but not for the activation of caspase-3. *Mol Cell*, 23, 121 - 132.
- LU, E. & WOLFE, J. 2001. Lysosomal enzymes in the macronucleus of Tetrahymena during its apoptosis-like degradation. *Cell Death Differ*, 8, 289 - 297.
- LU, J. & HOLMGREN, A. 2009. Selenoproteins. *Journal of Biological Chemistry*, 284, 723-727.
- LUDWIG, B., BENDER, E., ARNOLD, S., HÜTTEMANN, M., LEE, I. & KADENBACH, B. 2001. Cytochrome c Oxidase and the Regulation of Oxidative Phosphorylation. *ChemBioChem*, 2, 392-403.
- LUKIW, W. J. & BAZAN, N. G. 1998. Strong nuclear factor-kappaB-DNA binding parallels cyclooxygenase-2 gene transcription in aging and in sporadic Alzheimer's disease superior temporal lobe neocortex. *J Neurosci Res*, 53, 583 - 592.
- MACKENZIE, S. H. & CLARK, A. C. 2012. Death by Caspase Dimerization Protein Dimerization and Oligomerization in Biology. In: MATTHEWS, J. M. (ed.). Springer New York.
- MAHYAR, A., AYAZI, P., FALLAHI, M. & JAVADI, A. 2010. Correlation Between Serum Selenium Level and Febrile Seizures. *Pediatric Neurology*, 43, 331-334.
- MAIORINO, M., CHU, F. F., URSINI, F., DAVIES, K. J., DOROSHOW, J. H. & ESWORTHY, R. S. 1991a. Phospholipid hydroperoxide glutathione peroxidase is the 18-kDa selenoprotein expressed in human tumor cell lines. *Journal of Biological Chemistry*, 266, 7728-7732.
- MAIORINO, M., THOMAS, J., GIROTTI, A. & URSINI, F. 1991b. Reactivity of phospholipid hydroperoxide glutathione peroxidase with membrane and lipoprotein lipid hydroperoxides. *free Radic Res Commun*, 12-13, 131-5.
- MAITI, B., ARBOGAST, S., ALLAMAND, V., MOYLE, M. W., ANDERSON, C. B., RICHARD, P., GUICHENEY, P., FERREIRO, A., FLANIGAN, K. M. & HOWARD, M. T. 2009. A mutation in the SEPNI selenocysteine redefinition element (SRE) reduces selenocysteine incorporation and leads to SEPNI-related myopathy. *Human Mutation*, 30, 411-416.
- MANNES, A. M., SEILER, A., BOSELLO, V., MAIORINO, M. & CONRAD, M. 2011. Cysteine mutant of mammalian GPx4 rescues cell death induced by disruption of the wild-type selenoenzyme. *The FASEB Journal*, 25, 2135-2144.
- MARCOCCI, C., KAHALY, G. J., KRASSAS, G. E., BARTALENA, L., PRUMMEL, M., STAHL, M., ALTEA, M. A., NARDI, M., PITZ, S., BOBORIDIS, K., SIVELLI, P., VON ARX, G.,

- MOURITS, M. P., BALDESCHI, L., BENCIVELLI, W. & WIERSINGA, W. 2011. Selenium and the Course of Mild Graves' Orbitopathy. *New England Journal of Medicine*, 364, 1920-1931.
- MARCUS, C. 2009. Transgenic mouse models for the vital selenoenzymes cytosolic thioredoxin reductase, mitochondrial thioredoxin reductase and glutathione peroxidase 4. *Biochimica et Biophysica Acta (BBA) - General Subjects*, 1790, 1575-1585.
- MARGARET P, R. 2009. Selenoproteins and human health: Insights from epidemiological data. *Biochimica et Biophysica Acta (BBA) - General Subjects*, 1790, 1533-1540.
- MARGIS, R., DUNAND, C., TEIXEIRA, F.K., MARGIS-PINHEIRO, M. 2008. Glutathione peroxidase family – an evolutionary overview. *FEBS J.*, 275, 3959-70.
- MARTEAU, P., LEPAGE, P., MANGIN, I., SAUAU, A., DORE, J., PORCHAR, T. P. & SEKSIK, P. 2004. Review article: gut flora and inflammatory bowel disease. *Aliment Pharmacol Ther*, 18-23.
- MATSUMOTO, S., UCHIUMI, T., TANAMACHI, H., SAITO, T., YAGI, M., TAKAZAKI, S., KANKI, T. & KANG, D. 2012. Ribonucleoprotein Y-box-binding protein-1 regulates mitochondrial oxidative phosphorylation (OXPHOS) protein expression after serum stimulation through binding to OXPHOS mRNA. *Biochemical Journal*, 443, 573-584.
- MATTSON, M. P., GOODMAN, Y., LUO, H., FU, W. & FURUKAWA, K. 1997. Activation of NF-kappaB protects hippocampal neurons against oxidative stress-induced apoptosis: evidence for induction of manganese superoxide dismutase and suppression of peroxynitrite production and protein tyrosine nitration. *J Neurosci Res*, 49, 681 - 697.
- MAY, M. J., D'ACQUISTO, F., MADGE, L. A., GLOCKNER, J., POBER, J. S. & GHOSH, S. 2000. Selective inhibition of NF-kappaB activation by a peptide that blocks the interaction of NEMO with the IkappaB kinase complex. *Science*, 289, 1550 - 1554.
- MCCANN, J. C. & AMES, B. N. 2011. Adaptive dysfunction of selenoproteins from the perspective of the triage theory: why modest selenium deficiency may increase risk of diseases of aging. *The FASEB Journal*, 25, 1793-1814.
- MCKENZIE, M., LAZAROU, M. & RYAN, M. T. 2009. Analysis of Respiratory Chain Complex Assembly with Radiolabeled Nuclear- and Mitochondrial-Encoded Subunits. In: WILLIAM, S. A. & IMMO, E. S. (eds.) *Methods in Enzymology*. Academic Press.
- MCKENZIE, M., LIOLITSA, D. & HANNA, M. 2004. Mitochondrial Disease: Mutations and Mechanisms. *Neurochemical Research*, 29, 589-600.
- MEBERG, P. J., KINNEY, W. R., VALCOURT, E. G. & ROUTTENBERG, A. 1996. Gene expression of the transcription factor NF-kappaB in hippocampus: regulation by synaptic activity. *Mol Brain Res*, 38, 179 - 190.
- MÉPLAN, C., CROSLEY, L. K., NICOL, F., BECKETT, G. J., HOWIE, A. F., HILL, K. E., HORGAN, G., MATHERS, J. C., ARTHUR, J. R. & HESKETH, J. E. 2007. Genetic polymorphisms in the human selenoprotein P gene determine the response of selenoprotein markers to selenium supplementation in a gender-specific manner (the SELGEN study). *The FASEB Journal*, 21, 3063-3074.
- MÉPLAN, C., CROSLEY, L. K., NICOL, F., HORGAN, G. W., MATHERS, J. C., ARTHUR, J. R. & HESKETH, J. E. 2008. Functional effects of a common single-nucleotide polymorphism (GPX4c718t) in the glutathione peroxidase 4 gene: interaction with sex. *The American Journal of Clinical Nutrition*, 87, 1019-1027.
- MÉPLAN, C., HUGHES, D. J., PARDINI, B., NACCARATI, A., SOUCEK, P., VODICKOVA, L., HLAVATÁ, I., VRÁNA, D., VODICKA, P. & HESKETH, J. E. 2010. Genetic variants in selenoprotein genes increase risk of colorectal cancer. *Carcinogenesis*, 31, 1074-1079.

- MESEGUER, M., DE LOS SANTOS, M. J., SIMÓN, C., PELLICER, A., REMOHÍ, J. & GARRIDO, N. 2006. Effect of sperm glutathione peroxidases 1 and 4 on embryo asymmetry and blastocyst quality in oocyte donation cycles. *Fertility and Sterility*, 86, 1376-1385.
- MESSAOUDIA, I., BANNI, M., SAÏDA, L., SAÏDA, K., & KERKENI, K. 2010. Involvement of selenoprotein P and GPx4 gene expression in cadmium-induced testicular pathophysiology in rat. *Chem Biol Interact* 188, 94-101.
- MEYER, F., GALAN, P., DOUVILLE, P., BAIRATI, I., KEGLE, P., BERTRAIS, S., ESTAQUIO, C. & HERCBERG, S. 2005. Antioxidant vitamin and mineral supplementation and prostate cancer prevention in the SU.VI.MAX trial. *International Journal of Cancer*, 116, 182-186.
- MIN-HYUK YOO, X. G., 2 XUE-MING XU,1 JIN-YOUNG KIM,1,3 BRADLEY A. CARLSON,1 ANDREW D. PATTERSON,1,* HUAIBIN CAI,2 VADIM N. GLADYSHEV,4,5 AND DOLPH L. HATFIELD 2010. Delineating the Role of Glutathione Peroxidase 4 in Protecting Cells Against Lipid Hydroperoxide Damage and in Alzheimer's Disease. *Antioxid Redox Signal*, 12, 819-827.
- MIRAMAR, M. D., COSTANTINI, P., RAVAGNAN, L., SARAIVA, L. M., HAOUZI, D., BROTHERS, G., PENNINGER, J. M., PELEATO, M. L., KROEMER, G. & SUSIN, S. A. 2001. NADH Oxidase Activity of Mitochondrial Apoptosis-inducing Factor. *Journal of Biological Chemistry*, 276, 16391-16398.
- MISTRY, H. D., KURLAK, L. O., WILLIAMS, P. J., RAMSAY, M. M., SYMONDS, M. E. & BROUGHTON PIPKIN, F. 2010. Differential expression and distribution of placental glutathione peroxidases 1, 3 and 4 in normal and preeclamptic pregnancy. *Placenta*, 31, 401-408.
- MITCHELL, T., ROTARU, D., SABA, H., SMITH, R. A. J., MURPHY, M. P. & MACMILLAN-CROW, L. A. 2011. The Mitochondria-Targeted Antioxidant Mitoquinone Protects against Cold Storage Injury of Renal Tubular Cells and Rat Kidneys. *Journal of Pharmacology and Experimental Therapeutics*, 336, 682-692.
- MIYAKE, K., BEKISZ, J., ZHAO, T., CLARK, C. R. & ZOON, K. C. 2012. Apoptosis-inducing factor (AIF) is targeted in IFN- α 2a-induced Bid-mediated apoptosis through Bak activation in ovarian cancer cells. *Biochimica et Biophysica Acta (BBA) - Molecular Cell Research*, 1823, 1378-1388.
- MODJTAHEDI, N., GIORDANETTO, F., MADEO, F. & KROEMER, G. 2006. Apoptosis-inducing factor: vital and lethal. *Trends in Cell Biology*, 16, 264-272.
- MODJTAHEDI, N., GIORDANETTO, F. & KROEMER, G. 2010. A human mitochondriopathy caused by AIF mutation. *Cell Death Differ*, 17, 1525-1528.
- MOGHADASZADEH, B. & BEGGS, A. H. 2006. Selenoproteins and Their Impact on Human Health Through Diverse Physiological Pathways. *Physiology*, 21, 307-315.
- MOORE, K. & ROBERTS, L. J. 1998. Measurement of lipid peroxidation. *Free radic Res*, 28, 659-71.
- MPOKE, S. & WOLFE, J. 1996. DNA digestion and chromatin condensation during nuclear death in Tetrahymena. *Exp Cell Res*, 225, 357 - 365.
- MUKHERJEE, B., KESSINGER, C., KOBAYASHI, J., CHEN, B. P., CHEN, D. J., CHATTERJEE, A. & BURMA, S. 2006. DNA-PK phosphorylates histone H2AX during apoptotic DNA fragmentation in mammalian cells. *DNA Repair*, 5, 575 - 590.
- MUKHOPADHYAY, P., HORVÁTH, B., ZSENGELLÉR, Z., BÁTKAI, S., CAO, Z., KECHRID, M., HOLOVAC, E., ERDÉLYI, K., TANCHIAN, G., LIAUDET, L., STILLMAN, I. E., JOSEPH, J., KALYANARAMAN, B. & PACHER, P. 2012a. Mitochondrial reactive oxygen species generation triggers inflammatory response and tissue injury associated with hepatic ischemia-reperfusion: Therapeutic potential of mitochondrially targeted antioxidants. *Free Radical Biology and Medicine*, 53, 1123-1138.
- MUKHOPADHYAY, P., HORVÁTH, B., ZSENGELLÉR, Z., ZIELONKA, J., TANCHIAN, G., HOLOVAC, E., KECHRID, M., PATEL, V., STILLMAN, I. E., PARIKH, S. M., JOSEPH, J.,

- KALYANARAMAN, B. & PACHER, P. 2012b. Mitochondrial-targeted antioxidants represent a promising approach for prevention of cisplatin-induced nephropathy. *Free Radical Biology and Medicine*, 52, 497-506.
- MULLER, F. L., LIU, Y. & VAN REMMEN, H. 2004. Complex III Releases Superoxide to Both Sides of the Inner Mitochondrial Membrane. *Journal of Biological Chemistry*, 279, 49064-49073.
- MURAHASHI, H., AZUMA, H., ZAMZAMI, N., FURUYA, K.-J., IKEBUCHI, K., YAMAGUCHI, M., YAMADA, Y., SATO, N., FUJIHARA, M., KROEMER, G. & IKEDA, H. 2003. Possible contribution of apoptosis-inducing factor (AIF) and reactive oxygen species (ROS) to UVB-induced caspase-independent cell death in the T cell line Jurkat. *J Leukoc Biol*, 73, 399-406.
- MURPHY, M. P. 2008. Targeting lipophilic cations to mitochondria. *Biochimica et Biophysica Acta (BBA) - Bioenergetics*, 1777, 1028-1031.
- NACAMULLI, D., MIAN, C., PETRICCA, D., LAZZAROTTO, F., BAROLLO, S., POZZA, D., MASIERO, S., FAGGIAN, D., PLEBANI, M., GIRELLI, M. E., MANTERO, F. & BETTERLE, C. 2010. Influence of physiological dietary selenium supplementation on the natural course of autoimmune thyroiditis. *Clinical Endocrinology*, 73, 535-539.
- NAGATA, S. 2000. Apoptotic DNA Fragmentation. *Experimental Cell Research*, 256, 12-18.
- NAHA, P. C., DAVOREN, M., LYNG, F. M. & BYRNE, H. J. 2010. Reactive oxygen species (ROS) induced cytokine production and cytotoxicity of PAMAM dendrimers in J774A.1 cells. *Toxicology and Applied Pharmacology*, 246, 91-99.
- NATARAJAN SK, B., DF 2012. Role of apoptosis-inducing factor, proline dehydrogenase, and NADPH oxidase in apoptosis and oxidative stress. *Cell Health Cytoskelet.*, 4, 11-27.
- NEGRO, R., GRECO, G., MANGIERI, T., PEZZAROSSA, A., DAZZI, D. & HASSAN, H. 2007. The Influence of Selenium Supplementation on Postpartum Thyroid Status in Pregnant Women with Thyroid Peroxidase Autoantibodies. *Journal of Clinical Endocrinology & Metabolism*, 92, 1263-1268.
- NELSEN, B., HELLMAN, L. & SEN, R. 1988. The NF-kappaB-binding site mediates phorbol ester-inducible transcription in nonlymphoid cells. *Mol Cell Biol*, 8, 3526 - 3531.
- NEUZIL, J., WIDÉN, C., GELLERT, N., SWETTENHAM, E., ZOBALOVA, R., DONG, L.-F., WANG, X.-F., LIDEBJER, C., DALEN, H., HEADRICK, J. & WITTING, P. 2007. Mitochondria transmit apoptosis signalling in cardiomyocyte-like cells and isolated hearts exposed to experimental ischemia-reperfusion injury. *Redox Report*, 12, 148-162.
- NGU, L. H., NIJTMANS, L. G., DISTELMAIER, F., VENSELAAR, H., VAN EMST-DE VRIES, S. E., VAN DEN BRAND, M. A. M., STOLTENBORG, B. J. M., WINTJES, L. T., WILLEMS, P. H., VAN DEN HEUVEL, L. P., SMEITINK, J. A. & RODENBURG, R. J. T. 2012. A catalytic defect in mitochondrial respiratory chain complex I due to a mutation in NDUFS2 in a patient with Leigh syndrome. *Biochimica et Biophysica Acta (BBA) - Molecular Basis of Disease*, 1822, 168-175.
- NIEHAUS, W. J. & SAMUELSSON, B. 1968. Formation of malonaldehyde from phospholipid arachidonate during microsomal lipid peroxidation. *Eur J Biochem*, 6, 126-30.
- NIEROBISZ, L. S., MCFARLAND, D. C. & MOZDZIAK, P. E. 2011. MitoQ10 induces adipogenesis and oxidative metabolism in myotube cultures. *Comparative Biochemistry and Physiology Part B: Biochemistry and Molecular Biology*, 158, 125-131.
- NOBLANC, A., KOCER, A., CHABORY, E., VERNET, P., SAEZ, F., CADET, R., CONRAD, M. & DREVET, J. R. 2011. Glutathione Peroxidases at Work on Epididymal Spermatozoa: An Example of the Dual Effect of Reactive Oxygen Species on Mammalian Male Fertilizing Ability. *J Androl*, 32, 641-650.
- NOJI, H. & YOSHIDA, M. 2001. The Rotary Machine in the Cell, ATP Synthase. *Journal of Biological Chemistry*, 276, 1665-1668.

- NOMURA, K., IMAI, H., KOUMURA, T., ARAI, M. & NAKAGAWA, Y. 1999. Mitochondrial Phospholipid Hydroperoxide Glutathione Peroxidase Suppresses Apoptosis Mediated by a Mitochondrial Death Pathway. *Journal of Biological Chemistry*, 274, 29294-29302.
- NOOTEBOOM, M., JOHNSON, R., TAYLOR, R. W., WRIGHT, N. A., LIGHTOWLERS, R. N., KIRKWOOD, T. B. L., MATHERS, J. C., TURNBULL, D. M. & GREAVES, L. C. 2010. Age-associated mitochondrial DNA mutations lead to small but significant changes in cell proliferation and apoptosis in human colonic crypts. *Aging Cell*, 9, 96-99.
- NORBERG, E., GOGVADZE, V., OTT, M., HORN, M., UHLEN, P., ORRENIUS, S. & ZHIVOTOVSKY, B. 2008. An increase in intracellular Ca²⁺ is required for the activation of mitochondrial calpain to release AIF during cell death. *Cell Death Differ*, 15, 1857-1864.
- OESTERGAARD, M. Z., TYRER, J., CEBRIAN, A., SHAH, M., DUNNING, A. M., PONDER, B. A. J., EASTON, D. F. & PHAROAH, P. D. P. 2006. Interactions between genes involved in the antioxidant defence system and breast cancer risk. *Br J Cancer*, 95, 525-531.
- O'NEILL, L. A. J. & KALTSCHMIDT, C. 1997. NF-kappaB: a crucial transcription factor for glial and neuronal cell function. *Trends Neurosci*, 20, 252 - 258.
- ORRENIUS, S. 2007. Reactive Oxygen Species in Mitochondria-Mediated Cell Death. *Drug Metabolism Reviews*, 39, 443-455.
- PAGMANTIDIS, V., BERMANO, G., VILLETTE, S., BROOM, I., ARTHUR, J. & HESKETH, J. 2005. Effects of Se-depletion on glutathione peroxidase and selenoprotein W gene expression in the colon. *FEBS Letters*, 579, 792-796.
- PARK, Y. P., CHOI, S. C., CHO, M. Y., SONG, E. Y., KIM, J. W., PAIK, S. G., KIM, Y. K., KIM, J. W., & LEE, H. G. 2006. Modulation of telomerase activity and human telomerase reverse transcriptase expression by caspases and bcl-2 family proteins in Cisplatin-induced cell death. *Korean J Lab Med*, 26, 287-93.
- PELEG, S., SANANBENESI, F., ZOVOILIS, A., BURKHARDT, S., BAHARI-JAVAN, S., AGIS-BALBOA, R. C., COTA, P., WITTNAM, J. L., GOGOL-DOERING, A., OPITZ, L., SALINAS-RIESTER, G., DETTENHOFER, M., KANG, H., FARINELLI, L., CHEN, W. & FISCHER, A. 2010. Altered Histone Acetylation Is Associated with Age-Dependent Memory Impairment in Mice. *Science*, 328, 753-756.
- PETERS, U., CHATTERJEE, N., HAYES, R. B., SCHOEN, R. E., WANG, Y., CHANOCK, S. J. & FOSTER, C. B. 2008. Variation in the Selenoenzyme Genes and Risk of Advanced Distal Colorectal Adenoma. *Cancer Epidemiology Biomarkers & Prevention*, 17, 1144-1154.
- PETROSILLO, G., MATERA, M., MORO, N., RUGGIERO, F. M. & PARADIES, G. 2009. Mitochondrial complex I dysfunction in rat heart with aging: critical role of reactive oxygen species and cardiolipin. *Free Radical Biology and Medicine*, 46, 88-94.
- PFEIFER, H., CONRAD, M., ROETHLEIN, D., KYRIAKOPOULOS, A., BRIELMEIER, M., BORNKAMM, G. W. & BEHNE, D. 2001. Identification of a specific sperm nuclei selenoenzyme necessary for protamine thiol cross-linking during sperm maturation. *The FASEB Journal*.
- PIERRON, D., WILDMAN, D., HUTTEMANN, M., LETELLIER, T. & GROSSMAN, L. 2012. Evolution of the couple cytochrome c and cytochrome c oxidase in primates. *Adv Exp Med Biol*, 748, 185-213.
- PLECITÁ-HLAVATÁ, L., JEŽEK, J. & JEŽEK, P. 2009. Pro-oxidant mitochondrial matrix-targeted ubiquinone MitoQ10 acts as anti-oxidant at retarded electron transport or proton pumping within Complex I. *The International Journal of Biochemistry & Cell Biology*, 41, 1697-1707.
- POLONIKOV, A. V., VIALYKH, E. K., CHURNOSOV, M. I., ILLIG, T., FREIDIN, M. B., VASIL'EVA, O. V., BUSHUEVA, O. Y., RYZHAEVA, V. N., BULGAKOVA, I. V. & SOLODILOVA, M. A. 2011. The C718T polymorphism in the 3[prime]-untranslated region of

glutathione peroxidase-4 gene is a predictor of cerebral stroke in patients with essential hypertension. *Hypertens Res*.

- POSPISILIK, J. A., KNAUF, C., JOZA, N., BENIT, P., ORTHOFER, M., CANI, P. D., EBERSBERGER, I., NAKASHIMA, T., SARAO, R., NEELY, G., ESTERBAUER, H., KOZLOV, A., KAHN, C. R., KROEMER, G., RUSTIN, P., BURCELIN, R. & PENNINGER, J. M. 2007. Targeted Deletion of AIF Decreases Mitochondrial Oxidative Phosphorylation and Protects from Obesity and Diabetes. *Cell*, 131, 476-491.
- PRASAD, A. V., PILCHER, W. H. & JOSEPH, S. A. 1994. Nuclear factor-kappa B in rat brain: enhanced DNA-binding activity following convulsant-induced seizures. *Neurosci Lett*, 170, 145 - 148.
- PRESCOTT, D. M. 1994. The DNA of ciliated protozoa. *Microbiol Rev*, 58, 233 - 267.
- PUTCHA, G. V., DESHMUKH, M., JOHNSON, E.M Jr. 1999. BAX translocation is a critical event in neuronal apoptosis: regulation by neuroprotectants, BCL-2, and caspases. *J Neurosci*, 19, 7476-85.
- QIAO, Y.-L., DAWSEY, S. M., KAMANGAR, F., FAN, J.-H., ABNET, C. C., SUN, X.-D., JOHNSON, L. L., GAIL, M. H., DONG, Z.-W., YU, B., MARK, S. D. & TAYLOR, P. R. 2009. Total and Cancer Mortality After Supplementation With Vitamins and Minerals: Follow-up of the Linxian General Population Nutrition Intervention Trial. *Journal of the National Cancer Institute*, 101, 507-518.
- RAJAGOPALAN, K., WATT, D. S. & HALEY, B. E. 1999. Orientation of GTP and ADP within their respective binding sites in glutamate dehydrogenase. *European Journal of Biochemistry*, 265, 564-571.
- RAN, Q., VAN REMMEN, H., GU, M., QI, W., ROBERTS, L. J., PROLLA, T. & RICHARDSON, A. 2003. Embryonic fibroblasts from Gpx4^{+/-} mice: a novel model for studying the role of membrane peroxidation in biological processes. *Free Radical Biology and Medicine*, 35, 1101-1109.
- RAN, Q., LIANG, H., GU, M., QI, W., WALTER, C. A., ROBERTS, L. J., HERMAN, B., RICHARDSON, A. & VAN REMMEN, H. 2004. Transgenic Mice Overexpressing Glutathione Peroxidase 4 Are Protected against Oxidative Stress-induced Apoptosis. *Journal of Biological Chemistry*, 279, 55137-55146.
- RAN, Q., GU, M., VAN REMMEN, H., STRONG, R., ROBERTS, J. L. & RICHARDSON, A. 2006. Glutathione peroxidase 4 protects cortical neurons from oxidative injury and amyloid toxicity. *Journal of Neuroscience Research*, 84, 202-208.
- RAN, Q., LIANG, H., IKENO, Y., QI, W., PROLLA, T. A., ROBERTS, L. J., 2ND, WOLF, N., VAN REMMEN, H. & RICHARDSON, A. 2007. Reduction in glutathione peroxidase 4 increases life span through increased sensitivity to apoptosis. *J Gerontol A Biol Sci Med Sci*, 62, 932-42.
- RAO, B., SOUFIR, J., MARTIN, M. & DAVID, G. 1989. Lipid peroxidation in human spermatozoa as related to midpiece abnormalities and motility. *Gamete Res*, 24, 127-34.
- RAVAGNAN, L., GURBUXANI, S., SUSIN, S. A., MAISSE, C., DAUGAS, E., ZAMZAMI, N., MAK, T., JAATTELA, M., PENNINGER, J. M., GARRIDO, C. & KROEMER, G. 2001. Heat-shock protein 70 antagonizes apoptosis-inducing factor. *Nat Cell Biol*, 3, 839-843.
- RAVAGNAN, L., ROUMIER, T. & KROEMER, G. 2002. Mitochondria, the killer organelles and their weapons. *Journal of Cellular Physiology*, 192, 131-137.
- RAYMAN, M. P. 2000. The importance of selenium to human health. *The Lancet*, 356, 233-241.
- RAYMAN, M. P., THOMPSON, A. J., BEKAERT, B., CATTERICK, J., GALASSINI, R., HALL, E., WARREN-PERRY, M. & BECKETT, G. J. 2008. Randomized controlled trial of the effect of selenium supplementation on thyroid function in the elderly in the United Kingdom. *The American Journal of Clinical Nutrition*, 87, 370-378.

- RAYMAN, M. P. 2009. Selenoproteins and human health: Insights from epidemiological data. *Biochimica et Biophysica Acta (BBA) - General Subjects*, 1790, 1533-1540.
- RAYMAN, M. P. 2012. Selenium and human health. *The Lancet*, 379, 1256-1268.
- REBSCH, C. M., PENNA, F. J. & COPELAND, P. R. 2006. Selenoprotein expression is regulated at multiple levels in prostate cells. *Cell Res*, 16, 940-948.
- REEVES, M. & HOFFMANN, P. 2009. The human selenoproteome: recent insights into functions and regulation. *Cellular and Molecular Life Sciences*, 66, 2457-2478.
- REID, M. E., DUFFIELD-LILLICO, A. J., SUNGA, A., FAKIH, M., ALBERTS, D. S. & MARSHALL, J. R. 2006. Selenium supplementation and colorectal adenomas: An analysis of the nutritional prevention of cancer trial. *International Journal of Cancer*, 118, 1777-1781.
- REYNOLDS, A., LEAKE, D., BOESE, Q., SCARINGE, S., MARSHALL, W. S. & KHVOROVA, A. 2004. Rational siRNA design for RNA interference. *Nat Biotech*, 22, 326-330.
- RHOADS, M., UMBACH, A., SUBBAIAH, C. & SIEDOW, J. 2006. Mitochondrial reactive oxygen species. Contribution to oxidative stress and interorganellar signaling. *Plant Physiol*, 141, 357-66.
- RICHTER, C., PARK, J. W. & AMES, B. N. 1988. Normal oxidative damage to mitochondrial and nuclear DNA is extensive. *Proceedings of the National Academy of Sciences*, 85, 6465-6467.
- ROBBLEE, J. P., CAO, W., HENN, A., HANNEMANN, D. E. & DE LA CRUZ, E. M. 2005. Thermodynamics of Nucleotide Binding to Actomyosin V and VI: A Positive Heat Capacity Change Accompanies Strong ADP Binding†. *Biochemistry*, 44, 10238-10249.
- ROGAKOU, E. P., NIEVES-NEIRA, W., BOON, C., POMMIER, Y. & BONNER, W. M. 2000. Initiation of DNA fragmentation during apoptosis induces phosphorylation of H2AX histone at serine 139. *J Biol Chem*, 275, 9390 - 9395.
- ROGERIO, M., CHRISTOPHE, D., FELIPE, K. T. & MARCIA, M.-P. 2008. Glutathione peroxidase family – an evolutionary overview. *FEBS Journal*, 275, 3959-3970.
- ROHR-UDILOVA, N., SIEGHART, W., EFERL, R., STOIBER, D., BJÖRKHEM-BERGMAN, L., C.ERIKSSON, L., STOLZE, K., HAYDEN, H., KEPPLER, B., SAGMEISTER, S., GRASL-KRAUPP, B., SCHULTE-HERMANN, R. & PECK-RADOSAVLJEVIC, M. 2011. Antagonistic effects of selenium and lipid peroxides on growth control in early hepatocellular carcinoma. *Hepatology*, n/a-n/a.
- ROHR-UDILOVA, N., SIEGHART, W., EFERL, R., STOIBER, D., BJÖRKHEM-BERGMAN, L., ERIKSSON, L. C., STOLZE, K., HAYDEN, H., KEPPLER, B., SAGMEISTER, S., GRASL-KRAUPP, B., SCHULTE-HERMANN, R. & PECK-RADOSAVLJEVIC, M. 2012. Antagonistic effects of selenium and lipid peroxides on growth control in early hepatocellular carcinoma. *Hepatology*, 55, 1112-1121.
- ROMANOWSKA, M., KIKAWA, K. D., FIELDS, J. R., MACIAG, A., NORTH, S. L., SHIAO, Y.-H., KASPRZAK, K. S. & ANDERSON, L. M. 2007. Effects of selenium supplementation on expression of glutathione peroxidase isoforms in cultured human lung adenocarcinoma cell lines. *Lung Cancer*, 55, 35-42.
- RORBACH, J., RICHTER, R., WESSELS, H. J., WYDRO, M., PEKALSKI, M., FARHOUD, M., KÜHL, I., GAISNE, M., BONNEFOY, N., SMEITINK, J. A., LIGHTOWLERS, R. N. & CHRZANOWSKA-LIGHTOWLERS, Z. M. A. 2008. The human mitochondrial ribosome recycling factor is essential for cell viability. *Nucleic Acids Research*, 36, 5787-5799.
- ROSS, M., KELSO, G., BLAIKIE, F., JAMES, A., COCHEMÉ, H., FILIPOVSKA, A., DA ROS, T., HURD, T., SMITH, R. & MURPHY, M. 2005. Lipophilic triphenylphosphonium cations as tools in mitochondrial bioenergetics and free radical biology. *Biochemistry (Moscow)*, 70, 222-230.
- ROTHWARF, D. M., ZANDI, E., NATOLI, G. & KARIN, M. 1998. IKK-gamma is an essential regulatory subunit of the I kappa B kinase complex. *Nature*, 395, 297 - 300.

- ROUZER, C. A. & SAMUELSSON, B. 1986. The importance of hydroperoxide activation for the detection and assay of mammalian 5-lipoxygenase. *FEBS Letters*, 204, 293-296.
- RUBBO, H., RADI, R., TRUJILLO, M., TELLERI, R., KALYANARAMAN, B., BARNES, S., KIRK, M. & FREEMAN, B. A. 1994. Nitric oxide regulation of superoxide and peroxynitrite-dependent lipid peroxidation. Formation of novel nitrogen-containing oxidized lipid derivatives. *Journal of Biological Chemistry*, 269, 26066-26075.
- RUSSO, M. W., MURRAY, S. C., WURZELMANN, J. I., WOOSLEY, J. T. & SANDIER, R. S. 1997. Plasma selenium levels and the risk of colorectal adenomas. *Nutrition and Cancer*, 28, 125-129.
- SAKAMOTO, H., IMAI, H. & NAKAGAWA, Y. 2000. Involvement of Phospholipid Hydroperoxide Glutathione Peroxidase in the Modulation of Prostaglandin D2 Synthesis. *Journal of Biological Chemistry*, 275, 40028-40035.
- SAKAMURU, S., LI, X., ATTENE-RAMOS, M. S., HUANG, R., LU, J., SHOU, L., SHEN, M., TICE, R. R., AUSTIN, C. P. & XIA, M. 2012. Application of a homogenous membrane potential assay to assess mitochondrial function. *Physiological Genomics*, 44, 495-503.
- SALAS-VIDAL, E., LOMELI, AMP, X, HILDA, CASTRO-OBREGÓN, S., CUERVO, R., ESCALANTE-ALCALDE, D. & COVARRUBIAS, L. 1998. Reactive Oxygen Species Participate in the Control of Mouse Embryonic Cell Death. *Experimental Cell Research*, 238, 136-147.
- SAMAD, T. A., MOORE, K. A., SAPIRSTEIN, A., BILLET, S., ALLCHORNE, A., POOLE, S., BONVENTRE, J. V. & WOOLF, C. J. 2001. Interleukin-1beta-mediated induction of Cox-2 in the CNS contributes to inflammatory pain hypersensitivity. *Nature*, 410, 471 - 475.
- SANJUÁN-PLA, A., CERVERA, A. M., APOSTOLOVA, N., GARCIA-BOU, R., VÍCTOR, V. M., MURPHY, M. P. & MCCREATH, K. J. 2005. A targeted antioxidant reveals the importance of mitochondrial reactive oxygen species in the hypoxic signaling of HIF-1 α . *FEBS Letters*, 579, 2669-2674.
- SARETZKI, G., MURPHY, M. P. & VON ZGLINICKI, T. 2003. MitoQ counteracts telomere shortening and elongates lifespan of fibroblasts under mild oxidative stress. *Aging Cell*, 2, 141-143.
- SAVASKAN, N. E., BORCHERT, A., BRÄUER, A. U. & KUHN, H. 2007a. Role for glutathione peroxidase-4 in brain development and neuronal apoptosis: Specific induction of enzyme expression in reactive astrocytes following brain injury. *Free Radical Biology and Medicine*, 43, 191-201.
- SAVASKAN, N. E., BORCHERT, A., BRÄUER, A. U. & KUHN, H. 2007b. Molecular biology of glutathione peroxidase 4: from genomic structure to developmental expression and neural function. *Biol Chem*, 388, 1007-17.
- SCHEERER, P., BORCHERT, A., KRAUSS, N., WESSNER, H., GERTH, C., HÖHNE, W. & KUHN, H. 2007. Structural Basis for Catalytic Activity and Enzyme Polymerization of Phospholipid Hydroperoxide Glutathione Peroxidase-4 (GPx4)^{†,‡,§}. *Biochemistry*, 46, 9041-9049.
- SCHMIDT-ULLRICH, R., MEMET, S., LILIENBAUM, A., FEUILLARD, J., RAPHAEL, M. & ISRAEL, A. 1996. NF-kappaB activity in transgenic mice: developmental regulation and tissue specificity. *Development*, 122, 2117 - 2128.
- SCHMITZ, M. L. & BAEUERLE, P. A. 1991. The p53 subunit is responsible for the strong transcription activating potential of NF-kappaB. *EMBO J*, 10, 3805 - 3817.
- SCHNABEL, D., SALAS-VIDAL, E., NARVÁEZ, V., DEL RAYO SÁNCHEZ-CARBENTE, M., HERNÁNDEZ-GARCÍA, D., CUERVO, R. & COVARRUBIAS, L. 2006. Expression and regulation of antioxidant enzymes in the developing limb support a function of ROS in interdigital cell death. *Developmental Biology*, 291, 291-299.
- SCHNABEL, R., LUBOS, E., MESSOW, C. M., SINNING, C. R., ZELLER, T., WILD, P. S., PEETZ, D., HANDY, D. E., MUNZEL, T., LOSCALZO, J., LACKNER, K. J. & BLANKENBERG, S.

2008. Selenium supplementation improves antioxidant capacity in vitro and in vivo in patients with coronary artery disease: The Selenium Therapy in Coronary Artery disease Patients (SETCAP) Study. *American Heart Journal*, 156, 1201.e1-1201.e11.
- SCHNEIDER, M., FÖRSTER, H., BOERSMA, A., SEILER, A., WEHNES, H., SINOWATZ, F., NEUMÜLLER, C., DEUTSCH, M. J., WALCH, A., HRABÉ DE ANGELIS, M., WURST, W., URSINI, F., ROVERI, A., MALESZEWSKI, M., MAIORINO, M. & CONRAD, M. 2009. Mitochondrial glutathione peroxidase 4 disruption causes male infertility. *The FASEB Journal*, 23, 3233-3242.
- SCHNEIDER M, W. M., MANDAL PK, ARPORNCHAYANON W, JANNASCH K, ALVES F, STRIETH S, CONRAD M, BECK H. 2010. Absence of glutathione peroxidase 4 affects tumor angiogenesis through increased 12/15-lipoxygenase activity. *Neoplasia*, 12, 254-63.
- SCHNURR, K., BELKNER, J., URSINI, F., SCHEWE, T. & KÜHN, H. 1996. The Selenoenzyme Phospholipid Hydroperoxide Glutathione Peroxidase Controls the Activity of the 15-Lipoxygenase with Complex Substrates and Preserves the Specificity of the Oxygenation Products. *Journal of Biological Chemistry*, 271, 4653-4658.
- SCHOMBURG, L. & KÖHRLE, J. 2008. On the importance of selenium and iodine metabolism for thyroid hormone biosynthesis and human health. *Molecular Nutrition & Food Research*, 52, 1235-1246.
- SCHRIEVER, S. C., BARNES, K. M., EVENSON, J. K., RAINES, A. M. & SUNDE, R. A. 2009. Selenium Requirements Are Higher for Glutathione Peroxidase-1 mRNA than Gpx1 Activity in Rat Testis. *Experimental Biology and Medicine*, 234, 513-521.
- SCHUH, R. A., JACKSON, K. C., KHAIRALLAH, R. J., WARD, C. W. & SPANGENBURG, E. E. 2012. Measuring mitochondrial respiration in intact single muscle fibers. *American Journal of Physiology - Regulatory, Integrative and Comparative Physiology*, 302, R712-R719.
- SCHULTHESS, F. T., KATZ, S., ARDESTANI, A., KAWAHIRA, H., GEORGIA, S., BOSCO, D., BHUSHAN, A. & MAEDLER, K. 2009. Deletion of the Mitochondrial Flavoprotein Apoptosis Inducing Factor (AIF) Induces β -Cell Apoptosis and Impairs β -Cell Mass. *PLoS ONE*, 4, e4394.
- SCHWEIZER, U., BRÄUER, A. U., KÖHRLE, J., NITSCH, R. & SAVASKAN, N. E. 2004a. Selenium and brain function: a poorly recognized liaison. *Brain Research Reviews*, 45, 164-178.
- SCHWEIZER, U., MICHAELIS, M., KOHRLE, J. & SCHOMBURG, L. 2004b. Efficient selenium transfer from mother to offspring in selenoprotein-P-deficient mice enables dose-dependent rescue of phenotypes associated with selenium deficiency. *Biochem. J.*, 378, 21-6.
- SCHWEIZER, U., SCHOMBURG, L. & SAVASKAN, N. E. 2004c. The Neurobiology of Selenium: Lessons from Transgenic Mice. *The Journal of Nutrition*, 134, 707-710.
- SCIMECA, M. S., LISK, D. J., PROLLA, T. & LEI, X. G. 2005. Effects of gpx4 Haploid Insufficiency on GPx4 Activity, Selenium Concentration, and Paraquat-Induced Protein Oxidation in Murine Tissues. *Experimental Biology and Medicine*, 230, 709-714.
- SEILER, A., SCHNEIDER, M., FÖRSTER, H., ROTH, S., WIRTH, E. K., CULMSEE, C., PLESNILA, N., KREMMER, E., RÅDMARK, O., WURST, W., BORNKAMM, G. W., SCHWEIZER, U. & CONRAD, M. 2008. Glutathione Peroxidase 4 Senses and Translates Oxidative Stress into 12/15-Lipoxygenase Dependent- and AIF-Mediated Cell Death. *Cell Metabolism*, 8, 237-248.
- SEVRIOUKOVA, I. F. 2009. Redox-Linked Conformational Dynamics in Apoptosis-Inducing Factor. *Journal of Molecular Biology*, 390, 924-938.
- SEVRIOUKOVA, I. 2011. Apoptosis-inducing factor: structure, function, and redox regulation. *Antioxid Redox Signal*, 14, 2545-79.
- SHAHAR, A., PATEL, K. V., SEMBA, R. D., BANDINELLI, S., SHAHAR, D. R., FERRUCCI, L. & GURALNIK, J. M. 2010. Plasma selenium is positively related to performance in neurological tasks assessing coordination and motor speed. *Movement Disorders*, 25, 1909-1915.

- SHAMA, G. & MALIK, D. J. 2012. The uses and abuses of rapid bioluminescence-based ATP assays. *International Journal of Hygiene and Environmental Health*.
- SHANG, Y., SONG, X., BOWEN, J., CORSTANJE, R., GAO, Y., GAERTIG, J. & GOROVSKY, M. A. 2002. A robust inducible-repressible promoter greatly facilitates gene knockouts, conditional expression, and overexpression of homologous and heterologous genes in *Tetrahymena thermophila*. *Proc Natl Acad Sci USA*, 19, 3734 - 3739.
- SHARMA, L. K., LU, J. & BAI, Y. 2009. Mitochondrial Respiratory Complex I: Structure, Function and Implication in Human Diseases. *Current Medicinal Chemistry*, 16, 1266-1277.
- SHCHEDRINA, V. A., ZHANG, Y., LABUNSKY, V.M., HATFIELD, D. L. & GLADYSHEV, V. N. 2010. Structure-function relations, physiological roles, and evolution of mammalian ER-resident selenoproteins. *Antioxid Redox Signal*, 12, 839-49.
- SHIMIZU, S., KONISHI, A. & TUJIMOTO, Y. 2004. X-ray-induced DNA damage and apoptosisX-ray-induced DNA damage and apoptosis. *Tanpakushitsu Kakusan Koso*, 49, 601-7.
- SHIMIZU, T., NUMATA, T. & OKADA, Y. 2004. A role of reactive oxygen species in apoptotic activation of volume-sensitive Cl⁻ channel. *Proceedings of the National Academy of Sciences of the United States of America*, 101, 6770-6773.
- SHUREIQI, I., WU, Y., CHEN, D., YANG, X. L., GUAN, B., MORRIS, J. S., YANG, P., NEWMAN, R. A., BROADDUS, R., HAMILTON, S. R., LYNCH, P., LEVIN, B., FISCHER, S. M. & LIPPMAN, S. M. 2005. The Critical Role of 15-Lipoxygenase-1 in Colorectal Epithelial Cell Terminal Differentiation and Tumorigenesis. *Cancer Research*, 65, 11486-11492.
- SIBBING, D., PFEUFER, A., PERISIC, T., MANNES, A. M., FRITZ-WOLF, K., UNWIN, S., SINNER, M. F., GIEGER, C., GLOECKNER, C. J., WICHMANN, H.-E., KREMMER, E., SCHÄFER, Z., WALCH, A., HINTERSEER, M., NÄBAUER, M., KÄÄB, S., KASTRATI, A., SCHÖMIG, A., MEITINGER, T., BORNKAMM, G. W., CONRAD, M. & VON BECKERATH, N. 2011. Mutations in the mitochondrial thioredoxin reductase gene TXNRD2 cause dilated cardiomyopathy. *European Heart Journal*, 32, 1121-1133.
- SIDDIQUI, A., RIVERA-SÁNCHEZ, S., CASTRO, M. D. R., ACEVEDO-TORRES, K., RANE, A., TORRES-RAMOS, C. A., NICHOLLS, D. G., ANDERSEN, J. K. & AYALA-TORRES, S. 2012. Mitochondrial DNA damage Is associated with reduced mitochondrial bioenergetics in Huntington's disease. *Free Radical Biology and Medicine*.
- SKULACHEV, V. P. 1998. Cytochrome c in the apoptotic and antioxidant cascades. *FEBS Letters*, 423, 275-280.
- SMEITINK, J. & VAN DEN HEUVEL, L. 1999. Human Mitochondrial Complex I in Health and Disease. *The American Journal of Human Genetics*, 64, 1505-1510.
- SMITH, D. G., GAWRYLUK, R. M., SPENCER, D. F., PEARLMAN, R. E., SIU, K. W. & GRAY, M. W. 2007. Exploring the mitochondrial proteome of the ciliate protozoon *Tetrahymena thermophila*: direct analysis by tandem mass spectrometry. *J Mol Biol*, 30, 837 - 867.
- SMITH, R. A. J., KELSO, G. F., JAMES, A. M. & MURPHY, M. P. 2004. Targeting Coenzyme Q Derivatives to Mitochondria. In: HELMUT, S. & LESTER, P. (eds.) *Methods in Enzymology*. Academic Press.
- SMITH, R. A. J., ADLAM, V. J., BLAIKIE, F. H., MANAS, A.-R. B., PORTEOUS, C. M., JAMES, A. M., ROSS, M. F., LOGAN, A., COCHEMÉ, H. M., TRNKA, J., PRIME, T. A., ABAKUMOVA, I., JONES, B. A., FILIPOVSKA, A. & MURPHY, M. P. 2008. Mitochondria-Targeted Antioxidants in the Treatment of Disease. *Annals of the New York Academy of Sciences*, 1147, 105-111.
- SMITH, R. A. J. & MURPHY, M. P. 2010. Animal and human studies with the mitochondria-targeted antioxidant MitoQ. *Annals of the New York Academy of Sciences*, 1201, 96-103.
- SNEDDON, A. A., WU, H.-C., FARQUHARSON, A., GRANT, I., ARTHUR, J. R., ROTONDO, D., CHOE, S.-N. & WAHLE, K. W. J. 2003. Regulation of selenoprotein GPx4 expression and

- activity in human endothelial cells by fatty acids, cytokines and antioxidants. *Atherosclerosis*, 171, 57-65.
- SONG, X., GJONESKA, E., REN, Q., TAVERNA, S. D., ALLIS, C. D. & GOROVSKY, M. A. 2007. Phosphorylation of the SQ H2A.X motif is required for proper meiosis and mitosis in *Tetrahymena thermophila*. *Mol Cell Biol*, 27, 2648 - 2660.
- SORDILLO, L. M., STREICHER, K. L., MULLARKY, I. K., GANDY, J. C., TRIGONA, W. & CORL, C. M. 2008. Selenium inhibits 15-hydroperoxyoctadecadienoic acid-induced intracellular adhesion molecule expression in aortic endothelial cells. *Free Radical Biology and Medicine*, 44, 34-43.
- SPECKMANN, B., BIDMON, H.-J., PINTO, A., ANLAUF, M., SIES, H. & STEINBRENNER, H. 2011. Induction of Glutathione Peroxidase 4 Expression during Enterocytic Cell Differentiation. *Journal of Biological Chemistry*, 286, 10764-10772.
- STADTMAN, E. R. & LEVINE, R. L. 2000. Protein Oxidation. *Annals of the New York Academy of Sciences*, 899, 191-208.
- STAMBOLSKY, P., WEISZ, L., SHATS, I., KLEIN, Y., GOLDFINGER, N., OREN, M. & ROTTER, V. 2006. Regulation of AIF expression by p53. *Cell Death Differ*, 13, 2140-2149.
- STANLEY, B. A., SIVAKUMARAN, V., SHI, S., MCDONALD, I., LLOYD, D., WATSON, W. H., AON, M. A. & PAOLOCCI, N. 2011. Thioredoxin Reductase-2 Is Essential for Keeping Low Levels of H₂O₂ Emission from Isolated Heart Mitochondria. *Journal of Biological Chemistry*, 286, 33669-33677.
- STEEVENS, J., VAN DEN BRANDT, P. A., GOLDBOHM, R. A. & SCHOUTEN, L. J. 2010. Selenium Status and the Risk of Esophageal and Gastric Cancer Subtypes: The Netherlands Cohort Study. *Gastroenterology*, 138, 1704-1713.
- STEINBRECHER, A., MÉPLAN, C., HESKETH, J., SCHOMBURG, L., ENDERMANN, T., JANSEN, E., ÅKESSON, B., ROHRMANN, S. & LINSEISEN, J. 2010. Effects of Selenium Status and Polymorphisms in Selenoprotein Genes on Prostate Cancer Risk in a Prospective Study of European Men. *Cancer Epidemiology Biomarkers & Prevention*, 19, 2958-2968.
- STEINER, C. & KALTSCHMIDT, C. 1989. An automated method for calcium phosphate-mediated gene transfer. *Trends Genet*, 5, 138.
- STOLL, M., CORNELIUSSEN, B., COSTELLO, C. M., WAETZIG, G. H., MELLGARD, B., KOCH, W. A., ROSENSTIEL, P., ALBRECHT, M., CROUCHER, P. J. P., SEEGERT, D., NIKOLAUS, S., HAMPE, J., LENGAUER, T., PIERROU, S., FOELSCH, U. R., MATHEW, C. G., LAGERSTROM-FERMER, M. & SCHREIBER, S. 2004. Genetic variation in DLG5 is associated with inflammatory bowel disease. *Nat Genet*, 36, 476-480.
- STOPPINI, L., BUCHS, P. A. & MULLER, D. 1991. A simple method for organotypic cultures of nervous tissue. *J Neurosci Methods*, 37, 173 - 182.
- STRAIF, D., WERZ, O., KELLNER, R., BAHR, U. & STEINHILBER, D. 2000. Glutathione peroxidase-1 but not -4 is involved in the regulation of cellular 5-lipoxygenase activity in monocytic cells. *Biochem. J.*, 349, 455-461.
- SUNDE, R. A., RAINES, A. M., BARNES, K. M. & EVENSON, J. K. 2009a. Selenium status highly regulates selenoprotein mRNA levels for only a subset of the selenoproteins in the selenoproteome. *Biosci Rep*, 29, 329-38.
- SUNDE, R. A. & THOMPSON, K. M. 2009b. Dietary selenium requirements based on tissue selenium concentration and glutathione peroxidase activities in old female rats. *Journal of Trace Elements in Medicine and Biology*, 23, 132-137.
- SUNDE, R. A. & HADLEY, K. B. 2010. Phospholipid hydroperoxide glutathione peroxidase (Gpx4) is highly regulated in male turkey poult and can be used to determine dietary selenium requirements. *Experimental Biology and Medicine*, 235, 23-31.

- SUNDE, R. A. & RAINES, A. M. 2011. Selenium Regulation of the Selenoprotein and Nonselenoprotein Transcriptomes in Rodents. *Advances in Nutrition: An International Review Journal*, 2, 138-150.
- SUPINSKI, G. S., MURPHY, M. P. & CALLAHAN, L. A. 2009. MitoQ administration prevents endotoxin-induced cardiac dysfunction. *American Journal of Physiology - Regulatory, Integrative and Comparative Physiology*, 297, R1095-R1102.
- SUSIN, S. A., ZAMZAMI, N., CASTEDO, M., HIRSCH, T., MARCHETTI, P., MACHO, A., DAUGAS, E., GEUSKENS, M. & KROEMER, G. 1996. Bcl-2 inhibits the mitochondrial release of an apoptogenic protease. *J Exp Med*, 184, 1331-41.
- SUSIN, S. A., DAUGAS, E., RAVAGNAN, L., SAMEJIMA, K., ZAMZAMI, N., LOEFFLER, M., COSTANTINI, P., FERRI, K. F., IRINOPOULOU, T., PREVOST, M. C., BROTHERS, G., MAK, T. W., PENNINGER, J., EARNSHAW, W. C. & KROEMER, G. 2000. Two distinct pathways leading to nuclear apoptosis. *J Exp Med*, 192, 571 - 579.
- SUTHERLAND, M., SHANKARANARAYANAN, P., SCHEWE, T. & NIGAM, S. 2001. Evidence for the presence of phospholipid hydroperoxide glutathione peroxidase in human platelets: implications for its involvement in the regulatory network of the 12-lipoxygenase pathway of arachidonic acid metabolism. *Biochem. J.*, 353, 91-100.
- SUZUKI, G., HARPER, K. M., HIRAMOTO, T., FUNKE, B., LEE, M., KANG, G., BUELL, M., GEYER, M. A., KUCHERLAPATI, R., MORROW, B., MÄNNISTÖ, P. T., AGATSUMA, S. & HIROI, N. 2009. Over-expression of a human chromosome 22q11.2 segment including TXNRD2, COMT and ARVCF developmentally affects incentive learning and working memory in mice. *Human Molecular Genetics*, 18, 3914-3925.
- SWEETLOVE, L. J., HEAZLEWOOD, J. L., HERALD, V., HOLTZAPFFEL, R., DAY, D. A., LEAVER, C. J. & MILLAR, A. H. 2002. The impact of oxidative stress on Arabidopsis mitochondria. *The Plant Journal*, 32, 891-904.
- SZETO, H. H., LIU, S., SOONG, Y., WU, D., DARRAH, S. F., CHENG, F.-Y., ZHAO, Z., GANGER, M., TOW, C. Y. & SESHAN, S. V. 2011. Mitochondria-Targeted Peptide Accelerates ATP Recovery and Reduces Ischemic Kidney Injury. *Journal of the American Society of Nephrology*, 22, 1041-1052.
- SZETO, T. H., ROWLAND, S. L., ROTHFIELD, L. I. & KING, G. F. 2002. Membrane localization of MinD is mediated by a C-terminal motif that is conserved across eubacteria, archaea, and chloroplasts. *Proceedings of the National Academy of Sciences*, 99, 15693-15698.
- SZTILLER-SIKORSKA, M., JAKUBOWSKA, J., WOZNIAK, M., STASIAK, M. & CZYZ, M. 2009. A non-apoptotic function of caspase-3 in pharmacologically-induced differentiation of K562 cells. *British Journal of Pharmacology*, 157, 1451-1462.
- TAKENAKA, Y., HAGA, N., HARUMOTO, T., MATSUURA, T. & MITSUI, Y. 2002. Transformation of Paramecium caudatum with a novel expression vector harboring codon-optimized GFP gene. *Gene*, 284, 233 - 240.
- TARIN, F., MIGUEL-GARCIA, A., LINARES, M., SANCHEZ, M., ORERO, M., HERNANDEZ, F., BLANQUER, A., MIQUEL-SOSA, A., CARBONELL, F. & MATUTES, E. 1996. Peripheral blood identification of neoplastic cells and the tumoral growth fraction by double immunocytochemical study in a case of anaplastic CD30-positive large cell lymphoma. *Leukemia*, 10, 1560.
- TAZAWA, R., XU, X. M., WU, K. K. & WANG, L. H. 1994. Characterization of the genomic structure, chromosomal location and promoter of human prostaglandin H synthase-2 gene. *Biochem Biophys Res Commun*, 203, 190 - 199.
- TEGEDER, I., NIEDERBERGER, E., ISRAR, E., GUHRING, H., BRUNE, K., EUCHENHOFER, C., GROSCH, S. & GEISSLINGER, G. 2001. Inhibition of NF-kappaB and AP-1 activation by R- and S-flurbiprofen. *FASEB J*, 15, 2 - 4.

- THATI, B., NOBLE, A., CREAVER, B. S., WALSH, M., MCCANN, M., KAVANAGH, K., DEVEREUX, M. & EGAN, D. A. 2007. A study of the role of apoptotic cell death and cell cycle events mediating the mechanism of action of 6-hydroxycoumarin-3-carboxylatesilver in human malignant hepatic cells. *Cancer Letters*, 250, 128-139.
- THOMAS, J., GEIGER, P., MAIORINO, M., URSINI, F. & GIROTTI, A. 1990a. Enzymatic reduction of phospholipid and cholesterol hydroperoxides in artificial bilayers and lipoproteins. *Biochem Biophys Acta*, 1045, 252-60.
- THOMAS, J. P., MAIORINO, M., URSINI, F. & GIROTTI, A. W. 1990b. Protective action of phospholipid hydroperoxide glutathione peroxidase against membrane-damaging lipid peroxidation. In situ reduction of phospholipid and cholesterol hydroperoxides. *Journal of Biological Chemistry*, 265, 454-61.
- THOMPSON, J. L., SEE, V. H. L., THOMAS, P. M. & SCHULLER, K. A. 2010. Cloning and characterization of two glutathione peroxidase cDNAs from southern bluefin tuna (*Thunnus maccoyii*). *Comparative Biochemistry and Physiology Part B: Biochemistry and Molecular Biology*, 156, 287-297.
- THOMPSON, K. M., HAIBACH, H., EVENSON, J. K. & SUNDE, R. A. 1998. Liver Selenium and Testis Phospholipid Hydroperoxide Glutathione Peroxidase Are Associated with Growth during Selenium Repletion of Second-Generation Se-Deficient Male Rats. *The Journal of Nutrition*, 128, 1289-1295.
- TIAN, Y., KELEMEN, S. E. & AUTIERI, M. V. 2006. Inhibition of AIF-1 expression by constitutive siRNA expression reduces macrophage migration, proliferation, and signal transduction initiated by atherogenic stimuli. *American Journal of Physiology - Cell Physiology*, 290, C1083-C1091.
- TIROSH, O., LEVY, E. & REIFEN, R. 2007. High selenium diet protects against TNBS-induced acute inflammation, mitochondrial dysfunction, and secondary necrosis in rat colon. *Nutrition*, 23, 878-886.
- TISSIER, R., CHENOUNE, M., PONS, S., ZINI, R., DARBERA, L., LIDOUREN, F., GHALEH, B., BERDEAUX, A. & MORIN, D. Mild hypothermia reduces per-ischemic reactive oxygen species production and preserves mitochondrial respiratory complexes. *Resuscitation*.
- TOULIS, K., ANASTASILAKIS, A., TZELLO, S. T., GOULIS, D. & KOUVELAS, D. 2010. Selenium supplementation in the treatment of Hashimoto's thyroiditis: a systematic review and a meta-analysis. *Thyroid*, 20, 1163-73.
- UDLER, M., MAIA, A.-T., CEBRIAN, A., BROWN, C., GREENBERG, D., SHAH, M., CALDAS, C., DUNNING, A., EASTON, D., PONDER, B. & PHAROAH, P. 2007. Common Germline Genetic Variation in Antioxidant Defense Genes and Survival After Diagnosis of Breast Cancer. *Journal of Clinical Oncology*, 25, 3015-3023.
- UETA, T., INOUE, T., FURUKAWA, T., TAMAKI, Y., NAKAGAWA, Y., IMAI, H. & YANAGI, Y. 2011. Glutathione Peroxidase 4 is Required for Maturation of Photoreceptor Cells. *Journal of Biological Chemistry*.
- UETA, T., INOUE, T., FURUKAWA, T., TAMAKI, Y., NAKAGAWA, Y., IMAI, H. & YANAGI, Y. 2012. Glutathione Peroxidase 4 Is Required for Maturation of Photoreceptor Cells. *Journal of Biological Chemistry*, 287, 7675-7682.
- UFER, C., WANG, C. C., FÄHLING, M., SCHIEBEL, H., THIELE, B. J., BILLETT, E. E., KUHN, H. & BORCHERT, A. 2008. Translational regulation of glutathione peroxidase 4 expression through guanine-rich sequence-binding factor 1 is essential for embryonic brain development. *Genes & Development*, 22, 1838-1850.
- UFER, C., WANG, C., BORCHERT, A., HEYDECK, D. & KUHN, H. 2010. Redox control in mammalian embryo development. *Antioxid Redox Signal*, 13, 833-75.
- UFER, C. & WANG, C. C. 2011. The roles of glutathione peroxidases during embryo development. *Frontiers in Molecular Neuroscience*, 4.

- UI-TEI, K. & SAIGO, K. 2004. Molecular mechanism of RNA interference and the selection of highly effective siRNA sequences. *Tanpakushitsu Kakusan Koso*, 49, 2662-70.
- UI-TEI, K., NAITO, Y. & SAIGO, K. 2006. Essential notes regarding the design of functional siRNAs for efficient mammalian RNAi. *J Biomed Biotechnol*, 2006, 65052.
- URSINI, F., MAIORINO, M. & C, G. 1985. The selenoenzyme phospholipid hydroperoxide glutathione peroxidase. *Biochem Biophys Acta*, 839, 62-70.
- URSINI, F., HEIM, S., KIESS, M., MAIORINO, M., ROVERI, A., WISSING, J. & FLOHÉ, L. 1999. Dual Function of the Selenoprotein PHGPx During Sperm Maturation. *Science*, 285, 1393-1396.
- USUI, S., OVESON, B. C., IWASE, T., LU, L., LEE, S. Y., JO, Y.-J., WU, Z., CHOI, E.-Y., SAMULSKI, R. J. & CAMPOCHIARO, P. A. 2011. Overexpression of SOD in retina: Need for increase in H₂O₂-detoxifying enzyme in same cellular compartment. *Free Radical Biology and Medicine*, 51, 1347-1354.
- VAHSEN N, C. C., BRIÈRE JJ, BÉNIT P, JOZA N, LAROCLETTE N, MASTROBERARDINO PG, PEQUIGNOT MO, CASARES N, LAZAR V, FERAUD O, DEBILI N, WISSING S, ENGELHARDT S, MADEO F, PIACENTINI M, PENNINGER JM, SCHÄGGER H, RUSTIN P, KROEMER G. 2004. AIF deficiency compromises oxidative phosphorylation. *EMBO J*, 23, 4679-89.
- VALASEK, M. A. & REPA, J. J. 2005. The power of real-time PCR. *Advances in Physiology Education*, 29, 151-159.
- VAN BLERKOM, J., DAVIS, P., MATHWIG, V. & ALEXANDER, S. 2002. Domains of high-polarized and low-polarized mitochondria may occur in mouse and human oocytes and early embryos. *Human Reproduction*, 17, 393-406.
- VAN DEN BOGERT, C., DEKKER, H. L., CORNELISSEN, J. C., VAN KUILENBURG, A. B. P., BOLHUIS, P. A. & MUIJSERS, A. O. 1992. Isoforms of cytochrome c oxidase in tissues and cell lines of the mouse. *Biochimica et Biophysica Acta (BBA) - Bioenergetics*, 1099, 118-122.
- VAN LAAR, V. S. & BERMAN, S. B. 2012. The interplay of neuronal mitochondrial dynamics and bioenergetics: Implications for Parkinson's disease. *Neurobiology of Disease*.
- VARECHA, M., AMRICOVA, J., ZIMMERMANN, M., ULMAN, V., LUKASOVA, E. & KOZUBEK, M. 2007. Bioinformatic and image analyses of the cellular localization of the apoptotic proteins endonuclease G, AIF, and AMID during apoptosis in human cells. *Apoptosis*, 12, 1155 - 1171.
- VIDYA PRIYADARSINI, R., SENTHIL MURUGAN, R., MAITREYI, S., RAMALINGAM, K., KARUNAGARAN, D. & NAGINI, S. 2010. The flavonoid quercetin induces cell cycle arrest and mitochondria-mediated apoptosis in human cervical cancer (HeLa) cells through p53 induction and NF- κ B inhibition. *European Journal of Pharmacology*, 649, 84-91.
- VILLETTE, S., KYLE, J. A. M., BROWN, K. M., PICKARD, K., MILNE, J. S., NICOL, F., ARTHUR, J. R. & HESKETH, J. E. 2002. A Novel Single Nucleotide Polymorphism in the 3' Untranslated Region of Human Glutathione Peroxidase 4 Influences Lipoxigenase Metabolism. *Blood Cells, Molecules, and Diseases*, 29, 174-178.
- VOETS, A. M., HUIGSLOOT, M., LINDSEY, P. J., LEENDERS, A. M., KOOPMAN, W. J. H., WILLEMS, P. H. G. M., RODENBURG, R. J., SMEITINK, J. A. M. & SMEETS, H. J. M. 2011. Transcriptional changes in OXPHOS complex I deficiency are related to anti-oxidant pathways and could explain the disturbed calcium homeostasis. *Biochimica et Biophysica Acta (BBA) - Molecular Basis of Disease*, 1822, 1161-8.
- VOGT, T. M., ZIEGLER, R. G., GRAUBARD, B. I., SWANSON, C. A., GREENBERG, R. S., SCHOENBERG, J. B., SWANSON, G. M., HAYES, R. B. & MAYNE, S. T. 2003. Serum selenium and risk of prostate cancer in U.S. blacks and whites. *International Journal of Cancer*, 103, 664-670.

- VOISINE, C., CRAIG, E. A., ZUFALL, N., VON AHSEN, O., PFANNER, N. & VOOS, W. 1999. The Protein Import Motor of Mitochondria: Unfolding and Trapping of Preproteins Are Distinct and Separable Functions of Matrix Hsp70. *Cell*, 97, 565-574.
- VOUDOURI, A., CHADIO, S., MENEGATOS, J., ZERVAS, G., NICOL, F. & ARTHUR, J. 2003. Selenoenzyme activities in selenium- and iodine-deficient sheep. *Biological Trace Element Research*, 94, 213-224.
- WALKER, J., SARASTE, M., RUNSWICK, M. & GAY, N. 1982. Distantly related sequences in the alpha- and beta-subunits of ATP synthase, myosin, kinases and other ATP-requiring enzymes and a common nucleotide binding fold. *EMBO J*, 1, 945-51.
- WALLACE, E., CALVIN, H. & COOPER, G. 1983a. Progressive defects observed in mouse sperm during the course of 3 generation of selenium deficiency. *Gamete Res*, 7, 377-384.
- WALLACE, E., COOPER, G. & CALVIN, H. 1983b. Effects of selenium deficiency of the shape and arrangement of rodent sperm mitochondria. *Gamete Res*, 7.
- WANG, G. Q., DAWSEY, S. M., LI, J. Y., TAYLOR, P. R., LI, B., BLOT, W. J., WEINSTEIN, W. M., LIU, F. S., LEWIN, K. J. & WANG, H. 1994. Effects of vitamin/mineral supplementation on the prevalence of histological dysplasia and early cancer of the esophagus and stomach: results from the General Population Trial in Linxian, China. *Cancer Epidemiology Biomarkers & Prevention*, 3, 161-166.
- WANG, H. P., QIAN, S. Y., SCHAFER, F. Q., DOMANN, F. E., OBERLEY, L. W. & BUETTNER, G. R. 2001. Phospholipid hydroperoxide glutathione peroxidase protects against singlet oxygen-induced cell damage of photodynamic therapy. *Free Radical Biology and Medicine*, 30, 825-835.
- WANG, L., LIU, L., SHI, Y., CAO, H., CHATURVEDI, R., CALCUTT, M. W., HU, T., REN, X., WILSON, K. T., POLK, D. B. & YAN, F. 2012. Berberine Induces Caspase-Independent Cell Death in Colon Tumor Cells through Activation of Apoptosis-Inducing Factor. *PLoS ONE*, 7, e36418.
- WANG, X., YANG, C., CHAI, J., SHI, Y. & XUE, D. 2002. Mechanisms of AIF-mediated apoptotic DNA degradation in *Caenorhabditis elegans*. *Science*, 298, 1587 - 1592.
- WANI, W. Y., GUDUP, S., SUNKARIA, A., BAL, A., SINGH, P. P., KANDIMALLA, R. J. L., SHARMA, D. R. & GILL, K. D. 2011. Protective efficacy of mitochondrial targeted antioxidant MitoQ against dichlorvos induced oxidative stress and cell death in rat brain. *Neuropharmacology*, 61, 1193-1201.
- WEGNER, M., HELFTENBEIN, E., MULLER, F., MEINECKE, M., MULLER, S. & GRUMMT, F. 1989. Identification of an amplification promoting DNA sequence from the hypotrichous ciliate *Stylonychia lemnae*. *Nucleic Acids Res*, 17, 8783 - 8802.
- WEIR, C. P. & ROBAIRE, B. 2007. Spermatozoa Have Decreased Antioxidant Enzymatic Capacity and Increased Reactive Oxygen Species Production During Aging in the Brown Norway Rat. *J Androl*, 28, 229-240.
- WEISS, S.S. & SUNDE R.A. 2001. Selenium regulation of transcript abundance and translational efficiency of glutathione peroxidase-1 and -4 in rat liver. *Biochem. J.*, 357, 851-858.
- WELLMANN, H., KALTSCHMIDT, B. & KALTSCHMIDT, C. 2001. Retrograde transport of transcription factor NF-kappaB in living neurons. *J Biol Chem*, 276, 11821 - 11829.
- WEN, Z. & FIOCCHI, C. 2004. Inflammatory Bowel Disease: Autoimmune or Immune-mediated Pathogenesis? *Clin Dev Immunol*, 195-204.
- WHANGE, R. P. 2004. Selenium and its relationship to cancer: an update. *Br J Nutr*, 11-28.
- WHITEMAN M, S. J., SZETO HH, ARMSTRONG JS. 2008. Do mitochondriotropic antioxidants prevent chlorinative stress-induced mitochondrial and cellular injury? *Antioxid Redox Signal*, 10, 641-50.

- WIDLAK, P., LI, L. Y., WANG, X. & GARRARD, W. T. 2001. Action of recombinant human apoptotic endonuclease G on naked DNA and chromatin substrates: cooperation with exonuclease and DNase I. *J Biol Chem*, 276, 48404 - 48409.
- WIERENGA, R. K., TERPSTRA, P. & HOL, W. G. J. 1986. Prediction of the occurrence of the ADP-binding $\beta\alpha\beta$ -fold in proteins, using an amino acid sequence fingerprint. *Journal of Molecular Biology*, 187, 101-107.
- WILDING, J. R., JOUBERT, F., DE ARAUJO, C., FORTIN, D., NOVOTOVA, M., VEKSLER, V. & VENTURA-CLAPIER, R. 2006. Altered energy transfer from mitochondria to sarcoplasmic reticulum after cytoarchitectural perturbations in mice hearts. *The Journal of Physiology*, 575, 191-200.
- WILLET, T. W., POLK, B., MORRIS, J., STAMPFER, M., PRESSE, L. S., ROSNER, B., TAYLOR, J., SCHNEIDE, R. K. & HAMES, C. 1983. Prediagnostic serum selenium and risk of cancer. *Lancet*, 130-4.
- WINGER, A. M., MILLAR, A. H. & DAY, D. A. 2005. Sensitivity of plant mitochondrial terminal oxidases to the lipid peroxidation product 4-hydroxy-2-nonenal (HNE). *Biochem. J.*, 387, 865-870.
- WINGLER, K., BÖCHER, M., FLOHÉ, L., KOLLMUS, H. & BRIGELIUS-FLOHÉ, R. 1999. mRNA stability and selenocysteine insertion sequence efficiency rank gastrointestinal glutathione peroxidase high in the hierarchy of selenoproteins. *European Journal of Biochemistry*, 259, 149-157.
- WOLTER, K. G., HSU, Y.-T., SMITH, C. L., NECHUSHTAN, A., XI, X.-G. & YOULE, R. J. 1997. Movement of Bax from the Cytosol to Mitochondria during Apoptosis. *The Journal of Cell Biology*, 139, 1281-1292.
- XIAO D, Z. L. 2008. Upregulation of Bax and Bcl-2 following prenatal cocaine exposure induces apoptosis in fetal rat brain. *Int J Med Sci*, 5, 295-302.
- XU, J. D., CAO, X. X., LONG, Z. W., LIU, X. P., FURUYA, T., XU, J. W., LIU, X. L., DE XU, Z., SASAKI, K. & LI, Q. Q. 2011. BCL2L10 protein regulates apoptosis/proliferation through differential pathways in gastric cancer cells. *The Journal of Pathology*, 223, 400-409.
- XU, X.-M., CARLSON, B. A., MIX, H., ZHANG, Y., SAIRA, K., GLASS, R. S., BERRY, M. J., GLADYSHEV, V. N. & HATFIELD, D. L. 2006. Biosynthesis of Selenocysteine on Its tRNA in Eukaryotes. *PLoS Biol*, 5, e4.
- YAGI, K., KOMURA, S., KOJIMA, H., SUN, Q., NAGATA, N., OHISHI, N. & NISHIKIMI, M. 1996. Expression of human phospholipid hydroperoxide glutathione peroxidase gene for protection of host cells from lipid hydroperoxide-mediated injury. *Biochem Biophys Res Commun*, 219, 486-91.
- YAGUBLU, V., ARTHUR, J. R., BABAYEVA, S. N., NICOL, F., POST, S. & KEESE, M. 2011. Expression of Selenium-containing Proteins in Human Colon Carcinoma Tissue. *Anticancer Research*, 31, 2693-2698.
- YAMAGATA, K., ANDREASSON, K. I., KAUFMANN, W. E., BARNES, C. A. & WORLEY, P. F. 1993. Expression of a mitogen-inducible cyclooxygenase in brain neurons: regulation by synaptic activity and glucocorticoids. *Neuron*, 11, 371 - 386.
- YAMAMOTO, S., NISHIMURA, M., CONNERS, M. S., STOLTZ, R. A., FALCK, J. R., CHAUHAN, K. & LANIADO-SCHWARTZMAN, M. 1994. Oxidation and keto reduction of 12-hydroxy-5,8,10,14-eicosatetraenoic acids in bovine corneal epithelial microsomes. *Biochimica et Biophysica Acta (BBA) - Lipids and Lipid Metabolism*, 1210, 217-225.
- YAMAOKA, S., COURTOIS, G., BESSIA, C., WHITESIDE, S. T., WEIL, R., AGOU, F., KIRK, H. E., KAY, R. J. & ISRAEL, A. 1998. Complementation cloning of NEMO, a component of the I κ B kinase complex essential for NF- κ B activation. *Cell*, 93, 1231 - 1240.

- YANG, F., CHEN, W., DENG, R., LI, D., WU, K., FENG, G., LI, H. & ZHU, X. 2012. Hirsutanol A Induces Apoptosis and Autophagy via Reactive Oxygen Species Accumulation in Breast Cancer MCF-7 Cells. *J Pharmacol*, 119, 214-20.
- YANG, X.-F., WEBER, G. F. & CANTOR, H. 1997. A Novel Bcl-x Isoform Connected to the T Cell Receptor Regulates Apoptosis in T Cells. *Immunity*, 7, 629-639.
- YANT, L. J., RAN, Q., RAO, L., VAN REMMEN, H., SHIBATANI, T., BELTER, J. G., MOTTA, L., RICHARDSON, A. & PROLLA, T. A. 2003. The selenoprotein GPX4 is essential for mouse development and protects from radiation and oxidative damage insults. *Free Radical Biology and Medicine*, 34, 496-502.
- YE, H., CANDE, C., STEPHANOU, N. C., JIANG, S., GURBUXANI, S., LAROCLETTE, N., DAUGAS, E., GARRIDO, C., KROEMER, G. & WU, H. 2002. DNA binding is required for the apoptogenic action of apoptosis inducing factor. *Nat Struct Biol*, 9, 680 - 684.
- YIN, M. J., YAMAMOTO, Y. & GAYNOR, R. B. 1998. The anti-inflammatory agents aspirin and salicylate inhibit the activity of IkappaB kinase-beta. *Nature*, 396, 77 - 80.
- YOO, M., GU, X., XU, X., KIM, J., CARLSON, B., PATTERSON, A., CAI, H., GLADYSHEV, V. N. & HATFIELD, D. L. 2010. Delineating the role of glutathione peroxidase 4 in protecting cells against lipid hydroperoxide damage and in Alzheimer's disease. *Antioxid Redox Signal*, 12, 819-27.
- YOO, S.-E., CHEN, L., NA, R., LIU, Y., RIOS, C., VAN REMMEN, H., RICHARDSON, A. & RAN, Q. 2012. Gpx4 ablation in adult mice results in a lethal phenotype accompanied by neuronal loss in brain. *Free Radical Biology and Medicine*, 52, 1820-1827.
- YU, C. J., JIA, L. T., MENG, Y. L., ZHAO, J., ZHANG, Y., QIU, X. C., XU, Y. M., WEN, W. H., YAO, L. B., FAN, D. M., JIN, B. Q., CHEN, S. Y. & YANG, A. G. 2005. Selective proapoptotic activity of a secreted recombinant antibody//AIF fusion protein in carcinomas overexpressing HER2. *Gene Ther*, 13, 313-320.
- YU, L. & GOROVSKY, M. A. 1997. Constitutive expression, not a particular primary sequence, is the important feature of the H3 replacement variant hv2 in *Tetrahymena thermophila*. *Mol Cell Biol*, 17, 6303 - 6310.
- YU, S. W., WANG, H., POITRAS, M. F., COOMBS, C., BOWERS, W. J., FEDEROFF, H. J., POIRIER, G. G., DAWSON, T. M. & DAWSON, V. L. 2002. Mediation of poly (ADP-ribose) polymerase-1-dependent cell death by apoptosis-inducing factor. *Science*, 297, 259 - 263.
- YU, Z., ZHOU, D., CHENG, G. & MATTSO, M. P. 2000. Neuroprotective role for the p50 subunit of NF-kappaB in an experimental model of Huntington's disease. *J Mol Neurosci*, 15, 31 - 44.
- YUAN, C.-Q., LI, Y.-N. & ZHANG, X.-F. 2004. Down-regulation of apoptosis-inducing factor protein by RNA interference inhibits UVA-induced cell death. *Biochemical and Biophysical Research Communications*, 317, 1108-1113.
- YUAN, J., SHAHAM, S., LEDOUX, S., ELLIS, H. M. & HORVITZ, H. R. 1993. The *C. elegans* cell death gene *ced-3* encodes a protein similar to mammalian interleukin-1 beta-converting enzyme. *Cell*, 75, 641 - 652.
- ZAFIRIOU, M. P., DEVA, R., CICCOLI, R., SIAFAKA-KAPADAI, A. & NIGAM, S. 2007. Biological role of hepxilins: Upregulation of phospholipid hydroperoxide glutathione peroxidase as a cellular response to oxidative stress? *Prostaglandins, Leukotrienes and Essential Fatty Acids*, 77, 209-215.
- ZANDI, E., CHEN, Y. & KARIN, M. 1998. Direct phosphorylation of IkappaB by IKKalpha and IKKbeta: discrimination between free and NF-kappaB-bound substrate. *Science*, 281, 1360 - 1363.
- ZANGGER, H., MOTTRAM, J. C. & FASEL, N. 2002. Cell death in *Leishmania* induced by stress and differentiation: programmed cell death or necrosis? *Cell Death Differ*, 9, 1126 - 1139.

- ZHANG, J., PENG, W. D., HUI, H. X., JIN, M., WANG, D. N., WANG, C. J. & QIAN, H. W. 1999. Inducible Expression of bcl-2 Antisense RNA Promotes Apoptosis of Human Gastric Cancer Cell Line. *Sheng Wu Hua Xue Yu Sheng Wu Wu Li Xue Bao (Shanghai)*, 31, 278-283.
- ZHANG, K. & KAUFMAN, R. J. 2008. From endoplasmic-reticulum stress to the inflammatory response. *Nature*, 454, 455-462.
- ZHANG, Y. & CHEN, X. 2010. Selenoproteins and the aging brain. *Mech Ageing Dev*, 131, 253-60.
- ZHANG, Y.-B., YE, Y.-P., WU, X.-D. & SUN, H.-X. 2009. Astilbotriterpenic Acid Induces Growth Arrest and Apoptosis in HeLa Cells through Mitochondria-Related Pathways and Reactive Oxygen Species (ROS) Production. *Chemistry & Biodiversity*, 6, 218-230.
- ZHAO, L., WANG, H. P., ZHANG, H. J., WEYDERT, C. J., DOMANN, F. E., OBERLEY, L. W. & BUETTNER, G. R. 2003. L-PhGPx expression can be suppressed by antisense oligodeoxynucleotides. *Archives of Biochemistry and Biophysics*, 417, 212-218.
- ZHI, L., USTYUGOVA, I. V., CHEN, X., ZHANG, Q. & WU, M. X. 2012. Enhanced Th17 Differentiation and Aggravated Arthritis in IEX-1-Deficient Mice by Mitochondrial Reactive Oxygen Species-Mediated Signaling. *The Journal of Immunology*, 189, 1639-1647.
- ZHOU, J.-C., ZHAO, H., LI, J.-G., XIA, X.-J., WANG, K.-N., ZHANG, Y.-J., LIU, Y., ZHAO, Y. & LEI, X. G. 2009. Selenoprotein Gene Expression in Thyroid and Pituitary of Young Pigs Is Not Affected by Dietary Selenium Deficiency or Excess. *The Journal of Nutrition*, 139, 1061-1066.
- ZHU, C., WANG, X., DEINUM, J., HUANG, Z., GAO, J., MODJTAHEDI, N., NEAGU, M. R., NILSSON, M., ERIKSSON, P. S., HAGBERG, H., LUBAN, J., KROEMER, G. & BLOMGREN, K. 2007. Cyclophilin A participates in the nuclear translocation of apoptosis-inducing factor in neurons after cerebral hypoxia-ischemia. *The Journal of Experimental Medicine*, 204, 1741-1748.
- ZOIDIS, E., PAPPAS, A. C., GEORGIU, C. A., KOMAITIS, E. & FEGGEROS, K. 2010. Selenium affects the expression of GPx4 and catalase in the liver of chicken. *Comparative Biochemistry and Physiology Part B: Biochemistry and Molecular Biology*, 155, 294-300.
- ZOU, H., HENZEL, W. J., LIU, X., LUTSCHG, A. & WANG, X. 1997. Apaf-1, a Human Protein Homologous to *C. elegans* CED-4, Participates in Cytochrome c-Dependent Activation of Caspase-3. *Cell*, 90, 405-413.

Appendix A1 : List of genes of which expression were up-regulated

FOLD CHANGE	PROBE ID	REGULATION	SYMBOL	ENTREZ GENE NAME	P.VALUE	RP/SUM	PFP
1.395	10347	UP	ABCA7	ATP-binding cassette, sub-family A (ABC1), member 7	1.00E-04	6.8987	9.00E-04
1.276	22985	UP	ACIN1	apoptotic chromatin condensation inducer 1	1.00E-04	17.2908	9.00E-04
1.231	123	UP	ADFP	adipose differentiation-related protein	1.00E-04	18.0271	9.00E-04
1.303	11047	UP	ADRM1	adhesion regulating molecule 1	1.00E-04	50.6873	9.00E-04
1.216	10598	UP	AHSA1	AHA1, activator of heat shock 90kDa protein ATPase homolog 1 (yeast)	1.00E-04	56.39	9.00E-04
1.379	23600	UP	AMACR	alpha-methylacyl-CoA racemase	1.00E-04	73.4084	8.00E-04
1.718	336	UP	APOA2	apolipoprotein A-II	1.00E-04	75.2338	0.0011
1.307	381	UP	ARF5	ADP-ribosylation factor 5	1.00E-04	80.7635	0.001
1.292	402	UP	ARL2	ADP-ribosylation factor-like 2	1.00E-04	80.9704	0.001
1.305	10124	UP	ARL4A	ADP-ribosylation factor-like 4A	1.00E-04	91.5363	0.001
1.217	10094	UP	ARPC3	actin related protein 2/3 complex, subunit 3, 21kDa	1.00E-04	97.2508	0.0011
1.506	430	UP	ASCL2	achaete-scute complex homolog 2 (Drosophila)	1.00E-04	97.6242	0.0011
1.573	467	UP	ATF3	activating transcription factor 3	1.00E-04	101.8706	0.0012
1.23	64422	UP	ATG3	ATG3 autophagy related 3 homolog (S. cerevisiae)	1.00E-04	104.9955	0.0012
1.339	475	UP	ATOX1	ATX1 antioxidant protein 1 homolog (yeast)	1.00E-04	106.3461	0.0012
1.582	516	UP	ATP5G1	ATP synthase, H+ transporting, mitochondrial F0 complex, subunit C1 (subunit 9)	1.00E-04	110.6685	0.0012
1.498	517	UP	ATP5G2	ATP synthase, H+ transporting, mitochondrial F0 complex, subunit C2 (subunit 9)	1.00E-04	111.9969	0.0012
1.336	10476	UP	ATP5H (includes EG:10476)	ATP synthase, H+ transporting, mitochondrial F0 complex, subunit d	1.00E-04	127.8549	0.0012
1.717	521	UP	ATP5I	ATP synthase, H+ transporting, mitochondrial F0 complex, subunit E	1.00E-04	128.2946	0.0012
1.385	522	UP	ATP5J	ATP synthase, H+ transporting, mitochondrial F0 complex, subunit F6	1.00E-04	148.0875	0.0012
1.472	9551	UP	ATP5J2	ATP synthase, H+ transporting, mitochondrial F0 complex, subunit F2	1.00E-04	167.0592	0.0012
1.39	10632	UP	ATP5L	ATP synthase, H+ transporting, mitochondrial F0 complex, subunit G	1.00E-04	167.1144	0.0012
1.489	8313	UP	AXIN2	axin 2	1.00E-04	170.7812	0.0012
1.623	25805	UP	BAMBI	BMP and activin membrane-bound inhibitor homolog (Xenopus laevis)	1.00E-04	180.3614	0.0014
1.497	8815	UP	BANF1	barrier to autointegration factor 1	1.00E-04	183.2308	0.0014
1.387	581	UP	BAX	BCL2-associated X protein	1.00E-04	190.2291	0.0014
1.226	56647	UP	BCCIP	BRCA2 and CDKN1A interacting protein	1.00E-04	191.0652	0.0014
1.207	633	UP	BGN	biglycan	1.00E-04	197.3306	0.0014
1.265	8553	UP	BHLHE40	basic helix-loop-helix family, member e40	1.00E-04	201.1657	0.0014
1.317	652	UP	BMP4	bone morphogenetic protein 4	1.00E-04	202.2411	0.0014
1.769	552900	UP	BOLA2	bolA homolog 2 (E. coli)	1.00E-04	218.8481	0.0013
1.596	388962	UP	BOLA3	bolA homolog 3 (E. coli)	1.00E-04	220.9539	0.0014
1.212	9577	UP	BRE	brain and reproductive organ-expressed (TNFRSF1A modulator)	1.00E-04	231.6802	0.0015
1.394	25798	UP	BRI3	brain protein I3	1.00E-04	233.448	0.0016
1.293	684	UP	BST2	bone marrow stromal cell antigen 2	1.00E-04	240.5581	0.0017
1.288	84154	UP	BXDC1	brix domain containing 1	1.00E-04	242.2872	0.0017
1.549	746	UP	C11ORF10	chromosome 11 open reading frame 10	1.00E-04	245.8365	0.0017
1.379	79081	UP	C11ORF48	chromosome 11 open reading frame 48	1.00E-04	246.2932	0.0019
1.449	28984	UP	C13ORF15	chromosome 13 open reading frame 15	1.00E-04	248.0156	0.0023

1.635	81892	UP	C14ORF156	chromosome 14 open reading frame 156	1.00E-04	256.738	0.0023
1.404	145853	UP	C15ORF61	chromosome 15 open reading frame 61	1.00E-04	257.405	0.0023
1.338	55009	UP	C19ORF24	chromosome 19 open reading frame 24	1.00E-04	258.9334	0.0022
1.377	163183	UP	C19ORF46	chromosome 19 open reading frame 46	1.00E-04	260.6572	0.0023
1.397	125988	UP	C19ORF70	chromosome 19 open reading frame 70	1.00E-04	262.423	0.0024
1.269	708	UP	C1QBP	complement component 1, q subcomponent binding protein	1.00E-04	262.8811	0.0026
1.272	84319	UP	C3ORF26	chromosome 3 open reading frame 26	1.00E-04	266.4045	0.0026
1.425	114915	UP	C5ORF26	chromosome 5 open reading frame 26	1.00E-04	277.7207	0.0026
1.284	84300	UP	C6ORF125	chromosome 6 open reading frame 125	1.00E-04	279.4649	0.0026
1.39	387103	UP	C6ORF173	chromosome 6 open reading frame 173	1.00E-04	286.775	0.0026
1.291	84310	UP	C7ORF50	chromosome 7 open reading frame 50	1.00E-04	290.4644	0.0025
1.318	401466	UP	C8ORF59	chromosome 8 open reading frame 59	1.00E-04	297.3441	0.0025
1.366	375757	UP	C9ORF119	chromosome 9 open reading frame 119	1.00E-04	298.4375	0.0029
1.24	55450	UP	CAMK2N1	calcium/calmodulin-dependent protein kinase II inhibitor 1	1.00E-04	306.86	0.0031
1.255	826	UP	CAPNS1	calpain, small subunit 1	1.00E-04	306.8793	0.0031
1.29	865	UP	CBFB	core-binding factor, beta subunit	1.00E-04	313.2691	0.0032
1.321	131076	UP	CCDC58	coiled-coil domain containing 58	1.00E-04	313.6573	0.0031
1.272	29080	UP	CCDC59	coiled-coil domain containing 59	1.00E-04	327.4419	0.0032
1.385	51372	UP	CCDC72	coiled-coil domain containing 72	1.00E-04	331.3861	0.0032
1.292	79080	UP	CCDC86	coiled-coil domain containing 86	1.00E-04	332.5706	0.0032
1.203	898	UP	CCNE1	cyclin E1	1.00E-04	337.4269	0.0038
1.232	908	UP	CCT6A	chaperonin containing TCP1, subunit 6A (zeta 1)	1.00E-04	343.7884	0.0039
1.279	993	UP	CDC25A	cell division cycle 25 homolog A (S. pombe)	1.00E-04	343.9013	0.004
1.22	1027	UP	CDKN1B	cyclin-dependent kinase inhibitor 1B (p27, Kip1)	1.00E-04	345.8174	0.004
1.214	634	UP	CEACAM1	carcinoembryonic antigen-related cell adhesion molecule 1 (biliary glycoprotein)	1.00E-04	347.1911	0.0041
1.365	4680	UP	CEACAM6 (includes EG:4680)	carcinoembryonic antigen-related cell adhesion molecule 6 (non-specific cross reacting antigen)	1.00E-04	347.3339	0.004
1.427	400916	UP	CHCHD10	coiled-coil-helix-coiled-coil-helix domain containing 10	1.00E-04	362.6719	0.0043
1.464	55847	UP	CISD1	CDGSH iron sulfur domain 1	1.00E-04	382.1312	0.005
1.425	51192	UP	CKLF	chemokine-like factor	1.00E-04	383.8655	0.005
1.364	1163	UP	CKS1B	CDC28 protein kinase regulatory subunit 1B	1.00E-04	386.128	0.0054
1.696	1281	UP	COL3A1	collagen, type III, alpha 1	1.00E-04	388.1599	0.0054
1.372	51241	UP	COX16	COX16 cytochrome c oxidase assembly homolog (S. cerevisiae)	2.00E-04	388.7678	0.0054
1.508	10063	UP	COX17	COX17 cytochrome c oxidase assembly homolog (S. cerevisiae)	2.00E-04	389.922	0.0058
1.243	9377	UP	COX5A	cytochrome c oxidase subunit Va	2.00E-04	392.7933	0.0061
1.354	1337	UP	COX6A1	cytochrome c oxidase subunit VIa polypeptide 1	2.00E-04	399.9263	0.0062
1.392	1340	UP	COX6B1	cytochrome c oxidase subunit VIb polypeptide 1 (ubiquitous)	2.00E-04	400.7022	0.0062
1.403	1347	UP	COX7A2	cytochrome c oxidase subunit VIIa polypeptide 2 (liver)	2.00E-04	403.2707	0.0062
1.506	1351	UP	COX8A	cytochrome c oxidase subunit 8A (ubiquitous)	2.00E-04	404.4191	0.0062
1.465	1382	UP	CRABP2	cellular retinoic acid binding protein 2	2.00E-04	408.4344	0.0066
1.364	92359	UP	CRB3	crumbs homolog 3 (Drosophila)	2.00E-04	409.1106	0.0067
1.741	1469	UP	CST1	cystatin SN	2.00E-04	413.7525	0.0069
1.4	1476	UP	CSTB	cystatin B (stefin B)	2.00E-04	423.8551	0.0071
1.314	1622	UP	DBI	diazepam binding inhibitor (GABA receptor modulator, acyl-Coenzyme A binding protein)	2.00E-04	431.3047	0.007
1.251	84259	UP	DCUN1D5	DCN1, defective in cullin neddylation 1, domain containing 5 (S. cerevisiae)	2.00E-04	433.7799	0.0071

1.406	1649	UP	DDIT3	DNA-damage-inducible transcript 3	2.00E-04	434.3888	0.0071
1.374	1652	UP	DDT	D-dopachrome tautomerase	2.00E-04	435.857	0.0072
1.274	9188	UP	DDX21	DEAD (Asp-Glu-Ala-Asp) box polypeptide 21	2.00E-04	438.4136	0.0072
1.326	1716	UP	DGUOK	deoxyguanosine kinase	2.00E-04	439.7845	0.0072
1.205	54505	UP	DHX29	DEAH (Asp-Glu-Ala-His) box polypeptide 29	2.00E-04	442.7527	0.0072
1.236	1660	UP	DHX9	DEAH (Asp-Glu-Ala-His) box polypeptide 9	2.00E-04	444.4709	0.0073
1.202	1736	UP	DKC1	dyskeratosis congenita 1, dyskerin	2.00E-04	446.4573	0.0073
1.331	22943	UP	DKK1	dickkopf homolog 1 (<i>Xenopus laevis</i>)	2.00E-04	449.4813	0.0073
1.327	84661	UP	DPY30	dpy-30 homolog (<i>C. elegans</i>)	2.00E-04	450.2332	0.0073
1.328	8655	UP	DYNLL1	dynein, light chain, LC8-type 1	2.00E-04	451.6256	0.0073
1.381	83658	UP	DYNLRB1	dynein, light chain, roadblock-type 1	2.00E-04	456.6785	0.0074
1.213	10969	UP	EBNA1BP2	EBNA1 binding protein 2	2.00E-04	459.4885	0.0074
1.42	9718	UP	ECE2	endothelin converting enzyme 2	2.00E-04	460.7188	0.0073
1.343	8721	UP	EDF1	endothelial differentiation-related factor 1	2.00E-04	462.9098	0.0073
1.291	1933	UP	EEF1B2	eukaryotic translation elongation factor 1 beta 2	2.00E-04	464.0912	0.0074
1.204	1948	UP	EFNB2	ephrin-B2	2.00E-04	464.3649	0.0075
1.419	1958	UP	EGR1	early growth response 1	2.00E-04	465.9492	0.0079
1.231	1981	UP	EIF4G1	eukaryotic translation initiation factor 4 gamma, 1	3.00E-04	469.4701	0.0079
1.21	1982	UP	EIF4G2	eukaryotic translation initiation factor 4 gamma, 2	3.00E-04	473.6155	0.0081
1.288	1983	UP	EIF5	eukaryotic translation initiation factor 5	3.00E-04	473.9116	0.0082
1.282	3692	UP	EIF6	eukaryotic translation initiation factor 6	3.00E-04	478.562	0.0082
1.386	10436	UP	EMG1	EMG1 nucleolar protein homolog (<i>S. cerevisiae</i>)	3.00E-04	489.2744	0.0082
1.329	2077	UP	ERF	Ets2 repressor factor	3.00E-04	493.6935	0.0082
1.207	10961	UP	ERP29	endoplasmic reticulum protein 29	3.00E-04	495.4011	0.0084
1.28	2114	UP	ETS2	v-ets erythroblastosis virus E26 oncogene homolog 2 (avian)	3.00E-04	504.3943	0.0083
1.298	51013	UP	EXOSC1	exosome component 1	3.00E-04	512.5037	0.0085
1.38	26071	UP	FAM127B	family with sequence similarity 127, member B	3.00E-04	513.111	0.0086
1.367	2197	UP	FAU	Finkel-Biskis-Reilly murine sarcoma virus (FBR-MuSV) ubiquitously expressed	3.00E-04	513.2056	0.0085
1.39	51024	UP	FIS1	fission 1 (mitochondrial outer membrane) homolog (<i>S. cerevisiae</i>)	3.00E-04	517.0463	0.0085
1.211	51303	UP	FKBP11	FK506 binding protein 11, 19 kDa	3.00E-04	519.0091	0.0085
1.358	2280	UP	FKBP1A	FK506 binding protein 1A, 12kDa	3.00E-04	521.866	0.0084
1.289	2288	UP	FKBP4	FK506 binding protein 4, 59kDa	3.00E-04	522.2852	0.0084
1.264	8087	UP	FXR1	fragile X mental retardation, autosomal homolog 1	3.00E-04	529.2431	0.0086
1.899	51083	UP	GAL	galanin prepropeptide	3.00E-04	529.8449	0.0086
1.387	54433	UP	GAR1	GAR1 ribonucleoprotein homolog (yeast)	3.00E-04	533.0673	0.009
1.275	54552	UP	GNL3L (includes EG:54552)	guanine nucleotide binding protein-like 3 (nucleolar)-like	3.00E-04	537.2724	0.009
1.239	2821	UP	GPI	glucose phosphate isomerase	3.00E-04	538.5022	0.009
1.997	2876	UP	GPX1	glutathione peroxidase 1	3.00E-04	552.1627	0.009
1.37	404672	UP	GTF2H5	general transcription factor IIH, polypeptide 5	3.00E-04	557.9946	0.0089
1.214	2971	UP	GTF3A	general transcription factor IIIA	3.00E-04	558.0776	0.009
1.372	10542	UP	HBXIP	hepatitis B virus x interacting protein	3.00E-04	558.4924	0.009
1.523	650646	UP	HCG 2033311	ribosomal protein S26 pseudogene 15	3.00E-04	558.9583	0.009
1.291	3094	UP	HINT1	histidine triad nucleotide binding protein 1	3.00E-04	563.006	0.0091
1.38	85236	UP	HIST1H2BK	histone cluster 1, H2bk	3.00E-04	565.5634	0.0091

1.453	8364	UP	HIST1H4C	histone cluster 1, H4c	3.00E-04	571.8632	0.0095
1.21	81502	UP	HM13	histocompatibility (minor) 13	3.00E-04	573.9724	0.0095
1.322	3159	UP	HMG1	high mobility group AT-hook 1	3.00E-04	576.0082	0.0095
1.259	3182	UP	HNRNPAB	heterogeneous nuclear ribonucleoprotein A/B	4.00E-04	577.062	0.0096
1.493	3218	UP	HOXB8	homeobox B8	4.00E-04	577.1509	0.0096
1.294	3320	UP	HSP90AA1	heat shock protein 90kDa alpha (cytosolic), class A member 1	4.00E-04	586.1633	0.0095
1.328	51504	UP	HSPC152	hypothetical protein HSPC152	4.00E-04	586.7796	0.0096
1.429	3336	UP	HSPE1	heat shock 10kDa protein 1 (chaperonin 10)	4.00E-04	594.7471	0.0096
1.613	3397	UP	ID1	inhibitor of DNA binding 1, dominant negative helix-loop-helix protein	4.00E-04	597.3071	0.0097
1.596	3399	UP	ID3	inhibitor of DNA binding 3, dominant negative helix-loop-helix protein	4.00E-04	603.0025	0.0102
1.411	2537	UP	IFI6	interferon, alpha-inducible protein 6	4.00E-04	604.1088	0.0101
1.371	3481	UP	IGF2	insulin-like growth factor 2 (somatomedin A)	4.00E-04	605.96	0.0103
1.892	3484	UP	IGFBP1	insulin-like growth factor binding protein 1	4.00E-04	610.8075	0.0105
1.328	3487	UP	IGFBP4	insulin-like growth factor binding protein 4	4.00E-04	617.0922	0.0106
1.619	147920	UP	IGFL2	IGF-like family member 2	4.00E-04	623.0137	0.0106
1.276	79711	UP	IPO4	importin 4	4.00E-04	623.7442	0.0106
1.387	10265	UP	IRX5	iroquois homeobox 5	4.00E-04	624.0803	0.0105
1.496	3725	UP	JUN	jun oncogene	4.00E-04	624.6687	0.0111
1.292	23277	UP	KIAA0664	KIAA0664	4.00E-04	629.4972	0.0112
1.304	200185	UP	KRTCAP2	keratinocyte associated protein 2	4.00E-04	630.1046	0.0117
1.386	8270	UP	LAGE3	L antigen family, member 3	4.00E-04	634.5545	0.0117
1.254	3936	UP	LCP1	lymphocyte cytosolic protein 1 (L-plastin)	4.00E-04	637.6802	0.012
1.503	51176	UP	LEF1	lymphoid enhancer-binding factor 1	4.00E-04	638.3155	0.0128
1.34	3955	UP	LFNG	LFNG O-fucosylpeptide 3-beta-N-acetylglucosaminyltransferase	4.00E-04	641.1095	0.0134
1.383	56891	UP	LGALS14	lectin, galactoside-binding, soluble, 14	4.00E-04	645.6671	0.0138
1.264	3957	UP	LGALS2	lectin, galactoside-binding, soluble, 2	4.00E-04	646.369	0.0142
1.227	389421	UP	LIN28B	lin-28 homolog B (C. elegans)	4.00E-04	647.1977	0.0144
1.341	127295	UP	LOC127295	ribosomal protein L36 pseudogene 5	4.00E-04	648.8884	0.0149
1.233	283412	UP	LOC283412	ribosomal protein L29 pseudogene 12	5.00E-04	649.7014	0.015
1.415	441377	UP	LOC441377	ribosomal protein S26 pseudogene 35	5.00E-04	650.8293	0.0151
1.339	644844	UP	LOC644844	hypothetical protein LOC644844	5.00E-04	652.3817	0.0151
1.679	644934	UP	LOC644934	ribosomal protein S26 pseudogene 50	5.00E-04	652.4835	0.0151
1.251	652595	UP	LOC652595	similar to U2 small nuclear ribonucleoprotein A (U2 snRNP-A)	5.00E-04	652.5103	0.0151
1.202	9361	UP	LONP1	lon peptidase 1, mitochondrial	5.00E-04	656.9767	0.0155
1.431	27258	UP	LSM3	LSM3 homolog, U6 small nuclear RNA associated (S. cerevisiae)	5.00E-04	657.3352	0.0159
1.26	23658	UP	LSM5	LSM5 homolog, U6 small nuclear RNA associated (S. cerevisiae)	5.00E-04	660.3926	0.0159
1.443	51690	UP	LSM7	LSM7 homolog, U6 small nuclear RNA associated (S. cerevisiae)	5.00E-04	663.8365	0.0162
1.203	4074	UP	M6PR	mannose-6-phosphate receptor (cation dependent)	5.00E-04	664.6181	0.0161
1.346	51025	UP	MAGMAS	mitochondria-associated protein involved in granulocyte-macrophage colony-stimulating factor signal transduction	5.00E-04	668.6934	0.0161
1.398	4192	UP	MDK	midkine (neurite growth-promoting factor 2)	5.00E-04	669.8613	0.0161
1.333	29081	UP	METTL5	methyltransferase like 5	5.00E-04	673.5496	0.0161
1.565	4258	UP	MGST2	microsomal glutathione S-transferase 2	5.00E-04	675.7213	0.0162
1.278	6182	UP	MRPL12	mitochondrial ribosomal protein L12	5.00E-04	678.208	0.0162
1.319	29074	UP	MRPL18	mitochondrial ribosomal protein L18	5.00E-04	680.7218	0.0168

1.454	219927	UP	MRPL21	mitochondrial ribosomal protein L21	5.00E-04	681.8875	0.0167
1.332	29093	UP	MRPL22	mitochondrial ribosomal protein L22	5.00E-04	684.1374	0.0167
1.41	6150	UP	MRPL23	mitochondrial ribosomal protein L23	5.00E-04	687.5518	0.017
1.41	51264	UP	MRPL27	mitochondrial ribosomal protein L27	5.00E-04	687.6463	0.0176
1.469	9553	UP	MRPL33	mitochondrial ribosomal protein L33	5.00E-04	691.2431	0.018
1.239	54148	UP	MRPL39	mitochondrial ribosomal protein L39	6.00E-04	693.5437	0.018
1.301	51258	UP	MRPL51	mitochondrial ribosomal protein L51	6.00E-04	694.4283	0.018
1.272	64960	UP	MRPS15	mitochondrial ribosomal protein S15	6.00E-04	695.3962	0.0183
1.334	51373	UP	MRPS17	mitochondrial ribosomal protein S17	6.00E-04	696.687	0.0183
1.567	51023	UP	MRPS18C	mitochondrial ribosomal protein S18C	6.00E-04	697.1264	0.0187
1.298	64951	UP	MRPS24	mitochondrial ribosomal protein S24	6.00E-04	697.5959	0.0188
1.23	10884	UP	MRPS30	mitochondrial ribosomal protein S30	6.00E-04	700.9888	0.0188
1.309	51650	UP	MRPS33	mitochondrial ribosomal protein S33	6.00E-04	701.2804	0.0189
1.289	4487	UP	MSX1	msh homeobox 1	6.00E-04	702.9232	0.0189
1.434	4501	UP	MT1X	metallothionein 1X	6.00E-04	706.8982	0.0189
1.244	91663	UP	MYADM	myeloid-associated differentiation marker	6.00E-04	707.1389	0.0191
1.97	4608	UP	MYBPH	myosin binding protein H	7.00E-04	707.5486	0.019
1.31	10627	UP	MYL12A	myosin, light chain 12A, regulatory, non-sarcomeric	7.00E-04	708.7965	0.0191
1.297	10787	UP	NCKAP1	NCK-associated protein 1	7.00E-04	708.8348	0.0194
1.472	126328	UP	NDUFA11	NADH dehydrogenase (ubiquinone) 1 alpha subcomplex, 11, 14.7kDa	7.00E-04	710.1011	0.0201
1.366	55967	UP	NDUFA12	NADH dehydrogenase (ubiquinone) 1 alpha subcomplex, 12	7.00E-04	710.7575	0.0203
1.596	4696	UP	NDUFA3	NADH dehydrogenase (ubiquinone) 1 alpha subcomplex, 3, 9kDa	7.00E-04	712.6796	0.0204
1.321	4697	UP	NDUFA4	NADH dehydrogenase (ubiquinone) 1 alpha subcomplex, 4, 9kDa	7.00E-04	712.8144	0.0203
1.254	4706	UP	NDUFAB1	NADH dehydrogenase (ubiquinone) 1, alpha/beta subcomplex, 1, 8kDa	7.00E-04	713.3761	0.0203
1.435	91942	UP	NDUFAF2	NADH dehydrogenase (ubiquinone) 1 alpha subcomplex, assembly factor 2	7.00E-04	719.4195	0.0203
1.397	29078	UP	NDUFAF4	NADH dehydrogenase (ubiquinone) 1 alpha subcomplex, assembly factor 4	7.00E-04	720.9612	0.0209
1.404	4708	UP	NDUFB2	NADH dehydrogenase (ubiquinone) 1 beta subcomplex, 2, 8kDa	7.00E-04	721.5186	0.0209
1.423	4709	UP	NDUFB3	NADH dehydrogenase (ubiquinone) 1 beta subcomplex, 3, 12kDa	7.00E-04	722.2524	0.0214
1.625	4712	UP	NDUFB6	NADH dehydrogenase (ubiquinone) 1 beta subcomplex, 6, 17kDa	7.00E-04	725.0502	0.0225
1.346	4713	UP	NDUFB7	NADH dehydrogenase (ubiquinone) 1 beta subcomplex, 7, 18kDa	7.00E-04	726.2598	0.0228
1.392	4717	UP	NDUFC1	NADH dehydrogenase (ubiquinone) 1, subcomplex unknown, 1, 6kDa	7.00E-04	727.5049	0.0229
1.347	4725	UP	NDUFS5	NADH dehydrogenase (ubiquinone) Fe-S protein 5, 15kDa (NADH-coenzyme Q reductase)	7.00E-04	732.2632	0.0229
1.283	27247	UP	NFU1	NFU1 iron-sulfur cluster scaffold homolog (<i>S. cerevisiae</i>)	8.00E-04	732.5166	0.0229
1.311	55651	UP	NHP2	NHP2 ribonucleoprotein homolog (yeast)	8.00E-04	737.6291	0.0228
1.325	4809	UP	NHP2L1	NHP2 non-histone chromosome protein 2-like 1 (<i>S. cerevisiae</i>)	8.00E-04	738.0046	0.023
1.966	85407	UP	NKD1	naked cuticle homolog 1 (<i>Drosophila</i>)	8.00E-04	740.5457	0.0232
1.402	4830	UP	NME1	non-metastatic cells 1, protein (NM23A) expressed in	8.00E-04	747.3529	0.0233
1.386	654364	UP	NME1-NME2	NME1-NME2 readthrough transcript	8.00E-04	747.6315	0.0234
1.236	51406	UP	NOL7	nucleolar protein 7, 27kDa	8.00E-04	747.7923	0.0234
1.291	55505	UP	NOP10	NOP10 ribonucleoprotein homolog (yeast)	8.00E-04	748.1906	0.0236
1.367	4839	UP	NOP2	NOP2 nucleolar protein homolog (yeast)	8.00E-04	756.2838	0.0237
1.507	10360	UP	NPM3	nucleophosmin/nucleoplasm, 3	8.00E-04	757.903	0.0239
1.407	54959	UP	ODAM	odontogenic, ameloblast associated	8.00E-04	762.3838	0.0238
1.214	4953	UP	ODC1	ornithine decarboxylase 1	8.00E-04	763.0438	0.0239

1.261	5036	UP	PA2G4	proliferation-associated 2G4, 38kDa	8.00E-04	767.5953	0.0239
1.287	8106	UP	PABPN1	poly(A) binding protein, nuclear 1	8.00E-04	777.4239	0.0242
2.774	9506	UP	PAGE4	P antigen family, member 4 (prostate associated)	9.00E-04	777.8541	0.0244
1.546	5092	UP	PCBD1	pterin-4 alpha-carbinolamine dehydratase/dimerization cofactor of hepatocyte nuclear factor 1 alpha	9.00E-04	785.8578	0.0249
1.459	9141	UP	PDCD5	programmed cell death 5	9.00E-04	798.5674	0.025
1.319	5144	UP	PDE4D	phosphodiesterase 4D, cAMP-specific (phosphodiesterase E3 dunce homolog, Drosophila)	9.00E-04	803.648	0.0249
1.678	22822	UP	PHLDA1	pleckstrin homology-like domain, family A, member 1	9.00E-04	806.1151	0.0249
1.315	84457	UP	PHYHIPL	phytanoyl-CoA 2-hydroxylase interacting protein-like	9.00E-04	807.1986	0.0252
1.366	51227	UP	PIGP	phosphatidylinositol glycan anchor biosynthesis, class P	9.00E-04	808.2781	0.0251
1.323	11145	UP	PLA2G16	phospholipase A2, group XVI	9.00E-04	808.6303	0.025
1.428	5435	UP	POLR2F	polymerase (RNA) II (DNA directed) polypeptide F	9.00E-04	809.8626	0.0252
1.326	51728	UP	POLR3K	polymerase (RNA) III (DNA directed) polypeptide K, 12.3 kDa	9.00E-04	817.0725	0.0253
1.392	51371	UP	POMP	proteasome maturation protein	9.00E-04	823.2081	0.0256
1.278	26472	UP	PPP1R14B	protein phosphatase 1, regulatory (inhibitor) subunit 14B	9.00E-04	823.3912	0.0259
1.242	51029	UP	PPPDE1	PPPDE peptidase domain containing 1	9.00E-04	823.814	0.0259
1.257	27166	UP	PRELID1	PRELI domain containing 1	9.00E-04	827.4955	0.0259
1.401	29964	UP	PRICKLE4 (includes EG:29964)	prickle homolog 4 (Drosophila)	9.00E-04	827.7588	0.026
1.285	27339	UP	PRPF19	PRP19/PSO4 pre-mRNA processing factor 19 homolog (S. cerevisiae)	9.00E-04	827.8679	0.0263
1.688	11098	UP	PRSS23	protease, serine, 23	9.00E-04	829.1686	0.0264
1.206	5687	UP	PSMA6	proteasome (prosome, macropain) subunit, alpha type, 6	9.00E-04	829.24	0.027
1.404	5699	UP	PSMB10	proteasome (prosome, macropain) subunit, beta type, 10	9.00E-04	832.2041	0.0269
1.33	8624	UP	PSMG1	proteasome (prosome, macropain) assembly chaperone 1	9.00E-04	832.6955	0.0277
1.424	5805	UP	PTS	6-pyruvoyltetrahydropterin synthase	0.001	839.5307	0.0278
1.292	29920	UP	PYCR2	pyrroline-5-carboxylate reductase family, member 2	0.001	840.5638	0.0278
1.333	9584	UP	RBM39	RNA binding motif protein 39	0.001	841.7394	0.028
1.307	9978	UP	RBX1 (includes EG:9978)	ring-box 1	0.001	847.4905	0.0283
1.34	9986	UP	RCE1	RCE1 homolog, prenyl protein peptidase (S. cerevisiae)	0.001	851.3709	0.0286
1.249	9104	UP	RGN	regucalcin (senescence marker protein-30)	0.001	851.5459	0.029
1.346	440400	UP	RNASEK	ribonuclease, RNase K	0.001	854.7577	0.0305
1.395	51255	UP	RNF181	ring finger protein 181	0.001	856.2135	0.0311
1.339	140823	UP	ROMO1	reactive oxygen species modulator 1	0.001	856.6301	0.0311
1.288	84268	UP	RPAIN	RPA interacting protein	0.001	861.4403	0.0319
1.367	6136	UP	RPL12 (includes EG:6136)	ribosomal protein L12	0.001	862.5925	0.0322
1.274	649821	UP	RPL14L	ribosomal protein L14 pseudogene 1	0.001	866.0162	0.0327
1.437	6164	UP	RPL34	ribosomal protein L34	0.001	867.995	0.0333
1.305	25873	UP	RPL36 (includes EG:25873)	ribosomal protein L36	0.001	868.3356	0.0333
1.347	6166	UP	RPL36AL	ribosomal protein L36a-like	0.001	870.9072	0.0337
1.315	6169	UP	RPL38 (includes EG:6169)	ribosomal protein L38	0.001	874.4163	0.034
1.321	6128	UP	RPL6	ribosomal protein L6	0.0011	874.433	0.0342
1.461	6176	UP	RPLP1	ribosomal protein, large, P1	0.0011	875.5767	0.0343
1.303	79897	UP	RPP21	ribonuclease P/MRP 21kDa subunit	0.0011	878.1926	0.0343
1.273	10799	UP	RPP40	ribonuclease P/MRP 40kDa subunit	0.0011	882.8566	0.0349
1.299	6207	UP	RPS13	ribosomal protein S13	0.0011	884.5535	0.0348
1.371	6210	UP	RPS15A	ribosomal protein S15a	0.0011	885.9976	0.0348

1.461	6227	UP	RPS21	ribosomal protein S21	0.0011	886.588 9	0.0347
1.372	6229	UP	RPS24 (includes EG:6229)	ribosomal protein S24	0.0011	887.815 7	0.035
1.651	6231	UP	RPS26	ribosomal protein S26	0.0011	888.021 8	0.0358
1.306	6232	UP	RPS27	ribosomal protein S27	0.0011	894.813 9	0.0368
1.32	51065	UP	RPS27L (includes EG:51065)	ribosomal protein S27-like	0.0011	901.293 3	0.0368
1.226	6234	UP	RPS28	ribosomal protein S28	0.0011	902.717 9	0.0368
1.284	6235	UP	RPS29	ribosomal protein S29	0.0011	907.032 6	0.0371
1.487	6201	UP	RPS7	ribosomal protein S7	0.0011	909.452 9	0.0373
1.339	6275	UP	S100A4	S100 calcium binding protein A4	0.0011	914.304 7	0.0375
1.31	389432	UP	SAMD5	sterile alpha motif domain containing 5	0.0012	914.618 6	0.0378
1.243	23478	UP	SEC11A	SEC11 homolog A (<i>S. cerevisiae</i>)	0.0012	914.668	0.0379
1.293	10952	UP	SEC61B	Sec61 beta subunit	0.0012	914.986 9	0.0378
1.348	23480	UP	SEC61G	Sec61 gamma subunit	0.0012	918.297 4	0.0382
1.216	81929	UP	SEH1L	SEH1-like (<i>S. cerevisiae</i>)	0.0012	919.673 5	0.0384
1.388	58515	UP	SELK	selenoprotein K	0.0012	922.103 9	0.0384
1.281	728492	UP	SERF1B	small EDRK-rich factor 1B (centromeric)	0.0012	923.352 8	0.0394
1.296	871	UP	SERPINH1	serpin peptidase inhibitor, clade H (heat shock protein 47), member 1, (collagen binding protein 1)	0.0012	923.893 4	0.0393
1.328	51639	UP	SF3B14	splicing factor 3B, 14 kDa subunit	0.0012	926.163 4	0.0395
1.337	83443	UP	SF3B5	splicing factor 3b, subunit 5, 10kDa	0.0012	927.693 8	0.0396
1.2	119559	UP	SFXN4	sideroflexin 4	0.0012	930.618 5	0.0402
1.257	291	UP	SLC25A4	solute carrier family 25 (mitochondrial carrier; adenine nucleotide translocator), member 4	0.0012	932.049 7	0.0402
1.3	10237	UP	SLC35B1	solute carrier family 35, member B1	0.0012	933.008 9	0.0409
1.296	347734	UP	SLC35B2	solute carrier family 35, member B2	0.0012	935.596	0.0409
1.33	8884	UP	SLC5A6	solute carrier family 5 (sodium-dependent vitamin transporter), member 6	0.0013	936.734 3	0.0412
1.373	387066	UP	SNHG5	small nucleolar RNA host gene 5 (non-protein coding)	0.0012	939.456 8	0.0415
1.286	79622	UP	SNRNP25	small nuclear ribonucleoprotein 25kDa (U11/U12)	0.0012	944.184 3	0.0416
1.429	6629	UP	SNRPB2	small nuclear ribonucleoprotein polypeptide B"	0.0012	944.192 9	0.0415
1.607	6636	UP	SNRPF	small nuclear ribonucleoprotein polypeptide F	0.0012	944.689 2	0.0416
1.466	6637	UP	SNRPG	small nuclear ribonucleoprotein polypeptide G	0.0012	946.335 7	0.0418
1.563	389058	UP	SP5	Sp5 transcription factor	0.0012	946.539 8	0.042
1.301	28972	UP	SPCS1 (includes EG:28972)	signal peptidase complex subunit 1 homolog (<i>S. cerevisiae</i>)	0.0012	950.100 5	0.0424
1.344	6690	UP	SPINK1	serine peptidase inhibitor, Kazal type 1	0.0012	950.155 3	0.0425
1.292	6727	UP	SRP14	signal recognition particle 14kDa (homologous Alu RNA binding protein)	0.0011	951.098 7	0.0425
1.46	6728	UP	SRP19	signal recognition particle 19kDa	0.0012	954.493 1	0.0426
1.257	6734	UP	SRPR	signal recognition particle receptor (docking protein)	0.0012	955.671 5	0.0427
1.615	6742	UP	SSBP1	single-stranded DNA binding protein 1	0.0013	957.265 3	0.043
1.224	8148	UP	TAF15	TAF15 RNA polymerase II, TATA box binding protein (TBP)-associated factor, 68kDa	0.0013	959.446 5	0.0429
1.285	6876	UP	TAGLN	transgelin	0.0013	960.042 9	0.0431
1.309	6902	UP	TBCA	tubulin folding cofactor A	0.0013	960.600 8	0.0431
1.314	6921	UP	TCEB1	transcription elongation factor B (SIII), polypeptide 1 (15kDa, elongin C)	0.0013	961.323 1	0.043
1.331	6923	UP	TCEB2	transcription elongation factor B (SIII), polypeptide 2 (18kDa, elongin B)	0.0013	965.253 6	0.0429
1.203	6942	UP	TCF20	transcription factor 20 (AR1)	0.0013	966.176 2	0.0433
1.422	255758	UP	TCTEX1D2	Tctex1 domain containing 2	0.0013	971.400 9	0.0432
1.273	7035	UP	TFPI	tissue factor pathway inhibitor (lipoprotein-associated coagulation inhibitor)	0.0013	971.692 1	0.0432

1.375	10189	UP	THOC4	THO complex 4	0.0014	982.073 7	0.0439
1.266	7064	UP	THOP1	thimet oligopeptidase 1	0.0014	982.402 3	0.0439
1.477	26519	UP	TIMM10	translocase of inner mitochondrial membrane 10 homolog (yeast)	0.0014	985.867 6	0.0445
1.405	10431	UP	TIMM23	translocase of inner mitochondrial membrane 23 homolog (yeast)	0.0014	989.483 1	0.0454
1.234	7082	UP	TJP1	tight junction protein 1 (zona occludens 1)	0.0014	994.429 8	0.0454
1.357	84233	UP	TMEM126A	transmembrane protein 126A	0.0014	1004.92 81	0.0458
1.212	55863	UP	TMEM126B	transmembrane protein 126B	0.0015	1010.00 75	0.0461
1.307	10430	UP	TMEM147	transmembrane protein 147	0.0015	1010.18 76	0.0466
1.252	51522	UP	TMEM14C	transmembrane protein 14C	0.0016	1015.87 4	0.0467
1.274	90809	UP	TMEM55B	transmembrane protein 55B	0.0017	1019.59 82	0.0468
1.352	83460	UP	TMEM93	transmembrane protein 93	0.0017	1023.10 81	0.0468
1.295	401505	UP	TOMM5 (includes EG:401505)	translocase of outer mitochondrial membrane 5 homolog (yeast)	0.0017	1027.40 59	0.0478
1.436	54543	UP	TOMM7	translocase of outer mitochondrial membrane 7 homolog (yeast)	0.0019	1027.68 61	0.0478
1.473	51693	UP	TRAPPC2L	trafficking protein particle complex 2-like	0.0023	1028.31 68	0.0477
1.36	7295	UP	TXN	thioredoxin	0.0023	1030.31 55	0.0477
1.238	11338	UP	U2AF2 (includes EG:11338)	U2 small nuclear RNA auxiliary factor 2	0.0023	1030.92 18	0.0477
1.366	59286	UP	UBL5	ubiquitin-like 5	0.0022	1032.79 86	0.0476
1.271	29979	UP	UBQLN1	ubiquilin 1	0.0023	1034.85 16	0.0479
1.279	7347	UP	UCHL3	ubiquitin carboxyl-terminal esterase L3 (ubiquitin thiolesterase)	0.0024	1036.17 43	0.0479
1.345	8409	UP	UXT	ubiquitously-expressed transcript	0.0025	1037.28 1	0.0483
1.224	114049	UP	WBSCR22	Williams Beuren syndrome chromosome region 22	0.0026	1041.76 94	0.0487
1.284	7529	UP	YWHAB	tyrosine 3-monooxygenase/tryptophan 5-monooxygenase activation protein, beta polypeptide	0.0025	1042.06 79	0.0487
1.291	55954	UP	ZMAT5	zinc finger, matrin type 5	0.0026	1042.24 25	0.0492
1.504	84858	UP	ZNF503	zinc finger protein 503	0.0026	1042.67 96	0.0493
1.306	30834	UP	ZNRD1	zinc ribbon domain containing 1	0.0026	1044.71 99	0.0497

Table 1. Analysis of genes affected by reduced GPX4 expression by (siRNA). Genes with increased expression by 1.2 or greater (ranked) for 72 hours in response to GPX4 knock-down in Caco-2 cells by siRNA are listed. Genes identified through the in silico analysis as upregulated due to GPX4 knock-down includes Human gene symbols and Entrez identifiers

Appendix A2: List of genes of which expression were down-regulated

FOLD CHANGE	PROBE ID	REGULATION	SYMBOL	ENTREZ GENE NAME	P.VA LUE	RP/S UM	PPF
1.314	29974	DOWN	A1CF	APOBEC1 complementation factor	2.00E-04	5.7068	0
1.324	10058	DOWN	ABCB6	ATP-binding cassette, sub-family B (MDR/TAP), member 6	2.00E-04	13.6685	0
1.276	8714	DOWN	ABCC3	ATP-binding cassette, sub-family C (CFTR/MRP), member 3	2.00E-04	15.8502	0
1.347	79575	DOWN	ABHD8	abhydrolase domain containing 8	2.00E-04	17.2948	0
1.404	26	DOWN	ABP1	amiloride binding protein 1 (amine oxidase (copper-containing))	2.00E-04	17.5886	0
1.379	41	DOWN	ACCN2	amiloride-sensitive cation channel 2, neuronal	2.00E-04	21.797	0
1.309	11332	DOWN	ACOT7	acyl-CoA thioesterase 7	2.00E-04	31.115	0
1.310	8309	DOWN	ACOX2	acyl-Coenzyme A oxidase 2, branched chain	2.00E-04	39.0591	0
1.310	6296	DOWN	ACSM3	acyl-CoA synthetase medium-chain family member 3	3.00E-04	41.228	0
1.377	90	DOWN	ACVR1	activin A receptor, type I	3.00E-04	43.0222	0
1.303	91	DOWN	ACVR1B	activin A receptor, type IB	5.00E-04	47.5665	0
1.331	118	DOWN	ADD1	adducin 1 (alpha)	5.00E-04	50.4311	0
1.239	132	DOWN	ADK	adenosine kinase	4.00E-04	52.7382	0
1.885	174	DOWN	AFP	alpha-fetoprotein	4.00E-04	65.4513	0
1.289	9131	DOWN	AIFM1	apoptosis-inducing factor, mitochondrion-associated, 1	4.00E-04	76.3587	0
1.400	9465	DOWN	AKAP7	A kinase (PRKA) anchor protein 7	6.00E-04	94.1054	0
1.305	8644	DOWN	AKR1C3	aldo-keto reductase family 1, member C3 (3-alpha hydroxysteroid dehydrogenase, type II)	6.00E-04	95.8709	0
1.828	213	DOWN	ALB	albumin	6.00E-04	103.2966	2.00E-04
1.344	216	DOWN	ALDH1A1	aldehyde dehydrogenase 1 family, member A1	5.00E-04	114.3335	2.00E-04
1.300	4329	DOWN	ALDH6A1	aldehyde dehydrogenase 6 family, member A1	6.00E-04	1155.4874	2.00E-04
1.236	501	DOWN	ALDH7A1	aldehyde dehydrogenase 7 family, member A1	7.00E-04	124.1512	2.00E-04
1.278	51321	DOWN	AMZ2	archaelysin family metallopeptidase 2	6.00E-04	124.815	2.00E-04
1.492	8907	DOWN	AP1M1	adaptor-related protein complex 1, mu 1 subunit	6.00E-04	126.9185	2.00E-04
1.696	335	DOWN	APOA1	apolipoprotein A-I	6.00E-04	136.1924	2.00E-04
1.359	369	DOWN	ARAF	v-raf murine sarcoma 3611 viral oncogene homolog	6.00E-04	138.2483	2.00E-04
1.384	64411	DOWN	ARAP3	ArfGAP with RhoGAP domain, ankyrin repeat and PH domain 3	6.00E-04	140.1404	2.00E-04
1.377	55114	DOWN	ARHGAP17	Rho GTPase activating protein 17	6.00E-04	147.4309	2.00E-04
1.340	397	DOWN	ARHGDIB	Rho GDP dissociation inhibitor (GDI) beta	8.00E-04	149.8521	3.00E-04
1.366	10550	DOWN	ARL6IP5	ADP-ribosylation-like factor 6 interacting protein 5	0.001	150.732	3.00E-04
1.359	10776	DOWN	ARPP19	cAMP-regulated phosphoprotein, 19kDa	9.00E-04	151.9979	3.00E-04
1.370	84164	DOWN	ASCC2	activating signal cointegrator 1 complex subunit 2	9.00E-04	155.2893	4.00E-04
1.269	432	DOWN	ASGR1	asialoglycoprotein receptor 1	9.00E-04	156.8225	4.00E-04
1.581	79170	DOWN	ATAD4	ATPase family, AAA domain containing 4	0.001	157.2122	4.00E-04
1.285	476	DOWN	ATP1A1	ATPase, Na ⁺ /K ⁺ transporting, alpha 1 polypeptide	0.001	175.6125	7.00E-04

1.212	481	DOWN	ATP1B1	ATPase, Na+/K+ transporting, beta 1 polypeptide	0.0014	175.8058	7.00E-04
1.379	509	DOWN	ATP5C1	ATP synthase, H+ transporting, mitochondrial F1 complex, gamma polypeptide 1	0.0014	180.5184	7.00E-04
1.329	647340	DOWN	ATP5C2	ATP synthase, H+ transporting, mitochondrial F1 complex, gamma polypeptide 2	0.0015	181.664	7.00E-04
1.235	537	DOWN	ATP6AP1	ATPase, H+ transporting, lysosomal accessory protein 1	0.0015	183.3768	7.00E-04
1.263	155066	DOWN	ATP6V0E2	ATPase, H+ transporting V0 subunit e2	0.0015	189.9351	9.00E-04
1.375	558	DOWN	AXL	AXL receptor tyrosine kinase	0.0015	195.1795	9.00E-04
1.544	9334	DOWN	B4GALT5	UDP-Gal:betaGlcNAc beta 1,4- galactosyltransferase, polypeptide 5	0.0017	198.2168	9.00E-04
1.311	11285	DOWN	B4GALT7	xylosylprotein beta 1,4-galactosyltransferase, polypeptide 7 (galactosyltransferase I)	0.0016	203.5852	9.00E-04
1.398	593	DOWN	BCKDHA	branched chain keto acid dehydrogenase E1, alpha polypeptide	0.0016	206.0507	9.00E-04
1.376	10295	DOWN	BCKDK	branched chain ketoacid dehydrogenase kinase	0.0016	208.5591	9.00E-04
1.238	274	DOWN	BIN1	bridging integrator 1	0.0016	215.5276	9.00E-04
1.289	8548	DOWN	BLZF1	basic leucine zipper nuclear factor 1	0.0017	216.0266	9.00E-04
1.244	738	DOWN	C11ORF2	chromosome 11 open reading frame2	0.0017	217.3378	8.00E-04
1.442	79703	DOWN	C11ORF80	chromosome 11 open reading frame 80	0.0018	221.5212	8.00E-04
1.388	79762	DOWN	C1ORF115	chromosome 1 open reading frame 115	0.0018	221.6028	0.0011
1.331	25966	DOWN	C2CD2	C2 calcium-dependent domain containing 2	0.0018	228.4403	0.001
1.292	55845	DOWN	C3ORF10	chromosome 3 open reading frame 10	0.0018	228.934	0.001
1.489	725	DOWN	C4BPB	complement component 4 binding protein, beta	0.0019	239.1057	0.001
1.349	201895	DOWN	C4ORF34	chromosome 4 open reading frame 34	0.0019	239.1221	0.0011
1.308	221927	DOWN	C7ORF27	chromosome 7 open reading frame 27	0.0019	251.3178	0.0011
1.397	784	DOWN	CACNB3	calcium channel, voltage-dependent, beta 3 subunit	0.002	254.224	0.0012
1.405	23705	DOWN	CADM1	cell adhesion molecule 1	0.002	259.8967	0.0012
1.281	808	DOWN	CALM3	calmodulin 3 (phosphorylase kinase, delta)	0.002	262.5064	0.0012
1.390	818	DOWN	CAMK2G	calcium/calmodulin-dependent protein kinase II gamma	0.0019	263.5209	0.0012
1.563	726	DOWN	CAPN5	calpain 5	0.0021	264.1178	0.0012
1.366	847	DOWN	CAT	catalase	0.0022	277.8732	0.0012
1.389	875	DOWN	CBS	cystathionine-beta-synthase	0.0022	281.4995	0.0012
1.299	896	DOWN	CCND3	cyclin D3	0.0022	287.2722	0.0012
1.422	900	DOWN	CCNG1	cyclin G1	0.0022	289.2514	0.0012
1.257	10983	DOWN	CCNI	cyclin I	0.0022	290.7075	0.0012
1.376	7203	DOWN	CCT3	chaperonin containing TCP1, subunit 3 (gamma)	0.0023	292.9708	0.0012
1.296	928	DOWN	CD9	CD9 molecule	0.0023	302.2536	0.0012
1.223	4267	DOWN	CD99 (includes EG:4267)	CD99 molecule	0.0023	303.9589	0.0012
1.265	146059	DOWN	CDAN1	congenital dyserythropoietic anemia, type I	0.0025	314.5203	0.0012
1.412	8555	DOWN	CDC14B	CDC14 cell division cycle 14 homolog B (S. cerevisiae)	0.0026	317.1492	0.0014
1.446	999	DOWN	CDH1	cadherin 1, type 1, E-cadherin (epithelial)	0.0028	317.5345	0.0014

1.270	1015	DOWN	CDH17	cadherin 17, LI cadherin (liver-intestine)	0.0028	321.3004	0.0014
1.231	91368	DOWN	CDKN2AIPNL	CDKN2A interacting protein N-terminal like	0.0028	329.1749	0.0014
1.373	91368	DOWN	CDKN2AIPNL	CDKN2A interacting protein N-terminal like	0.0028	339.4503	0.0014
1.397	91368	DOWN	CDKN2AIPNL	CDKN2A interacting protein N-terminal like	0.0031	342.9462	0.0014
1.313	81620	DOWN	CDT1	chromatin licensing and DNA replication factor 1	0.0032	350.5827	0.0014
1.314	131474	DOWN	CHCHD4	coiled-coil-helix-coiled-coil-helix domain containing 4	0.0032	353.7992	0.0013
1.208	166012	DOWN	CHST13	carbohydrate (chondroitin 4) sulfotransferase 13	0.0033	355.4054	0.0013
1.298	63924	DOWN	CIDEA	cell death-inducing DFFA-like effector c	0.0033	356.9938	0.0014
1.339	23274	DOWN	CLEC16A	C-type lectin domain family 16, member A	0.0032	365.1194	0.0015
2.708	29121	DOWN	CLEC2D (includes EG:29121)	C-type lectin domain family 2, member D	0.0033	367.9093	0.0015
1.486	119467	DOWN	CLRN3	clarin 3	0.0033	369.64	0.0016
1.257	80790	DOWN	CMIP	c-Maf-inducing protein	0.0032	373.8272	0.0017
1.229	1266	DOWN	CNN3	calponin 3, acidic	0.0033	375.6908	0.0017
1.339	55330	DOWN	CNO	cappuccino homolog (mouse)	0.0033	384.5502	0.0017
1.291	80347	DOWN	COASY	Coenzyme A synthase	0.0033	386.5388	0.0019
1.582	22837	DOWN	COBLL1	COBL-like 1	0.0035	391.1578	0.0023
1.297	22796	DOWN	COG2	component of oligomeric golgi complex 2	0.0035	394.5228	0.0023
1.567	1303	DOWN	COL12A1	collagen, type XII, alpha 1	0.0035	398.2869	0.0023
1.366	10087	DOWN	COL4A3BP	collagen, type IV, alpha 3 (Goodpasture antigen) binding protein	0.0036	401.2048	0.0022
1.223	149951	DOWN	COMMD7	COMM domain containing 7	0.0036	404.206	0.0023
1.343	23603	DOWN	CORO1C	coronin, actin binding protein, 1C	0.0036	406.2356	0.0024
1.297	54504	DOWN	CPVL	carboxypeptidase, vitellogenic-like	0.0036	411.9762	0.0026
1.353	51747	DOWN	CROP	cisplatin resistance-associated overexpressed protein	0.0036	416.053	0.0026
1.307	1429	DOWN	CRYZ	crystallin, zeta (quinone reductase)	0.0037	422.2502	0.0026
1.327	1438	DOWN	CSF2RA (includes EG:1438)	colony stimulating factor 2 receptor, alpha, low-affinity (granulocyte-macrophage)	0.0037	428.0362	0.0026
1.267	10106	DOWN	CTDSP2	CTD (carboxy-terminal domain, RNA polymerase II, polypeptide A) small phosphatase 2	0.0038	430.4944	0.0026
1.261	1495	DOWN	CTNNA1	catenin (cadherin-associated protein), alpha 1, 102kDa	0.0038	431.7868	0.0026
1.306	1508	DOWN	CTSB	cathepsin B	0.0044	446.4891	0.0025
1.218	1512	DOWN	CTSH	cathepsin H	0.0044	447.5745	0.0025
1.346	1515	DOWN	CTSL2	cathepsin L2	0.0045	449.3516	0.0029
1.434	404093	DOWN	CUEDC1	CUE domain containing 1	0.0046	456.1893	0.0031
1.328	26999	DOWN	CYFIP2 (includes EG:26999)	cytoplasmic FMR1 interacting protein 2	0.0048	457.5081	0.0031
1.296	27071	DOWN	DAPP1	dual adaptor of phosphotyrosine and 3-phosphoinositides	0.0049	464.4514	0.0032
1.344	79007	DOWN	DBNDD1	dysbindin (dystrobrevin binding protein 1) domain containing 1	0.0049	466.4678	0.0031
1.219	1642	DOWN	DDB1	damage-specific DNA binding protein 1, 127kDa	0.0049	467.71	0.0032
1.564	1672	DOWN	DEFB1	defensin, beta 1	0.0052	471.6073	0.0032

1.322	8560	DOWN	DEGS1	degenerative spermatocyte homolog 1, lipid desaturase (<i>Drosophila</i>)	0.005 2	471.9 604	0.00 32
1.378	1687	DOWN	DFNA5	deafness, autosomal dominant 5	0.005 3	475.7 744	0.00 38
1.541	8694	DOWN	DGAT1	diacylglycerol O-acyltransferase homolog 1 (mouse)	0.005 2	477.5 203	0.00 39
1.236	1725	DOWN	DHPS	deoxyhypusine synthase	0.005 2	479.5 811	0.00 4
1.346	11581 7	DOWN	DHRS1	dehydrogenase/reductase (SDR family) member 1	0.005 6	484.2 411	0.00 4
1.367	84925	DOWN	DIRC2	disrupted in renal carcinoma 2	0.005 8	484.5 572	0.00 41
1.246	79962	DOWN	DNAJC22	DnaJ (Hsp40) homolog, subfamily C, member 22	0.005 9	487.0 292	0.00 4
1.259	79746	DOWN	ECHDC3	enoyl Coenzyme A hydratase domain containing 3	0.006	493.4 745	0.00 43
1.248	1892	DOWN	ECHS1	enoyl Coenzyme A hydratase, short chain, 1, mitochondrial	0.006	495.6	0.00 43
1.581	1917	DOWN	EEF1A2	eukaryotic translation elongation factor 1 alpha 2	0.006 1	496.6 818	0.00 5
1.327	1942	DOWN	EFNA1	ephrin-A1	0.006 4	499.7 438	0.00 5
1.388	1949	DOWN	EFNB3	ephrin-B3	0.006 4	501.6 321	0.00 5
1.309	10938	DOWN	EHD1	EH-domain containing 1	0.006 5	507.3 827	0.00 54
1.215	51386	DOWN	EIF3L	eukaryotic translation initiation factor 3, subunit L	0.007 2	507.4 617	0.00 54
1.294	2034	DOWN	EPAS1	endothelial PAS domain protein 1	0.007 4	510.7 8	0.00 54
1.284	29924	DOWN	EPN1	epsin 1	0.007 6	512.7 274	0.00 58
1.393	2064	DOWN	ERBB2	v-erb-b2 erythroblastic leukemia viral oncogene homolog 2, neuro/glioblastoma derived oncogene homolog (avian)	0.007 8	513.6 842	0.00 61
1.648	12150 6	DOWN	ERP27	endoplasmic reticulum protein 27	0.007 8	518.9 779	0.00 62
1.326	2122	DOWN	EVI1	ecotropic viral integration site 1	0.007 9	519.4 662	0.00 62
2.163	51466	DOWN	EVL	Enah/Vasp-like	0.007 9	524.4 771	0.00 62
1.291	7430	DOWN	EZR	ezrin	0.007 9	525.0 101	0.00 62
1.262	2159	DOWN	F10	coagulation factor X	0.008 4	526.2 134	0.00 66
1.319	50848	DOWN	F11R	F11 receptor	0.008 4	526.7 479	0.00 67
1.360	2150	DOWN	F2RL1	coagulation factor II (thrombin) receptor-like 1	0.009 2	528.4 007	0.00 69
1.336	23197	DOWN	FAF2	Fas associated factor family member 2	0.009 3	530.1 463	0.00 71
1.579	83641	DOWN	FAM107B	family with sequence similarity 107, member B	0.009 3	530.3 444	0.00 7
1.332	63901	DOWN	FAM111A	family with sequence similarity 111, member A	0.009 4	536.0 104	0.00 71
1.700	33809 4	DOWN	FAM151A	family with sequence similarity 151, member A	0.009 6	536.8 854	0.00 71
1.337	28363 5	DOWN	FAM177A1	family with sequence similarity 177, member A1	0.009 7	538.9 095	0.00 72
1.259	2192	DOWN	FBLN1	fibulin 1	0.009 7	542.2 597	0.00 72
1.260	2222	DOWN	FDFT1	farnesyl-diphosphate farnesyltransferase 1	0.010 1	543.8 342	0.00 72
2.348	2243	DOWN	FGA	fibrinogen alpha chain	0.010 1	552.2 205	0.00 72
2.046	2244	DOWN	FGB	fibrinogen beta chain	0.010	554.1 691	0.00 73
1.521	89846	DOWN	FGD3	FYVE, RhoGEF and PH domain containing 3	0.010 1	554.4 831	0.00 73
1.296	2261	DOWN	FGFR3	fibroblast growth factor receptor 3	0.010 2	559.6 134	0.00 73
2.018	2266	DOWN	FGG	fibrinogen gamma chain	0.010 3	560.9 484	0.00 73
1.227	2271	DOWN	FH	fumarate hydratase	0.010 2	564.7 214	0.00 73

1.266	2218	DOWN	FKTN	fukutin	0.010 6	572.2 849	0.00 74
1.419	80164	DOWN	FLJ22184	hypothetical protein FLJ22184	0.010 7	575.2 287	0.00 74
1.264	28408 5	DOWN	FLJ40504	hypothetical protein FLJ40504	0.010 7	587.5 09	0.00 74
1.237	2319	DOWN	FLOT2	flotillin 2	0.010 9	588.4 152	0.00 74
1.327	23048	DOWN	FNBP1	formin binding protein 1	0.010 9	588.9 121	0.00 73
1.352	3169	DOWN	FOXA1	forkhead box A1	0.010 9	591.6 36	0.00 73
1.501	80144	DOWN	FRAS1	Fraser syndrome 1	0.010 9	593.2 276	0.00 74
1.320	10841	DOWN	FTCD	formiminotransferase cyclodeaminase	0.011	604.4 483	0.00 75
1.205	53827	DOWN	FXYD5	FXYD domain containing ion transport regulator 5	0.011 3	606.4 85	0.00 79
1.317	2584	DOWN	GALK1	galactokinase 1	0.011 4	611.1 03	0.00 79
1.260	2592	DOWN	GALT	galactose-1-phosphate uridylyltransferase	0.011 4	611.5 248	0.00 81
1.275	2621	DOWN	GAS6	growth arrest-specific 6	0.011 5	616.5 538	0.00 82
1.297	10985	DOWN	GCN1L1	GCN1 general control of amino-acid synthesis 1-like 1 (yeast)	0.011 9	617.4 511	0.00 82
1.249	10052	DOWN	GJC1	gap junction protein, gamma 1, 45kDa	0.012	618.9 611	0.00 82
1.220	2720	DOWN	GLB1	galactosidase, beta 1	0.012 1	621.0 534	0.00 82
1.385	15200 7	DOWN	GLIPR2	GLI pathogenesis-related 2	0.012 1	621.4 266	0.00 84
1.402	13215 8	DOWN	GLYCK	glycerate kinase	0.012 1	628.8 998	0.00 83
1.296	51292	DOWN	GMPR2	guanosine monophosphate reductase 2	0.012 4	629.9 76	0.00 85
1.533	2719	DOWN	GPC3	glypican 3	0.012 3	634.7 134	0.00 86
1.585	2262	DOWN	GPC5	glypican 5	0.012 7	635.7 019	0.00 85
1.328	57211	DOWN	GPR126	G protein-coupled receptor 126	0.012 7	636.3 109	0.00 85
1.328	27239	DOWN	GPR162	G protein-coupled receptor 162	0.012 8	640.5 028	0.00 85
2.175	2879	DOWN	GPX4	glutathione peroxidase 4 (phospholipid hydroperoxidase)	0.013	650.7 664	0.00 84
1.426	2888	DOWN	GRB14	growth factor receptor-bound protein 14	0.013	651.7 823	0.00 84
1.278	9380	DOWN	GRHPR	glyoxylate reductase/hydroxypyruvate reductase	0.013	662.9 739	0.00 84
1.436	2938	DOWN	GSTA1	glutathione S-transferase alpha 1	0.012 9	666.7 011	0.00 86
1.445	2939	DOWN	GSTA2	glutathione S-transferase alpha 2	0.013 3	676.0 86	0.00 86
1.294	2944	DOWN	GSTM1	glutathione S-transferase mu 1	0.013 6	678.5 655	0.00 87
1.325	2946	DOWN	GSTM2	glutathione S-transferase mu 2 (muscle)	0.013 9	678.6 233	0.00 9
1.447	2984	DOWN	GUCY2C	guanylate cyclase 2C (heat stable enterotoxin receptor)	0.013 9	680.4 539	0.00 9
1.266	2990	DOWN	GUSB	glucuronidase, beta	0.014	688.7 406	0.00 9
1.278	8908	DOWN	GYG2	glycogenin 2	0.013 9	689.9 21	0.00 9
1.369	9555	DOWN	H2AFY	H2A histone family, member Y	0.014	697.2 437	0.00 89
1.308	3033	DOWN	HADH	hydroxyacyl-Coenzyme A dehydrogenase	0.014 1	699.1 181	0.00 9
1.408	10866	DOWN	HCP5	HLA complex P5	0.014 2	699.6 822	0.00 9
1.288	51020	DOWN	HDDC2	HD domain containing 2	0.014 4	699.7 955	0.00 9
1.372	8226	DOWN	HDHD1A	haloacid dehalogenase-like hydrolase domain containing 1A	0.014 6	703.8 159	0.00 91

1.388	9843	DOWN	HEPH	hephaestin	0.014 7	704.6 46	0.00 91
1.265	3074	DOWN	HEXB	hexosaminidase B (beta polypeptide)	0.014 7	705.3 683	0.00 91
1.346	3081	DOWN	HGD	homogentisate 1,2-dioxygenase (homogentisate oxidase)	0.014 9	705.9 495	0.00 95
1.343	3156	DOWN	HMGCR	3-hydroxy-3-methylglutaryl-Coenzyme A reductase	0.015 2	713.4 526	0.00 95
1.363	3157	DOWN	HMGCS1	3-hydroxy-3-methylglutaryl-Coenzyme A synthase 1 (soluble)	0.015 1	714.0 463	0.00 95
1.524	3158	DOWN	HMGCS2	3-hydroxy-3-methylglutaryl-Coenzyme A synthase 2 (mitochondrial)	0.015 2	715.0 109	0.00 95
1.364	3178	DOWN	HNRNPA1	heterogeneous nuclear ribonucleoprotein A1	0.015 1	715.1 446	0.00 96
1.247	3281	DOWN	HSBP1	heat shock factor binding protein 1	0.015 1	715.7 917	0.00 96
1.589	3294	DOWN	HSD17B2	hydroxysteroid (17-beta) dehydrogenase 2	0.016 3	717.9 537	0.00 95
1.320	3283	DOWN	HSD3B1	hydroxy-delta-5-steroid dehydrogenase, 3 beta- and steroid delta-isomerase 1	0.016 3	720.3 81	0.00 96
1.251	3373	DOWN	HYAL1	hyaluronoglucosaminidase 1	0.016 2	720.7 417	0.00 96
1.457	3398	DOWN	ID2	inhibitor of DNA binding 2, dominant negative helix-loop-helix protein	0.016 2	720.8 8	0.00 97
1.213	3420	DOWN	IDH3B	isocitrate dehydrogenase 3 (NAD+) beta	0.016 1	720.9 761	0.00 97
1.278	83880	DOWN	IFP38	eukaryotic translation initiation factor 3, subunit F pseudogene 2	0.016 1	726.2 226	0.01 02
1.290	3321	DOWN	IGSF3	immunoglobulin superfamily, member 3	0.016 4	727.3 493	0.01 01
1.305	3588	DOWN	IL10RB	interleukin 10 receptor, beta	0.016 5	727.9 672	0.01 03
1.367	10994	DOWN	ILVBL	ilvB (bacterial acetolactate synthase)-like	0.016 6	730.6 025	0.01 05
1.443	64423	DOWN	INF2 (includes EG:64423)	inverted formin, FH2 and WH2 domain containing	0.016 7	732.4 673	0.01 06
1.342	55827	DOWN	IQWD1	IQ motif and WD repeats 1	0.016 8	733.4 964	0.01 06
1.315	51477	DOWN	ISYNA1	inositol-3-phosphate synthase 1	0.016 7	735.7 309	0.01 06
1.266	81618	DOWN	ITM2C	integral membrane protein 2C	0.016 7	738.1 265	0.01 05
1.331	3710	DOWN	ITPR3	inositol 1,4,5-triphosphate receptor, type 3	0.016 9	742.8 336	0.01 11
1.391	38943 4	DOWN	IYD	iodotyrosine deiodinase	0.016 9	743.7 583	0.01 12
1.354	9929	DOWN	JOSD1	Josephin domain containing 1	0.017 3	746.6 124	0.01 17
1.262	9798	DOWN	KIAA0174	KIAA0174	0.017 4	753.2 532	0.01 17
1.349	23588	DOWN	KLHDC2	kelch domain containing 2	0.017 3	754.5 821	0.01 2
1.792	3827	DOWN	KNG1 (includes EG:3827)	kininogen 1	0.017 4	759.1 518	0.01 28
2.395	3875	DOWN	KRT18	keratin 18	0.017 5	759.1 567	0.01 28
1.628	28421 7	DOWN	LAMA1	laminin, alpha 1	0.018 5	760.3 635	0.01 34
1.462	3920	DOWN	LAMP2	lysosomal-associated membrane protein 2	0.018 5	762.5 715	0.01 38
1.238	51451	DOWN	LCMT1	leucine carboxyl methyltransferase 1	0.019	766.4 197	0.01 42
1.353	64077	DOWN	LHPP	phospholysine phosphohistidine inorganic pyrophosphate phosphatase	0.019	768.4 185	0.01 44
1.209	11025	DOWN	LILRB3 (includes EG:11025)	leukocyte immunoglobulin-like receptor, subfamily B (with TM and ITIM domains), member 3	0.019	771.8 788	0.01 49
1.591	3990	DOWN	LIPC	lipase, hepatic	0.019 1	773.7 104	0.01 5
1.319	4000	DOWN	LMNA	lamin A/C	0.019 6	774.8 97	0.01 51
1.457	28573 3	DOWN	LOC285733	hypothetical LOC285733	0.019 8	775.6 527	0.01 51
1.344	40250 9	DOWN	LOC402509	similar to solute carrier family 29 (nucleoside transporters), member 4	0.019 9	775.6 567	0.01 51

1.360	64293 4	DOWN	LOC642934	hypothetical LOC642934	0.020 2	776.0 3	0.01 51
1.370	64716 9	DOWN	LOC647169	similar to glutathione transferase	0.020 2	776.4 98	0.01 55
1.215	65323 2	DOWN	LOC653232	ribosomal protein L15 pseudogene 3	0.020 2	782.2 943	0.01 59
1.269	73216 5	DOWN	LOC729708	TPI1 pseudogene	0.020 5	785.1 755	0.01 59
1.362	73002 4	DOWN	LOC730024	hypothetical LOC730024	0.020 5	787.1 399	0.01 59
1.467	4036	DOWN	LRP2	low density lipoprotein-related protein 2	0.020 6	788.5 231	0.01 62
1.363	11606 4	DOWN	LRR58	leucine rich repeat containing 58	0.020 6	789.2 961	0.01 61
1.353	4048	DOWN	LTA4H	leukotriene A4 hydrolase	0.021 2	789.5 84	0.01 61
1.287	9500	DOWN	MAGED1	melanoma antigen family D, 1	0.021 3	791.8 799	0.01 61
1.308	63905	DOWN	MANBAL	mannosidase, beta A, lysosomal-like	0.021 4	794.5 857	0.01 61
1.289	4082	DOWN	MARCKS (includes EG:4082)	myristoylated alanine-rich protein kinase C substrate	0.021 5	798.5 995	0.01 62
1.218	9782	DOWN	MATR3	matrin 3	0.021 5	802.2 092	0.01 62
1.276	9477	DOWN	MED20	mediator complex subunit 20	0.021 7	803.4 823	0.01 68
1.332	4240	DOWN	MFGE8	milk fat globule-EGF factor 8 protein	0.021 7	804.2 626	0.01 67
1.233	11365 5	DOWN	MFSD3	major facilitator superfamily domain containing 3	0.021 7	805.9 867	0.01 67
1.290	4320	DOWN	MMP11	matrix metalloproteinase 11 (stromelysin 3)	0.021 7	808.8 424	0.01 67
1.325	65258	DOWN	MPPE1	metallophosphoesterase 1	0.021 6	809.2 712	0.01 7
1.351	9019	DOWN	MPZL1	myelin protein zero-like 1	0.021 8	809.6 909	0.01 76
1.419	12499 5	DOWN	MRPL10	mitochondrial ribosomal protein L10	0.021 8	811.1 064	0.01 76
1.403	64978	DOWN	MRPL38	mitochondrial ribosomal protein L38	0.022	813.6 191	0.01 8
1.311	84311	DOWN	MRPL45	mitochondrial ribosomal protein L45	0.021 9	823.9 833	0.01 8
1.332	64419	DOWN	MTMR14	myotubularin related protein 14	0.022 1	825.0 695	0.01 8
1.362	10608	DOWN	MXD4	MAX dimerization protein 4	0.022 2	825.3 799	0.01 83
1.373	54820	DOWN	NDE1	nudE nuclear distribution gene E homolog 1 (A. nidulans)	0.022 1	825.5 161	0.01 83
1.336	10397	DOWN	NDRG1	N-myc downstream regulated 1	0.022 5	825.8 505	0.01 87
1.305	4705	DOWN	NDUFA10 (includes EG:4705)	NADH dehydrogenase (ubiquinone) 1 alpha subcomplex, 10, 42kDa	0.022 5	826.5 292	0.01 88
1.367	10783	DOWN	NEK6	NIMA (never in mitosis gene a)-related kinase 6	0.022 5	829.8 933	0.01 88
1.365	64332	DOWN	NFKBIZ	nuclear factor of kappa light polypeptide gene enhancer in B-cells inhibitor, zeta	0.022 6	831.4 663	0.01 89
1.297	8508	DOWN	NIPSNAP1	nipsnap homolog 1 (C. elegans)	0.022 8	833.2 513	0.01 89
1.294	12620 5	DOWN	NLRP8	NLR family, pyrin domain containing 8	0.022 7	835.7 814	0.01 89
1.391	11281 7	DOWN	NPL2	N-acetylneuraminatase pyruvate lyase 2 (putative)	0.022 8	836.7 994	0.01 91
1.336	27020	DOWN	NPTN	neuroplastin	0.023 1	836.8 578	0.01 9
1.339	1728	DOWN	NQO1	NAD(P)H dehydrogenase, quinone 1	0.023 2	837.9 167	0.01 91
1.473	7026	DOWN	NR2F2	nuclear receptor subfamily 2, group F, member 2	0.023 1	840.5 218	0.01 94

1.256	54940	DOWN	OCIAD1	OCIA domain containing 1	0.023 3	842.0 335	0.01 99
1.407	4973	DOWN	OLR1	oxidized low density lipoprotein (lectin-like) receptor 1	0.023 4	842.1 588	0.02 01
1.373	5004	DOWN	ORM1	orosomuroid 1	0.023 3	846.7 685	0.02 03
1.578	5005	DOWN	ORM2	orosomuroid 2	0.023 6	847.5 631	0.02 04
1.310	54623	DOWN	PAF1	Paf1, RNA polymerase II associated factor, homolog (<i>S. cerevisiae</i>)	0.023 7	848.4 069	0.02 03
1.552	5064	DOWN	PALM	paralemmin	0.023 7	849.4 122	0.02 03
1.300	19674 3	DOWN	PAOX (includes EG:196743)	polyamine oxidase (exo-N4-amino)	0.023 6	849.7 346	0.02 03
1.491	64282	DOWN	PAPD5	PAP associated domain containing 5	0.023 6	854.3 986	0.02 09
1.240	5094	DOWN	PCBP2	poly(rC) binding protein 2	0.023 5	855.1 113	0.02 09
1.289	5111	DOWN	PCNA	proliferating cell nuclear antigen	0.023 7	858.4 269	0.02 14
1.330	5118	DOWN	PCOLCE	procollagen C-endopeptidase enhancer	0.023 6	860.3 193	0.02 15
1.327	27250	DOWN	PDCD4	programmed cell death 4 (neoplastic transformation inhibitor)	0.023 6	865.9 134	0.02 22
1.282	5143	DOWN	PDE4C	phosphodiesterase 4C, cAMP-specific (phosphodiesterase E1 dunce homolog, <i>Drosophila</i>)	0.023 7	866.7 41	0.02 25
1.315	5159	DOWN	PDGFRB	platelet-derived growth factor receptor, beta polypeptide	0.023 7	869.2 378	0.02 28
1.372	8566	DOWN	PDXK	pyridoxal (pyridoxine, vitamin B6) kinase	0.023 7	870.9 774	0.02 29
1.373	57026	DOWN	PDXP (includes EG:57026)	pyridoxal (pyridoxine, vitamin B6) phosphatase	0.023 8	876.3 165	0.02 29
1.390	64065	DOWN	PERP	PERP, TP53 apoptosis effector	0.023 8	880.4 625	0.02 29
1.210	10857	DOWN	PGRMC1	progesterone receptor membrane component 1	0.023 9	881.5 768	0.02 28
1.288	10424	DOWN	PGRMC2	progesterone receptor membrane component 2	0.024 7	884.3 768	0.02 3
1.339	5297	DOWN	PI4KA	phosphatidylinositol 4-kinase, catalytic, alpha	0.024 4	885.0 293	0.02 32
1.467	9091	DOWN	PIGQ	phosphatidylinositol glycan anchor biosynthesis, class Q	0.024 6	887.0 663	0.02 31
1.375	12886 9	DOWN	PIGU	phosphatidylinositol glycan anchor biosynthesis, class U	0.024 7	889.1 884	0.02 33
1.259	5296	DOWN	PIK3R2	phosphoinositide-3-kinase, regulatory subunit 2 (beta)	0.024 7	889.8 963	0.02 34
1.348	23646	DOWN	PLD3	phospholipase D family, member 3	0.025 4	890.7 387	0.02 34
1.278	5372	DOWN	PMM1	phosphomannomutase 1	0.025 9	891.4 852	0.02 36
1.474	5376	DOWN	PMP22	peripheral myelin protein 22	0.026 9	895.4 254	0.02 37
1.262	87178	DOWN	PNPT1	polyribonucleotide nucleotidyltransferase 1	0.026 4	896.7 533	0.02 39
1.266	8495	DOWN	PPFIBP2	PTPRF interacting protein, binding protein 2 (liprin beta 2)	0.026 4	898.5 937	0.02 38
1.295	5515	DOWN	PPP2CA	protein phosphatase 2 (formerly 2A), catalytic subunit, alpha isoform	0.026 3	899.1 11	0.02 39
1.323	13081 4	DOWN	PQLC3	PQ loop repeat containing 3	0.026 3	900.8 069	0.02 39
1.464	8842	DOWN	PROM1	prominin 1	0.026 8	901.1 124	0.02 42
1.316	15069 6	DOWN	PROM2	prominin 2	0.026 8	902.6 337	0.02 44
1.410	5627	DOWN	PROS1	protein S (alpha)	0.027 4	903.5 739	0.02 49
1.300	5636	DOWN	PRPSAP2	phosphoribosyl pyrophosphate synthetase-associated protein 2	0.028 1	903.9 941	0.02 48
1.301	78994	DOWN	PRR14	proline rich 14	0.028 1	905.1 038	0.02 48
1.469	5652	DOWN	PRSS8	protease, serine, 8	0.028 5	905.1 879	0.02 5
1.415	56952	DOWN	PRTFDC1	phosphoribosyl transferase domain containing 1	0.028 4	907.2 378	0.02 49

1.490	5660	DOWN	PSAP	prosaposin	0.028 5	908.8 963	0.02 49
1.371	22949	DOWN	PTGR1	prostaglandin reductase 1	0.028 8	913.1 431	0.02 52
1.260	5747	DOWN	PTK2	PTK2 protein tyrosine kinase 2	0.028 8	915.1 12	0.02 51
1.354	5786	DOWN	PTPRA	protein tyrosine phosphatase, receptor type, A	0.028 7	915.7 674	0.02 5
1.522	5792	DOWN	PTPRF	protein tyrosine phosphatase, receptor type, F	0.028 8	915.9 086	0.02 52
1.430	28411 9	DOWN	PTRF	polymerase I and transcript release factor	0.028 8	919.0 889	0.02 53
1.395	25945	DOWN	PVRL3	poliovirus receptor-related 3	0.028 8	919.3 379	0.02 56
1.380	5859	DOWN	QARS	glutamyl-tRNA synthetase	0.029 4	919.7 133	0.02 59
1.286	80223	DOWN	RAB11FIP1	RAB11 family interacting protein 1 (class I)	0.029 7	922.2 762	0.02 59
1.369	9727	DOWN	RAB11FIP3	RAB11 family interacting protein 3 (class II)	0.029 6	925.0 475	0.02 59
1.829	11031	DOWN	RAB31	RAB31, member RAS oncogene family	0.029 8	925.3 453	0.02 6
1.261	32662 4	DOWN	RAB37	RAB37, member RAS oncogene family	0.030 2	926.4 133	0.02 63
1.366	5899	DOWN	RALB	v-ral simian leukemia viral oncogene homolog B (ras related; GTP binding protein)	0.031	928.8 746	0.02 64
1.506	10928	DOWN	RALBP1	ralA binding protein 1	0.031 1	930.0 007	0.02 7
1.392	51285	DOWN	RASL12	RAS-like, family 12	0.031	930.0 506	0.02 69
1.331	34809 3	DOWN	RBPM52	RNA binding protein with multiple splicing 2	0.031 3	932.5 875	0.02 77
1.356	92840	DOWN	REEP6	receptor accessory protein 6	0.031 4	932.9 69	0.02 78
1.343	29803	DOWN	REPIN1	replication initiator 1	0.031 3	933.3 806	0.02 78
1.349	23180	DOWN	RFTN1	raftlin, lipid raft linker 1	0.031 4	936.8 728	0.02 78
1.218	6001	DOWN	RGS10	regulator of G-protein signaling 10	0.031 4	938.3 058	0.02 8
1.242	387	DOWN	RHOA	ras homolog gene family, member A	0.031 4	939.2 276	0.02 83
1.336	389	DOWN	RHOC	ras homolog gene family, member C	0.031 4	940.2 18	0.02 86
1.284	6038	DOWN	RNASE4	ribonuclease, RNase A family, 4	0.032 1	940.4 819	0.02 9
1.517	8635	DOWN	RNASET2	ribonuclease T2	0.032 1	941.3 478	0.03 05
1.305	26001	DOWN	RNF167	ring finger protein 167	0.032	942.8 808	0.03 11
1.382	6051	DOWN	RNPEP	arginyl aminopeptidase (aminopeptidase B)	0.031 9	942.9 217	0.03 11
1.555	4736	DOWN	RPL10A (includes EG:4736)	ribosomal protein L10a	0.032	943.2 923	0.03 19
1.247	6137	DOWN	RPL13	ribosomal protein L13	0.032	943.7 686	0.03 22
1.429	23521	DOWN	RPL13A	ribosomal protein L13a	0.032 1	944.7 884	0.03 27
1.299	6138	DOWN	RPL15	ribosomal protein L15	0.032 1	945.1 058	0.03 33
1.991	6144	DOWN	RPL21 (includes EG:6144)	ribosomal protein L21	0.032 1	945.7 473	0.03 33
1.301	6154	DOWN	RPL26	ribosomal protein L26	0.032	946.0 195	0.03 34
1.378	6158	DOWN	RPL28	ribosomal protein L28	0.032	947.7 589	0.03 37
1.640	6130	DOWN	RPL7A	ribosomal protein L7a	0.032 2	950.6 867	0.03 37
1.231	28585 5	DOWN	RPL7L1	ribosomal protein L7-like 1	0.032 3	953.9 539	0.03 4
1.269	6184	DOWN	RPN1	ribophorin I	0.032 5	955.4 844	0.03 42
1.369	6185	DOWN	RPN2	ribophorin II	0.033	956.3 052	0.03 43

1.333	6199	DOWN	RPS6KB2	ribosomal protein S6 kinase, 70kDa, polypeptide 2	0.033	956.9 019	0.03 43
1.530	56681	DOWN	SAR1A	SAR1 homolog A (<i>S. cerevisiae</i>)	0.033	963.9 779	0.03 49
1.351	51435	DOWN	SCARA3	scavenger receptor class A, member 3	0.033	970.4 834	0.03 48
1.421	29970	DOWN	SCHIP1	schwannomin interacting protein 1	0.033 2	972.1 263	0.03 48
1.337	57410	DOWN	SCYL1	SCY1-like 1 (<i>S. cerevisiae</i>)	0.033 3	975.9 31	0.03 47
1.680	6382	DOWN	SDC1	syndecan 1	0.033 3	976.4 117	0.03 51
1.481	22928	DOWN	SEPHS2	selenophosphate synthetase 2	0.033 4	976.8 96	0.03 5
1.269	4735	DOWN	SEPT2	septin 2	0.033 5	977.2 586	0.03 58
1.315	5413	DOWN	SEPT5	septin 5	0.033 8	982.1 059	0.03 58
1.289	5104	DOWN	SERPINA5	serpin peptidase inhibitor, clade A (alpha-1 antiproteinase, antitrypsin), member 5	0.033 8	982.7 157	0.03 68
1.284	5269	DOWN	SERPINB6	serpin peptidase inhibitor, clade B (ovalbumin), member 6	0.034 9	988.5 886	0.03 68
1.354	462	DOWN	SERPINC1	serpin peptidase inhibitor, clade C (antithrombin), member 1	0.035 6	993.4 059	0.03 68
1.235	6430	DOWN	SFRS5	splicing factor, arginine/serine-rich 5	0.036	994.1 238	0.03 71
1.254	6431	DOWN	SFRS6	splicing factor, arginine/serine-rich 6	0.036 2	997.6 468	0.03 73
1.348	15376 9	DOWN	SH3RF2	SH3 domain containing ring finger 2	0.036 3	997.7 595	0.03 75
1.296	51092	DOWN	SIDT2	SID1 transmembrane family, member 2	0.036 2	999.2 031	0.03 75
1.331	7884	DOWN	SLBP	stem-loop binding protein	0.036 2	1002. 8427	0.03 78
1.451	6554	DOWN	SLC10A1	solute carrier family 10 (sodium/bile acid cotransporter family), member 1	0.036 1	1003. 7515	0.03 79
1.301	38770 0	DOWN	SLC16A12	solute carrier family 16, member 12 (monocarboxylic acid transporter 12)	0.036 1	1003. 9048	0.03 78
1.326	9121	DOWN	SLC16A5	solute carrier family 16, member 5 (monocarboxylic acid transporter 6)	0.036 1	1005. 2128	0.03 82
1.268	51312	DOWN	SLC25A37	solute carrier family 25, member 37	0.036	1005. 9407	0.03 83
1.465	22296 2	DOWN	SLC29A4	solute carrier family 29 (nucleoside transporters), member 4	0.037 6	1006. 4934	0.03 84
1.405	2542	DOWN	SLC37A4	solute carrier family 37 (glucose-6-phosphate transporter), member 4	0.037 5	1006. 7054	0.03 84
1.487	54946	DOWN	SLC41A3 (includes EG:54946)	solute carrier family 41, member 3	0.037 9	1014. 7883	0.03 94
1.250	23446	DOWN	SLC44A1	solute carrier family 44, member 1	0.038 3	1014. 9258	0.03 93
1.723	9056	DOWN	SLC7A7	solute carrier family 7 (cationic amino acid transporter, y+ system), member 7	0.038 2	1016. 409	0.03 95
1.417	9368	DOWN	SLC9A3R1	solute carrier family 9 (sodium/hydrogen exchanger), member 3 regulator 1	0.038 3	1020. 1983	0.03 96
1.263	4090	DOWN	SMAD5	SMAD family member 5	0.038 2	1023. 458	0.04 02
1.305	27131	DOWN	SNX5	sorting nexin 5	0.038 5	1024. 7569	0.04 02
1.222	64847	DOWN	SPATA20	spermatogenesis associated 20	0.038 5	1025. 2445	0.04 09
1.262	56848	DOWN	SPHK2	sphingosine kinase 2	0.038 6	1029. 1641	0.04 09
1.343	10653	DOWN	SPINT2	serine peptidase inhibitor, Kunitz type, 2	0.038 6	1030. 2163	0.04 12
1.443	55304	DOWN	SPTLC3	serine palmitoyltransferase, long chain base subunit 3	0.038 5	1030. 2755	0.04 15
1.311	10402	DOWN	ST3GAL6	ST3 beta-galactoside alpha-2,3-sialyltransferase 6	0.039 6	1032. 6779	0.04 16
1.311	6773	DOWN	STAT2	signal transducer and activator of transcription 2, 113kDa	0.039 6	1033. 9682	0.04 15
1.290	8614	DOWN	STC2	stanniocalcin 2	0.039 7	1035. 1833	0.04 16
2.027	2040	DOWN	STOM	stomatin	0.040 1	1036. 0108	0.04 18

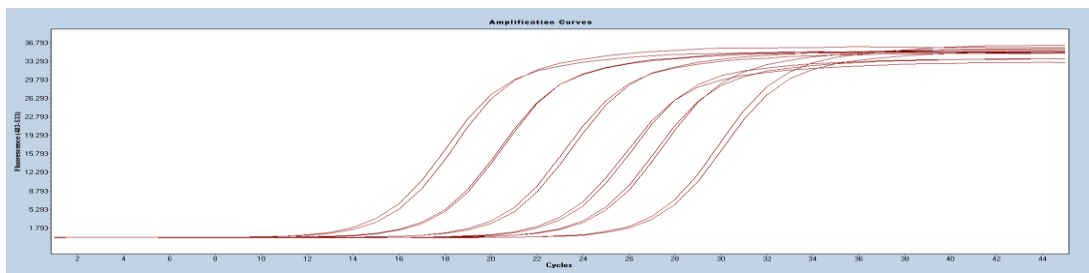
1.575	6811	DOWN	STX5	syntaxis 5	0.04	1041.0031	0.0418
1.270	8802	DOWN	SUCLG1	succinate-CoA ligase, alpha subunit	0.0402	1041.0414	0.0402
1.314	6817	DOWN	SULT1A1	sulfotransferase family, cytosolic, 1A, phenol-preferring, member 1	0.0403	1041.1463	0.0424
1.580	56241	DOWN	SUSD2	sushi domain containing 2	0.0404	1042.2754	0.0425
1.335	55333	DOWN	SYNJ2BP	synaptojanin 2 binding protein	0.0403	1042.5665	0.0425
1.388	26123	DOWN	TCTN3	tectonic family member 3	0.0403	1043.1112	0.0426
1.407	7045	DOWN	TGFBI	transforming growth factor, beta-induced, 68kDa	0.0403	1043.2405	0.0427
1.401	26277	DOWN	TINF2	TERF1 (TRF1)-interacting nuclear factor 2	0.0415	1043.9309	0.0403
1.355	27134	DOWN	TJP3	tight junction protein 3 (zona occludens 3)	0.0417	1044.042	0.0429
1.239	4071	DOWN	TM4SF1	transmembrane 4 L six family member 1	0.0417	1044.8326	0.0431
1.408	79022	DOWN	TMEM106C	transmembrane protein 106C	0.0421	1046.0933	0.0431
1.545	387521	DOWN	TMEM189	transmembrane protein 189	0.0423	1046.9511	0.0403
1.365	440026	DOWN	TMEM41B	transmembrane protein 41B	0.0423	1047.901	0.0429
1.445	757	DOWN	TMEM50B	transmembrane protein 50B	0.0422	1051.2343	0.0433
1.278	51669	DOWN	TMEM66	transmembrane protein 66	0.0425	1051.6246	0.0432
1.398	10140	DOWN	TOB1	transducer of ERBB2, 1	0.0426	1051.7964	0.0432
1.345	8459	DOWN	TPST2	tyrosylprotein sulfotransferase 2	0.0435	1052.8136	0.0433
1.335	10758	DOWN	TRAF3IP2	TRAF3 interacting protein 2	0.0436	1055.2347	0.0437
1.329	89122	DOWN	TRIM4	tripartite motif-containing 4	0.0436	1056.6837	0.0439
1.287	8295	DOWN	TRRAP	transformation/transcription domain-associated protein	0.044	1057.189	0.0439
1.374	27075	DOWN	TSPAN13	tetraspanin 13	0.0447	1058.642	0.0445
1.408	90139	DOWN	TSPAN18	tetraspanin 18	0.0446	1059.4039	0.0405
1.364	10099	DOWN	TSPAN3	tetraspanin 3	0.0447	1062.6395	0.0454
1.312	6302	DOWN	TSPAN31	tetraspanin 31	0.0449	1062.8833	0.0454
1.239	7263	DOWN	TST	thiosulfate sulfurtransferase (rhodanese)	0.045	1070.7392	0.0458
1.491	337867	DOWN	UBAC2	UBA domain containing 2	0.0451	1074.8959	0.0461
1.385	140739	DOWN	UBE2F	ubiquitin-conjugating enzyme E2F (putative)	0.0452	1079.2519	0.0466
1.335	9246	DOWN	UBE2L6	ubiquitin-conjugating enzyme E2L 6	0.0453	1081.4066	0.0467
1.265	9690	DOWN	UBE3C	ubiquitin protein ligase E3C	0.0454	1082.3881	0.0468
1.298	8408	DOWN	ULK1	unc-51-like kinase 1 (C. elegans)	0.0454	1082.5836	0.0468
1.294	55245	DOWN	UQCC	ubiquinol-cytochrome c reductase complex chaperone	0.0463	1082.7392	0.0478
1.259	7390	DOWN	UROS	uroporphyrinogen III synthase	0.0467	1083.8441	0.0478
1.311	10083	DOWN	USH1C	Usher syndrome 1C (autosomal recessive, severe)	0.0468	1084.4072	0.0477
1.321	8239	DOWN	USP9X	ubiquitin specific peptidase 9, X-linked	0.047	1084.566	0.0477
1.460	7411	DOWN	VBP1	von Hippel-Lindau binding protein 1	0.0475	1094.6139	0.0477
1.384	9686	DOWN	VGLL4	vestigial like 4 (Drosophila)	0.0479	1100.0318	0.0476
1.292	7429	DOWN	VIL1	villin 1	0.0484	1100.1869	0.0479

1.271	7448	DOWN	VTN	vitronectin	0.048 3	1102. 0199	0.04 79
1.332	25676 4	DOWN	WDR72	WD repeat domain 72	0.048 2	1102. 1919	0.04 83
1.270	25844	DOWN	YIPF3	Yip1 domain family, member 3	0.048 1	1103. 5268	0.04 87
1.353	7528	DOWN	YY1	YY1 transcription factor	0.048 8	1103. 8819	0.04 87
1.353	7766	DOWN	ZNF223	zinc finger protein 223	0.049 1	1106. 8563	0.04 92
1.353	14046 7	DOWN	ZNF358	zinc finger protein 358	0.049 5	1107. 2774	0.04 93
1.314	65249	DOWN	ZSWIM4	zinc finger, SWIM-type containing 4	0.049 9	1108. 3324	0.04 97

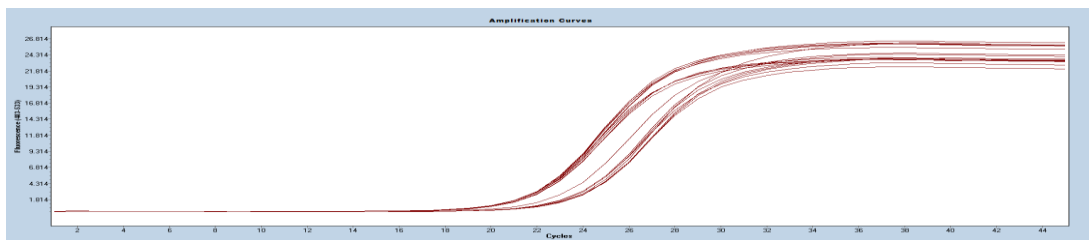
Table 2. Analysis of genes affected by reduced GPX4 expression by (siRNA). Genes with reduced expression by 1.2 or greater (ranked) for 72 hours in response to GPX4 knock-down in Caco-2 cells by siRNA are listed. Genes identified through the in silico analysis as upregulated due to GPX4 knock-down includes Human gene symbols and Entrez identifiers.

Appendix B: Amplification and Standard Curves for qPCR

i



ii



iii

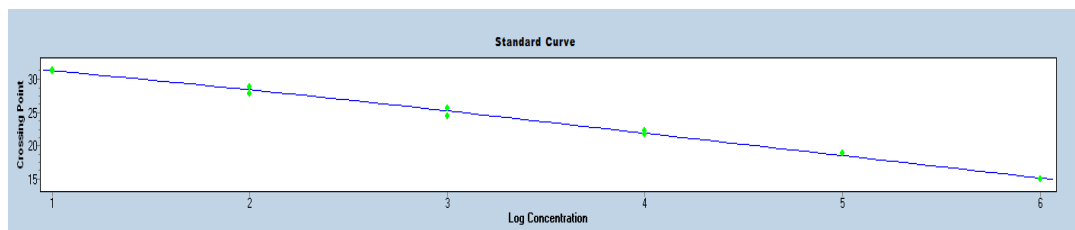
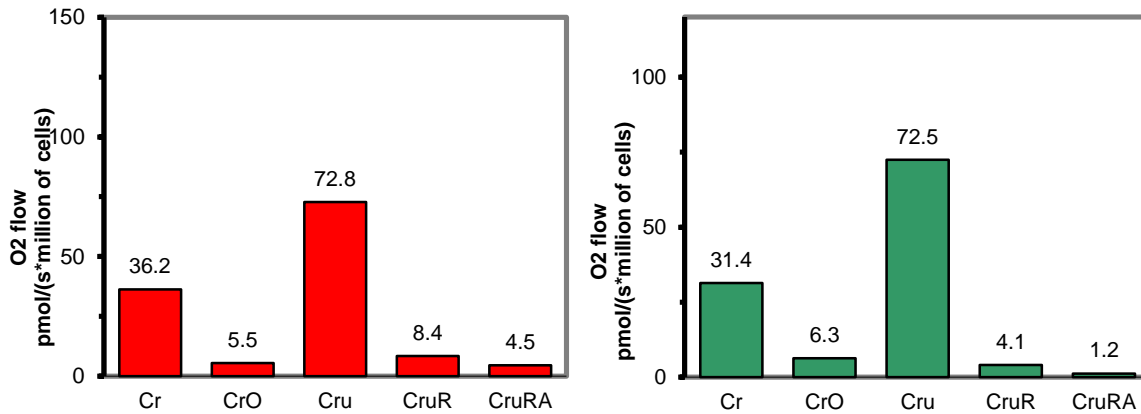


Figure 1. RT-qPCR for Apoptosis inducing factor (AIF) (i) RT-qPCR amplification using PCR product of AIF (ii) RT-qPCR amplification of unknown samples using cDNA from siRNA and scrambled control treated cells (iii) standard curves using primers for GAPDH and β -actin on reverse-transcribed Caco-2 cell RNA. i – Typical amplification curves generated using primers for GAPDH and β -actin. Fluorescence intensity generated by amplification of PCR product used to generate standard curve was measured and plotted against PCR cycle number to determine the threshold crossing point (CT values). ii- Fluorescence intensity generated by amplification of cDNA of unknown concentration was measured and plotted against PCR cycle number to determine the threshold crossing point (CT values). Each sample was measured in duplicate. iii – Typical standard curve generated for GAPDH and β -actin. The mean log concentration of each PCR and cDNA sample within a ten- fold dilution series was plotted against the CT value. The standard curve was then used to calculate the relative levels of GAPDH and β -actin in each unknown sample.

Appendix C: A typical Oxygen Electrode (Oxygraph) recording of cellular respiration in Caco-2 cells.

A



B

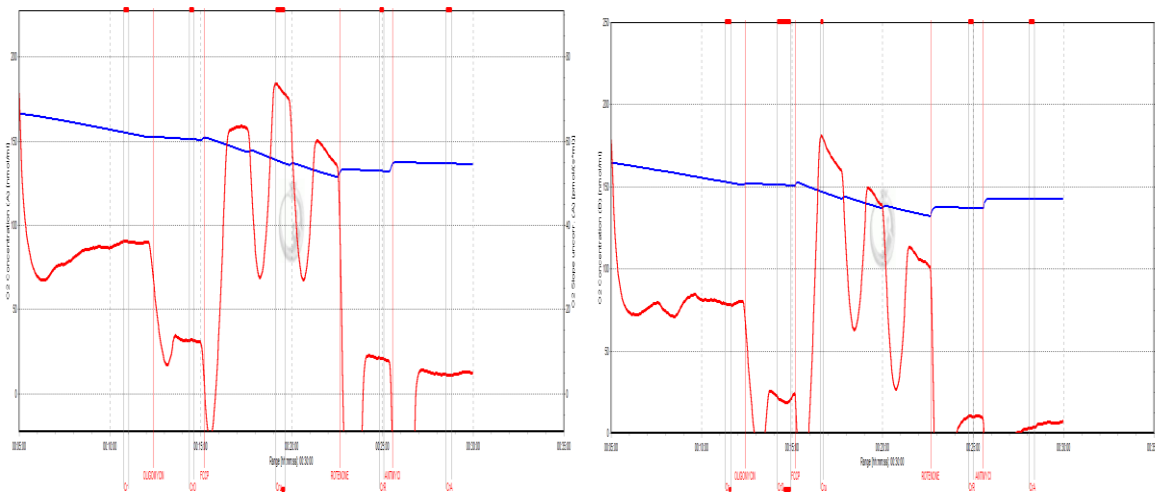


Figure 2. Cellular respiration and oxygen consumption assesment. (A) Oxygen flow after addition of specific inhibitors of the mitochondrial electron transport chains; Cr- cell resting respiration, CrO- respiration after addition of Oligomycin (Inhibitor of ATP synthase-Complex V), Cru- addition of FCCP (Uncoupler) to assess maximum respiration, CruR-addition of Rotenone (inhibitor of complex I) and CruRA- addition of Antimycin A (inhibitor of complex III). (B) A typical O_2 concentration generated from the respirometry experiment Blue-Oxygen concentration [μM] and Red-Oxygen flux per volume [$pmol/ml$] corrected for instrumental background.

Appendix D: Composition of cell culture medium

DMEM-Dulbecco's Modified Eagle Medium (Caco-2)

Components	Concentration (mg/L)	Molarity (mM)
------------	----------------------	---------------

Amino Acids:

Glycine	30	0.4
L-Alanyl-L-Glutamine	862	3.97
L-Arginine hydrochloride	84	0.398
L-Cystine 2HCl	63	0.201
L-Histidine hydrochloride-H ₂ O	42	0.2
L-Isoleucine	105	0.802
L-Leucine	105	0.802
L-Lysine hydrochloride	146	0.798
L-Methionine	30	0.201
L-Phenylalanine	66	0.4
L-Serine	42	0.4
L-Threonine	95	0.798
L-Tryptophan	16	0.0784
L-Tyrosine	72	0.398
L-Valine	94	0.803

Vitamins

Choline chloride	4	0.0286
D-Calcium pantothenate	4	0.00839
Folic Acid	4	0.00907
Niacinamide	4	0.0328
Pyridoxine hydrochloride	4	0.0196
Riboflavin	0.4	0.00106
Thiamine hydrochloride	4	0.0119
i-Inositol	7.2	0.04

Inorganic Salts:

Calcium Chloride (CaCl ₂ -2H ₂ O)	264	1.8
Ferric Nitrate (Fe(NO ₃) ₃ -9H ₂ O)	0.1	0.000248
Magnesium Sulfate (MgSO ₄ -7H ₂ O)	200	0.813
Potassium Chloride (KCl)	400	5.33
Sodium Bicarbonate (NaHCO ₃)	3700	44.05
Sodium Chloride (NaCl)	6400	110.34
Sodium Phosphate monobasic (NaH ₂ PO ₄ -2H ₂ O)	141	0.916

Other Components:

D-Glucose (Dextrose)	4500	25
Phenol Red	15	0.0399
Sodium Pyruvate	110	1